NAVAL POSTGRADUATE SCHOOL

MONTEREY, CALIFORNIA

THESIS

AUTHORSHIP ATTRIBUTION OF SHORT MESSAGES USING MULTIMODAL FEATURES

by

Sarah R. Boutwell

March 2011

Thesis Co-Advisors: Robert Beverly
Craig H. Martell

Approved for public release; distribution is unlimited

THIS PAGE INTENTIONALLY LEFT BLANK

REPORT DOCUMENTATION PAGE

Form Approved OMB No. 0704-0188

1. AGENCY USE ONLY *(Leave blank)*	**2. REPORT DATE** March 2011	**3. REPORT TYPE AND DATES COVERED** Master’s Thesis

4. TITLE AND SUBTITLE
Authorship Attribution of Short Messages Using Multimodal Features

5. FUNDING NUMBERS

6. AUTHOR(S) Sarah R. Boutwell

7. PERFORMING ORGANIZATION NAME(S) AND ADDRESS(ES)
Naval Postgraduate School
Monterey, CA 93943-5000

8. PERFORMING ORGANIZATION REPORT NUMBER

9. SPONSORING /MONITORING AGENCY NAME(S) AND ADDRESS(ES)
N/A

10. SPONSORING/MONITORING AGENCY REPORT NUMBER

11. SUPPLEMENTARY NOTES The views expressed in this thesis are those of the author and do not reflect the official policy or position of the Department of Defense or the U.S. Government. IRB Protocol number: n/a ________________.

12a. DISTRIBUTION / AVAILABILITY STATEMENT
Approved for public release; distribution is unlimited

12b. DISTRIBUTION CODE

13. ABSTRACT (maximum 200 words)

In this thesis, we develop a multimodal classifier for authorship attribution of short messages. Standard natural language processing authorship attribution techniques are applied to a Twitter text corpus. Using character n-gram features and a Naïve Bayes classifier, we build statistical models of the set of authors. The social network of the selected Twitter users is analyzed using the screen names referenced in their messages. The timestamps of the messages are used to generate a pattern-of-life model. We analyze the physical layer of a network by measuring modulation characteristics of GSM cell phones. A statistical model of each cell phone is created using a Naïve Bayes classifier. Each phone is assigned to a Twitter user, and the probability outputs of the individual classifiers are combined to show that the combination of natural-language and network-feature classifiers identifies a user to phone binding better than when the individual classifiers are used independently.

14. SUBJECT TERMS Authorship Attribution, Machine Learning, Twitter, GSM, Device Identification, Multimodal Classifier, Naïve Bayes

15. NUMBER OF PAGES
187

16. PRICE CODE

17. SECURITY CLASSIFICATION OF REPORT	**18. SECURITY CLASSIFICATION OF THIS PAGE**	**19. SECURITY CLASSIFICATION OF ABSTRACT**	**20. LIMITATION OF ABSTRACT**
Unclassified	Unclassified	Unclassified	UU

THIS PAGE INTENTIONALLY LEFT BLANK

AUTHORSHIP ATTRIBUTION OF SHORT MESSAGES USING MULTIMODAL FEATURES

Sarah R. Boutwell
Lieutenant, United States Navy
B.S., Johns Hopkins University, 1996

Submitted in partial fulfillment of the
requirements for the degree of

MASTER OF SCIENCE IN COMPUTER SCIENCE

from the

NAVAL POSTGRADUATE SCHOOL
March 2011

Author: Sarah R. Boutwell

Approved by: Robert Beverly
Thesis Co-Advisor

Craig H. Martell
Thesis Co-Advisor

Peter J. Denning
Chair, Department of Computer Science

THIS PAGE INTENTIONALLY LEFT BLANK

ABSTRACT

In this thesis, we develop a multimodal classifier for authorship attribution of short messages. Standard natural language processing authorship attribution techniques are applied to a Twitter text corpus. Using character n-gram features and a Naïve Bayes classifier, we build statistical models of the set of authors. The social network of the selected Twitter users is analyzed using the screen names referenced in their messages. The timestamps of the messages are used to generate a pattern-of-life model. We analyze the physical layer of a network by measuring modulation characteristics of GSM cell phones. A statistical model of each cell phone is created using a Naïve Bayes classifier. Each phone is assigned to a Twitter user, and the probability outputs of the individual classifiers are combined to show that the combination of natural-language and network-feature classifiers identifies a user to phone binding better than when the individual classifiers are used independently.

THIS PAGE INTENTIONALLY LEFT BLANK

TABLE OF CONTENTS

LIST OF FIGURES

THIS PAGE INTENTIONALLY LEFT BLANK

LIST OF TABLES

THIS PAGE INTENTIONALLY LEFT BLANK

LIST OF ACRONYMS AND ABBREVIATIONS

3GPP	3rd Generation Partnership Project
API	Application Programming Interface
ARFCN	Absolute Radio Frequency Channel Number
BSC	Base Station Controller
BTS	Base Transceiver Station
ETSI	European Telecommunications Standards Institute
FDM	Frequency Division Multiplexing
FPGA	Field-Programmable Gate Array
GMSK	Gaussian Minimum-Shift Keying
GMT	Greenwich Mean Time
GSM	Global System for Mobile Communications
I/Q	In-phase/Quadrature
ICMP	Internet Control Message Protocol
IMEI	International Mobile Equipment Identifier
IMSI	International Mobile Subscriber Identity
JSON	JavaScript Object Notation
kNN	k-Nearest Neighbor
MAC	Media Access Control
NIC	Network Interface Card
NPSML	Naval Postgraduate School Machine Learning
NRZ	Non-Return-To-Zero
PARADIS	Passive Radiometric Device Identification System
PCH	Physical Channel
PSTN	Public Switched Telephone Network
QPSK	Quadrature Phase Shift Keying
RF	Radio Frequency
RMS	Root Mean Square
SCAP	Source Code Author Profiles
SIM	Subscriber Identity Module
SMS	Short Message Service

SVM	Support Vector Machine
TacBSR	Tactical Base Station Router
TCP	Transport Control Protocol
TDM	Time Division Multiplexing
UMOP	Unintentional Modulation on Pulse
URL	Uniform Resource Locator
WARP	Wireless Open-Access Research Platform
XML	Extensible Markup Language

ACKNOWLEDGMENTS

I would like to acknowledge the many people who helped make this work possible. I would like to thank my advisors Professor Rob Beverly and Professor Craig Martell. Without your guidance and insight, this work would not have been possible, and Professor Beverly’s critical eye and rigor helped make this an excellent product.

I would like to thank the other members of my cohort for the support in finishing this program. Particularly, I would like to thank the other members of the Natural Language Processing Lab, CDR Jody Grady, LT Charles Ahn, LT Randy Honaker, and LT Kori Levy-Minzie for help with software and all the shared suffering.

I would also like to thank Brandon for all the moral support through this process.

THIS PAGE INTENTIONALLY LEFT BLANK

I. INTRODUCTION

The cellular telephone has become ubiquitous. Teenagers carry them to school, and adults carry them to work. They provide connection and communication, information and entertainment. In the U.S., 93% of the population has access to a cell phone, and 24.5% of households have abandoned the landline to use cellular only [1]. Along with the cell phone, the short messaging service (SMS) has also gained popularity. Americans sent 7.2 billion SMS messages a month in 2005. In 2010, that value increased to 173.2 billion a month. The annualized value of 1.81 trillion text messages a year comes close to matching the 2.26 trillion minutes of cell phone use in 2010 [1]. SMS messages are an integral part of modern communication.

A. IDENTITY ISSUES

The benefits and convenience of SMS messaging, however, bring with them new difficulties for human identity. For example, one can answer a phone call and immediately detect that it is one’s sister on the other end of the line by the sound of her voice. However, upon receiving a text message from one’s sister, it may be her, or she may have her husband key the message while she is driving. While this is an innocuous example of an identity mismatch, it is easy to imagine more malicious behavior.

Identity is a crucial part of network security. Devices communicate their identity to a network at the network link layer in the form of a media access control (MAC) address; cell phones on a Global System for Mobile

Communications (GSM) network use an international mobile equipment identifier (IMEI). A sophisticated adversary can falsify or “spoof” these identification codes to appear as a different device. Users authenticate to the network at the application layer in the form of passwords or biometric information. Passwords have well-known vulnerabilities if they are not carefully selected, and biometrics have not achieved widespread use. Users can access web-based applications from any internet-capable device, allowing independence from a specific platform.

For authentication mechanisms in cell phone networks, the provider mandates the user have a physical token in the form of a registered phone or subscriber identity module (SIM) card to gain access to the network. Even this notion of “registration” is not uniformly employed. Legislators in the Philippines just introduced a bill in January 2011 regulating the sale and distribution of SIM cards. Currently, pre-paid SIM cards and cellular phones can be purchased in the Philippines and many other countries, without having to provide any identification or register a legal name with a network provider. More trivially, phones may also be lost or misappropriated. Thus, it is difficult to tie a cell phone used in an illegal activity, such as a kidnapping, with its user [2].

A registration system may improve accountability in cell phone use, but policy alone cannot guarantee that the name in the database associated with a phone is the same person using the phone at any point in time. This identity uncertainty can also be problematic in situations that do not involve illegal activities. A business that issues cell phones to its employees may not want those phones used for non-work-related communications. A government agency may want an unobtrusive way to ensure that an employee has not lost or loaned his phone to a family member. In these situations, an authority wants to establish and monitor a device-to-user binding, associating a specific user to a specific phone. Beyond security, a phone that is contextually aware may wish to display specific information or act differently depending on the user. We propose that it is possible to identify the user of a mobile wireless device based on the statistical analysis of user's text messaging characteristics and their phones' radio transmission signals.

B. RESEARCH QUESTIONS

This thesis addresses two questions related to identity determination on mobile devices. We first examine whether combining user-specific text authorship characteristics and device-specific signal characteristics in a naïve Bayes classifier improves upon the accuracy results of classifying these characteristics individually. The second question asks if this classifier can detect when a phone normally used by one individual begins to be used by a different individual. We use an authorship attribution analysis of the text of short messages as the user classifier, and an analysis of signal modulation characteristics as the device classifier.

C. SIGNIFICANT FINDINGS

This research produced the following significant results:

- Classification of 120 individual Twitter messages from 50 authors using a multiclass naïve Bayes classifier produced 40.3% authorship attribution accuracy, less than the 54.4% found by Layton, Watters, and Dazeley using the Source Code Author Profiles (SCAP) method [3].
- Combining multiple Twitter messages to generate a text feature vector for input to the classifier improves authorship attribution accuracy. Using a feature vector from 23 combined messages produces the best result of 99.6% accuracy.
- Classification of 120 individual cell phone radio signal modulation characteristic vectors for 20 GSM cell phones resulted in a 90% classification accuracy. This compares favorably to the 99% accuracy of Brik et al. for modulation characteristics of 802.11 devices [4].
- Sum rule combination of the text and phone classifiers improves upon the results of the text classifier. Multimodal classifier accuracies over 99% were attained when using individual classifiers that employed the method of combining multiple messages to create the input feature vectors.
- The multimodal classifier was able to detect a simulated new user on a phone 36% of the time in the best-performing configuration.

D. ORGANIZATION OF THESIS

This thesis is organized as follows:

- Chapter I discusses the difficulty of ascertaining identity on mobile devices and the research questions we address in our experimentation.
- Chapter II discusses prior work in authorship attribution, device identification, and the machine learning techniques used in this study.
- Chapter III describes the methods used to collect and process data and set up and execute the classification experiments.

- Chapter IV contains the results of the experiments and analysis of their significance.
- Chapter V contains conclusions drawn from the results and possible areas of future research.

THIS PAGE INTENTIONALLY LEFT BLANK

II. BACKGROUND

A. INTRODUCTION

Developing a binding between a user and a device involves merging the efforts to classify the user by applying authorship attribution methods, e.g., statistical word counts, social network structure, etc., and to classify the device using the characteristics of its wireless signal. This chapter describes the textual and signal domains that provide our data. We discuss authorship attribution and device identification techniques, followed by an overview of machine learning classification methods. A description of the software tools used in this research concludes the chapter.

B. TWITTER

Twitter provides a popular “microblogging” service, allowing users to communicate with messages of 140 characters or less known as tweets. Users subscribe to another user’s message “feed” to “follow” them, receiving messages from the user they follow. Twitter also provides a mechanism for users to reply to a tweet, directly send a message to another user, or repeat a received tweet to their own set of followers, thereby expanding the readership of that tweet. Users have the option to specify that their tweets are private, viewable only by their followers or the direct recipient of a tweet, or publicly viewable. Users post their messages to Twitter via twitter.com, text messages, or third party clients, including mobile applications. As of September 14, 2010, Twitter reports it has 175 million users, while 95 million tweets are sent per day [5]. We expect Twitter, and Twitter-like services, to continue to gain in popularity and that our work will be relevant to not only Twitter, but to new services that emerge.

1. Twitter Attributes

Twitter’s primary characteristic that differentiates it from e-mail, chat, or a standard blog is its 140-character length limit. In this respect, tweets have more in common with short message service (SMS) messages than any other communication technology [6]. Many language conventions of chat and SMS such as abbreviated spellings, acronyms, misspellings, and emoticons (i.e., combinations of characters that represent emotions, for instance a smiley face using a colon and a right parenthesis) are also used extensively in Twitter. While some misspellings are accidental, others are for effect, such as writing “sleeeepy” instead of “sleepy.” Another technique we note in our examination of our Twitter corpus is the chat convention where writers use asterisks before and after a statement to indicate action, for example “really? *bangs head on desk*.” The similarities noted between SMS and Twitter text imply that analysis methods that work in one domain will also work in the other.

Twitter adds two unique message attributes beyond SMS: the @ sign followed by a user’s screen name to indicate a reference to that user, and the # sign followed by a topic tag for use in grouping and searching messages by topic thread. We shall refer to these attributes as @names and #tags. In [7], Boyd, et al. found that, in a random sample of 720,000 tweets, 36% of them contain a @name and 5%

contain a #tag. Figure 1 is an anonymized example of a tweet using these attributes. In this example, the sender directs the tweet to @User1 in a conversational manner, referencing @User2 within the comment.

@User1 no wonder @User2 never wrote me back #epicfail

Figure 1. Typical Twitter Message

Another common message attribute is the Internet URL. As a text-only communication medium, Twitter users include Uniform Resource Locator (URL) links to outside content they wish to share [8]. This practice has given rise to URL shorteners, services such as http://bit.ly that provide redirection from a longer standard URL to a shortened URL (i.e., http://bit.ly/a1b2c3), enabling more efficient use of the limited message space.

C. PRIOR WORK IN AUTHORSHIP ATTRIBUTION

Authorship attribution takes a piece of written material and attempts to identify its author. Typically, this is done through a supervised learning process, taking material known to be written by an author and building a model from it, then gauging how well the writing in question fits the model. Researchers have found different ways to build these models. A discussion of several of these techniques follows, with an emphasis on those that have shown success with short messages.

1. Lexical Feature Analysis

Lexical features treat the text as a series of tokens, with a token consisting of a word, number, or punctuation mark, or some combination of alphanumeric characters. The author model consists of statistics such the distribution of sentence length, vocabulary richness, word frequencies, etc. An example of vocabulary richness is the ratio of the number of unique words in a corpus to the total number of words in the corpus. Vectors built from word frequencies that include the most common words, such as prepositions and pronouns, represent the author’s style, and are most often used in authorship detection. When vectors discard high frequency words with little semantic content, those prepositions and pronouns tend to perform better in topic detection [9].

In her 2007 thesis, Jane Lin used lexical features to profile authors of the NPS Chat Corpus by age and gender. In the processing of her corpus, she grouped Internet chat utterances by the age reported in the user’s profile, maintaining punctuation marks intact. This allowed her to build a dictionary of common emoticons and use them as a feature for classification. In her analysis she used the following features: emoticon token counts, emoticon types per sentence, punctuation token counts, punctuation types per sentence, average sentence length, and average count of word types per document (vocabulary richness). She used a naïve Bayes classifier, which we describe later, to compute classification accuracy both with and without prior probability [10].

Lin found that while classifying teens against 20-year-olds showed poor results, comparing them to increasingly older age groups improved the results. The top F-score, a metric of combined precision and recall that we detail later, of 0.932 came from comparing teens to 50-year-olds. As most sexual predators are 26 and older, she compared those under 26 to those over 26 with a resulting F-score of 0.702. Based on the results and her data, she suggested that other machine learning techniques may perform better [10].

2. N-Gram Feature Analysis

While the use of word features captures the style of the author well, it fails to capture certain features common to short messaging. Emoticons, abbreviations, and creative punctuation use may carry morphological information useful in stylistic discrimination. Custom-built parsers, such as used by Lin in the work described above, could pull these features out of the text but add a level of complexity to tokenizing and smoothing [9]. An alternative approach uses character-level n-grams as the feature type. This method disregards language-specific information such as word spacing, letter case, or new line markers. It also eliminates the need for taggers, parsers, or any other complex text preprocessing.

In [11], Keselj et al. used byte-level n-grams for authorship attribution of English, Greek, and Chinese texts. For each author they built a profile of the L most common character n-grams and their normalized frequencies. The basic theory of this method is that authorship is determined by the amount of similarity between the profiles of two texts, classifying a test profile as the author profile from which it is least dissimilar. The measure of dissimilarity is a normalized distance metric based on the n-gram frequencies within the text profiles. They refer to this measurement as the relative distance between two texts. For English texts by eight classic authors, they achieved 100% accuracy for several different n-gram and profile sizes. On Greek data sets drawn from newspaper texts they attained an accuracy of 85%, surpassing the previous best reported accuracy of 73% for that data set. These results suggest that byte-level n-grams have some useful application in authorship attribution.

Keselj’s method of determining the difference between two author profiles of byte-level n-gram features was expanded upon and simplified by [12] in order to apply the technique to a different textual domain. Instead of the normalized distance metric used by Keselj to differentiate authors, Frantzeskou et al. built profiles of the L most common n-grams used by the authors of computer source code samples. Unlike the previous method, this approach does not normalize the n-gram frequencies. They call this the Source Code Author Profiles (SCAP) method. The size of the set of n-grams in the intersection of the two author profile sets measures the distance between the authors. A test document gets classified as the author with whom this intersection set is largest.

Frantzeskou et al. used a corpus of C++ programs applying Keselj’s method and the SCAP method to data from six authors. While results were similarly good for both methods with 100% accuracy at higher profile size (L) values, or number of n-grams per author, SCAP performed slightly better at lower values of L, and significantly better with bi-grams. On a corpus consisting of Java code with no comments, SCAP again performed better with accuracies from 92 – 100% across several values of L and n-gram sizes. The relative distance method performed well at lower values of L, but poorly at the highest L value tested [12]. The SCAP method provides a mathematically simple and effective means of conducting authorship attribution on source code material. While computer program source code and short messages have very different structures, both domains may present at first glance the impression of very broken, oddly punctuated English. Although Twitter covers a wider vocabulary range, authorship attribution methods effective in one domain may show similar effectiveness in the other.

The success of the SCAP method with source code led to an examination by [3] of its viability for authorship attribution of short messages, specifically those sent via Twitter. Layton, Watters, and Dazeley examined 50 users randomly from a set of 14,000. The 140-character limit of Twitter messages restricted the amount of unique characters sufficiently that they used a value of L that encompassed all characters used by an author. The value of n was varied from 2 to 7 characters. The experiment used three different text preprocessing methods to gauge the effect of the tagging conventions unique to Twitter, with one method removing @names from the text, one removing #tags, and one removing both.

Applying the SCAP methodology to Twitter produced a best result of 72.9% accuracy using character 4-grams and with both @names and #tags included in the message text. The @name influenced results the most, showing an average 26% accuracy drop when removed. The #tags reduced accuracy by only 1% on average. This implies that the inclusion of user social network analysis can significantly improve the ability to identify that user. The threshold number of tweets per author beyond which accuracy did not significantly improve was found to be 120. This study showed that authorship attribution of short messages with the SCAP method performs much better than chance, with the addition of information on the user's social network significantly improving the classification performance [3]. As short messages sent via SMS do not generally contain this social network information, their best accuracy result of 54.4% with both @names and #tags removed is a more realistic benchmark for authorship attribution of short messages.

This subsection described several different methods for authorship attribution in a variety of textual domains. Figure 2 summarizes the key points discussed.

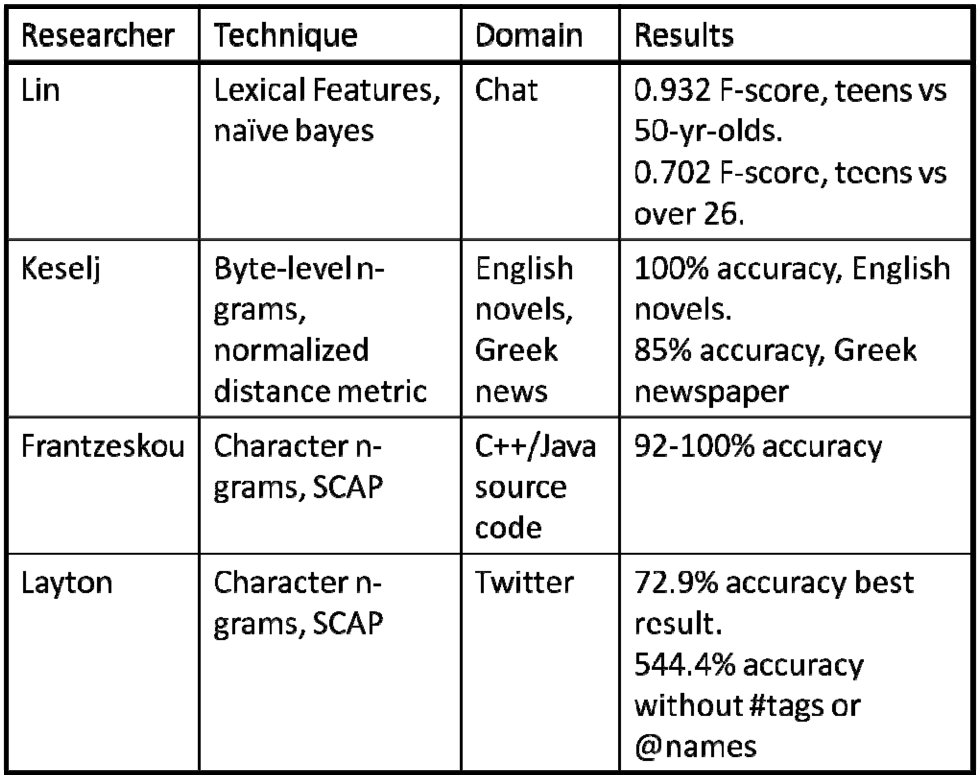

Researcher	Technique	Domain	Results
Lin	Lexical Features, naïve bayes	Chat	0.932 F-score, teens vs 50-yr-olds. 0.702 F-score, teens vs over 26.
Keselj	Byte-level n-grams, normalized distance metric	English novels, Greek news	100% accuracy, English novels. 85% accuracy, Greek newspaper
Frantzeskou	Character n-grams, SCAP	C++/Java source code	92-100% accuracy
Layton	Character n-grams, SCAP	Twitter	72.9% accuracy best result. 544.4% accuracy without #tags or @names

Figure 2. Comparison of Several Authorship Attribution Techniques on Different Textual Domains (After [10], [11], [12], [3])

D. PRIOR WORK IN DEVICE IDENTIFICATION

Accurate identification of individuals on a network is an important security concern. A number of security exploits involve mimicking an authorized user to gain access to a network. There is a parallel problem of trying to identify individuals involved in nefarious activities who may be trying to obfuscate their communications activities by routinely changing devices or otherwise misrepresenting themselves on a communications network. A passive means of correctly identifying an authorized device and its user by means of network characteristics, electronic emissions, and/or textual analysis could minimize the impact of spoofing attacks and contribute to intelligence or law enforcement efforts to track a specific individual.

Research in the 802.11 wireless domain shows that individual devices can be identified quite well by their radiometric signatures, even among users with the same brand of device. This is due to inherent variability in the manufacturing process. Other research has focused on authorship attribution based on analysis of an individual's language use. No known research to date has combined the two identification methods in an effort to improve the classification of users to devices in a network. This study will attempt to do so, with a focus on wireless and cellular SMS communications.

Identification of radio frequency (RF) transmitters by their signal characteristics has been accomplished with good success, particularly in the radar domain. That technology has advanced from basic measures of frequency, amplitude, and pulse width to fine-grained analysis of unintentional modulation on pulse (UMOP), which looks at pulse artifacts unique to individual transmitters. Once a radar is positively identified as transmitting a signal, that radar can be identified by that signal in the future. Unknown radars can be classified by manufacturer. A Litton Applied Technology UMOP analysis method was able to identify radars at 90–95% confidence level in the early 1990s [13].

1. Signal Transient Characteristic Method

Communications and data signals can be more complex than radars, with different modulation schemes, spread spectrum technology, and frequency hopping to enhance security, reliability, and capacity. Several methods have been proposed to "fingerprint" wireless transmitters by their physical, link, or application layer characteristics. Danev and Capkun have proposed a method to fingerprint 802.15.4 CC2420 radios by analyzing RF signal transient characteristics [14]. When a RF signal is transmitted, there is a period at the start of the signal where the amplitude ramps up from no energy to actual packet transmission at power. This part of the signal is the transient, and its characteristics vary depending on the analog hardware of the transmitter. Danev and Capkun extracted transients from 500 signals and applied a feature selection process to obtain distinctive templates of each. This process consisted of a transformation stage and a feature extraction stage. The transform method that gave them the best results was one that measured the relative differences between adjacent fast fourier transforms spectra. The feature extraction process took the transformed transient data and extracted spectral Fisher-features using a Linear Discriminant Analysis derived linear transformation. They show that their process identifies sensor nodes with an accuracy of 99.5%. This was on a set of 50 radios made by the same manufacturer. They did find that changes in antenna polarization reduced their accuracy, so this method works well only with fixed-location transmitters and receivers.

2. Steady State Signal Characteristic Method

Another identification method described by Candore, Kocabas, and Koushanfar, looks at the RF characteristics of the steady-state part of the signal for unique elements imparted by transmitter hardware [15]. They do this by developing individual classifiers that may be weak for the following characteristics: frequency difference, magnitude difference, phase difference, distance vector, and I/Q origin offset, where difference/distance/offset refers to difference between the ideal values and actual measured values of the signal. These individual classifiers are then combined with weighted voting to form a stronger classifier. Their work uses a Wireless Open-Access Research Platform (WARP) built around a computer, field-programmable gate array (FPGA) for the digital signal processing, and radio cards operating in the 2.4 GHz and 5 GHz bands. They use Differential Quadrature phase-shift keying modulation and extract their signal signatures in the modulation domain. After training the classifier on data collected from 200 frames of 1844 random symbols, they then use five frames to test it. At five frames, results were rather poor for six different radios. Testing with at least 25 frames, the individual characteristic classifiers each surpassed 50% identification accuracy. Combining the classifiers with weighted voting, they got 88% accuracy with a 12.8% false alarm probability of correct transmitter identification on five frames. One reason they suggested for the less than perfect identification results is that their WARP radio cards contain many digital components, which would have less inherent variability than other radios with more analog components in the transmission processing stream. If that is true, our software-oriented test system may show the same signal stability.

3. Modulation Characteristic Method

The modulation domain was used again in a paper by Brik et al., this time applied to 802.11 network interface cards (NIC) [4]. They developed a methodology called the passive radiometric device identification system (PARADIS). Four of the five characteristics they used were the same as in the WARP paper: frequency error, I/Q origin offset, magnitude error, and phase error. They also used another characteristic called SYNC correlation, which is the difference between the measured and ideal I/Q values of the SYNC, the short signal used to synchronize the transmitter and receiver prior to transmitting the data. The 802.11 physical layer, in many instances, encodes data with two sub-carriers, in-phase (I) and quadrature (Q) that are separated by $\pi/2$. In quadrature phase shift keying (QPSK), each symbol encodes two data bits and is represented by points in the modulation domain using a constellation diagram that plots the points in each of the four quadrants of a two-dimensional grid. Errors in modulation are usually measured by comparing vectors corresponding to the I and Q values at a point of time. Phase error is the angle between the ideal and measured phasor. Error vector magnitude is magnitude of vector difference between ideal and measured phasor. Those errors are taken as averages across all symbols in the frame in order to minimize the effects of channel noise. Figures 3 and 4 are a graphical display of the error measurements.

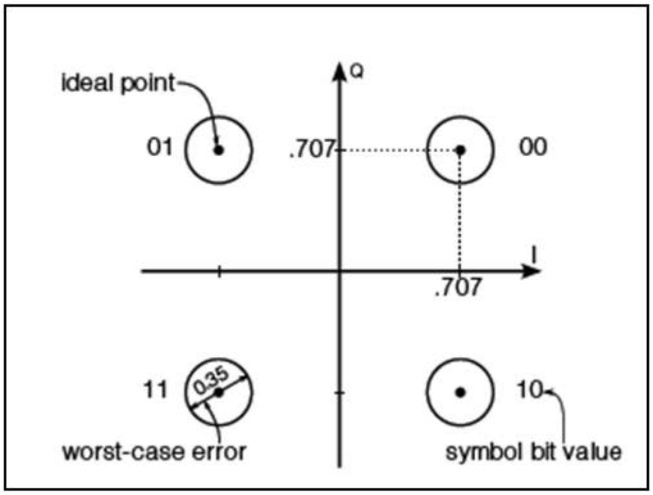

Figure 3. QPSK Error Shown on an I/Q Plane (From [4])

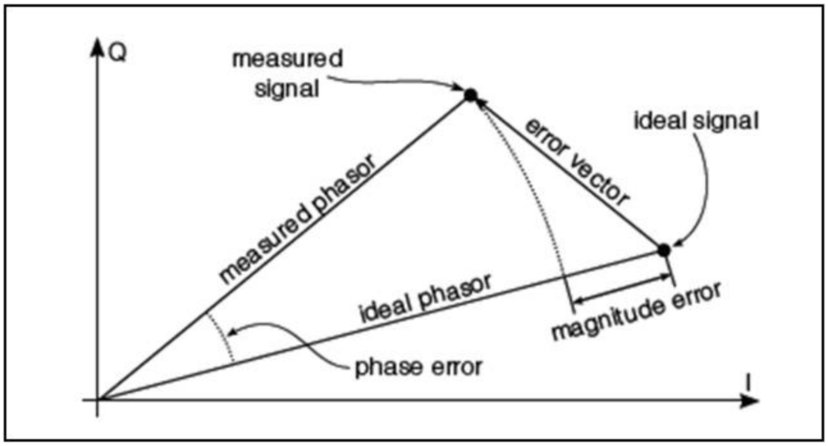

Figure 4. Vector Display of Modulation Errors (From [4])

For their experiment, the Brik group used identical Atheros NICs configured as 802.11b access points and an Agilent vector signal analyzer as the sensor. They tried both a k-Nearest Neighbor (kNN) and support vector machine (SVM) classification schemes to associate a MAC address to a NIC based on the collected modulation parameters. After evaluating data from 138 NICs, the best feature set was found to be, in order, frequency error, SYNC correlation, I/Q offset, magnitude and phase errors for SVM. Freq error, SYNC correlation, I/Q offset for kNN. The SVM classifier error rate was 0.34%, and kNN classifier error rate was 3%. Based on their data, no one NIC was able to masquerade as another. Modulation similarities were under 5% for 99% of the cards. One NIC had a similarity to others of 17% [4]. They also suggest that this method could work with any digital modulation scheme.

4. Transport Layer Characteristic Method

A passive fingerprinting technique proposed by Kohno, Broido, and Claffy, eschews the physical layer signal analysis, instead exploiting the transport layer for identity information by measuring clock skew in transport control protocol (TCP) timestamps [16]. Their method exploits two clocks on a computer: the system time clock and a TCP timestamps option clock internal to the TCP network stack. The system time clock may or may not be synchronized with true time by connection to a Network Time Protocol server. If not, the difference between system time and true time can be measured. Most modern operating systems enable the TCP timestamps option in their network stack. Thus, each TCP packet sent contains a 32-bit timestamp embedded in the packed header. They describe methods for passively collecting TCP timestamps from computers running various operating systems and formulas for calculating clock skew from the timestamps. They also describe a method for estimating system clock skew by sending Internet control message protocol ICMP Timestamp Requests to a targeted device, but focus on the TCP method, as most network stacks use clocks operating at lower frequencies than system clocks. Also, many routers and firewalls filter ICMP messages. For clock skew measurement to be effective, different devices must have different clock skews, and the skews must be consistent over time. Others have shown that both those assumptions hold, but they prove it by collecting two hours of traffic on a major link and using their process to find the clock skew of the first hour, second hour, and entire period and comparing them for each source that was active at least 30 minutes of each hour. A plot of their findings found that they were able to differentiate between some individual machines by their clock skew, but not all. This is an interesting method but not useful in our research, as cell phones synchronize their clocks with their network upon connection.

E. GSM OVERVIEW

The Global System for Mobile Communications (GSM) standard is the basis for the most popular mobile phone system in the world, with over 3 billion connections [17]. Its ubiquity and well-established hardware technology make it a good platform for experimentation and a good target for exploitation. GSM operates as a cellular network with a set of base stations distributed over a service area. The distribution is based on the desired coverage level, which depends on geography and connection demand. A rural area may have a few, high powered base stations spread out over a large area, while an urban area might have many lower powered units in close proximity [18]. The structure of a GSM network is shown in Figure 1. The two left blocks of Figure 1 contain the part of the network relevant to this study: the handset, the base transceiver station (BTS), and the air, or Um, interface between the two.

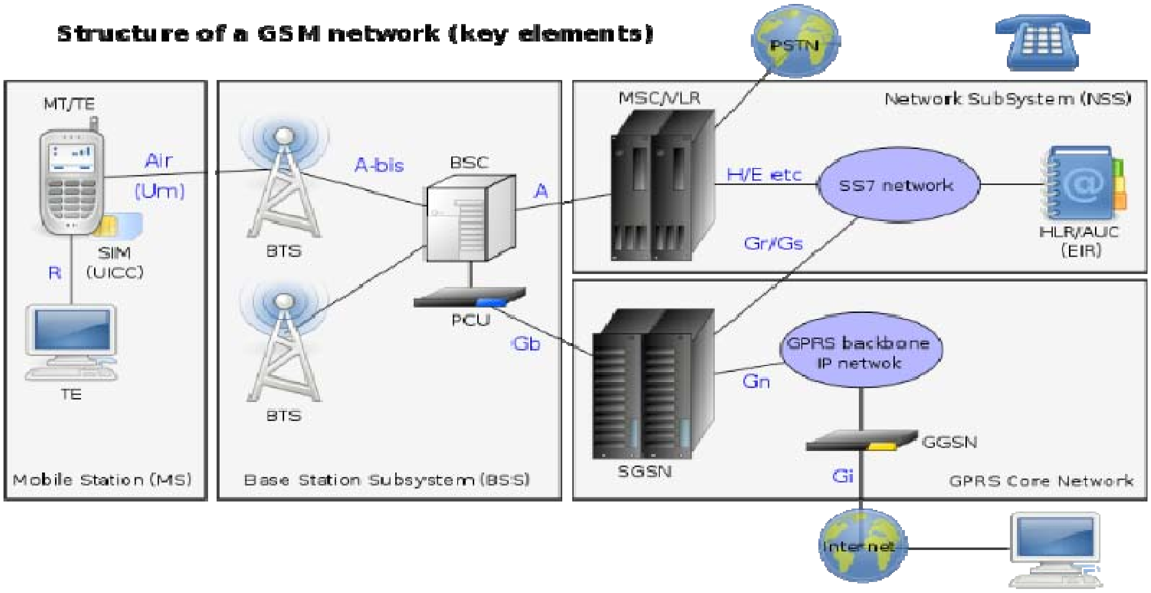

Figure 5. GSM Network Structure (From [19])

1. GSM Network Infrastructure

In a GSM network, the BTS contains the antennas, the transceivers for transmitting and receiving RF signals, and encryption gear as needed. While the complete capabilities of the BTS vary depending on the network provider, the minimum function is to receive the modulated analog RF signal from the handset, convert it to a modulated digital signal, and send it to the base station controller (BSC). The BTS can contain more functionality, to include handling handover between cells. The BTS is controlled by the BSC, which typically controls several BTSs in a network. The BSC manages the frequency channels used by its towers, handles handovers and switching among its towers, and may do the conversion from the air interface’s voice channel coding to the coding used in the circuit-switched Public

Switched Telephone Network (PSTN) [20]. A small and simple limited network can be assembled using only a BTS with appropriate software to manage a specific number of handsets. The network assembled for the experimentation conducted here is one such limited network.

2. Mobile Handset

The end of the cellular wireless network most familiar to typical users is the handset. Along with a transceiver and digital signal processing unit, a GSM handset also contains the subscriber identity module (SIM) card. The SIM card is what identifies the user to the network, allowing the network to choose to provide or deny access to the user. A user can easily switch phones and still access their subscribed services by transferring their SIM card to the new phone, assuming that phone is unlocked and compatible with the network technology. The indentifying feature of the SIM card is the International Mobile Subscriber Identity (IMSI) number. Each SIM card has a unique IMSI associated to the user. The phone itself also has a unique identifier, the International Mobile Equipment Identity (IMEI) number [20]. These two numbers are unrelated, though both may be transmitted through the network as part of control signal metadata.

The air interface between the handset and the BTS is the focus of part of the experimentation conducted here. GSM providers operate in the licensed 450 MHz, 850 MHz, 900 MHz, 1800 MHz, and 1900 MHz radio frequency bands. Uplink and downlink bands are typically each 25 MHz wide and separated by 45 – 50 MHz. Each of these bands is divided into 124 carrier frequencies with a 200 kHz bandwidth. An uplink/downlink channel pair is referred to by an absolute radio frequency channel number (ARFCN). Time-division multiplexing is used to divide each channel into eight time slots. A single timeslot in a specific ARFCN is called a physical channel (PCH) [21]. Thus, GSM combines FDM and TDM to make the most efficient use of its spectrum assignment. Each timeslot, or burst, generally consists of two 57 bit data fields separated by a 26 bit “training sequence” for equalization, three tail bits at each end, and an 8.25 bit guard sequence. Gaussian Minimum-Shift Keying (GMSK) is the signal modulation scheme used to modulate the digital data into the analog RF signal [21].

3. GSM Modulation

GSM uses the Gaussian Minimum Shift Keying modulation scheme. This modulation method applies a Gaussian filter to the data signal prior to the MSK modulator. MSK is a form of digital frequency modulation with a 0.5 modulation index. It has several properties that make it good for efficient mobile radio use: a constant envelope, a narrow bandwidth, and coherent detection capability. This makes it relatively impervious to noise. The one thing it lacks is the ability to minimize energy occurring out-of-band in transmission. The Gaussian filter has a narrow bandwidth and the cutoff properties to minimize extraneous frequencies, shaping the input data waveform so that the output fits a constant envelope. The single channel per carrier characteristic of GSM, with carriers spaced 200 kHz apart, minimizes off-carrier energy, and thus the Gaussian filter is important to clear transmission [22].

The modulation sequence of a typical GMSK signal modulator is shown in Figure 6. In this example, a stream of binary data formed in a Non-Return-To-Zero (NRZ) sequence is sampled and integrated into an analog signal. It is then convoluted with a Gaussian function to filter out the energy outside the Gaussian form. The real, in phase (I) and quadrature (Q) components of the data signal are calculated, then modulated onto the I and Q carrier waves. The two components are added, and the modulated signal is formed [23].

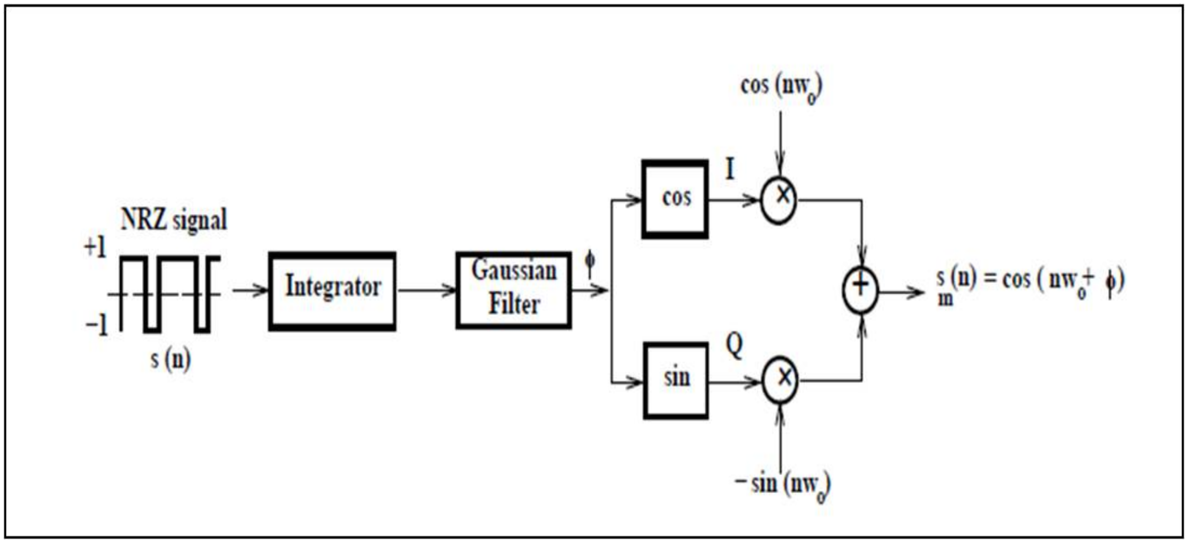

Figure 6. GMSK Modulation Block Diagram (From [23])

Demodulation of the GMSK signal is more complicated, particularly for GSM applications. Operating in the 900 MHz range, GSM is subject to a significant amount of interference, to include signal attenuation, multipath propagation, and co-channel or adjacent band interference. The GSM standard does not specify a demodulation algorithm, but does say that it has to be able to handle two multipath signals of equal power received at up to 16 μs apart. This implies that an equalizer is required to separate signals. Viterbi demodulation incorporates an assumption on the possible signal and additive noise and uses a probabilistic maximum likelihood calculation to produce the most probable received signal [23]. A diagram of a typical demodulator is shown in Figure 5. It splits the received signal into the I and Q components and demodulates each from its carrier wave. After going through a low-pass filter to clean up some of the noise, the I and Q components of the data stream are combined and the signal is converted back to a digital NRZ signal [23].

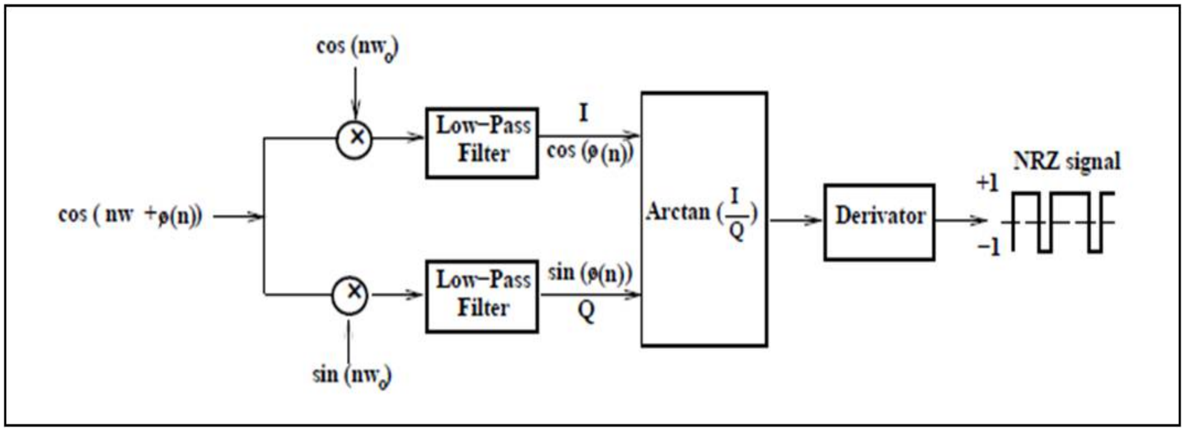

Figure 7. GMSK Demodulation Block Diagram (From [23])

F. MACHINE LEARNING TECHNIQUES

Authorship attribution entails creating a profile of an author and matching that pattern to a piece of text. Machine learning accomplishes this by building a model based on statistical methods, then customizing the model with training data or previous experience. The goal of the model is not to memorize the behavior of the training data, but to use it to decide if new data points fit into the pattern. While there are many machine learning techniques based on different statistical mechanisms, this research employs naïve Bayes.

1. Naïve Bayes Classifier

The naïve Bayes classifier uses Bayes' Rule of probability to assign a given set of features to a class.

$$P(C \mid \mathbf{F}) = \frac{P(\mathbf{F} \mid C)P(C)}{P(\mathbf{F})}$$

Bayes' rule is particularly useful in many practical situations where it is easier to estimate the conditional probability of a particular feature given a class. The conditional probability of the class given the features, P(C|**F**), depends on the probabilities of the class and the features and the probability of the features given the class. When **F** is a vector of d random feature values, **F** = $(f_1,\ldots,f_j,\ldots,f_d)$, and all documents fall into one of n random classes conditional on the feature set, C = $(c_1,\ldots,c_k,\ldots,c_n)$, Bayes' Rule may be expressed as [24]:

$$P(c_k \mid \mathbf{F}) = \frac{P(\mathbf{F} \mid c_k)P(c_k)}{P(\mathbf{F})}$$

The classification problem becomes simple when $P(c_k|F)$ is known; as discussed in [10], [25], and [26] the document with feature vector **F** is assigned to the class with the highest conditional probability value, c*:

$$c^* = \arg\max_{c_k \in C}\left[\frac{P(\mathbf{F} \mid c_k)P(c_k)}{P(\mathbf{F})}\right]$$

The P(**F**) term does not change between classes, which allows us to omit it from the argmax term, simplifying the above formula to:

$$c^* = \arg\max_{c_k \in C} \left[P(\mathbf{F} \mid c_k) P(c_k) \right]$$

In a standard authorship attribution problem, that conditional probability is not known and must be estimated from the data and Bayes' rule. One assumption we make in using naïve Bayes is that the occurrence of any one feature f_j is independent of any other feature $f_{j'}$ in a document of class c_k. Thus, the distribution of the feature vector over c_k may be modeled as:

$$P(\mathbf{F} \mid c_k) = \prod_{j=1}^{d} P(f_j \mid c_k)$$

Combining the two previous formulas gives the following:

$$c^* = \arg\max_{c_k \in C} \left[P(c_k) \prod_{j=1}^{d} P(f_j \mid c_k) \right]$$

The product operation applied to probabilities can cause the above equation to yield very small values for c*. This is a particular concern when working with n-gram features, as the probability values of some n-grams over a large amount of text may be very small to start with. Changing the product term to a sum of logarithms term can prevent numeric underflow:

$$c^* = \arg\max_{c_k \in C} \left[\log P(c_k) + \sum_{j=1}^{d} \log P(f_j \mid c_k) \right]$$

The P(c_k) term reflects the prior probability of the class occurring in the data set. This is typically modeled in one of two ways: as a uniform distribution of classes, or as the actual proportion of the count of the class in the training data. A training set containing equal occurrences of four classes gives a prior probability of 0.25. One in which half the class occurrences belong to c_1 gives that class a prior probability of 0.5. Thus the balance of classes in the training data affects the naïve Bayes classifier result.

2. Smoothing

The naïve Bayes classifier builds a probabilistic model of a class based on training data from that class. A problem arises when the test data contains features that the model has not seen in training. These zero counts have a zero probability, leaving the naïve Bayes classifier unable to predict a class. Smoothing, the process of shifting probability mass from frequently appearing features to zero count features while retaining their relative influence on the classifier, mitigates this problem. Two smoothing techniques, Laplace and Witten-Bell, are discussed here.

a. Laplace Smoothing

A simple algorithm, Laplace smoothing adds a value of 1 to each feature count in the data set, both test and training. This prevents a zero probability situation by ensuring every feature has a probability of occurring based on at least a single count, even if it does not appear in the training data. Adding to the feature counts requires a similar adjustment in the normalization step. If N is the total count of all tokens in the data set and V is the count of unique tokens, or types, a total of V is added to the individual counts by adding 1 to each [26]. The normalization must also be adjusted by V for a Laplace probability formula for a term:

$$P_{Laplace}(t_i) = \frac{c_i + 1}{N + V}$$

b. Witten-Bell Smoothing

Instead of altering the count of all features in the data set, Witten-Bell uses the probabilities of the features occurring in the training set to estimate the probability of an unseen feature. As the training set is processed, the probability that the next token will be of type i is given by [27]:

$$P_{W-B}(t_i) = \frac{c_i}{n + v}$$

where n is the number of tokens seen so far and v is the number of types seen so far. The total probability of an unseen type occurring next is based on the fact that it has already occurred v times in the training set and given by [27]:

$$P_{W-B}(t_{novel}) = \frac{v}{n + v}$$

3. Combining Classifiers

A classifier for detecting a device to user binding must derive information from both the user and the device. In this research, the user is modeled by their short message writing style and the device is modeled by signal characteristics. The variety of features used makes it mathematically difficult to simply plug them all into one high-dimensional classifier, though it is possible with appropriate normalization of the data. The fields of biometrics, image analysis, and handwriting analysis also use diverse feature sets for classification of target items. Researchers in these fields have developed methods to combine multiple classifiers, each focusing on a single feature type, into a multimodal classifier system producing accuracy rates superior to those of the individual classifiers used independently.

Design of a multimodal classifier depends on the outputs of the individual input classifiers. When combining single class labels, a majority vote scheme may be used. The class labels output by each component classifier are counted, with the class that collects the most votes selected as the output of the combined classifier [28]. Variants of this system may apply weights, potentially learned, to the inputs to the combined classifier based on a quality metric or require the winning class to have more than a simple majority. Input classifiers providing a set of ranked class labels use a combined classifier that joins the individual sets and re-ranks the labels, selecting the top-ranked label as the output [29].

The input classifiers that generate the greatest amount of classification information provide the probability distribution of the class labels, such as the posterior probabilities produced by a Bayesian classifier. [29] shows how the output probabilities $P_k(C_i|\mathbf{x})$ of several

Bayesian classifiers may be averaged to create posterior probabilities of the combined classifier:

$$P_E(C_i \mid \mathbf{x}) = \frac{1}{K}\sum_{k=1}^{K} P_k(C_i \mid \mathbf{x})$$

where i ranges from 1 to M classes and k from 1 to K classifiers. The class selected by the combined classifier is the one with the maximum value of $P_E(C_i|\mathbf{x})$. A similar method uses the median value of posterior probabilities, as averages can be skewed by large outlier values. The combined posterior priorities become:

$$P_E(C_i \mid \mathbf{x}) = \frac{P_m(C_i \mid \mathbf{x})}{\sum_{i=1}^{M} P_m(C_i \mid \mathbf{x})}$$

where $P_m(C_i|\mathbf{x})$ is the median value of $P_k(C_i|\mathbf{x})$ for the class. These methods provide a simplistic way to combine the output probabilities of Bayesian classifiers, with the median technique providing particularly good results as discussed in the biometric experimentation below.

Bayesian probability theory lends itself to developing classifier combination schemes using the probability distributions output by individual classifiers. [28] provides the derivation of the product and sum rules based on the joint probability distribution $P(x_1,\dots,x_R|C_i)$. Assuming the measurements are statistically independent, the probability distribution becomes the product of all the individual probability values $P(x_k|C_i)$. Applying Bayes' rule and the Bayes classifier decision process yields the product rule where Z is assigned to class C_i if:

$$p^{-(R-1)}(C_i)\prod_{j=1}^{R} P(C_i \mid x_j) = \max_{k=1}^{m} P^{-(R-1)}(C_k)\prod_{j=1}^{R} P(C_k \mid x_j)$$

The sum rule makes the assumption that the posterior probabilities of the individual classifiers will not differ significantly from the prior probabilities. In that situation, the posterior probabilities may be expressed as:

$$P(C_i \mid x_j) = P(C_i)(1+\sigma_{ij})$$

where $\sigma_{ij} << 1$. Substituting this value in the product rule form gives:

$$p^{-(R-1)}(C_i)\prod_{j=1}^{R} P(C_i \mid x_j) = P(C_i)\prod_{j=1}^{R}(1+\sigma_{ij})$$

Expanding the product on the right hand side of the above equation and ignoring the second and higher order terms, as they will approach zero in size, allows us to rewrite the equation as:

$$p^{-(R-1)}(C_i)\prod_{j=1}^{R} P(C_i \mid x_j) = P(C_i) + P(C_i)\sum_{j=1}^{R}\sigma_{ij}$$

The decision rule for the sum method then states that Z is assigned to C_i if:

$$(1-R)P(C_i) + \sum_{j=1}^{R} P(C_i \mid x_j) = \max_{k=1}^{m}\left[(1-R)P(C_k) + \sum_{j=1}^{R} P(C_k \mid x_j)\right]$$

In an experimental comparison of classifier combination methods [28] evaluated three biometric modalities, frontal face image, face profile image, and voice. For 37 users, the face images were trained with three pictures and tested with one. Similarity in facial images was gauged by distance measurements. The voice classifier used Hidden Markov Models to classify utterances of digits from zero to nine. Results for the individual classifiers showed speech provided the best performance with a 1.4% error rate, profile images with 8.5%, and frontal face images with 12.2%. When the results of the three classifiers were combined using the techniques described above, the sum rule provided the best results, with 0.7% error rate. The product rule gave 1.4% and the median rule 1.2%. While the product rule was unable to improve on the best individual classifier, the sum and median rules both yielded better results. The assumptions made by the sum rule, that posterior and prior probabilities will not differ much, are not very realistic, but the insensitivity of the method to estimation errors allows it to yield good accuracy rates. This work shows that combining individual classifiers of different features may improve the results of a multimodal classification problem.

G. EVALUATION CRITERIA

Once the classifier has run, we must have a way to evaluate the results and compare those of different experiments. Standard performance metrics include precision, recall, F-score, and accuracy. [26] and [30] explain these measurements.

Precision measures the proportion of documents correctly classified as belonging to a particular class, or the number of documents correctly labeled as a class divided by the total documents labeled as that class.

Recall measures the proportion of documents belonging to a particular class that the classifier actually identified, or the number of documents correctly labeled as a class divided by the total number of those documents in the data set. The formulas for precision and recall follow:

$$precision = \frac{TP}{TP + FP}$$

$$recall = \frac{TP}{TP + FN}$$

Where TP is a true positive, the number of documents correctly assigned to a class. FP is a false positive, the number of documents incorrectly assigned to a class. FN is a false negative, the number of documents of one class identified as a member of another class.

The F-score combines these two measures into one metric balanced so that neither one affects the result more than the other. This prevents the experimenter from making design adjustments that favor one measure or another. F-score is the harmonic mean of the precision and recall:

$$F = \frac{2}{\frac{1}{P} + \frac{1}{R}}$$

Accuracy is a generalized measure of the performance of the classifier, finding the proportion of documents labeled correctly. It is obtained by dividing the number of correctly classified documents by the total number of documents in the set. While accuracy gives some indication as to the effectiveness of the classifier, precision and recall do a better job of reflecting false negatives. False positives and false negatives are relevant in binary class problems but not in multiclass problems such as the one this research focuses on, meaning accuracy is a useful metric of evaluation.

THIS PAGE INTENTIONALLY LEFT BLANK

III. TECHNIQUES

A. INTRODUCTION

This chapter describes the design and analysis of the experiments conducted over the course of this research. We first explain how the Twitter data was collected and processed to generate the corpus. Then we discuss the authorship attribution analysis of the text data. Next is a description of the signal collection process followed by the device identification analysis of the signal data. Last, we detail the machine learning classifier combination scheme and analysis.

B. CORPUS GENERATION

1. Twitter Streaming

The text data for this research was collected from Twitter's public streaming Application Programming Interface (API). This interface allows users to write programs to collect and filter Twitter status updates, to include replies to other tweets, a user mentioned by another user, and direct messages, created by a non-protected public account. A Twitter account is required to access the streaming API. To initiate a connection to the Streaming API, the client forms an HTTP request to a Twitter server. Once the connection is established, the client consumes the resulting stream indefinitely. Closure of the connection may be initiated by the user, or because of duplicate log-ins, server restarts, lag in the connection due to bandwidth or a slow client, or Twitter network maintenance [31].

The streaming feed provides data in extensible markup language (XML) or JavaScript object notation (JSON) format. The stream can be filtered by any of the keys in the data structure, to include user ID, keyword, or geographic location. Twitter offers a service called Firehose, which delivers all public status update data for a fee. The free sample feed from the basic streaming API randomly samples 1% of the Firehose stream. The exception is when conducting a following filter on a user ID, which has the effect of "following" that user, capturing all status updates associated with him [31].

2. Text Data Collection and Processing

To build a representative, real-world, short-text messaging corpus, we collected the basic Twitter sample feed on a near-daily basis from June 16, 2010 to August 26, 2010. Collection of the feed occurred during weekdays and some nights and weekends. Any tweets in the stream flagged as retweets were removed in order to prevent associating text not written by a user with that user. The tweets were sorted into files by user ID. We manually discarded users with fewer than ten tweets, users that did not tweet in English, and users with tweets that appeared to be spam, news headlines, or overly repetitive. A goal of 50 users with over 500 tweets per user was set to provide a robust text corpus that would also allow comparison to the Twitter text analysis in [3]. From the group of "good" users, we selected the 53 most prolific and conducted further collection from November 8, 2010, to December 17, 2010, using the follow feed to obtain all tweets sent by, to, or referencing those users. Out of the 53, we were able to obtain 50 authors active enough to meet our tweet quantity goal.

The initial sample feed collection resulted in 4045 tweets by 53 users. The follow feed collection boosted this value to 114,000 tweets. The tweets were processed to remove @names and #tags from the text and throw out any tweets with fewer than three words. Those short tweets tended to consist of emoticons or brief comments of approval, amusement, disgust, or other expressions. Removing the short tweets changes the total tweet count to 97,090. Table 1 provides the total tweets and maximum, minimum, and median tweets per author for each collection run and following processing.

Table 1. Collection Quantities

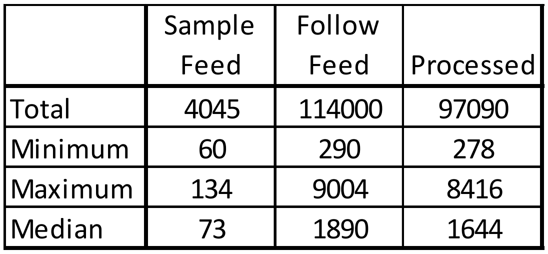

	Sample Feed	Follow Feed	Processed
Total	4045	114000	97090
Minimum	60	290	278
Maximum	134	9004	8416
Median	73	1890	1644

The next step in data preparation was to split the tweets into files by author. Each tweet constituted one line in the author file. To provide anonymity, the files were labeled with a randomly selected number code instead of the user ID. A line-by-line random shuffle was applied to each file to randomize the order of tweets. For the first set of experiments, the first 230 tweets of each file were taken as the text data set. As one tweet contains very little feature count information to build a profile, we tried combining several tweets into one document to represent the author. The 230 tweets were divided into ten documents of 23 tweets each to serve as the training set. In another set of experiments each document contained only one tweet, for a training set of 230 documents. This treats each utterance independently in the subsequent classification process. A third experiment used 120 tweets from each author with one tweet per document in order to compare results with those in [3]. The text files were shuffled prior to extracting the 120 tweets, generating a different text set than the 230 tweet set. Other experiments were conducted with varying tweet quantities and training set sizes, which are explained in the Results section of this thesis.

C. AUTHORSHIP ATTRIBUTION PROCESS

Figure 8 shows a flowchart of the text processing and classification process.

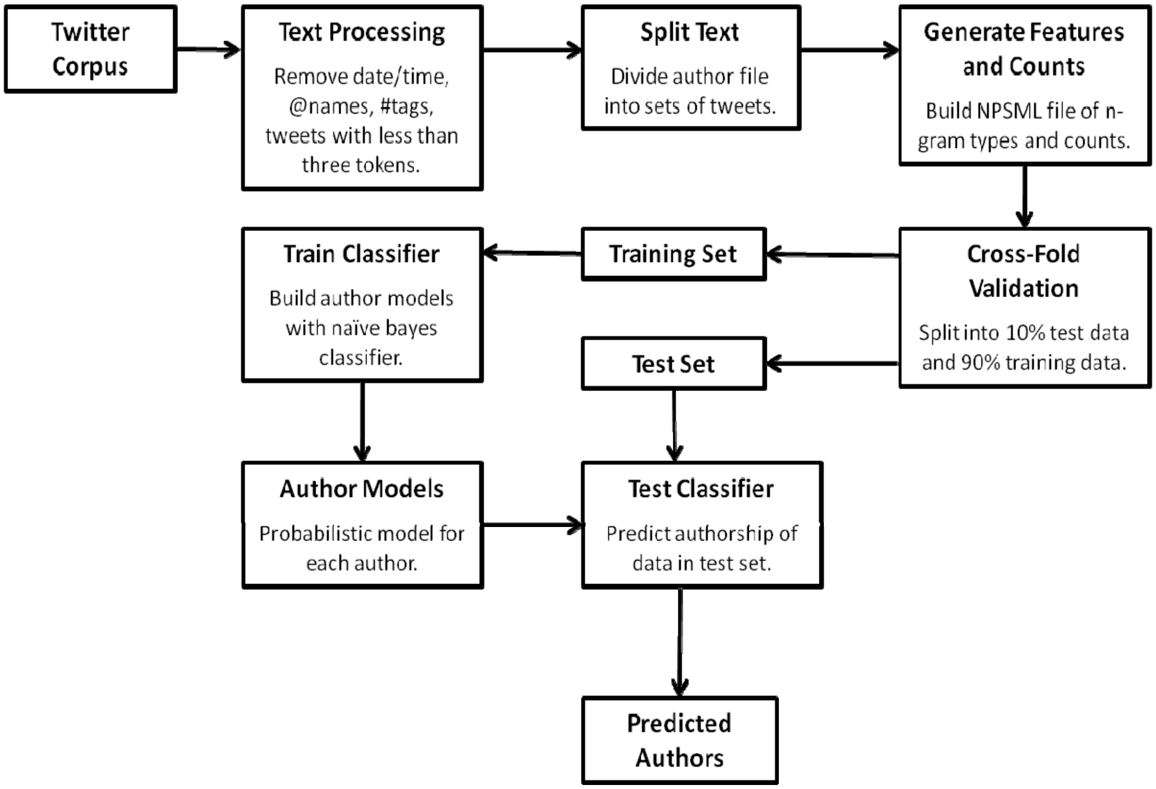
Twitter Corpus
Text Processing
Remove date/time, @names, #tags, tweets with less than three tokens.
Split Text
Divide author file into sets of tweets.
Generate Features and Counts
Build NPSML file of n-gram types and counts.
Cross-Fold Validation
Split into 10% test data and 90% training data.
Training Set
Test Set
Train Classifier
Build author models with naïve bayes classifier.
Author Models
Probabilistic model for each author.
Test Classifier
Predict authorship of data in test set.
Predicted Authors

Figure 8. Naïve Bayes Classification Process

1. Feature Extraction

From the data set, we derive the features used for classification. As explained in the previous chapter, character n-grams tolerate noise well and capture an author’s style and punctuation use, all important in classifying short messages like Twitter. This experimentation broke each tweet into character 2-, 3-, 4-, 5-, and 6-grams. The start and end of each post was indicated by a “_” character appended to the first and last character in the post to provide information on the placement of the n-gram. The “_” character also represented white space. Any capitalization or misspellings were preserved. Table 2 shows the top five n-grams and their counts for each value of n in the entire corpus.

Table 2. Top Five n-grams

2-gram	count	3-gram	count	4-gram	count	5-gram	count	6-gram	count
e_	131034	_th	53687	_the	29704	_the_	19574	_that_	7466
t_	99995	the	33572	_you	21952	_you_	13674	_like_	6282
_t	97549	ing	27566	ing_	21798	_that	10328	_just_	4910
s_	72470	he_	26976	the_	20004	_and_	9700	_have_	4856
th	68538	_to	26260	_to_	19066	that_	7732	_with_	3762

The n-grams are conceptually generated using a sliding window of size n moving over the utterance, recording and counting each n-character token. All punctuation marks and white spaces are included as characters. A software program parses each tweet and records the n-grams and counts associated with each author, saving them in a file in the NPSML format, one file for each value of n. NPSML format is shown in Figure 9. The key field was the name of the file from which the feature labels and counts were derived. All weights were set to 1.0 for all files. The class field was set to the identifier code of the author of the utterance.

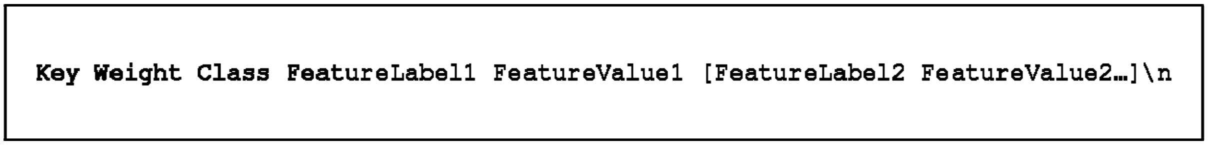

```
Key Weight Class FeatureLabel1 FeatureValue1 [FeatureLabel2 FeatureValue2…]\n
```

Figure 9. NPSML Format

Prior to running the classifier, we must split the feature count files into test and training sets. An internal line shuffle program randomized the order of the posts in the feature count files. A ten-fold cross validation was applied, in which a feature count file was split into ten subfiles, with nine used for training the classifier and one used for testing it. The nps-bTTSplit software program from the NPS Machine Learning Library [32] was used to generate the test and train files, ensuring each author was represented with an equal number of posts in each of the subfiles. None of the posts used in a training file were also used in the associated test file.

2. Naïve Bayes Classifier

This experimentation used the Naval Postgraduate School Natural Language Processing Lab naïve Bayes classification package. This software package uses the NPSML file format as input. The learning portion uses the smoothed feature counts from the input training data file to generate a probabilistic model. One set of experiments was conducted using Laplace add-one smoothing. A second set was conducted using Witten-Bell smoothing. The classification program used the model generated by the learning program and the NPSML-formatted test data to determine the most probable class assignment for each test utterance. The program output the key and predicted class for each utterance in the test file. Each fold of the 10-fold cross validation was run and the outputs averaged for the final classification result. As each author has an equal number of tweets in the data set, prior probabilities for each author were fixed and equal.

D. PATTERN OF LIFE ANALYSIS

Human beings often fall into habitual daily routines. The act of communicating with others may fit into this routine, allowing an observer to discern a pattern. A user may log into his computer at the same time every weekday morning, or call his mother to chat during his commute home every evening. Analyzing a user’s communication patterns may aid in the identification of the user.

1. Twitter Time Analysis

Each tweet collected includes a date/time field. Figure 10 shows the format of the date/time field. This analysis focused on a simple pattern analysis of send time by hour of the day. This may capture any user patterns centered on a work or school schedule.

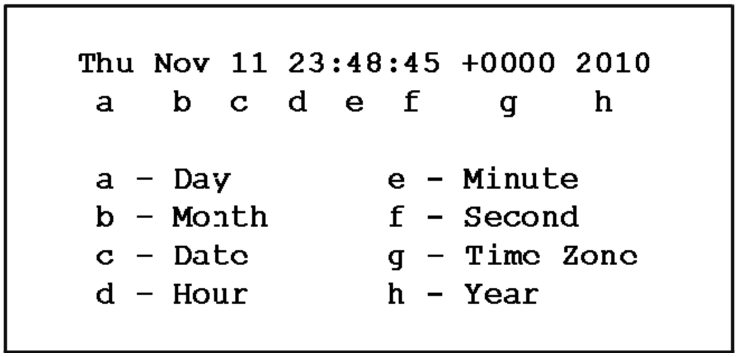

```
Thu Nov 11 23:48:45 +0000 2010
 a   b  c  d  e  f    g    h

 a - Day        e - Minute
 b - Month      f - Second
 c - Date       g - Time Zone
 d - Hour       h - Year
```

Figure 10. Date/Time Field Format

The date/time fields were stripped from each tweet and saved in a separate file for each user. A line-by-line shuffle program randomized the order of the timestamps. The first 120 were taken from each author file as a sample set. This sample set was then subdivided, grouping timestamps into files labeled with the author as the class. We used training set sizes of three, five, ten, and twelve for testing. The files were processed into the NPSML format with the sent hours and their counts as the keys and values contained in each file. The NPSML files were processed in the same manner as the text files. The hours and counts were divided into test and training groups, holding out 10% as a test set. The naïve Bayes learning and classify programs were run on a 10-fold cross validation using Witten-Bell smoothing and the results averaged to determine the final output class for each test input. Other experiments were conducted with varying timestamp quantities and training set sizes, which are explained in the Results section of this thesis.

2. Social Network Analysis

Another characteristic of an individual’s communication patterns is the group of people with whom he communicates. In a telephone or SMS network, discerning this would require some access to signaling information or service provider records. In Twitter, users often include the screen name of the user they are specifically speaking to or about in their tweet. Layton et al. noted a 26% reduction in the accuracy of their authorship attribution method when screen names were removed from the tweets. For a simple social network analysis, we examined the screen names referenced by the users in our corpus independent of the text of their tweets.

The data processing used to conduct the social network analysis was identical to the date analysis. Instead of pulling the date/time field out of each tweet, any @name found in parsing was saved to a file by author. The shuffling, splitting, and grouping into training sets was conducted using sets of three, six, ten, and twelve out of 120 @names per author. NPSML files of @names and their counts per author were built. These were divided into test and train sets, and naïve Bayes learning and classification with Witten-Bell smoothing was performed on a 10-fold cross validation with the results averaged to give final output classes for each input.

E. CELL PHONE SIGNAL ANALYSIS

Based on the success of [4], we focused on signal modulation features to build device characteristic vectors. GSM modulation parameters are governed by the European Telecommunications Standards Institute (ETSI) in their 3rd Generation Partnership Project (3GPP) standards [33], [34]. Cell phone manufacturers test their products for quality assurance purposes, ensuring phone users have an acceptable link quality and that phones do not interfere with other users. Three signal characteristics that are measured and controlled are peak phase error, root mean square (RMS) phase error, and frequency error. The Agilent 8922S GSM Test Set is a signal analyzer geared for measuring these standard modulation characteristics of a GSM mobile station.

1. Signal Collection

The equipment used in conducting the mobile station signal measurements was the Agilent 8922S GSM Test Set, the LGS Innovations Tactical Base Station Router (TacBSR), and an assortment of unlocked GSM-capable cell phones. The 8922S was run in test mode with small whip antenna serving as the RF input element. The use of an antenna required adjustment of the expected input amplitude decibel value. This varied by phone and was set based on Test Set measurements of the phone output power and the presence or absence of RF overload errors. Figure 11 shows the cell control screen where these values were set.

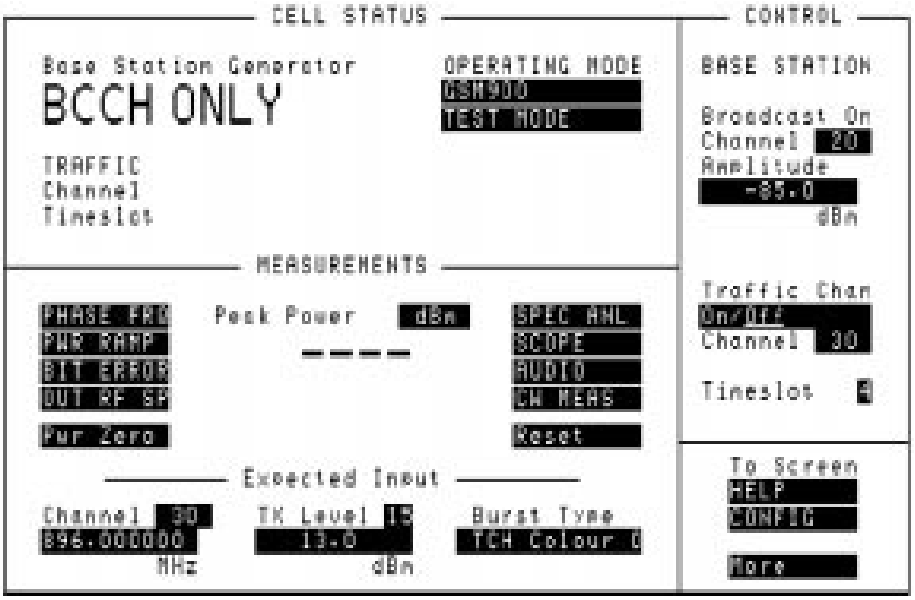

CELL STATUS

Base Station Generator
BCCH ONLY

OPERATING MODE
GSM900
TEST MODE

TRAFFIC
Channel
Timeslot

CONTROL

BASE STATION
Broadcast On
Channel 20
Amplitude -85.0 dBm

Traffic Chan
On/Off
Channel 30
Timeslot 4

MEASUREMENTS

Peak Power dBm

Expected Input

Channel 30
896.000000 MHz

TX Level 15
13.0 dBm

Burst Type
TCH Colour 0

Figure 11. Cell Control Screen (From [35])

In test mode, the 8922S transmits a GSM broadcast signal on a specified frequency channel, or absolute radio frequency channel number (ARFCN). It has a separate ARFCN designated for the traffic channel the phone will use to communicate with the BTS. Our phones could not connect to the 8922S as a BTS with the antenna and SIM cards we had available for use, so we used the TacBSR as the BTS. The TacBSR was configured to operate in the E-GSM900 spectrum using ARFCN 875 as the traffic channel. This correlates to an uplink frequency of 882.2 MHz. The 8922S was configured as a midpoint collector listening to ARFCN 875. All the phones we tested operated in this GSM band.

Besides the amplitude of the input, two other settings required adjustment before taking measurements, the traffic channel timeslot and the trigger delay. When setting up a call with the TacBSR, we noted the calling phone was assigned timeslot 2 and the called phone was assigned timeslot 3. To establish a traffic channel for measurement, we had to establish a voice call between two phones. The calling phone was noted and proper traffic channels were set when conducting measurements. The trigger delay sets the time delay between a valid trigger event and the beginning of a measurement. The 8922S uses the midamble of a GSM frame as a trigger, as it is easy to detect. The Data Bits screen of the Phase/Frequency page shows the bit sequence of the GSM frame, highlighting the midamble. Figure 12 shows an example of this screen. The trigger timing was set by observing the value of the First Bit field and adjusting the trigger delay to force that value close to zero.

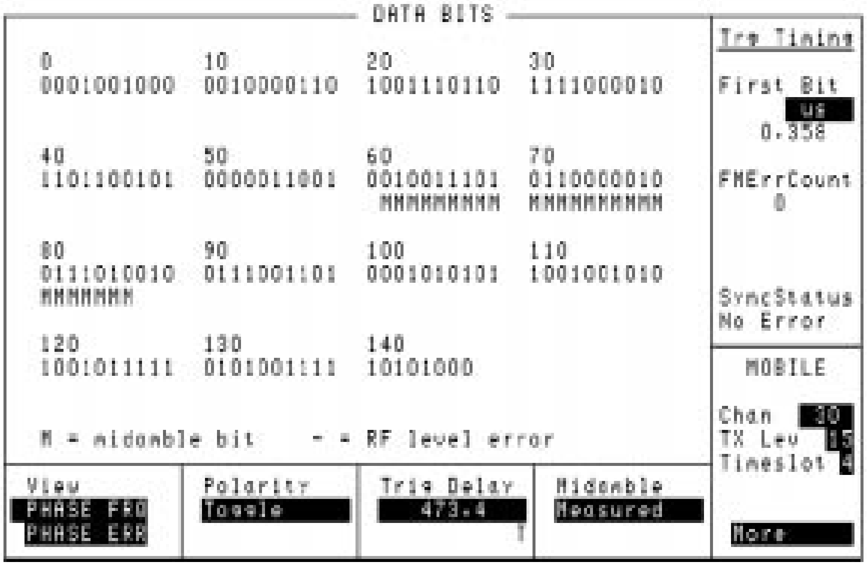

```
                         DATA BITS                               Trg Timing
0            10           20           30
0001001000   0010000110   1001110110   1111000010              First Bit
                                                                       uS
40           50           60           70                        0.358
1101100101   0000011001   0010011101   0110000010
                           MMMMMMMMM   MMMMMMMMMM              FMErrCount
80           90           100          110                        0
0111010010   0111001101   0001010101   1001001010
MMMMMMM                                                        SyncStatus
                                                               No Error
120          130          140
1001011111   0101001111   10101000                               MOBILE

M = midamble bit     - = RF level error                        Chan      30
                                                               TX Lev    15
View          Polarity      Trig Delay     Midamble            Timeslot   4
 PHASE FRQ    Toggle          473.4        Measured
 PHASE ERR                        ↑                            More
```

Figure 12. Data Bits Screen (From [35])

Once the amplitude, timeslot, and trigger delay were set, we measured the three modulation characteristics. A more detailed explanation of the modulation measurements is included in Appendix A. This was done from the Phase/Frequency page, shown in Figure 13. To get an average value over a fixed number of transmission bursts for each measurement, we used the multi-burst feature for ten bursts. The measured phone was held near the antenna of the 8922S, while the phone on the other end of the call was placed across the room to minimize cross-channel interference. We collected 30 values for peak phase, RMS phase, and frequency error as averaged over 10 transmission bursts. The values were read from the screen and recorded.

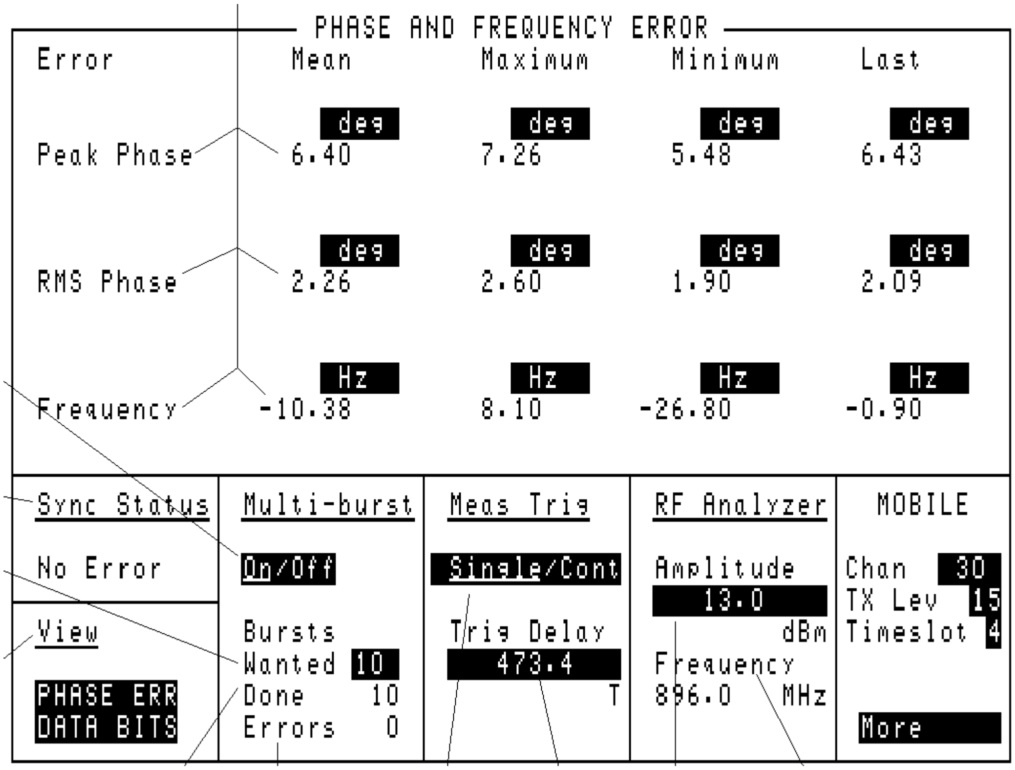

PHASE AND FREQUENCY ERROR

Error	Mean	Maximum	Minimum	Last
Peak Phase	deg 6.40	deg 7.26	deg 5.48	deg 6.43
RMS Phase	deg 2.26	deg 2.60	deg 1.90	deg 2.09
Frequency	Hz -10.38	Hz 8.10	Hz -26.80	Hz -0.90

Sync Status
No Error

View
PHASE ERR
DATA BITS

Multi-burst
On/Off
Bursts
Wanted 10
Done 10
Errors 0

Meas Trig
Single/Cont
Trig Delay
473.4
T

RF Analyzer
Amplitude
13.0
dBm
Frequency
896.0 MHz

MOBILE
Chan 30
TX Lev 15
Timeslot 4
More

Figure 13. Phase and Frequency Error Screen (Multi-burst on)(From [35])

The data collection method for the cell phone features was sufficiently time and labor intensive that we used the 30 data samples of each feature from each phone as the foundation for building a larger data set. The measured values of each feature were input into a program that built a probability density function based on a histogram of the results. The program smoothed the samples by building a histogram, and then used the scipy gaussian_kde module to create the probability density function. It then drew a specified number of random values weighted by the probability density [36]. We used this method to generate 160 more values representative of each handset.

2. Data Analysis and Classification

The modulation characteristic data required some preprocessing before use as an identification vector. An average and standard deviation value was calculated for each characteristic for each phone. The smallest standard deviation value of each feature was used as a bin size, and the raw data was binned, generating histograms for each phone. For example, if the standard deviation of the frequency error for phone 1 was 8.2, phone 2 was 9.5, and phone 3 was 7.3, the bin size for frequency error for the three phones would be 7.3. Binning the data reduced noise from the measurement process and discretized values from continuous domains to aid in feature counting for the classification step. Each set of {peak phase error, RMS phase error, frequency error} bin values for each collection data point served as a feature vector for the phone it was associated with.

For learning and classification, the feature vectors were split into separate files. As with the time and name analysis, we experimented with varying the size of the training set. A software program turned each set of files into an NPSML-formatted file of features and their counts. The NPSML files were provided as input to the NPS naive Bayes learning and classifying programs. The average results of a 10-fold cross validation were given as the output classes. We conducted experiments with varying numbers of feature vectors and document sizes, which are explained further in the next chapter of this thesis.

F. COMBINING CLASSIFIERS

Once the individual classification results were obtained, we experimented with combining these results to see if there was any subsequent improvement in accuracy. The NPS nb-classify program can provide as its output the logarithms of the probabilities for each class label. Based on the availability of that information and the prior work described in the previous chapter, we chose the sum rule combination scheme. The sum rule takes the probability outputs of a set of classifiers and adds the probability values of each class label. The class label with the maximum summed value is selected as the output label.

In the first set of experiments, one phone was assigned to one author. The output probability logarithms for each class label from the phone classifier were added to the output probability logarithms of the text classifier. The maximum combined value of each classification test was taken as the result. We conducted

20 experiments rotating the author assignment for each phone to verify the consistency of results across phone-author pairings. The accuracy results for each pairing were averaged to obtain the overall accuracy. Appendix E contains the phone-author pairing matrix.

To mitigate the influence of the differences in magnitudes of the text and device probability logarithms on the summation result, these values were normalized across the individual classes for each classifier output. The normalized output of the signal classifier for a particular phone was added to the normalized output of the text classifier for its associated author. The experimentation process was repeated on these values. The pattern of life classifier results were included in another set of experiments, adding the output values to the text and device output values to attain a combined output value.

Another experiment was conducted to gauge the effectiveness of the combined classifier at detecting a change of author on a single phone. Using the same set of 20 authors and phones as above, the tweet text set was modified to simulate a change of author. We chose two of the 20 authors to swap. Out of the 50 tweet per author data set, 10 tweets from each of the two authors were labeled as the other author. The labeling scheme included a flag so that we could identify the modified tweets after classification. The modified test set was classified using the classifier model trained previously. None of the tweets in the test data had been part of the training model. The results were normalized and added to the normalized phone classifier results. The results of the combined classifier were examined to determine if the modified tweets were detected and appropriately classified. This process was repeated using the 120 tweet per author data set with a training set size of five. In this case, 25 tweets from each of the two authors were labeled as the other author.

THIS PAGE INTENTIONALLY LEFT BLANK

IV. RESULTS AND ANALYSIS

A. TEXT RESULTS

This section examines the authorship attribution results from classification of the Twitter text corpus. We first present the effects of varying the size of the character n-gram in the feature set and the type of smoothing used. As 140 characters or less do not contain much feature information to make a profile, we experiment with combining several individual tweets from one author into a “document”, increasing the total word count of the experimental unit of analysis by using a set of multiple tweets rather than just one tweet, then training the classifier and testing with these “documents”. We experiment with classifying data sets consisting of different total quantities of tweets per author, combining these tweets into documents of varying tweet count. We then test the effect on classifier accuracy of changing the number of authors and the total number of tweets per author in the data set.

Analysis of the Twitter text showed that the author could be determined by a naïve Bayes classifier at a rate significantly better than chance. Table 3 shows the accuracy results averaged over a ten-fold cross validation of a multiclass classification of 50 authors using 230 tweets per author with character 2- through 6-grams as the feature set. Results for LaPlace add-one and Witten-Bell smoothing are presented. These smoothing techniques are explained in more detail in Chapter II, Section F. As expected, the Witten-Bell smoothing performed better than the add-one smoothing.

Table 3. Classification Accuracy Results for 50 Authors With 230 Tweets Per Author

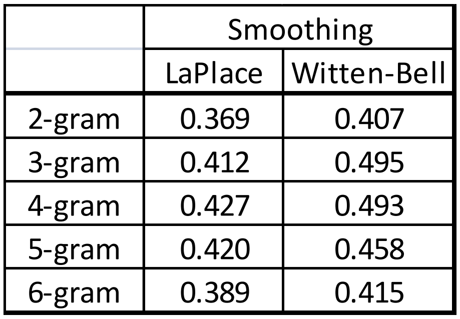

	Smoothing	
	LaPlace	Witten-Bell
2-gram	0.369	0.407
3-gram	0.412	0.495
4-gram	0.427	0.493
5-gram	0.420	0.458
6-gram	0.389	0.415

In order to compare our results to those published in [3], we performed the same analysis using 120 tweets per author. The SCAP method shows better results than our classifier. Table 4 shows our accuracy results compared to their results when their @name and #tag removal preprocessor is applied.

Table 4. Classification Accuracy Results for 50 Authors With 120 Tweets Per Author With Comparison to SCAP Method

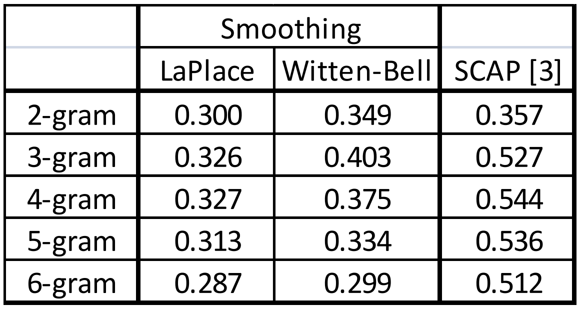

	Smoothing		
	LaPlace	Witten-Bell	SCAP [3]
2-gram	0.300	0.349	0.357
3-gram	0.326	0.403	0.527
4-gram	0.327	0.375	0.544
5-gram	0.313	0.334	0.536
6-gram	0.287	0.299	0.512

The results presented thus far use a single tweet as a document for classification purposes. Combining multiple tweets in a document and using a set of these documents to build the feature and count values for the training and test inputs to the classifier improves the accuracy results significantly. Table 5 shows the accuracy results of the classifier averaged over the ten-fold cross validation for 50 authors with 230 total tweets per author divided into ten documents of 23 tweets each, a value determined empirically to provide the best accuracy results as described next.

Table 5. Classification Accuracy Results for 50 Authors With 230 Tweets per Author Combined into Documents of Size 23 Tweets

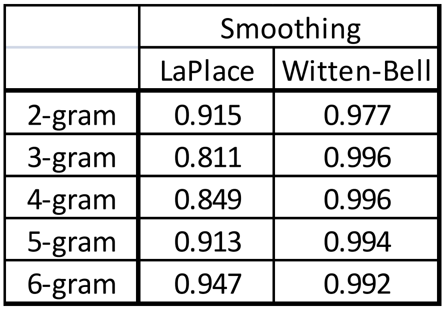

	Smoothing	
	LaPlace	Witten-Bell
2-gram	0.915	0.977
3-gram	0.811	0.996
4-gram	0.849	0.996
5-gram	0.913	0.994
6-gram	0.947	0.992

Grouping multiple tweets into a document improves the accuracy of the classifier significantly. As the character 3-gram feature and Witten-Bell smoothing process provided the best results in early testing, we continued further testing with those parameters fixed. The next set of tests evaluated the effects of document size, in tweets, on accuracy. To complete the 90%:10% train to test split, a minimum of ten documents are required for classification. We used ten documents with a range of five to 20 tweets per document. Table 6 shows the results of that experiment.

Table 6. Classification Accuracy Results for 50 Authors Using 10 Documents With Increasing Number of Tweets per Document

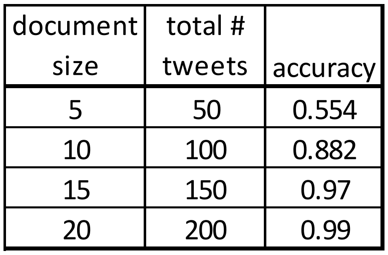

document size	total # tweets	accuracy
5	50	0.554
10	100	0.882
15	150	0.97
20	200	0.99

Fixing the previous experiment at ten documents caused the larger document sizes to use a proportionally larger total number of tweets for classification. To determine whether the accuracy improvement could be attributed to the document size or the total number of tweets in the data set, we conducted another experiment in which we set the total number of tweets at or near 150. In a situation where the available number of messages per author is limited, this distinction is important in designing an accurate classification process. If the use of multi-tweet documents enhances classifier accuracy in a fixed corpus size, acceptable results may be obtained using fewer tweets per author than if tweets are tested individually. The document size was varied from five to 15 tweets per document. The total number of tweets per classification run was the multiple of the document size closest to 150. Figure 14 shows the results of this experiment. The document size range from one to five tweets was examined further, finding the classification accuracy for 50, 100, and 150 tweets across that range. Those results are displayed in Figure 15.

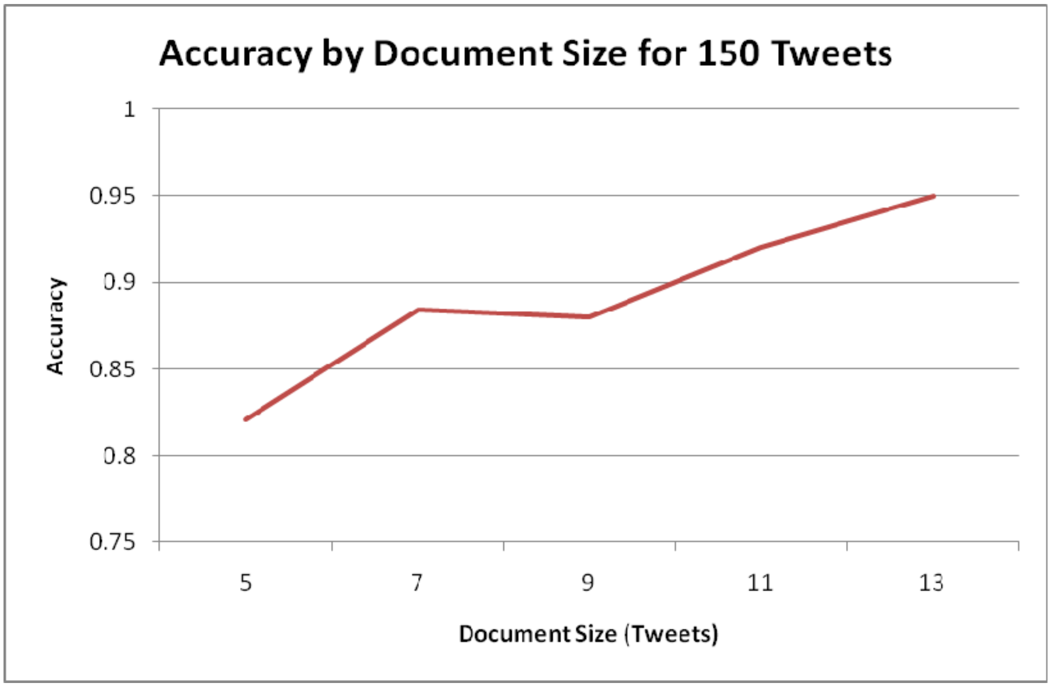

Figure 14. Classification Accuracy for 50 Authors Using 150 Tweets per Author With Increasing Document Size

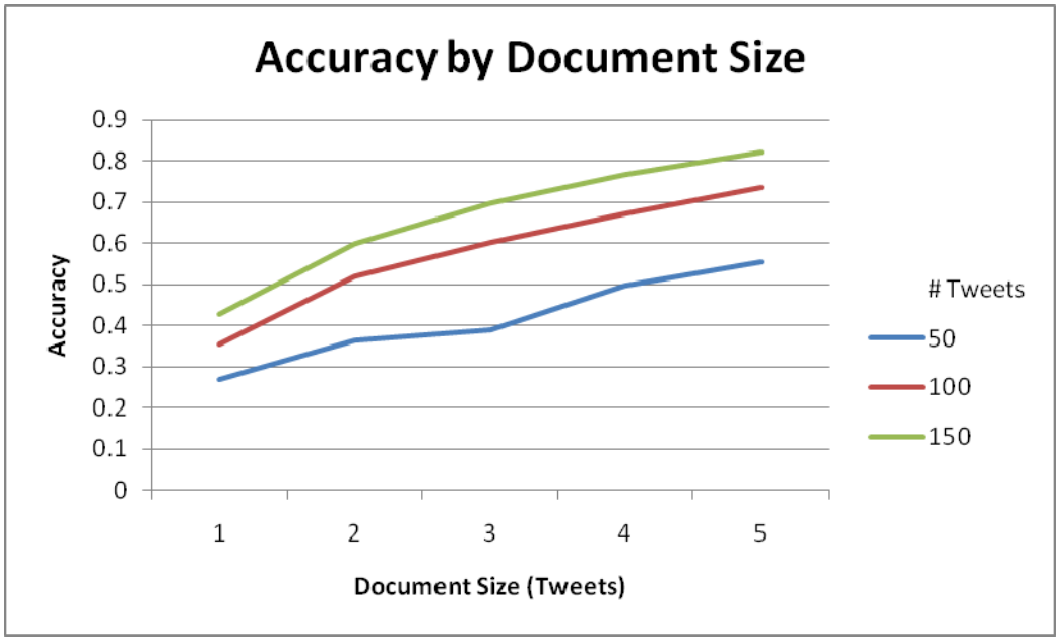

Figure 15. Classification Accuracy for 50 Authors by Document Size and Total Number of Tweets per Author

The effects of changing the number of tweets per author and changing the number of authors were evaluated in more detail. The number of authors in each trial was varied from two to 50, selected randomly from the set of 50 authors. The number of tweets was varied from 30 to 190 with a document size of one tweet. Figures 16 and 17 show graphs of the accuracy results over the range examined. Improvement in accuracy appears to level off at about 22 authors.

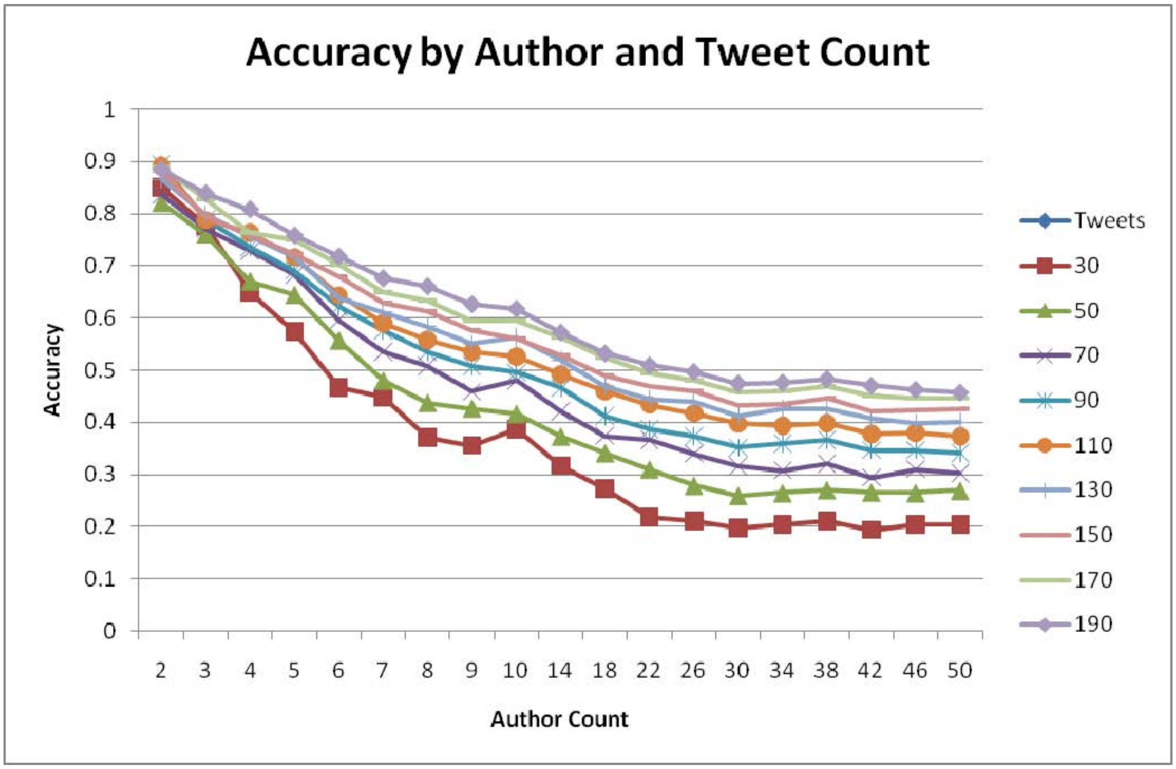

Figure 16. Classification Accuracy Results for Various Total Tweet Values Per Author With Increasing Author Count

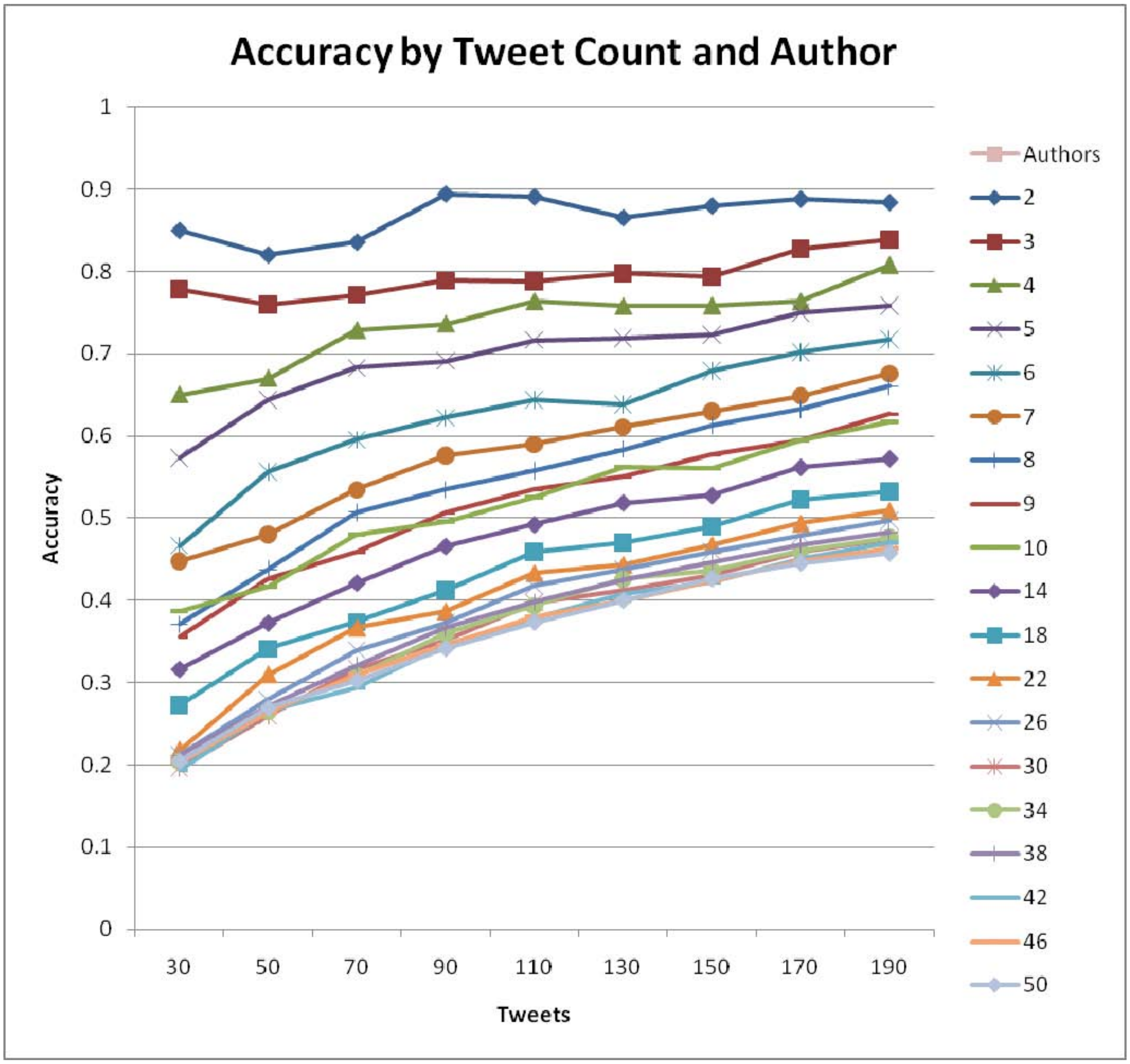

Figure 17. Classification Accuracy Results for Various Author Counts With Increasing Total Tweet Per Author Values

The classification accuracy curve for increasing number of authors in the data set levels out at 20 authors. We conducted further experimentation with a set of 20 authors randomly selected from the 50-author data set. We used total tweet per author values of 30, 50, 100, 120, and 150. The document sizes tested ranged from one to 15 tweets per document. Figures 18 and 19 show the classifier accuracy results averaged over a ten-fold cross validation for 20 authors with varying numbers of tweets per author and tweets per document.

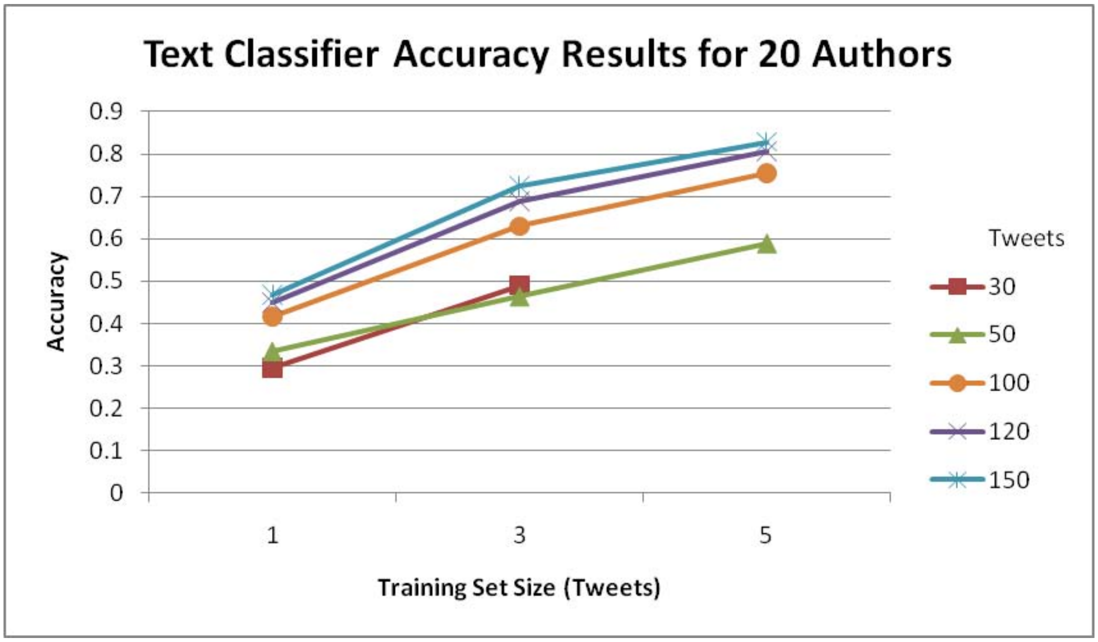

Figure 18. Classification Results for 20 Authors With Varying Values of Tweets per Author and Tweets per Document

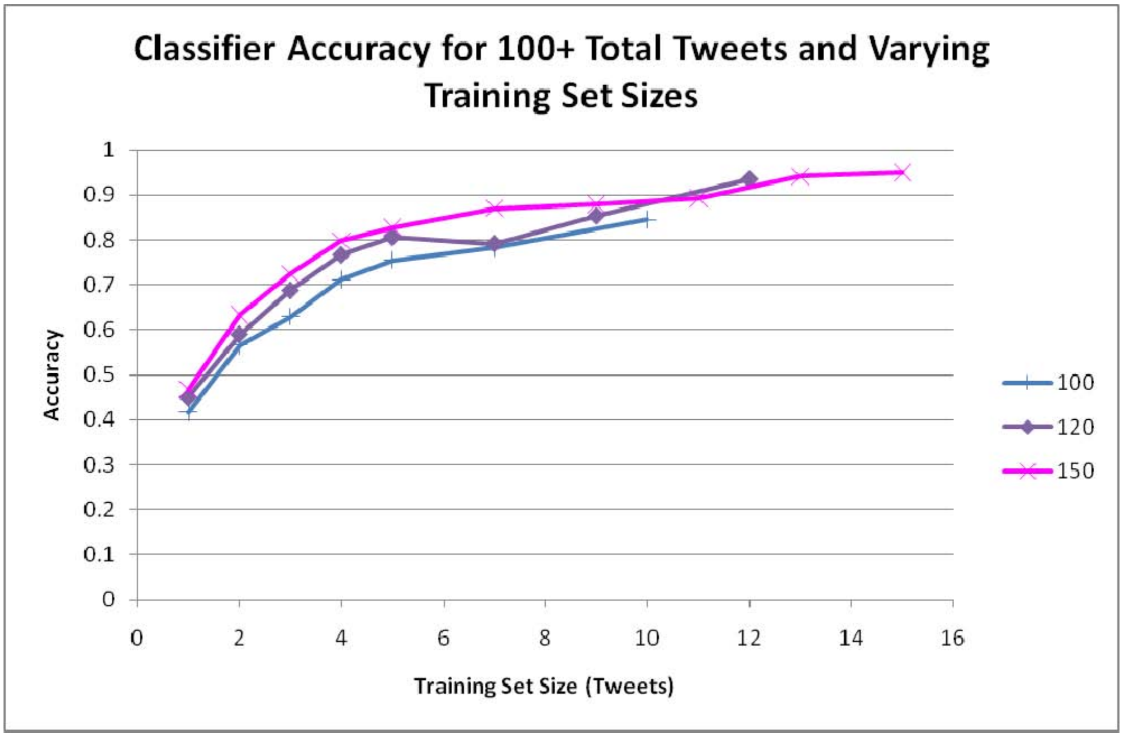

Figure 19. Classification Results for 20 Authors With More Than 100 Tweets per Author and Varying Tweets per Document

We next investigated if the improvement in classification accuracy results generated by combining multiple tweets into a document occurred during the training or the testing of the classifier. Using the set of 20 authors, we took the models built for 50 tweets per author with five tweets per document, 100 tweets per author with five and ten tweets per document, and 120 tweets per author with five and 12 tweets per document and tested a new set of single tweets of the appropriate size on each model. The results of these tests are presented in Table 7. The consistency of the accuracy results implies the added feature depth of the multi-tweet document generates its accuracy benefits during the testing of the classifier rather than the training.

Table 7. Classification Accuracy Results for Single Tweet Documents Tested on Models Trained on Multi-Tweet Documents of the Specified Quantity

Tweets per Author	Document Size Trained On	Accuracy
50	1	0.335
50	5	0.335
100	1	0.417
100	5	0.421
100	10	0.4275
120	1	0.4496
120	5	0.4554
120	12	0.4471

This section presented the results of a series of classification experiments conducted on a Twitter corpus of 50 authors. We found that using character 3-grams as a feature set and Witten-Bell smoothing produced the best accuracy results. Classification accuracy improved as the number of tweets per author increased, reaching 49.5% accuracy at 230 tweets per author, a value based on the smallest author data set in the corpus. Increasing the feature depth of the text by combining multiple tweets into a document and training and testing the classifier with the multi-tweet documents improves classification accuracy significantly, with accuracy levels reaching 90% at ten tweets per document for 120 and 150 tweets per author and 99% at 23 tweets per document for 230 tweets per author. Confusion matrices and per-author accuracy results for the above tests are provided in Appendix B.

B. PATTERN OF LIFE RESULTS

The pattern of life analysis builds a basic description of an author’s tweeting habits by examining the time of day he sends his messages. We use the hour of day the message is sent as the feature used for classification. Like in the text classification process, we try to increase the depth of the feature set by combining the send times of multiple tweets into one training set and using the <feature, count> values of the combined set as the input to the classifier.

Analysis of the hour of day the users tweet showed that the author of a tweet could be determined by a naïve Bayes classifier at an accuracy rate just slightly better than chance. We used the send hour (GMT) of 120 tweets for each author as the time value. As the send time is reported in hour:minute:second format, this serves to bin the times into 24 bins, one per hour. The 120-hour values were split into training sets, similar to grouping multiple tweets into documents as in the previous section. We experimented with training set sizes ranging from one to 12 tweet hours per set. As with the message text, accuracy improved when grouping multiple tweet times into a training set. The training sets are input into the naïve Bayes classifier and trained and tested using Witten-Bell smoothing. Figure 20 shows the classification accuracy results averaged over a ten-fold cross validation for 50 authors with 120 tweet time values per author grouped into training sets ranging in size from one to 12 tweet time values per set.

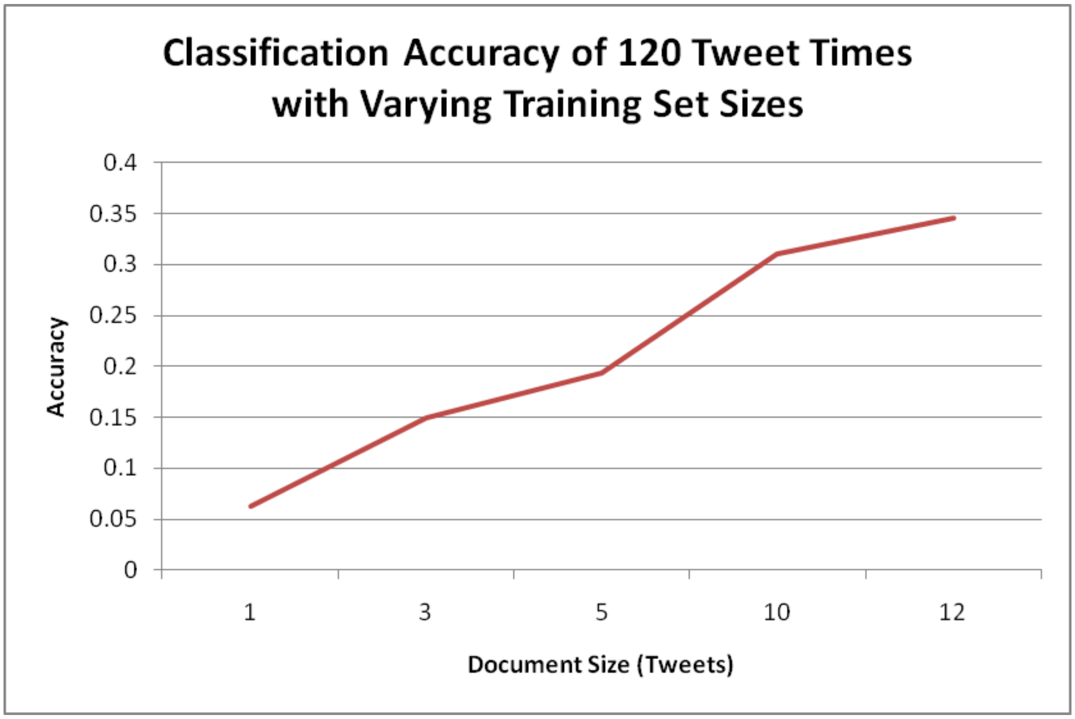

Figure 20. Classification Accuracy for 50 Authors of 120 Tweet Times per Author With Increasing Number of Tweet Times per Training Set

Compared to the text classification results, time of day was not an effective way to discriminate between authors. As the testing focused on English speakers, it is possible that many of the users were located in similar time zones, and thus maintained similar schedules. A few authors could be classified with very good results, with two authors identified at over 60% accuracy over 120 tweets with a training set size of three. Table 8 shows the accuracy result for each author for 120 tweets per author and training set sizes of three, five, ten, and 12 tweet hours per set. Histograms of the tweet send times for each author are presented in Appendix C.

Table 8. Classifier Accuracy Results for Each Author Using 120 Tweet Times per Author and Increasing Number of Tweet Times per Training Set

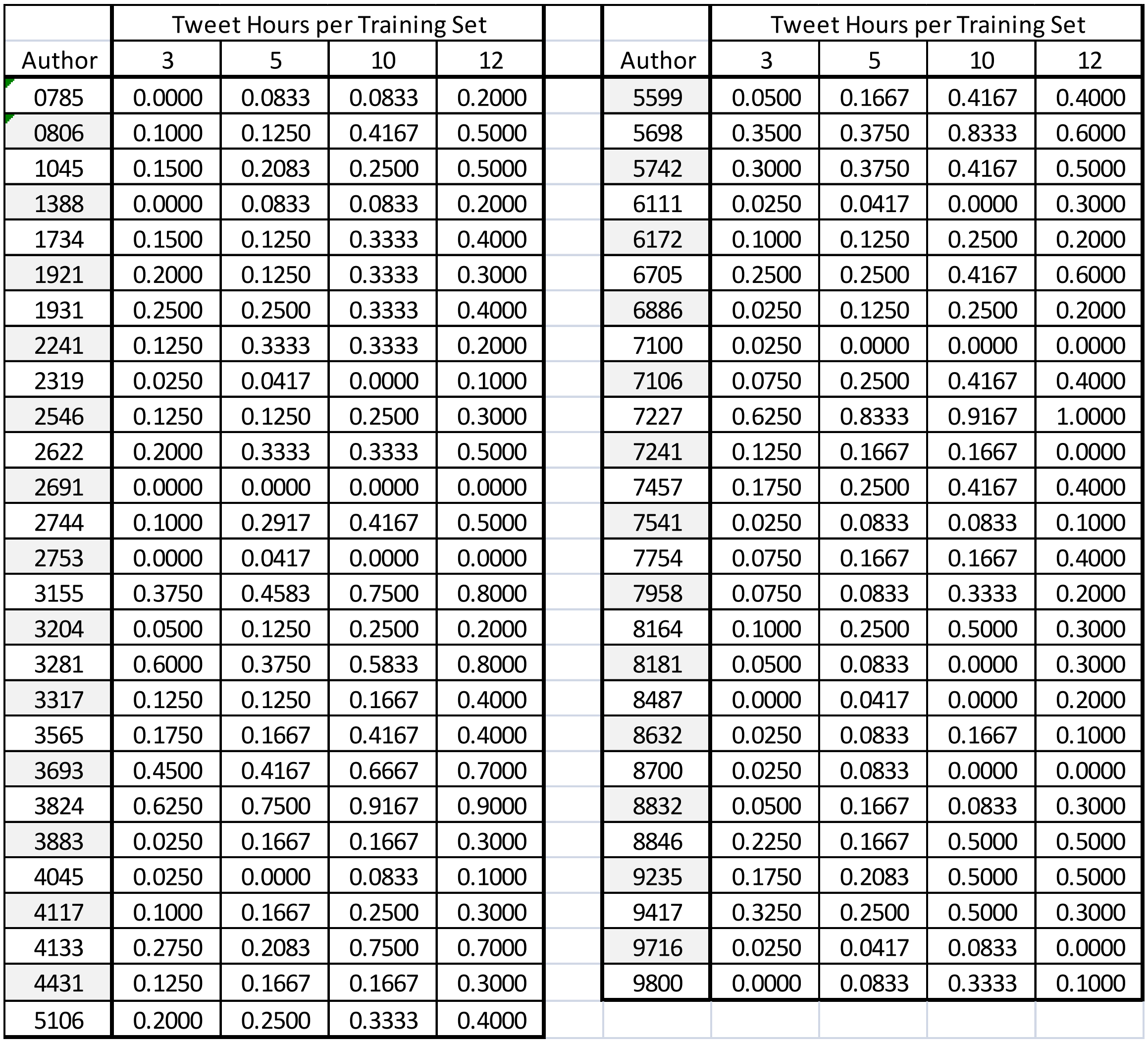

	Tweet Hours per Training Set			
Author	3	5	10	12
0785	0.0000	0.0833	0.0833	0.2000
0806	0.1000	0.1250	0.4167	0.5000
1045	0.1500	0.2083	0.2500	0.5000
1388	0.0000	0.0833	0.0833	0.2000
1734	0.1500	0.1250	0.3333	0.4000
1921	0.2000	0.1250	0.3333	0.3000
1931	0.2500	0.2500	0.3333	0.4000
2241	0.1250	0.3333	0.3333	0.2000
2319	0.0250	0.0417	0.0000	0.1000
2546	0.1250	0.1250	0.2500	0.3000
2622	0.2000	0.3333	0.3333	0.5000
2691	0.0000	0.0000	0.0000	0.0000
2744	0.1000	0.2917	0.4167	0.5000
2753	0.0000	0.0417	0.0000	0.0000
3155	0.3750	0.4583	0.7500	0.8000
3204	0.0500	0.1250	0.2500	0.2000
3281	0.6000	0.3750	0.5833	0.8000
3317	0.1250	0.1250	0.1667	0.4000
3565	0.1750	0.1667	0.4167	0.4000
3693	0.4500	0.4167	0.6667	0.7000
3824	0.6250	0.7500	0.9167	0.9000
3883	0.0250	0.1667	0.1667	0.3000
4045	0.0250	0.0000	0.0833	0.1000
4117	0.1000	0.1667	0.2500	0.3000
4133	0.2750	0.2083	0.7500	0.7000
4431	0.1250	0.1667	0.1667	0.3000
5106	0.2000	0.2500	0.3333	0.4000
5599	0.0500	0.1667	0.4167	0.4000
5698	0.3500	0.3750	0.8333	0.6000
5742	0.3000	0.3750	0.4167	0.5000
6111	0.0250	0.0417	0.0000	0.3000
6172	0.1000	0.1250	0.2500	0.2000
6705	0.2500	0.2500	0.4167	0.6000
6886	0.0250	0.1250	0.2500	0.2000
7100	0.0250	0.0000	0.0000	0.0000
7106	0.0750	0.2500	0.4167	0.4000
7227	0.6250	0.8333	0.9167	1.0000
7241	0.1250	0.1667	0.1667	0.0000
7457	0.1750	0.2500	0.4167	0.4000
7541	0.0250	0.0833	0.0833	0.1000
7754	0.0750	0.1667	0.1667	0.4000
7958	0.0750	0.0833	0.3333	0.2000
8164	0.1000	0.2500	0.5000	0.3000
8181	0.0500	0.0833	0.0000	0.3000
8487	0.0000	0.0417	0.0000	0.2000
8632	0.0250	0.0833	0.1667	0.1000
8700	0.0250	0.0833	0.0000	0.0000
8832	0.0500	0.1667	0.0833	0.3000
8846	0.2250	0.1667	0.5000	0.5000
9235	0.1750	0.2083	0.5000	0.5000
9417	0.3250	0.2500	0.5000	0.3000
9716	0.0250	0.0417	0.0833	0.0000
9800	0.0000	0.0833	0.3333	0.1000

C. SOCIAL NETWORK RESULTS

Analysis of the social network of the authors as determined by the @names referenced in their tweets provided excellent accuracy results. The corpus contained a total of 72,888 references to 6,105 unique @names. The least connected author, gauged by the author’s ratio of

@names to tweets in the corpus, made 1020 @name references in 9004 tweets, while the most connected author made 1570 @name references in 1174 tweets. We extracted the @names from each author’s tweets and selected 120 from each author. The @names were used as the features input to the naïve Bayes classifier using Witten-Bell smoothing. Like the text and time data, we experimented with combining multiple @names into a training set to increase the depth of the experimental unit. Accuracy improved when the @names drawn from multiple tweets were combined into one training set and this training set was used to generate the feature and count data. The averaged results of a ten-fold cross validation classification of 120 @names per author for 50 authors with a training set size ranging from three to 12 @names per set are presented in figure 21.

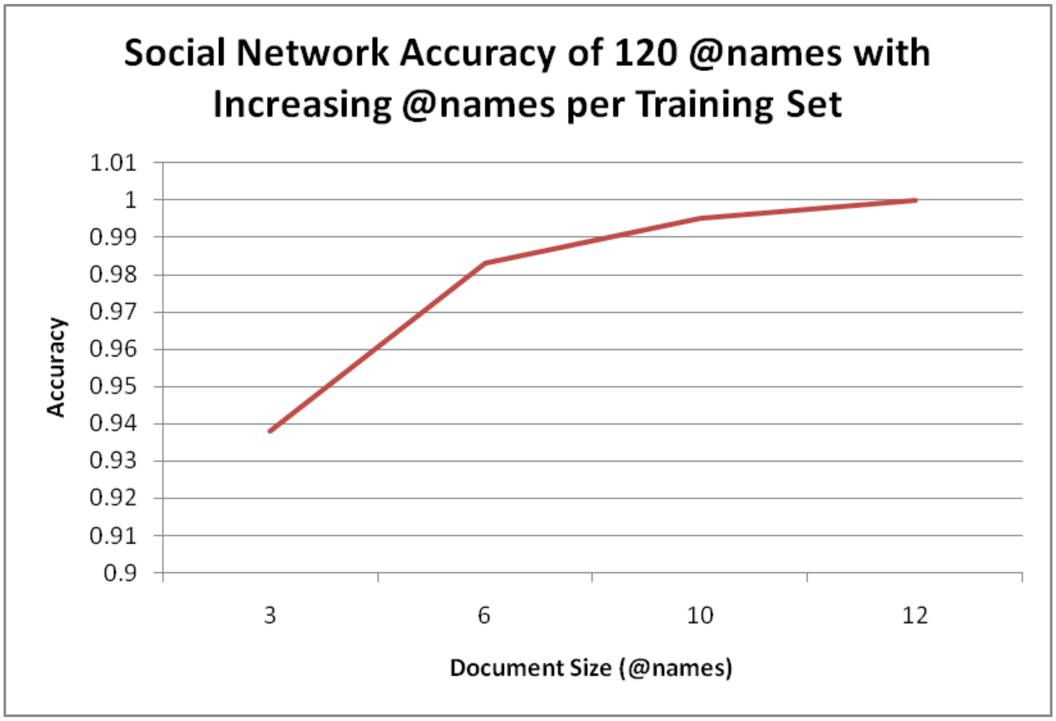

Figure 21. Classification Accuracy Results for Social Network Analysis of 120 @names per Author With Increasing Number of @names per Training Set

The very high classification accuracy rate implies that the authors randomly chosen for this study did not interact with each other or have many common acquaintances. In a practical application, this lack of interconnectivity may not apply. A work group or a criminal cell may have a large number of common nodes in their social network, making this sort of analysis less effective. For this study, the social network proved to be too discriminative, and we conducted no further experimentation with @names. In future work, we plan to examine the accuracy of the social network as a function of the number of classification classes, or authors.

D. PHONE SIGNAL ANALYSIS

This section presents the results of the classification of modulation characteristics collected from cell phone signals in an effort to correctly identify the specific device transmitting the signal. We form the three measured modulation characteristics (peak phase error, RMS phase error, and frequency error) into a feature vector, and then use a naïve Bayes classifier to predict the device associated with a set of signal feature vectors. As with the previous experiments, we combine multiple signal feature vectors into a training set in order to improve classification results by increasing the depth of the feature context in each training set. The classifier is trained and tested with a variety of total signal vector counts per device, and different quantities of signal vectors per training set.

Analysis of the phone signal modulation characteristics showed that devices could be identified by the naïve Bayes classifier at an accuracy level well above random chance. Figure 22 shows the accuracy results averaged over a ten-fold cross validation for 20 phones with a total signal feature vector quantity of 30 – 150 vectors per device and a training set size of one to five vectors per training set.

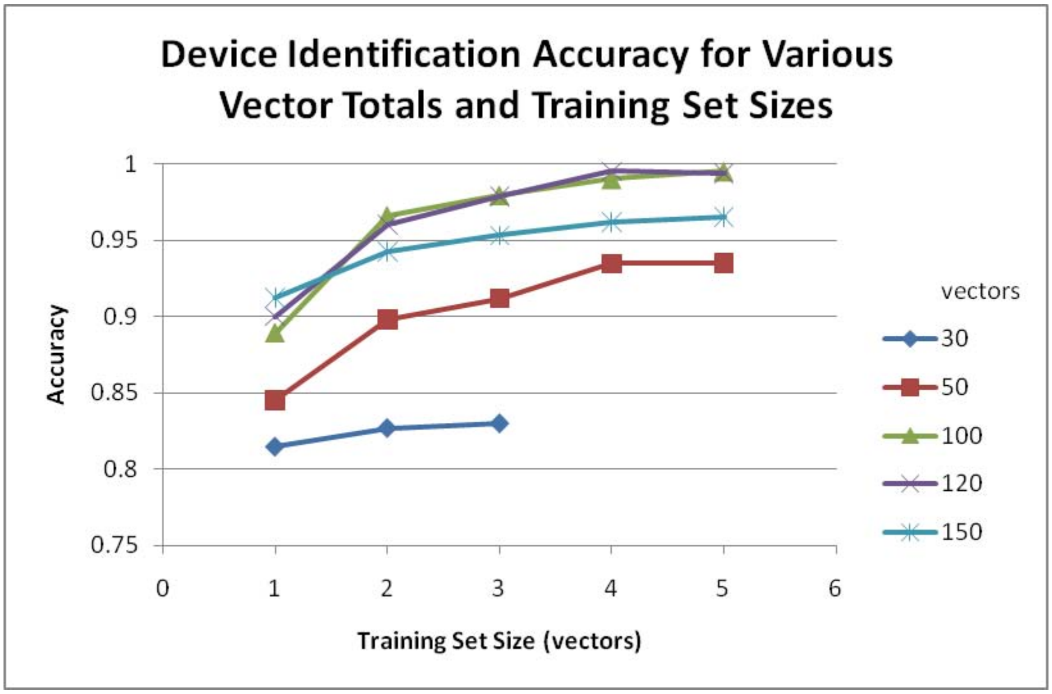

Figure 22. Classification Accuracy for 20 Devices With Varying Vectors per Training Set and Total Vectors per Device

Training set sizes larger than five vectors per set were explored using 150 total data vectors. Figure 23 shows the results of these experiments for 20 phones. As the training set size increases the total number of classification results per phone decreases, giving each incorrect classification a larger impact on the accuracy result. For example, 150 data vectors divided into five per training set gives 30 sets for classification. Incorrectly classifying one of these documents yields a 96.7% accuracy result. When 150 data vectors are grouped into training sets of size 15, ten sets are created for classification. Incorrectly classifying one set yields a 90% accuracy result. Figure 23 reflects this phenomenon.

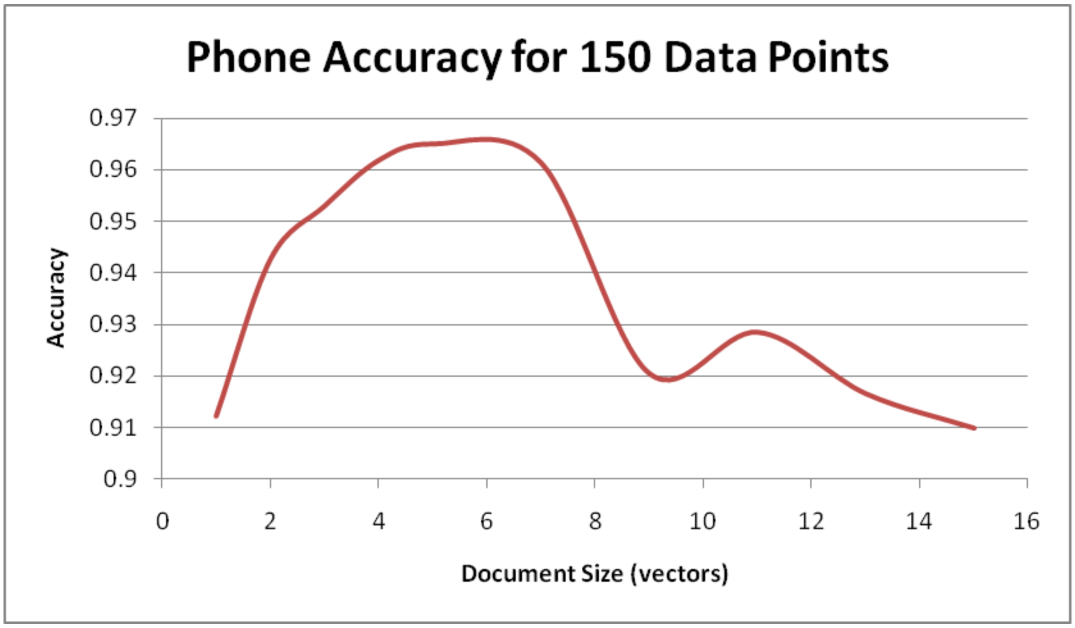

Figure 23. Classification Accuracy Results for 20 Phones With 150 Data Vectors and Varying Document Size

Confusion matrices and accuracy results per phone are included in Appendix D. In future work, we wish to investigate which features of the phone signals provide the most discriminatory classification power.

E. COMBINED CLASSIFIERS

Combining the outputs of the individual classifiers improved upon the authorship attribution results of the individual text classifier. Per the sum-rule combination scheme discussed in Chapter II, our experimentation added the output probability logarithms, averaged over a ten-fold cross validation, of the individual phone and text classifiers. The text data sets used in the experiments were the classification results from the 20 authors using 30, 50, 100, 120, and 150 tweets per author and document sizes of one to 15 tweets per document. The phone data sets used were the classification results from 20 phones using the same number of signal vectors per phone and signal vectors per training set as the text data sets. We repeated this process for selected data sets after normalizing the output probability logarithms. Figures 24-28 show the accuracy results of the individual and combined classifiers for the five data sets. Appendix E contains the accuracy results for each author-phone pairing tested.

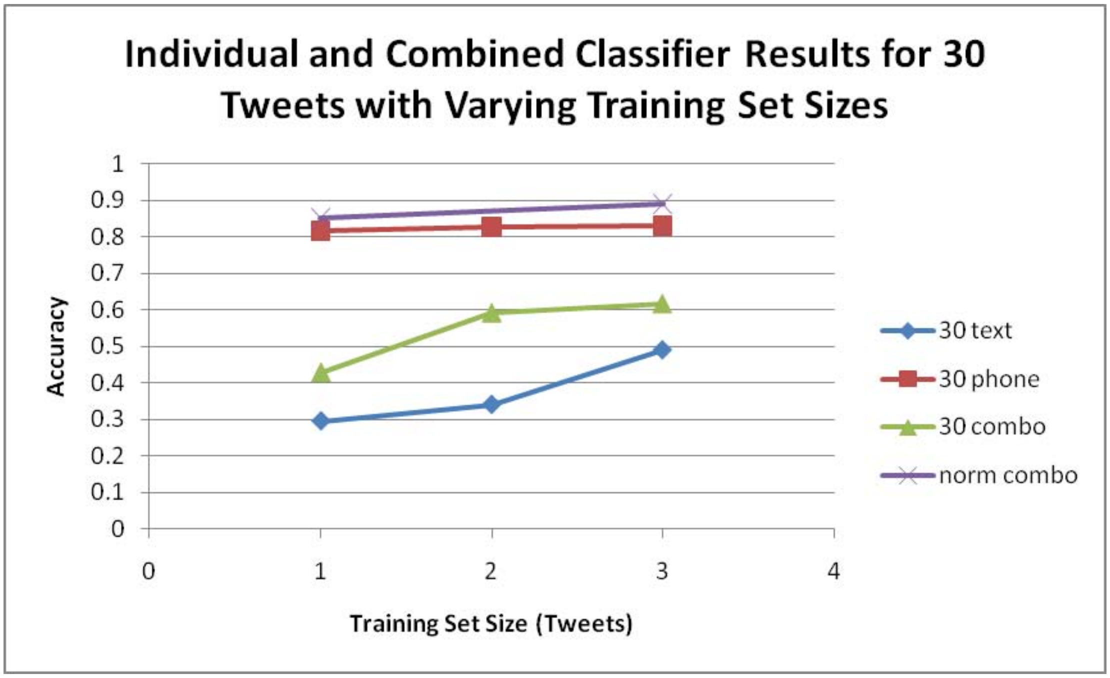

Figure 24. Classification Accuracy of Individual and Combined Classifiers for 30 Tweets/Signal Vectors and Various Training Set Sizes

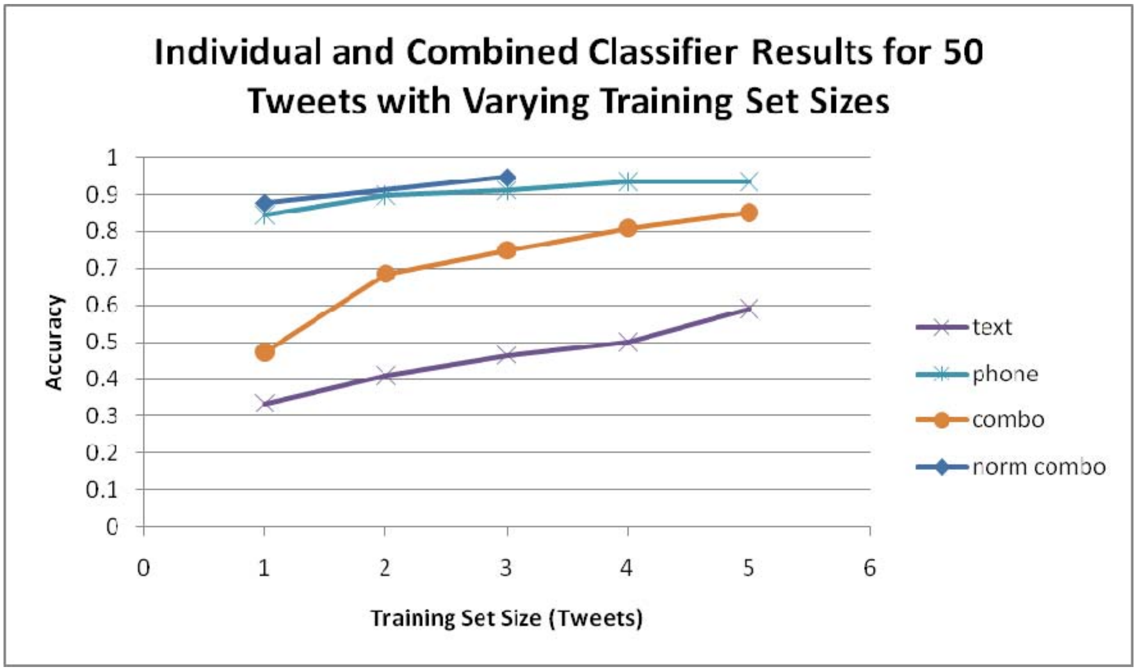

Figure 25. Classification Accuracy of Individual and Combined Classifiers for 50 Tweets/Signal Vectors and Various Training Set Sizes

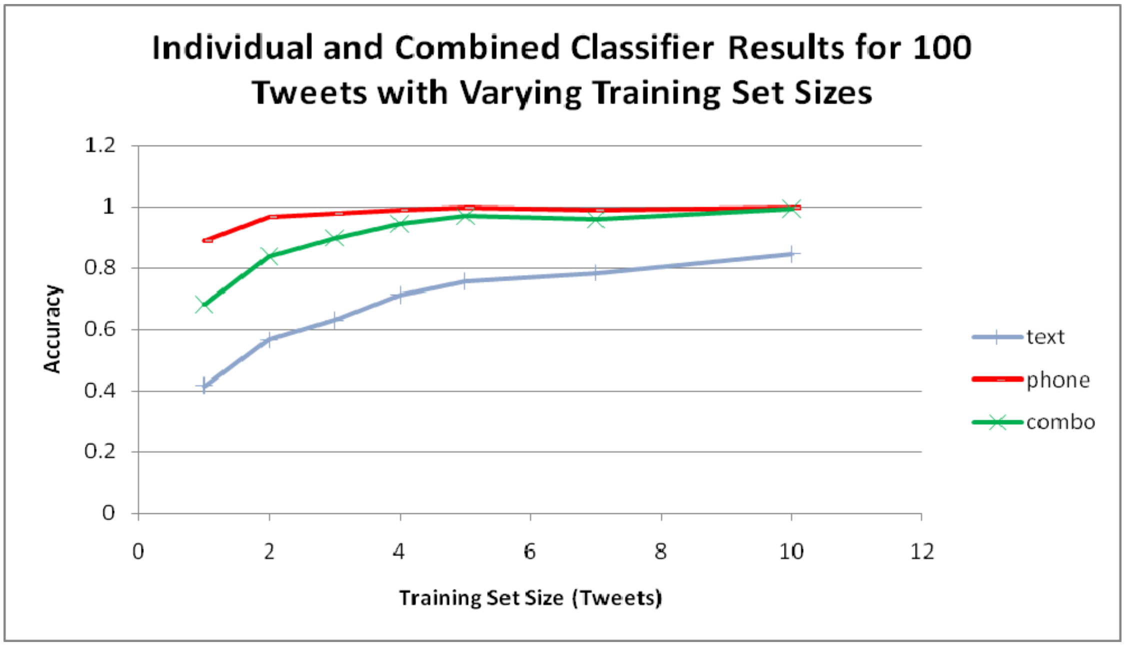

Figure 26. Classification Accuracy of Individual and Combined Classifiers for 100 Tweets/Signal Vectors and Various Training Set Sizes

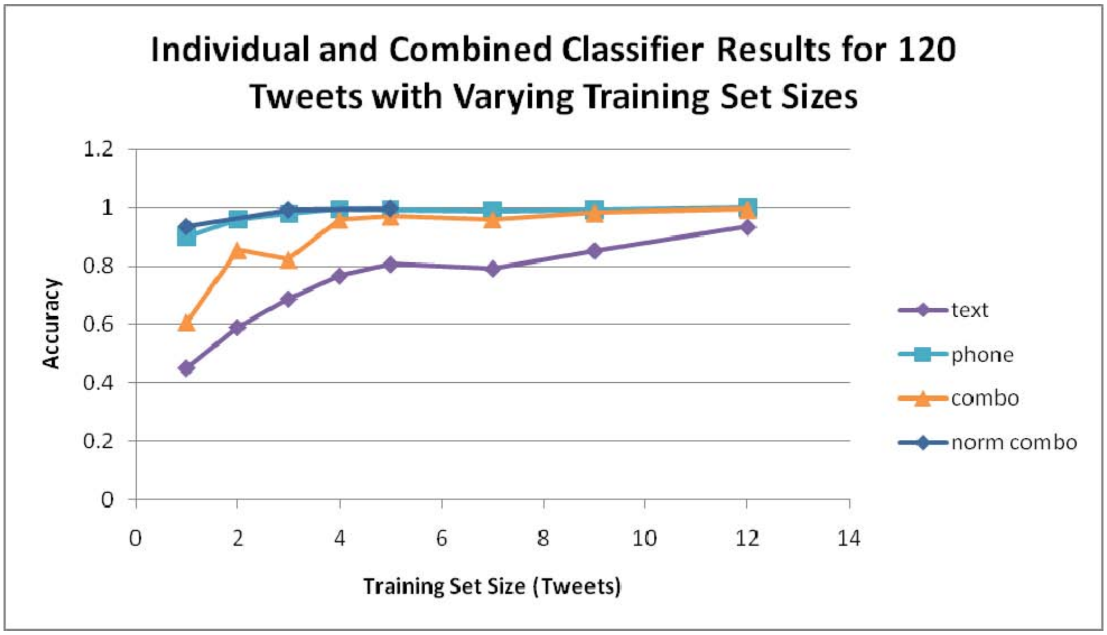

Figure 27. Classification Accuracy of Individual and Combined Classifiers for 120 Tweets/Signal Vectors and Various Training Set Sizes

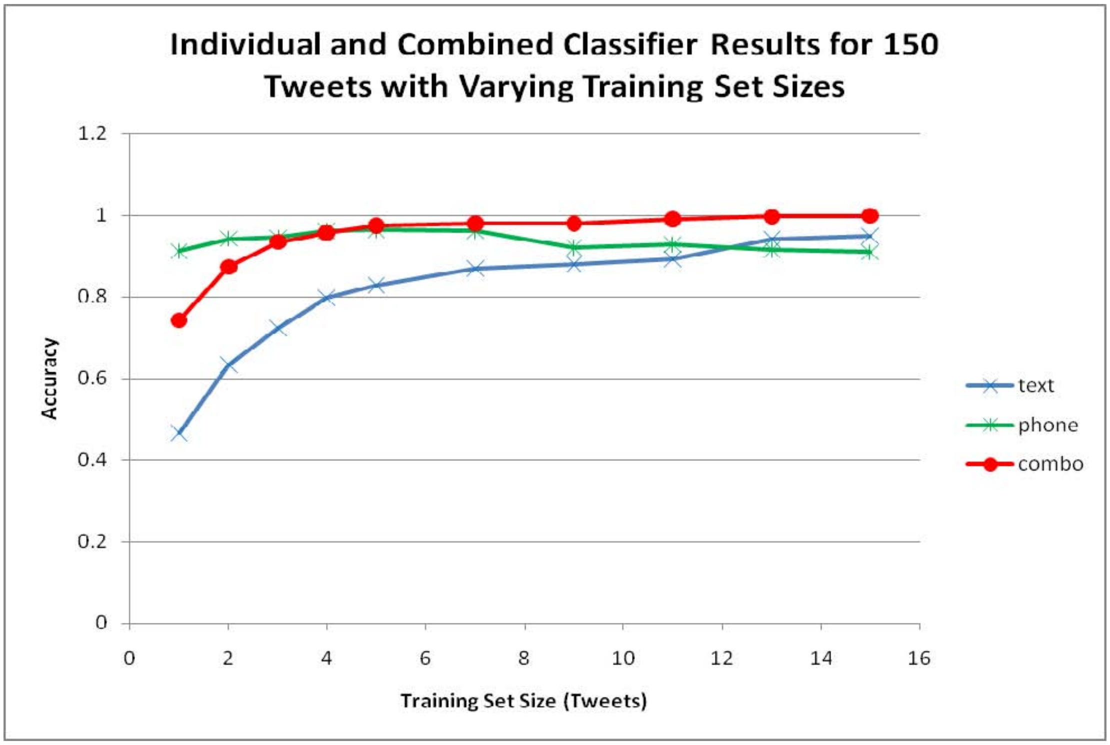

Figure 28. Classification Accuracy of Individual and Combined Classifiers for 150 Tweets/Signal Vectors and Various Training Set Sizes

Normalizing the output probability logarithms, before adding them together, results in accuracy values superior to either of the individual classifiers. The probability logarithm outputs of the text classifier are orders of magnitude smaller than the phone classifier, with bigger variance between the label values because of the much larger text feature space. Table 9 shows an example using the author 2744 and the phone htc376.

Table 9. Comparing Combination of Probability Logarithms and Combination of Normalized Probability Logarithms

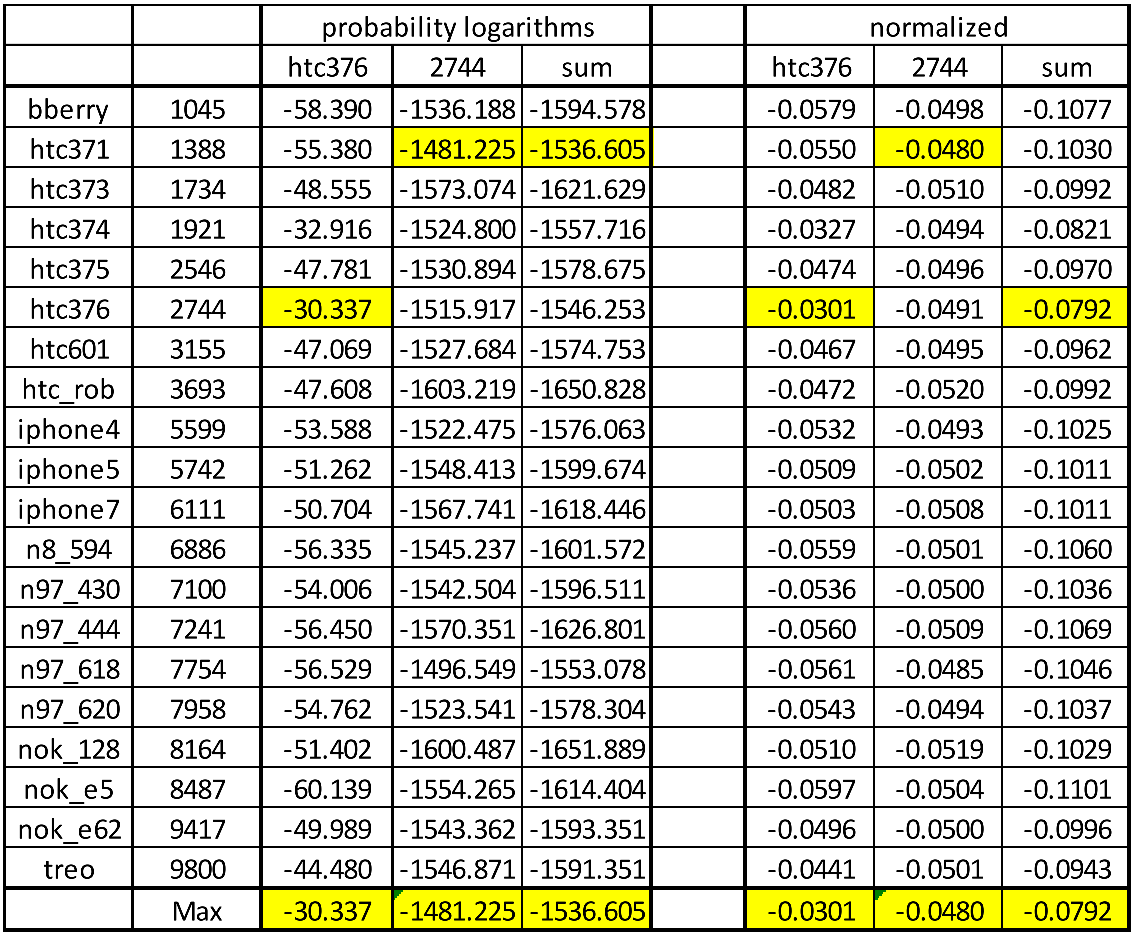

		probability logarithms				normalized		
		htc376	2744	sum		htc376	2744	sum
bberry	1045	-58.390	-1536.188	-1594.578		-0.0579	-0.0498	-0.1077
htc371	1388	-55.380	-1481.225	-1536.605		-0.0550	-0.0480	-0.1030
htc373	1734	-48.555	-1573.074	-1621.629		-0.0482	-0.0510	-0.0992
htc374	1921	-32.916	-1524.800	-1557.716		-0.0327	-0.0494	-0.0821
htc375	2546	-47.781	-1530.894	-1578.675		-0.0474	-0.0496	-0.0970
htc376	2744	-30.337	-1515.917	-1546.253		-0.0301	-0.0491	-0.0792
htc601	3155	-47.069	-1527.684	-1574.753		-0.0467	-0.0495	-0.0962
htc_rob	3693	-47.608	-1603.219	-1650.828		-0.0472	-0.0520	-0.0992
iphone4	5599	-53.588	-1522.475	-1576.063		-0.0532	-0.0493	-0.1025
iphone5	5742	-51.262	-1548.413	-1599.674		-0.0509	-0.0502	-0.1011
iphone7	6111	-50.704	-1567.741	-1618.446		-0.0503	-0.0508	-0.1011
n8_594	6886	-56.335	-1545.237	-1601.572		-0.0559	-0.0501	-0.1060
n97_430	7100	-54.006	-1542.504	-1596.511		-0.0536	-0.0500	-0.1036
n97_444	7241	-56.450	-1570.351	-1626.801		-0.0560	-0.0509	-0.1069
n97_618	7754	-56.529	-1496.549	-1553.078		-0.0561	-0.0485	-0.1046
n97_620	7958	-54.762	-1523.541	-1578.304		-0.0543	-0.0494	-0.1037
nok_128	8164	-51.402	-1600.487	-1651.889		-0.0510	-0.0519	-0.1029
nok_e5	8487	-60.139	-1554.265	-1614.404		-0.0597	-0.0504	-0.1101
nok_e62	9417	-49.989	-1543.362	-1593.351		-0.0496	-0.0500	-0.0996
treo	9800	-44.480	-1546.871	-1591.351		-0.0441	-0.0501	-0.0943
	Max	-30.337	-1481.225	-1536.605		-0.0301	-0.0480	-0.0792

The text classifier incorrectly selects author 1388 as the most probable class, with a probability logarithm output 34.691 orders of magnitude higher than the actual class. The phone classifier correctly selects htc376, but its probability logarithm output is only 25.043 orders of magnitude more than htc371, the phone associated with author 1388. Thus, the combined classifier selects the htc371-1388 pair. Once the probability logarithms are normalized, the relative variation between class labels decreases. The text classifier selection of 1388 is only 0.0011 orders of magnitude greater than the value for 2744, while the value of htc371 is now 0.0249 orders of magnitude less than the correct value of htc376. Thus, the combined classifier outputs the correct htc376-2744 pairing based on the strength of the phone classifier.

Another example using the same phone-author pair demonstrates how the normalized probability logarithms can have a negative effect on the combined classifier accuracy. Table 10 shows a set of classifier outputs in which the incorrect phone classifier causes the normalized probability logarithm combination to make an incorrect phone-author pair classification, while the non-normalized output combination selected the correct pair.

Table 10. Normalized Probability Logarithm Combination Resulting in Incorrect Classification

		probability logarithms				normalized		
		htc376	2744	sum		htc376	2744	sum
bberry	1045	-61.569	-1889.374	-1950.943		-0.0576	-0.0501	-0.1077
htc371	1388	-59.819	-1835.965	-1895.783		-0.0560	-0.0487	-0.1047
htc373	1734	-57.650	-1886.810	-1944.460		-0.0540	-0.0500	-0.1040
htc374	1921	-34.498	-1829.496	-1863.993		-0.0323	-0.0485	-0.0808
htc375	2546	-50.496	-1828.648	-1879.145		-0.0473	-0.0485	-0.0958
htc376	2744	-36.906	-1805.979	-1842.885		-0.0345	-0.0479	-0.0824
htc601	3155	-55.518	-1889.277	-1944.794		-0.0520	-0.0501	-0.1021
htc_rob	3693	-51.020	-2004.238	-2055.258		-0.0478	-0.0531	-0.1009
iphone4	5599	-55.867	-1855.938	-1911.805		-0.0523	-0.0492	-0.1015
iphone5	5742	-50.603	-1922.999	-1973.602		-0.0474	-0.0510	-0.0984
iphone7	6111	-47.807	-1902.916	-1950.723		-0.0448	-0.0505	-0.0952
n8_594	6886	-57.837	-1884.001	-1941.838		-0.0541	-0.0500	-0.1041
n97_430	7100	-57.482	-1879.858	-1937.340		-0.0538	-0.0498	-0.1037
n97_444	7241	-58.516	-1875.332	-1933.848		-0.0548	-0.0497	-0.1045
n97_618	7754	-59.387	-1894.904	-1954.291		-0.0556	-0.0502	-0.1058
n97_620	7958	-57.586	-1898.507	-1956.092		-0.0539	-0.0503	-0.1042
nok_128	8164	-51.677	-1920.182	-1971.859		-0.0484	-0.0509	-0.0993
nok_e5	8487	-58.015	-1891.816	-1949.830		-0.0543	-0.0502	-0.1045
nok_e62	9417	-54.917	-1923.301	-1978.218		-0.0514	-0.0510	-0.1024
treo	9800	-51.128	-1894.848	-1945.976		-0.0479	-0.0502	-0.0981
	Max	-34.498	-1805.979	-1842.885		-0.0323	-0.0479	-0.0808

In this case, the output probability logarithm combination provided the correct classification based on the strength of the text classifier, but the normalized outputs emphasized the phone classifier and produced an incorrect classification result. In future work we wish to investigate different classifier combination mechanisms to evaluate in more detail the effects of the individual classifier inputs on the combined result, and find ways to balance these effects on the final result.

F. DETECTING AUTHOR CHANGES

In this section, we test whether the combined classification system we have built is able to detect a simulated change in user. For example, a criminal may use a cell phone for a period of time, then sell the cell phone to someone else and get a new one in order to elude anyone who may be tracking the old cell phone. Our research question asks: in the absence of any other knowledge about the target user and device, can our classifier detect that someone new is using the phone. We do this by simulating a "change" in author in the combination scheme, exchanging tweets from two authors in our set of 20 and analyzing if the previously trained models of the text and combined classifiers can detect and correctly classify the mislabeled tweets in the test set.

Analysis of the combined classifiers, with the simulated change in author in two author-phone pairings, showed that the classifier combination could detect the change in tweet author less than 40% of the time. Tweets from authors 7958 and 9417 were exchanged to simulate a change in user on a phone. Testing was conducted using a set of 50 tweets per author with training set sizes of one and three tweets per set, and with a set of 120 tweets per author with a training set size of five tweets per set. The text classifier alone was able to detect the change up to 100% of the time, but the classification accuracy of the unaltered text, true positives, was also rather low. Tables 11-13 show the text-only classification confusion matrices for the two affected authors. The "Original" row shows the results for the unaffected tweets. The "Swapped" row shows the results for the tweets that were exchanged between the authors, listed under the labeled author. The true positives are highlighted. Table 14 lists the accuracy rates these matrices display and compares to the accuracy over all 20 authors.

Based on previous testing, adding the phone classifier output to the text classifier output should improve the true positive rate. Our analysis shows the true positive rate does improve, but the false positive rate also increases. When using the output probability logarithms in combination a small difference in accuracy between the actual and injected text is noted, with author 7958 more distinct than author 9147. When using the normalized output probability logarithms in combination, no difference between the actual and injected text can be detected. Tables 15–20 are the combined classifier confusion matrices for the two affected authors. Counts are added for all 20 phone-author pairs tested. The “Original” row shows the results for the unaffected tweets. The “Swapped” row shows the results for the tweets that were exchanged between the authors, listed under the labeled author. The true positives are highlighted. Table 21 shows the accuracy results averaged over all 20 author-phone pairings.

Table 11. Confusion Matrix for Text Classifier for Simulated Author Change Using 50 Tweets per Author With One Tweet per Document With Ten Tweets Exchanged Between Authors

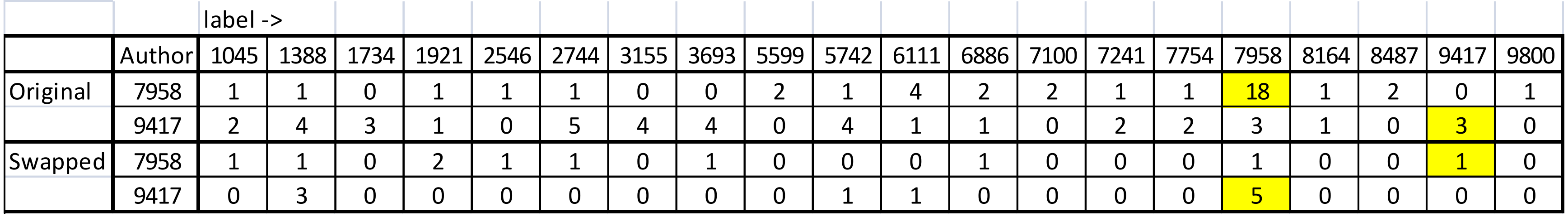

		label ->																			
	Author	1045	1388	1734	1921	2546	2744	3155	3693	5599	5742	6111	6886	7100	7241	7754	7958	8164	8487	9417	9800
Original	7958	1	1	0	1	1	1	0	0	2	1	4	2	2	1	1	18	1	2	0	1
	9417	2	4	3	1	0	5	4	4	0	4	1	1	0	2	2	3	1	0	3	0
Swapped	7958	1	1	0	2	1	1	0	1	0	0	0	1	0	0	0	1	0	0	1	0
	9417	0	3	0	0	0	0	0	0	0	1	1	0	0	0	0	5	0	0	0	0

Table 12. Confusion Matrix for Text Classifier for Simulated Author Change Using 50 Tweets per Author With Three Tweets per Document With Nine Tweets Exchanged Between Authors

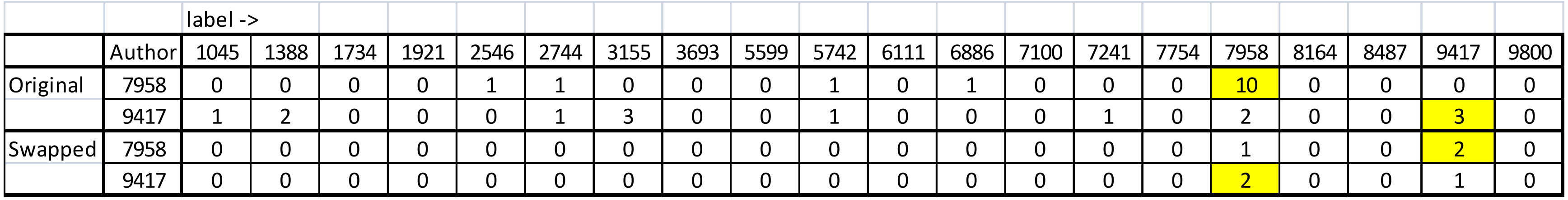

		label ->																			
	Author	1045	1388	1734	1921	2546	2744	3155	3693	5599	5742	6111	6886	7100	7241	7754	7958	8164	8487	9417	9800
Original	7958	0	0	0	0	1	1	0	0	0	1	0	1	0	0	0	10	0	0	0	0
	9417	1	2	0	0	0	1	3	0	0	1	0	0	0	1	0	2	0	0	3	0
Swapped	7958	0	0	0	0	0	0	0	0	0	0	0	0	0	0	0	1	0	0	2	0
	9417	0	0	0	0	0	0	0	0	0	0	0	0	0	0	0	2	0	0	1	0

Table 13. Confusion Matrix for Text Classifier for Simulated Author Change Using 120 Tweets per Author With Five Tweets per Document With 25 Tweets Exchanged Between Authors

		label ->																			
	Author	1045	1388	1734	1921	2546	2744	3155	3693	5599	5742	6111	6886	7100	7241	7754	7958	8164	8487	9417	9800
Original	7958	0	0	0	0	0	1	0	0	0	0	0	1	1	0	0	14	0	0	2	0
	9417	0	0	1	0	0	2	0	0	0	0	0	1	0	0	1	4	0	0	10	0
Swapped	7958	0	1	0	0	0	0	0	0	0	0	0	0	0	0	0	1	0	0	3	0
	9417	0	0	0	0	0	0	0	0	0	0	0	0	0	0	0	5	0	0	0	0

Table 14. Classification Accuracy of Text Classifier for Simulated Author Change – True Positives (non-swap) and False Positives (Swap)

Tweets	50		120
Train Set	1	3	5
Overall	0.319	0.4912	0.775
7958 non-swap	0.45	0.7143	0.7368
7958 Swap	0.1	0.3333	0.2
9147 non-swap	0.075	0.2143	0.5263
9147 Swap	0	0.3333	0

Table 15. Confusion Matrix for Normalized Combined Classifier for Simulated Author Change Using 50 Tweets per Author With One Tweet per Document With Ten Tweets Exchanged Between Authors

		label ->																			
	Author	1045	1388	1734	1921	2546	2744	3155	3693	5599	5742	6111	6886	7100	7241	7754	7958	8164	8487	9417	9800
Original	7958	2	0	2	0	1	1	0	1	2	3	5	4	14	15	14	707	13	4	8	4
	9417	9	14	8	2	2	2	0	2	0	0	1	1	1	3	6	17	19	20	680	13
Swapped	7958	3	1	1	0	2	0	1	2	0	4	0	1	3	4	2	170	5	0	0	1
	9417	0	3	2	1	2	1	0	0	0	1	0	0	6	0	0	6	5	4	164	5

Table 16. Confusion Matrix for Normalized Combined Classifier for Simulated Author Change Using 50 Tweets per Author With Three Tweets per Document With Nine Tweets Exchanged Between Authors

		label ->																			
	Author	1045	1388	1734	1921	2546	2744	3155	3693	5599	5742	6111	6886	7100	7241	7754	7958	8164	8487	9417	9800
Original	7958	1	0	0	0	0	0	1	0	0	1	0	1	3	2	6	262	1	1	1	0
	9417	2	1	1	1	1	0	0	0	0	1	0	0	2	0	1	5	2	7	256	0
Swapped	7958	0	1	0	0	0	0	0	0	0	1	0	0	0	1	0	57	0	0	0	0
	9417	0	0	0	0	0	0	0	0	0	0	0	1	1	0	0	0	0	0	58	0

Table 17. Confusion Matrix for Normalized Combined Classifier for Simulated Author Change Using 120 Tweets per Author With Five Tweets per Document With 25 Tweets Exchanged Between Authors

		label ->																			
	Author	1045	1388	1734	1921	2546	2744	3155	3693	5599	5742	6111	6886	7100	7241	7754	7958	8164	8487	9417	9800
Original	7958	0	0	0	0	0	0	0	0	0	0	0	0	0	0	1	359	0	0	0	0
	9417	0	0	0	0	0	0	0	0	0	0	0	0	0	0	0	0	0	1	359	0
Swapped	7958	0	0	0	0	0	0	0	0	0	0	0	0	0	0	0	100	0	0	0	0
	9417	0	0	0	0	0	0	0	0	0	0	0	0	0	0	0	0	0	0	100	0

Table 18. Confusion Matrix for Non-normalized Combined Classifier for Simulated Author Change Using 50 Tweets per Author With One Tweet per Document With Ten Tweets Exchanged Between Authors

		label ->																			
	Author	1045	1388	1734	1921	2546	2744	3155	3693	5599	5742	6111	6886	7100	7241	7754	7958	8164	8487	9417	9800
Original	7958	17	10	7	4	12	21	0	6	22	18	67	10	42	23	32	458	22	14	4	11
	9417	29	97	42	13	12	68	77	57	2	35	17	13	9	38	33	49	5	24	176	4
Swapped	7958	20	24	0	8	15	25	7	20	0	0	0	5	2	1	5	36	2	5	25	0
	9417	0	44	0	0	2	0	8	0	0	20	14	7	3	5	1	70	0	14	12	0

Table 19. Confusion Matrix for Non-normalized Combined Classifier for Simulated Author Change Using 50 Tweets per Author With Three Tweets per Document With Nine Tweets Exchanged Between Authors

		label ->																			
	Author	1045	1388	1734	1921	2546	2744	3155	3693	5599	5742	6111	6886	7100	7241	7754	7958	8164	8487	9417	9800
Original	7958	0	1	0	0	0	0	0	0	0	1	1	4	4	0	0	269	0	0	0	0
	9417	13	37	0	2	8	26	48	0	0	4	0	1	1	12	1	29	0	0	98	0
Swapped	7958	0	0	1	0	0	0	0	0	0	0	0	0	0	0	0	59	0	0	0	0
	9417	0	0	0	0	0	0	0	0	0	0	0	0	0	0	0	20	0	0	40	0

Table 20. Confusion Matrix for Non-normalized Combined Classifier for Simulated Author Change Using 120 Tweets per Author With Five Tweets per Document With 25 Tweets Exchanged Between Authors

		label ->																			
	Author	1045	1388	1734	1921	2546	2744	3155	3693	5599	5742	6111	6886	7100	7241	7754	7958	8164	8487	9417	9800
Original	7958	0	0	0	0	0	4	0	0	0	0	0	1	0	0	0	355	0	0	0	0
	9417	0	0	6	0	0	8	0	0	0	0	0	0	0	0	1	4	0	0	341	0
Swapped	7958	0	0	0	0	0	0	0	0	0	0	0	1	0	0	5	81	0	0	13	0
	9417	0	0	0	0	0	0	0	0	0	0	0	0	0	0	0	13	0	0	87	0

Table 21. Classification Accuracy of Combined Classifiers for Detecting Simulated Author Change – True Positives (non-swap) and False Positives (Swap)

	Non-normalized Outputs			Normalized Outputs		
Tweets	50		120	50		120
Train Set	1	3	5	1	3	5
Overall	0.4669	0.7607	0.9700	0.8738	0.9432	0.9966
7958 non-swap	0.5700	0.9714	0.9842	0.8838	0.9357	0.9974
7958 Swap	0.1900	0.9833	0.6400	0.8500	0.9500	0.9500
9147 non-swap	0.1900	0.3500	0.9500	0.8500	0.9143	1.0000
9147 Swap	0.0600	0.6667	0.8700	0.8200	0.9667	1.0000

THIS PAGE INTENTIONALLY LEFT BLANK

V. CONCLUSIONS

A. SUMMARY

This thesis asked two questions: can a multi-modal naïve Bayes classifier, combining user-specific text authorship characteristics and device-specific signal characteristics, improve on the accuracy results of a text classifier alone — especially for short messages — and can such a classifier detect if a phone, normally used by one individual, is unexpectedly used by a different individual. Our results show that the answer to the first question is *yes*, while the answer to the second is that *it is possible*, but our method requires further refinement to improve accuracy.

In our text classification experiments, classification of 120 individual Twitter messages from 50 authors using a multiclass naïve Bayes classifier produced 40.3% authorship attribution accuracy, less than the 54.4% found by Layton, Watters, and Dazeley, using the Source Code Author Profiles (SCAP) method [3], the most comparable related work to our own. However, combining multiple tweets to generate a text feature vector for input to the classifier improves authorship attribution accuracy. Using a feature vector from 23 combined messages produces the best result of 99.6% accuracy.

Analysis of a user’s message communication pattern by the time of day they sent tweets did not produce a good classifier. In the best case tested, using the send times of 120 tweets per author from 50 authors combined into 12 tweets per training set, the classification accuracy was

35%. It is possible that by selecting for English speakers we obtained a set of authors living in similar time zones. The social network analysis, classifying authors by the @names mentioned in their tweets, performed extremely well. We attained 94% accuracy classifying 120 @names per author from 50 authors combined into 3 @names per training set, with better accuracy results as training set size increased. The random selection of authors for the study likely chose users unrelated to each other, with distinctive social networks that enabled high classification accuracy, suggesting that the performance of such approaches may decrease as the author set size increases.

The device identification portion of the research performed very well. Classification of 120 individual cell phone radio signal modulation characteristic vectors for 20 GSM cell phones resulted in a 90% classification accuracy. This compares favorably to the 99% accuracy of Brik et al. for modulation characteristics of 802.11 devices [4]. Combining the signal vectors into training sets of five signal vectors per set improved classification accuracy to 99%.

Sum-rule combination of the text and phone classifiers, adding the probability logarithm outputs of the individual classifiers, improves upon the results of the text classifier. The multimodal classifier performed better than the text classifier in every experiment as the high device identification accuracies influenced the combined accuracy result. For 20 author-phone pairs with 120 tweets/signal vectors per pair the multimodal classifier accuracy was 60%. When the tweets/signal vectors were combined into 5 per training set, the multimodal classifier accuracy surpassed 98%. Predictably, summing the classifier outputs produces better accuracy results when the individual classifier accuracy results are also high.

The phone user change simulation testing showed that the multimodal classifier could not reliably detect if tweets from two of the authors were exchanged to simulate a different author in a phone-author pairing. The text classifier alone achieved the best results in detecting author change, achieving a false positive rate of 0% with a true positive rate of 52.6% for one author, and a false positive rate of 20% and true positive rate of 73.7% for the other. Those numbers were using 120 tweets per author grouped into training sets of five tweets per set. The multimodal classifier results on the same data set were a false positive rate of 87% and true positive rate of 95% for one author, and a false positive rate of 64% and true positive rate of 98.4% for the other. This indicates that the phone classifier results are skewing the multimodal classifier to favor the phone detection. A more accurate text classifier may produce better author change detection results.

These results suggest that the classification of the user-device binding is feasible. It could be employed as a secondary security layer for a business or government cell phone management scheme to detect unauthorized phone use or the loss or theft of a phone. In a law enforcement context, this method could help verify the author of SMS messages sent from a suspect’s phone. With improvement of the author change detection method, it may help detect when a suspect ceases to use or sells a temporary, or “burner”, phone. Authorship attribution of short messages is a difficult problem, but we have shown that a multimodal classifier can improve upon the current state of the art.

B. FUTURE WORK

This research suggests a number of avenues for further research in authorship attribution of short messages.

1. Social Network Analysis

The social network analysis conducted here was superficial, but showed potentially highly effective results. Future work could build a new Twitter corpus, possibly using some of the authors here as a basis. The follow-feed collection of a starting set of selected authors would gather tweets to and from users with whom they are routinely in contact. Then repeat this process to expand their networks. A larger set of interconnected users could be built through this discover-and-collect method. Once a satisfactorily sized corpus is built, the text-based authorship attribution methods used in this research could be repeated.

2. Other Machine Learning Methods

This research used naïve Bayes classification for every data type. Future research could try other machine learning techniques, particularly SVM, to try to improve accuracy results. The binning conducted to discretize continuous variables in the phone signal collection and in the time analysis may hurt accuracy results. SVM is better suited for machine learning of continuous variables. This research used a multiclass classifier. Developing an effective one-of-many classifier may have more practical application uses when searching for a specific individual in an undefined population set.

Another potential research avenue would be to further tune the multimodal classifier, experimenting with different classifier combination schemes, and possibly using input weighting to mitigate the heavy influence of the phone signal results on the multimodal results.

3. Expanded Phone Signal Analysis

We used three easily obtained modulation characteristics of the cell phone signal to conduct our classification testing. Future research could determine which of these three characteristics is the most discriminative. Other signal characteristics such as bit error rate and signal ramp time could also be explored.

An additional research area in the phone signal analysis would be to develop a means for measuring these signal characteristics with a software defined radio system. The test equipment used in our research is not a useful product for a practical application of phone signal analysis. A software defined radio receiver would be a more transportable and covert collection asset.

4. Segmentation Inside Boundaries

The author change in phone-author pairings experiment conducted here could be expanded upon. Our experiment used the technique of combining multiple tweets into a document and classifying the feature vector of that document in order to increase the feature space and improve classification accuracy. In the change of author experiment, all the tweets in one document belonged to the same author. The author change was simulated by exchanging the documents of two authors. Treating the document as a bounded feature space, one could exchange tweets within a document. The goal then would be to detect in which document the change of author in the author-phone pairing occurs, and where within that document it occurs.

5. Temporal Posting Aspects

The tweets used in this research were treated as independent slices of text data from an author. Tweets were selected randomly for use. In reality, tweets, and short message communication units in general, have a temporal linkage between each other, especially in a conversational context. Future work could examine the linkages between sequential tweets, and if those linkages could be defined and exploited. Also of interest is whether these linkages can be discriminated by topic or by stylistic characteristics.

C. CONCLUDING REMARKS

This research explores a holistic view of communication as a function of a user and a device together. We explore the user-to-device binding and our ability to detect this binding as a pair. The results of this work show that it is easier to detect an author when he is bound to a device than it is to detect this author alone, with a 50% accuracy improvement in the most disparate case. Knowing that in a real-world application a security professional may have a limited number of text and phone signal data points to work with, we tested our method on data sets of various sizes, looking to find ways to elicit quality accuracy results from minimal data sets. Authorship attribution of short messages is a difficult problem, but we have shown here that there are ways to effectively accomplish it. The practical applications of this research range from law enforcement and intelligence gathering to wireless network security.

THIS PAGE INTENTIONALLY LEFT BLANK

APPENDIX A: MEASURING GSM PHASE AND FREQUENCY ERRORS

Errors in signal modulation generated by a GSM transmitter cause degradation in the performance of the system. Small manufacturing variations in the electronics fabrication and assembly may cause persistent error in signal modulation and transmission. The ETSI 3GPP standards [33] and [34] impose quality standards on the allowable error for base stations and mobile stations. Manufacturers have developed quality control test mechanisms and equipment for their devices to ensure compliance with the standards and acceptable performance for users in the field. We use these mechanisms for test and identification of the mobile devices used in our experiments.

Once a call is established between the handset and the tower, the 8922S samples the uplink signal. This sampling collects the actual phase trajectory of the signal. In GMSK modulation, the signal carries bit-level data by affecting changes in carrier frequency, which cause corresponding changes in phase state. A one is represented by a carrier frequency change of +67.708 kHz, causing a phase state change of +90 degrees in the I/Q plane. A zero is represented by a carrier frequency change of -67.708 kHz, a phase state change of -90 degrees. The phase trajectory, then, consists of the phase state changes representing the series of data bits in the signal [37]. An error in the phase state change is reflected by a deviation from the 90 degree value. The signal analyzer collects the actual phase trajectory transmitted by the handset. It then demodulates the signal to determine the transmitted bit sequence. From the bit sequence, it calculates the ideal phase trajectory. The phase error is the difference between these two trajectories [38]. Figure 29 is a graphical representation of this process.

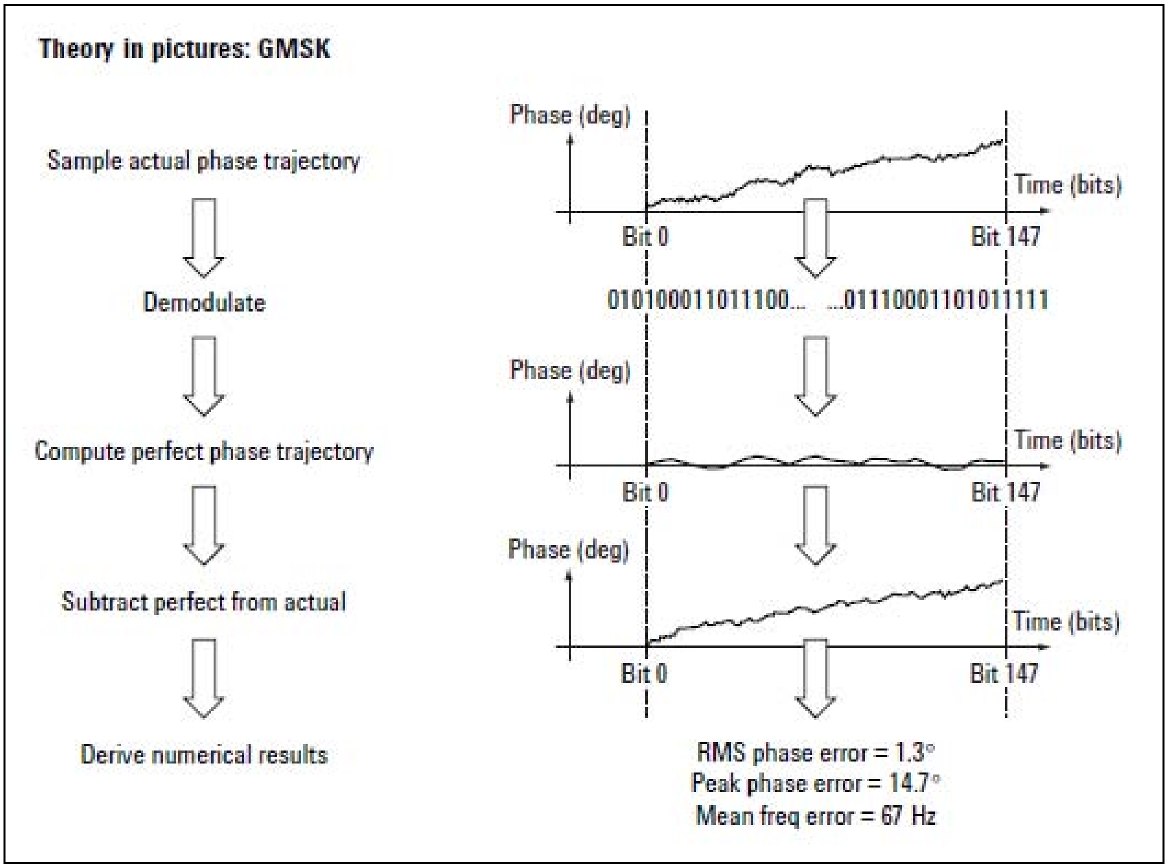

Figure 29. GMSK Phase Error Measurement (From [38])

The phase error measurement forms the basis of the three error values we use in our device identification scheme. The root mean square of the error measurement is calculated and reported as the RMS phase error. The largest phase deviation from ideal is reported as the peak phase error. The frequency error is the mean slope of the error line (phase/time) [38]. Figure 30 is a graphical representation of these error measurements relative to the calculated error line.

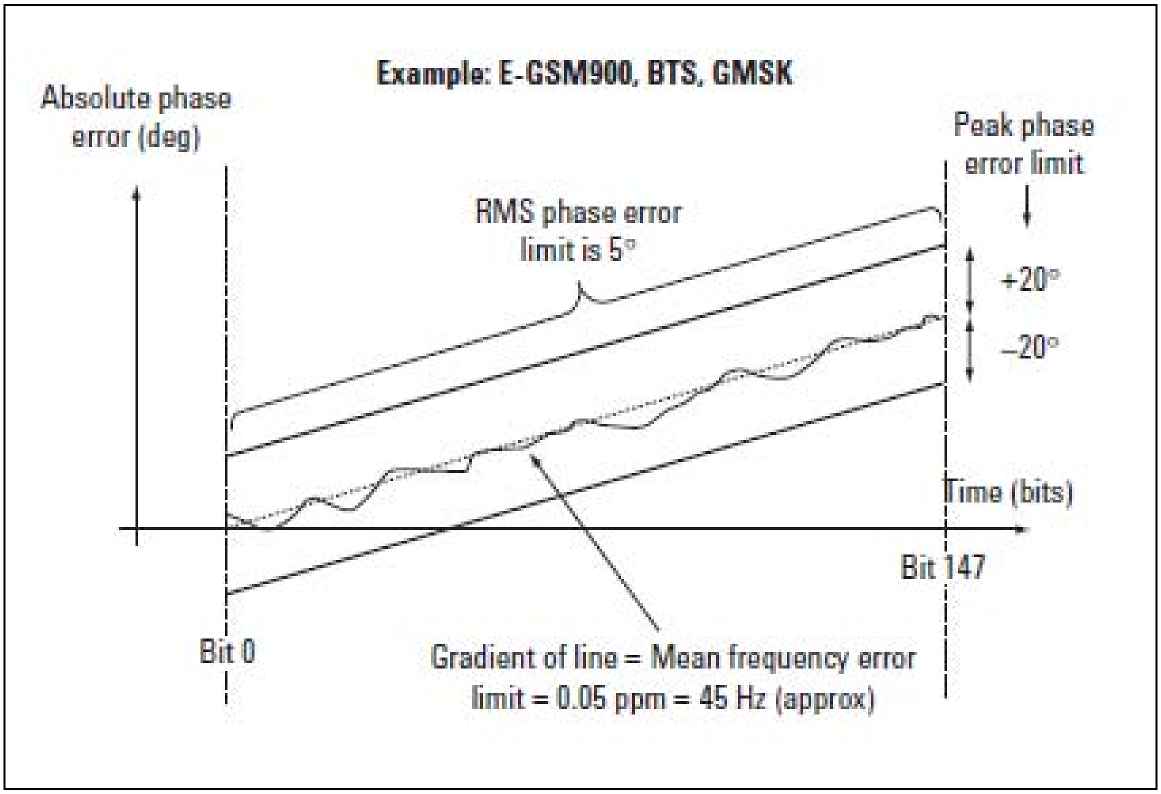
Example: E-GSM900, BTS, GMSK
Absolute phase error (deg)
Peak phase error limit
RMS phase error limit is 5°
+20°
–20°
Time (bits)
Bit 147
Bit 0
Gradient of line = Mean frequency error limit = 0.05 ppm = 45 Hz (approx)

Figure 30. GMSK Modulation Errors and Specified Limits (From [38])

The Agilent 8922S collects the GSM signal from the handset, performs the calculations described above over the signal bursts, and reports the peak phase error, RMS phase error, and frequency error. These modulation errors provide the basis for the device identification classification experiments conducted in this thesis.

THIS PAGE INTENTIONALLY LEFT BLANK

APPENDIX B: ADDITIONAL TEXT CLASSIFICATION DATA

Table 22. Confusion Matrix for 30 Tweets per Author With One Tweet per Document

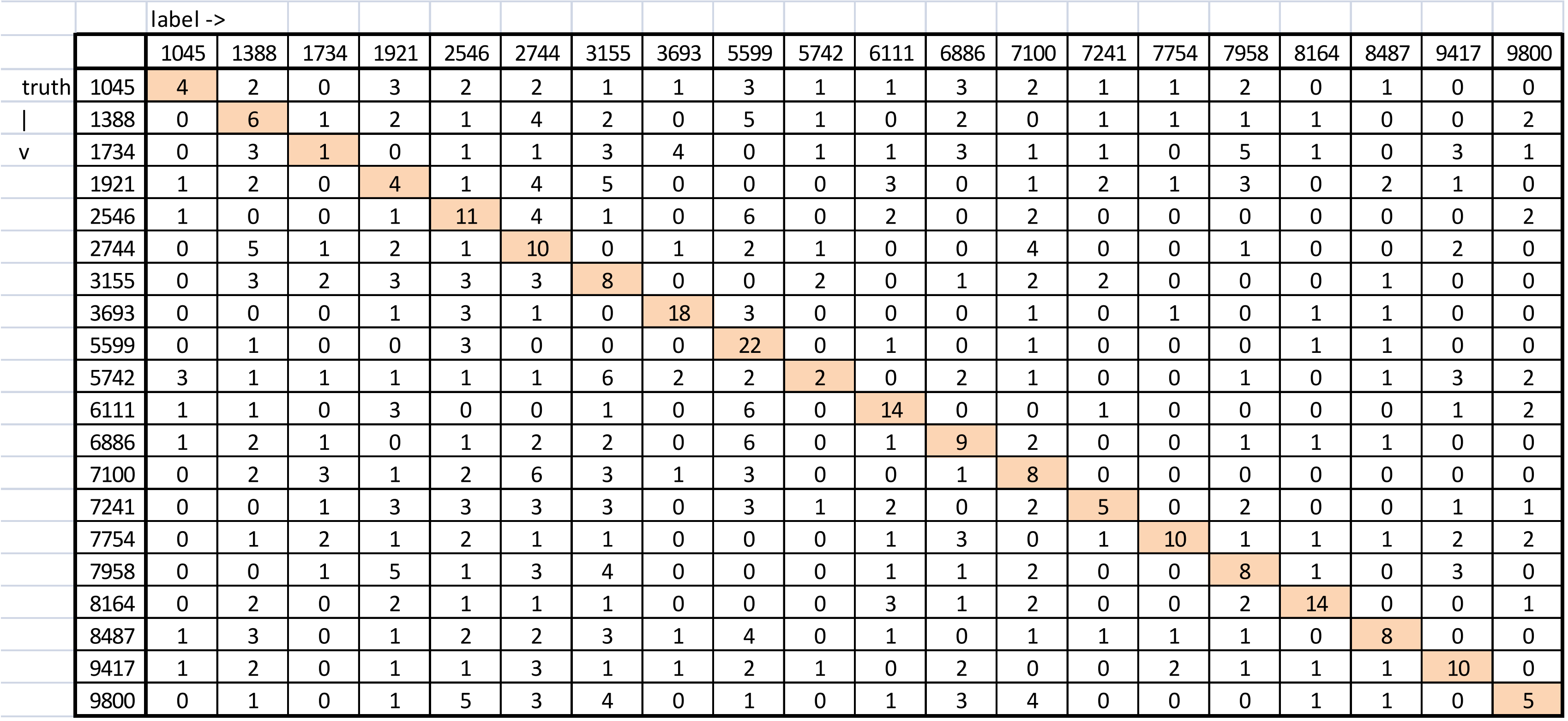

		label ->																			
		1045	1388	1734	1921	2546	2744	3155	3693	5599	5742	6111	6886	7100	7241	7754	7958	8164	8487	9417	9800
truth	1045	4	2	0	3	2	2	1	1	3	1	1	3	2	1	1	2	0	1	0	0
|	1388	0	6	1	2	1	4	2	0	5	1	0	2	0	1	1	1	1	0	0	2
v	1734	0	3	1	0	1	1	3	4	0	1	1	3	1	1	0	5	1	0	3	1
	1921	1	2	0	4	1	4	5	0	0	0	3	0	1	2	1	3	0	2	1	0
	2546	1	0	0	1	11	4	1	0	6	0	2	0	2	0	0	0	0	0	0	2
	2744	0	5	1	2	1	10	0	1	2	1	0	0	4	0	0	1	0	0	2	0
	3155	0	3	2	3	3	3	8	0	0	2	0	1	2	2	0	0	0	1	0	0
	3693	0	0	0	1	3	1	0	18	3	0	0	0	1	0	1	0	1	1	0	0
	5599	0	1	0	0	3	0	0	0	22	0	1	0	1	0	0	0	1	1	0	0
	5742	3	1	1	1	1	1	6	2	2	2	0	2	1	0	0	1	0	1	3	2
	6111	1	1	0	3	0	0	1	0	6	0	14	0	0	1	0	0	0	0	1	2
	6886	1	2	1	0	1	2	2	0	6	0	1	9	2	0	0	1	1	1	0	0
	7100	0	2	3	1	2	6	3	1	3	0	0	1	8	0	0	0	0	0	0	0
	7241	0	0	1	3	3	3	3	0	3	1	2	0	2	5	0	2	0	0	1	1
	7754	0	1	2	1	2	1	1	0	0	0	1	3	0	1	10	1	1	1	2	2
	7958	0	0	1	5	1	3	4	0	0	0	1	1	2	0	0	8	1	0	3	0
	8164	0	2	0	2	1	1	1	0	0	0	3	1	2	0	0	2	14	0	0	1
	8487	1	3	0	1	2	2	3	1	4	0	1	0	1	1	1	1	0	8	0	0
	9417	1	2	0	1	1	3	1	1	2	1	0	2	0	0	2	1	1	1	10	0
	9800	0	1	0	1	5	3	4	0	1	0	1	3	4	0	0	0	1	1	0	5

Table 23. Confusion Matrix for 30 Tweets per Author With Three Tweets per Document

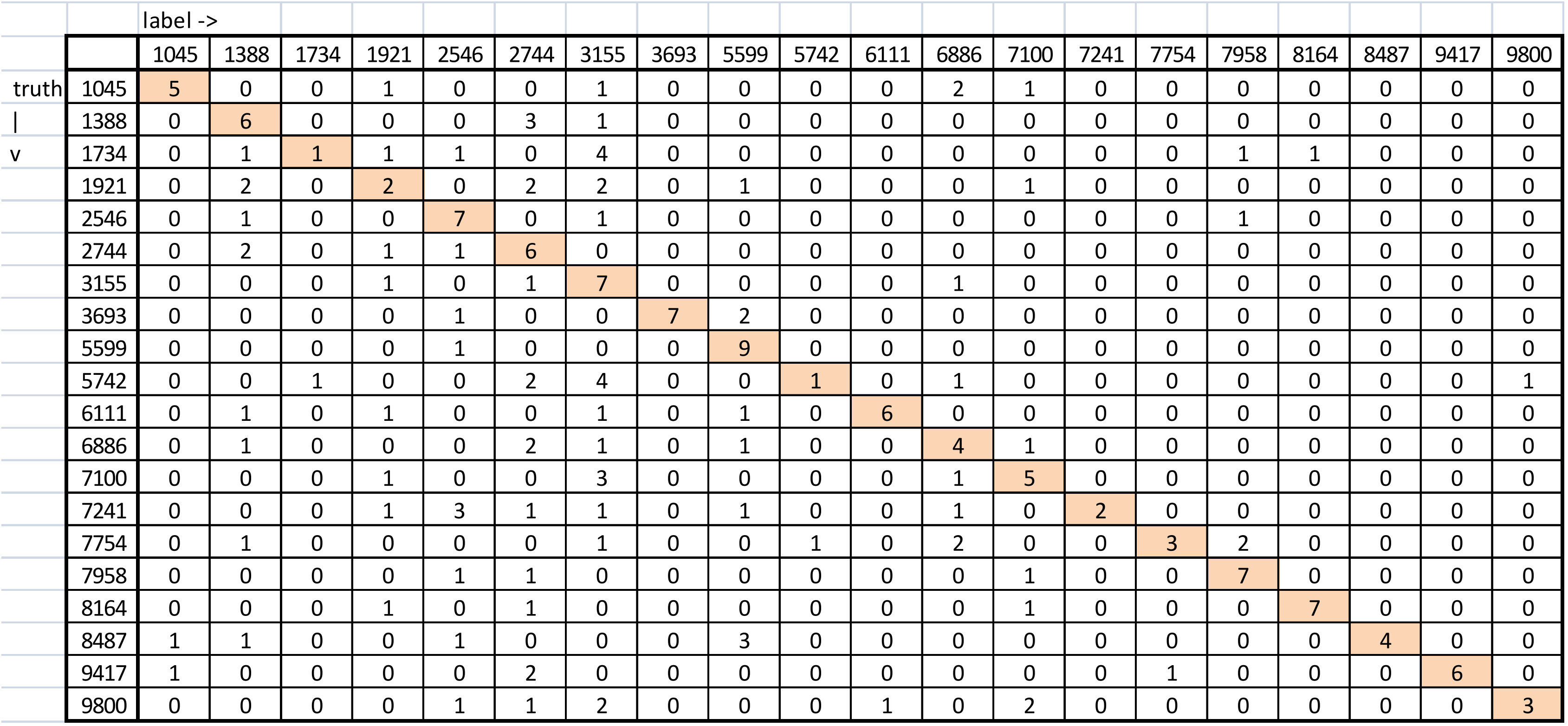

		label ->																			
		1045	1388	1734	1921	2546	2744	3155	3693	5599	5742	6111	6886	7100	7241	7754	7958	8164	8487	9417	9800
truth	1045	5	0	0	1	0	0	1	0	0	0	0	2	1	0	0	0	0	0	0	0
|	1388	0	6	0	0	0	3	1	0	0	0	0	0	0	0	0	0	0	0	0	0
v	1734	0	1	1	1	1	0	4	0	0	0	0	0	0	0	0	1	1	0	0	0
	1921	0	2	0	2	0	2	2	0	1	0	0	0	1	0	0	0	0	0	0	0
	2546	0	1	0	0	7	0	1	0	0	0	0	0	0	0	0	1	0	0	0	0
	2744	0	2	0	1	1	6	0	0	0	0	0	0	0	0	0	0	0	0	0	0
	3155	0	0	0	1	0	1	7	0	0	0	0	1	0	0	0	0	0	0	0	0
	3693	0	0	0	0	1	0	0	7	2	0	0	0	0	0	0	0	0	0	0	0
	5599	0	0	0	0	1	0	0	0	9	0	0	0	0	0	0	0	0	0	0	0
	5742	0	0	1	0	0	2	4	0	0	1	0	1	0	0	0	0	0	0	0	1
	6111	0	1	0	1	0	0	1	0	1	0	6	0	0	0	0	0	0	0	0	0
	6886	0	1	0	0	0	2	1	0	1	0	0	4	1	0	0	0	0	0	0	0
	7100	0	0	0	1	0	0	3	0	0	0	0	1	5	0	0	0	0	0	0	0
	7241	0	0	0	1	3	1	1	0	1	0	0	1	0	2	0	0	0	0	0	0
	7754	0	1	0	0	0	0	1	0	0	1	0	2	0	0	3	2	0	0	0	0
	7958	0	0	0	0	1	1	0	0	0	0	0	0	1	0	0	7	0	0	0	0
	8164	0	0	0	1	0	1	0	0	0	0	0	0	1	0	0	0	7	0	0	0
	8487	1	1	0	0	1	0	0	0	3	0	0	0	0	0	0	0	0	4	0	0
	9417	1	0	0	0	0	2	0	0	0	0	0	0	0	0	1	0	0	0	6	0
	9800	0	0	0	0	1	1	2	0	0	0	1	0	2	0	0	0	0	0	0	3

Table 24. Confusion Matrix for 50 Tweets per Author With One Tweet per Document

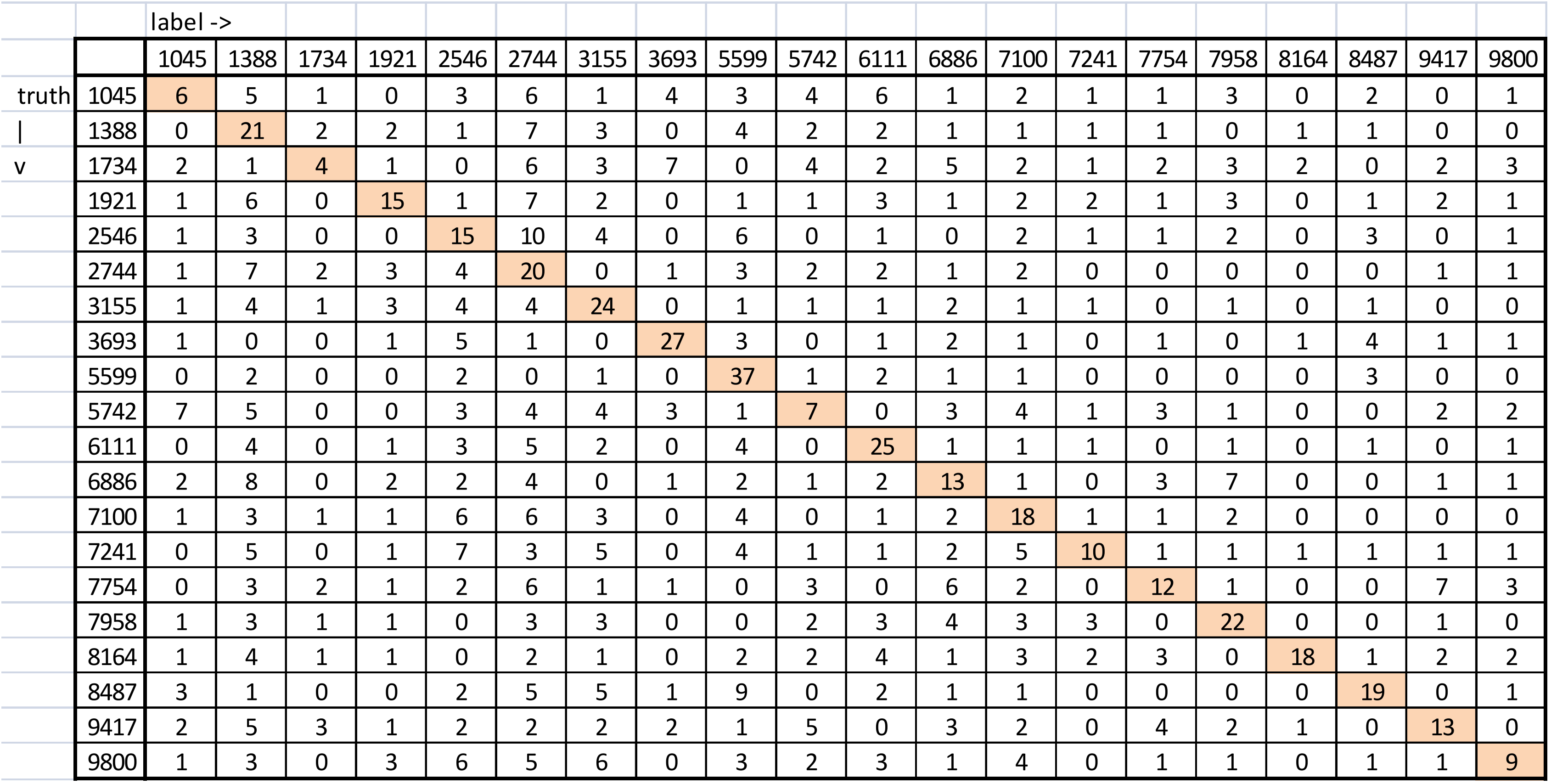

		label ->																			
		1045	1388	1734	1921	2546	2744	3155	3693	5599	5742	6111	6886	7100	7241	7754	7958	8164	8487	9417	9800
truth	1045	6	5	1	0	3	6	1	4	3	4	6	1	2	1	1	3	0	2	0	1
|	1388	0	21	2	2	1	7	3	0	4	2	2	1	1	1	1	0	1	1	0	0
v	1734	2	1	4	1	0	6	3	7	0	4	2	5	2	1	2	3	2	0	2	3
	1921	1	6	0	15	1	7	2	0	1	1	3	1	2	2	1	3	0	1	2	1
	2546	1	3	0	0	15	10	4	0	6	0	1	0	2	1	1	2	0	3	0	1
	2744	1	7	2	3	4	20	0	1	3	2	2	1	2	0	0	0	0	0	1	1
	3155	1	4	1	3	4	4	24	0	1	1	1	2	1	1	0	1	0	1	0	0
	3693	1	0	0	1	5	1	0	27	3	0	1	2	1	0	1	0	1	4	1	1
	5599	0	2	0	0	2	0	1	0	37	1	2	1	1	0	0	0	0	3	0	0
	5742	7	5	0	0	3	4	4	3	1	7	0	3	4	1	3	1	0	0	2	2
	6111	0	4	0	1	3	5	2	0	4	0	25	1	1	1	0	1	0	1	0	1
	6886	2	8	0	2	2	4	0	1	2	1	2	13	1	0	3	7	0	0	1	1
	7100	1	3	1	1	6	6	3	0	4	0	1	2	18	1	1	2	0	0	0	0
	7241	0	5	0	1	7	3	5	0	4	1	1	2	5	10	1	1	1	1	1	1
	7754	0	3	2	1	2	6	1	1	0	3	0	6	2	0	12	1	0	0	7	3
	7958	1	3	1	1	0	3	3	0	0	2	3	4	3	3	0	22	0	0	1	0
	8164	1	4	1	1	0	2	1	0	2	2	4	1	3	2	3	0	18	1	2	2
	8487	3	1	0	0	2	5	5	1	9	0	2	1	1	0	0	0	0	19	0	1
	9417	2	5	3	1	2	2	2	2	1	5	0	3	2	0	4	2	1	0	13	0
	9800	1	3	0	3	6	5	6	0	3	2	3	1	4	0	1	1	0	1	1	9

Table 25. Confusion Matrix for 50 Tweets per Author With Three Tweets per Document

		label ->																			
		1045	1388	1734	1921	2546	2744	3155	3693	5599	5742	6111	6886	7100	7241	7754	7958	8164	8487	9417	9800
truth	1045	5	1	1	0	0	1	2	0	1	3	0	0	0	0	0	2	0	0	1	0
|	1388	0	14	0	0	1	1	1	0	0	0	0	0	0	0	0	0	0	0	0	0
v	1734	0	1	1	0	0	4	2	0	0	2	0	2	0	0	2	1	1	0	1	0
	1921	0	4	0	5	1	4	2	0	0	0	0	0	0	0	0	1	0	0	0	0
	2546	0	2	0	0	11	1	0	0	1	0	1	0	0	0	0	1	0	0	0	0
	2744	0	3	0	0	2	10	1	0	0	0	0	0	1	0	0	0	0	0	0	0
	3155	0	2	0	1	0	1	13	0	0	0	0	0	0	0	0	0	0	0	0	0
	3693	0	0	0	0	2	0	0	11	1	0	0	1	0	0	0	0	0	2	0	0
	5599	0	0	0	0	1	0	0	0	16	0	0	0	0	0	0	0	0	0	0	0
	5742	1	1	1	1	0	2	1	0	0	5	0	2	1	0	1	0	0	0	0	1
	6111	0	0	0	3	2	2	1	0	0	0	8	0	0	1	0	0	0	0	0	0
	6886	0	4	0	0	1	2	0	0	1	0	0	5	1	0	0	2	0	0	1	0
	7100	0	0	0	0	3	3	1	0	1	0	0	0	9	0	0	0	0	0	0	0
	7241	0	0	0	1	4	2	1	0	1	0	0	1	0	6	0	0	0	0	0	1
	7754	2	1	1	0	2	1	1	0	0	2	0	2	0	0	1	2	0	0	2	0
	7958	2	1	0	1	0	0	0	0	0	0	0	3	0	1	0	9	0	0	0	0
	8164	0	2	0	2	0	0	0	0	1	0	1	1	1	0	1	0	8	0	0	0
	8487	0	1	0	0	3	0	1	0	0	1	0	0	0	0	0	1	0	10	0	0
	9417	0	1	0	1	1	2	0	0	0	0	0	2	1	0	1	1	0	0	7	0
	9800	0	0	0	1	3	1	2	0	0	1	2	1	2	0	0	0	0	0	0	4

Table 26. Confusion Matrix for 50 Tweets per Author With Five Tweets per Document

		label ->																			
		1045	1388	1734	1921	2546	2744	3155	3693	5599	5742	6111	6886	7100	7241	7754	7958	8164	8487	9417	9800
truth	1045	5	0	1	0	1	1	0	0	0	0	0	1	0	0	0	1	0	0	0	0
|	1388	0	9	0	0	1	0	0	0	0	0	0	0	0	0	0	0	0	0	0	0
v	1734	0	0	0	0	0	5	1	0	0	1	0	0	0	0	1	1	0	0	1	0
	1921	0	2	0	3	0	2	2	0	0	0	1	0	0	0	0	0	0	0	0	0
	2546	0	0	0	0	9	0	0	0	0	0	1	0	0	0	0	0	0	0	0	0
	2744	0	1	0	0	0	9	0	0	0	0	0	0	0	0	0	0	0	0	0	0
	3155	0	1	0	1	0	0	8	0	0	0	0	0	0	0	0	0	0	0	0	0
	3693	1	0	0	0	0	0	0	8	1	0	0	0	0	0	0	0	0	0	0	0
	5599	0	0	0	0	0	0	0	0	10	0	0	0	0	0	0	0	0	0	0	0
	5742	0	1	2	1	0	1	3	0	0	2	0	0	0	0	0	0	0	0	0	0
	6111	0	1	0	0	0	1	0	0	0	0	8	0	0	0	0	0	0	0	0	0
	6886	0	3	0	0	2	0	0	0	0	0	0	4	0	0	0	1	0	0	0	0
	7100	0	0	0	0	2	1	0	0	0	0	0	0	7	0	0	0	0	0	0	0
	7241	0	1	0	1	2	2	0	0	0	0	0	0	0	4	0	0	0	0	0	0
	7754	0	1	0	0	1	2	0	0	0	1	0	2	0	0	2	1	0	0	0	0
	7958	1	0	0	1	0	0	0	0	0	0	0	1	0	0	0	7	0	0	0	0
	8164	0	2	0	0	0	0	0	0	0	0	0	1	0	0	0	0	7	0	0	0
	8487	0	0	0	0	2	0	0	0	1	0	0	0	0	0	0	0	0	7	0	0
	9417	1	1	0	0	0	2	0	0	0	0	0	0	0	0	0	1	0	0	5	0
	9800	0	0	0	1	2	0	0	0	0	0	0	2	1	0	0	0	0	0	0	4

Table 27. Confusion Matrix for 120 Tweets per Author With One Tweet per Document

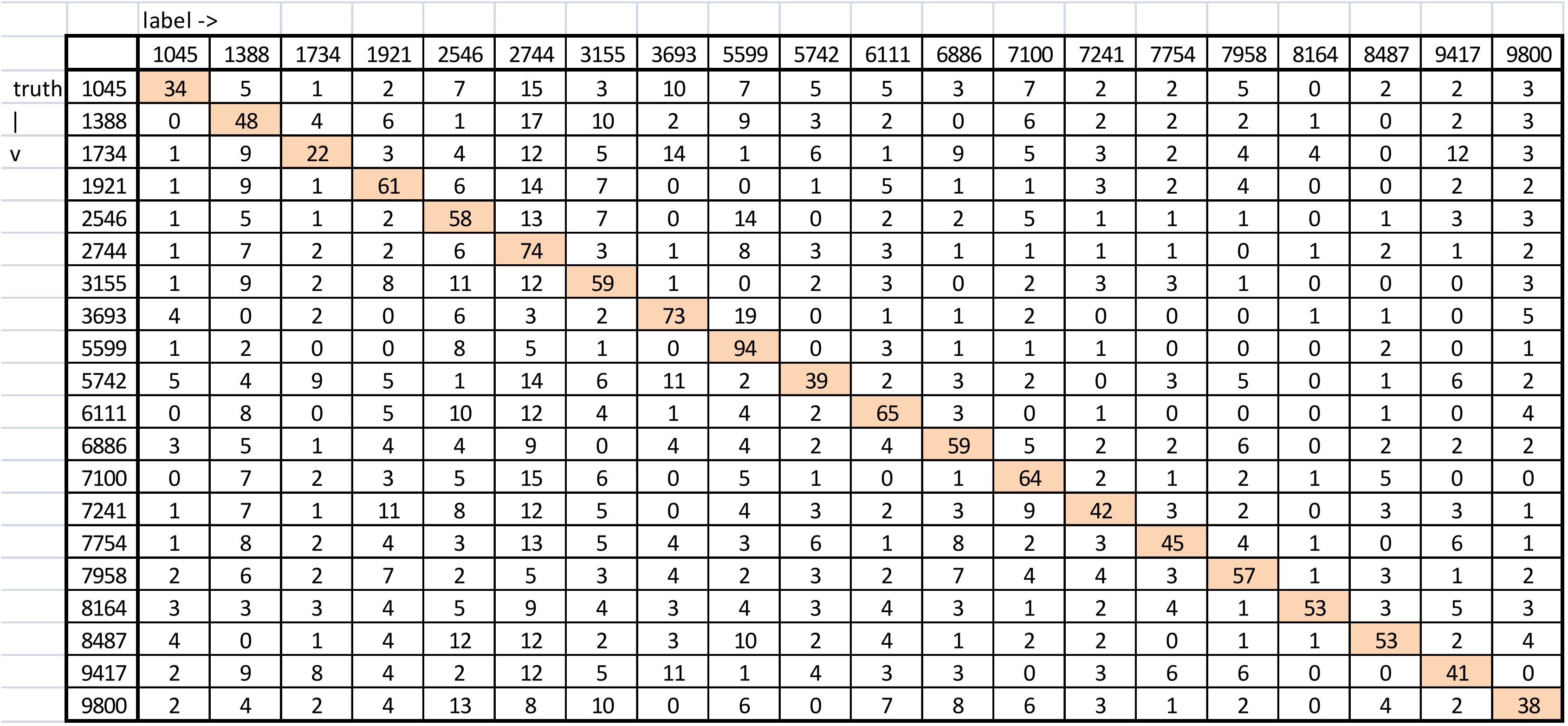

		label ->																			
		1045	1388	1734	1921	2546	2744	3155	3693	5599	5742	6111	6886	7100	7241	7754	7958	8164	8487	9417	9800
truth	1045	34	5	1	2	7	15	3	10	7	5	5	3	7	2	2	5	0	2	2	3
|	1388	0	48	4	6	1	17	10	2	9	3	2	0	6	2	2	2	1	0	2	3
v	1734	1	9	22	3	4	12	5	14	1	6	1	9	5	3	2	4	4	0	12	3
	1921	1	9	1	61	6	14	7	0	0	1	5	1	1	3	2	4	0	0	2	2
	2546	1	5	1	2	58	13	7	0	14	0	2	2	5	1	1	1	0	1	3	3
	2744	1	7	2	2	6	74	3	1	8	3	3	1	1	1	1	0	1	2	1	2
	3155	1	9	2	8	11	12	59	1	0	2	3	0	2	3	3	1	0	0	0	3
	3693	4	0	2	0	6	3	2	73	19	0	1	1	2	0	0	0	1	1	0	5
	5599	1	2	0	0	8	5	1	0	94	0	3	1	1	1	0	0	0	2	0	1
	5742	5	4	9	5	1	14	6	11	2	39	2	3	2	0	3	5	0	1	6	2
	6111	0	8	0	5	10	12	4	1	4	2	65	3	0	1	0	0	0	1	0	4
	6886	3	5	1	4	4	9	0	4	4	2	4	59	5	2	2	6	0	2	2	2
	7100	0	7	2	3	5	15	6	0	5	1	0	1	64	2	1	2	1	5	0	0
	7241	1	7	1	11	8	12	5	0	4	3	2	3	9	42	3	2	0	3	3	1
	7754	1	8	2	4	3	13	5	4	3	6	1	8	2	3	45	4	1	0	6	1
	7958	2	6	2	7	2	5	3	4	2	3	2	7	4	4	3	57	1	3	1	2
	8164	3	3	3	4	5	9	4	3	4	3	4	3	1	2	4	1	53	3	5	3
	8487	4	0	1	4	12	12	2	3	10	2	4	1	2	2	0	1	1	53	2	4
	9417	2	9	8	4	2	12	5	11	1	4	3	3	0	3	6	6	0	0	41	0
	9800	2	4	2	4	13	8	10	0	6	0	7	8	6	3	1	2	0	4	2	38

Table 28. Confusion Matrix for 120 Tweets per Author With Three Tweets per Document

		label ->																			
		1045	1388	1734	1921	2546	2744	3155	3693	5599	5742	6111	6886	7100	7241	7754	7958	8164	8487	9417	9800
truth	1045	21	3	0	1	1	3	0	3	1	0	0	0	1	0	0	3	0	1	2	0
|	1388	0	31	0	0	0	6	2	0	0	0	0	0	0	0	0	0	0	0	0	1
v	1734	0	3	9	0	0	6	2	1	0	5	0	1	0	0	1	4	1	0	7	0
	1921	1	0	0	32	0	4	1	0	0	1	0	0	0	0	0	1	0	0	0	0
	2546	0	0	0	0	30	5	0	0	1	0	1	0	0	0	0	1	0	1	0	1
	2744	0	2	0	0	3	34	1	0	0	0	0	0	0	0	0	0	0	0	0	0
	3155	0	2	0	1	2	1	32	0	0	0	0	0	0	0	1	0	0	0	1	0
	3693	1	0	0	0	1	1	0	31	5	0	0	0	0	0	0	1	0	0	0	0
	5599	0	0	0	0	1	1	0	0	38	0	0	0	0	0	0	0	0	0	0	0
	5742	0	2	2	2	0	8	2	1	0	18	0	1	2	0	1	0	0	0	1	0
	6111	0	0	0	0	1	4	1	0	0	0	34	0	0	0	0	0	0	0	0	0
	6886	0	0	0	0	1	6	0	0	0	0	1	29	1	0	0	1	0	1	0	0
	7100	0	1	0	0	1	4	0	0	0	0	0	0	33	0	0	1	0	0	0	0
	7241	0	1	0	3	2	7	1	0	1	0	0	0	1	23	0	0	0	0	1	0
	7754	0	3	0	1	0	7	1	0	0	2	0	2	0	0	23	0	0	0	1	0
	7958	1	1	0	1	0	2	0	0	0	2	0	0	2	0	0	29	0	0	2	0
	8164	0	1	0	1	2	1	0	1	0	0	1	1	2	0	0	0	30	0	0	0
	8487	0	0	0	1	4	2	0	0	0	0	1	0	1	1	0	0	0	29	0	1
	9417	0	1	1	1	1	5	1	0	0	2	1	0	0	0	1	1	0	0	25	0
	9800	0	2	0	4	1	4	4	0	0	0	1	2	1	0	0	0	0	2	0	19

Table 29. Confusion Matrix for 120 Tweets per Author With Five Tweets per Document

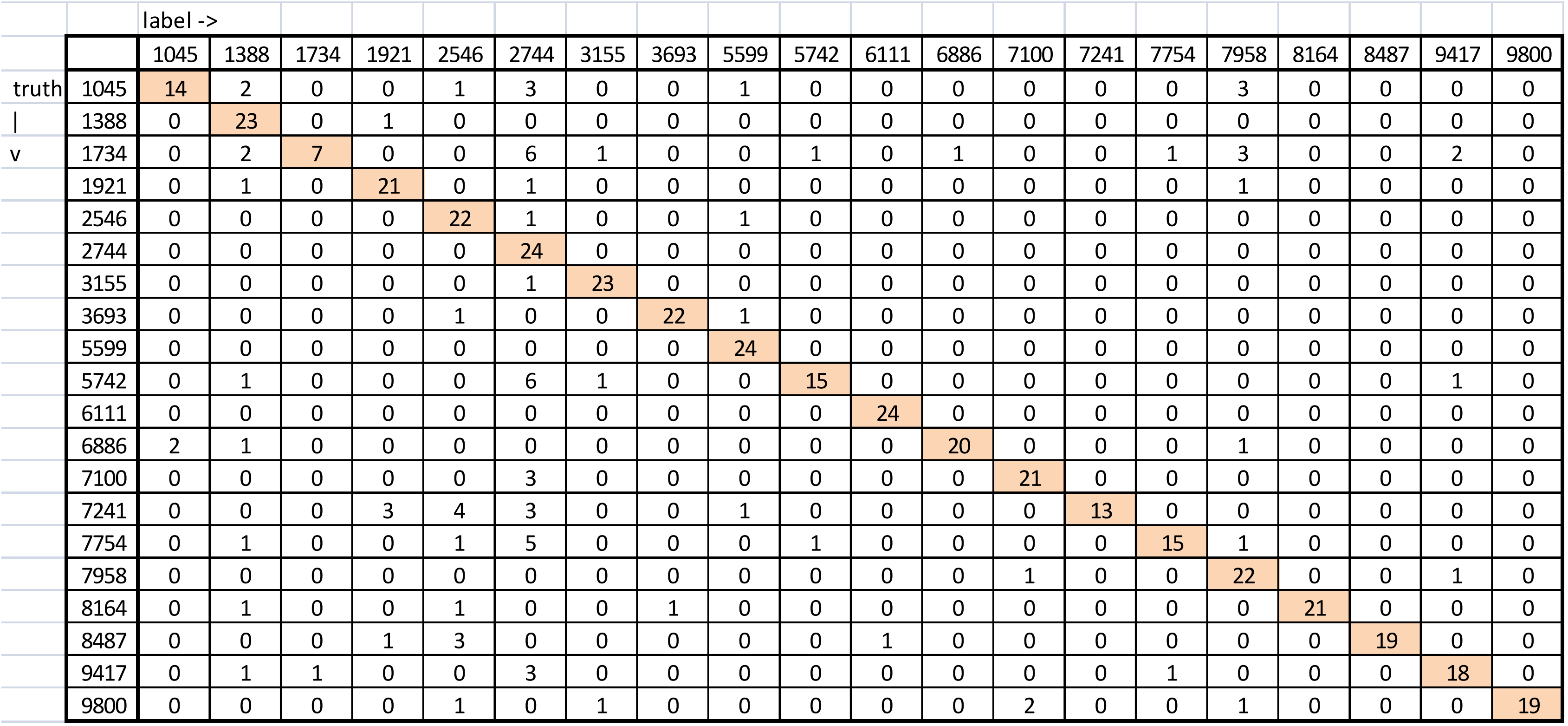

		label ->																			
		1045	1388	1734	1921	2546	2744	3155	3693	5599	5742	6111	6886	7100	7241	7754	7958	8164	8487	9417	9800
truth	1045	14	2	0	0	1	3	0	0	1	0	0	0	0	0	0	3	0	0	0	0
|	1388	0	23	0	1	0	0	0	0	0	0	0	0	0	0	0	0	0	0	0	0
v	1734	0	2	7	0	0	6	1	0	0	1	0	1	0	0	1	3	0	0	2	0
	1921	0	1	0	21	0	1	0	0	0	0	0	0	0	0	0	1	0	0	0	0
	2546	0	0	0	0	22	1	0	0	1	0	0	0	0	0	0	0	0	0	0	0
	2744	0	0	0	0	0	24	0	0	0	0	0	0	0	0	0	0	0	0	0	0
	3155	0	0	0	0	0	1	23	0	0	0	0	0	0	0	0	0	0	0	0	0
	3693	0	0	0	0	1	0	0	22	1	0	0	0	0	0	0	0	0	0	0	0
	5599	0	0	0	0	0	0	0	0	24	0	0	0	0	0	0	0	0	0	0	0
	5742	0	1	0	0	0	6	1	0	0	15	0	0	0	0	0	0	0	0	1	0
	6111	0	0	0	0	0	0	0	0	0	0	24	0	0	0	0	0	0	0	0	0
	6886	2	1	0	0	0	0	0	0	0	0	0	20	0	0	0	1	0	0	0	0
	7100	0	0	0	0	0	3	0	0	0	0	0	0	21	0	0	0	0	0	0	0
	7241	0	0	0	3	4	3	0	0	1	0	0	0	0	13	0	0	0	0	0	0
	7754	0	1	0	0	1	5	0	0	0	1	0	0	0	0	15	1	0	0	0	0
	7958	0	0	0	0	0	0	0	0	0	0	0	0	1	0	0	22	0	0	1	0
	8164	0	1	0	0	1	0	0	1	0	0	0	0	0	0	0	0	21	0	0	0
	8487	0	0	0	1	3	0	0	0	0	0	1	0	0	0	0	0	0	19	0	0
	9417	0	1	1	0	0	3	0	0	0	0	0	0	0	0	1	0	0	0	18	0
	9800	0	0	0	0	1	0	1	0	0	0	0	0	2	0	0	1	0	0	0	19

Table 30. Confusion Matrix for 150 Tweets per Author With One Tweet per Document

		label ->																			
		1045	1388	1734	1921	2546	2744	3155	3693	5599	5742	6111	6886	7100	7241	7754	7958	8164	8487	9417	9800
truth	1045	45	12	2	4	7	12	1	11	6	7	7	2	7	2	3	11	1	3	1	6
|	1388	2	68	3	7	7	21	11	2	3	5	2	2	5	1	3	2	0	2	1	3
v	1734	2	17	30	9	5	16	7	14	0	9	4	5	7	1	3	7	2	0	8	4
	1921	1	9	1	79	9	13	8	0	0	4	2	3	2	6	1	3	2	2	4	1
	2546	1	4	1	3	77	13	7	0	21	0	5	2	6	4	0	0	0	2	1	3
	2744	0	10	2	5	9	87	7	1	9	2	4	1	6	1	0	1	0	2	0	3
	3155	1	10	4	9	9	12	70	1	0	2	3	2	4	8	2	2	0	2	0	9
	3693	3	2	1	2	5	1	2	91	23	0	2	4	1	1	0	0	0	3	3	6
	5599	1	2	0	0	16	3	0	0	113	0	5	0	2	1	0	1	0	2	1	3
	5742	5	12	5	6	1	20	6	11	2	50	1	5	3	0	7	7	1	0	6	2
	6111	0	8	0	6	10	13	3	1	4	0	91	4	0	1	0	1	1	2	0	5
	6886	3	10	1	7	4	8	1	4	2	2	2	76	8	4	1	8	2	1	4	2
	7100	0	5	3	4	8	12	4	1	6	1	3	2	92	1	1	3	0	4	0	0
	7241	3	4	1	9	17	17	8	0	9	1	0	2	7	54	2	4	1	3	1	7
	7754	2	7	6	2	5	16	6	6	2	8	1	9	2	4	53	8	2	1	7	3
	7958	3	7	2	7	3	7	3	5	3	1	6	7	3	2	2	81	1	2	3	2
	8164	1	9	4	6	6	5	3	7	5	2	5	1	3	3	4	1	76	4	4	1
	8487	3	3	0	3	16	14	1	6	13	1	4	3	5	3	0	1	0	68	2	4
	9417	2	15	5	5	4	11	5	16	1	3	4	6	0	0	10	9	1	2	48	3
	9800	2	5	3	6	12	14	15	0	7	0	7	8	7	5	1	1	0	4	1	52

Table 31. Confusion Matrix for 150 Tweets per Author With Three Tweets per Document

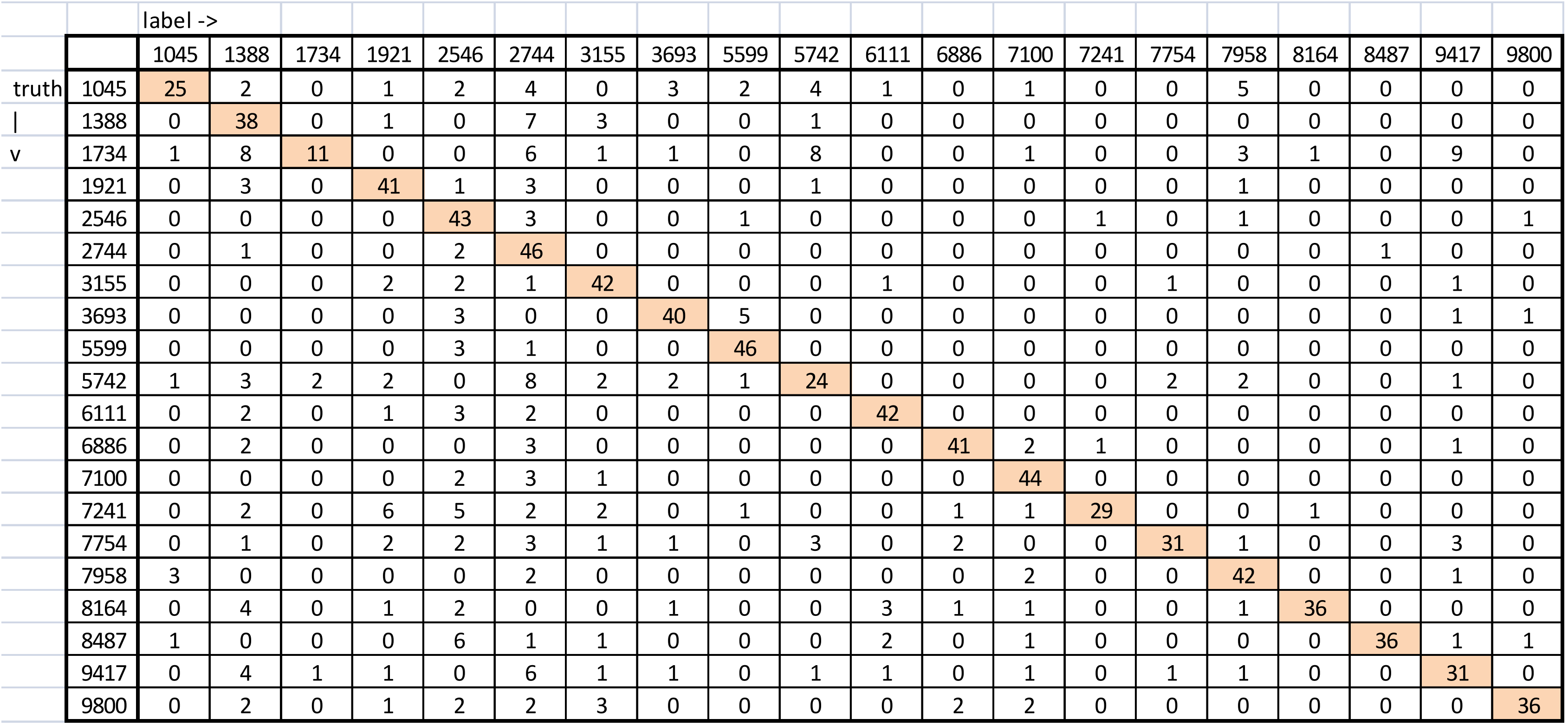

		label ->																			
		1045	1388	1734	1921	2546	2744	3155	3693	5599	5742	6111	6886	7100	7241	7754	7958	8164	8487	9417	9800
truth	1045	25	2	0	1	2	4	0	3	2	4	1	0	1	0	0	5	0	0	0	0
|	1388	0	38	0	1	0	7	3	0	0	1	0	0	0	0	0	0	0	0	0	0
v	1734	1	8	11	0	0	6	1	1	0	8	0	0	1	0	0	3	1	0	9	0
	1921	0	3	0	41	1	3	0	0	0	1	0	0	0	0	0	1	0	0	0	0
	2546	0	0	0	0	43	3	0	0	1	0	0	0	0	1	0	1	0	0	0	1
	2744	0	1	0	0	2	46	0	0	0	0	0	0	0	0	0	0	0	1	0	0
	3155	0	0	0	2	2	1	42	0	0	0	1	0	0	0	1	0	0	0	1	0
	3693	0	0	0	0	3	0	0	40	5	0	0	0	0	0	0	0	0	0	1	1
	5599	0	0	0	0	3	1	0	0	46	0	0	0	0	0	0	0	0	0	0	0
	5742	1	3	2	2	0	8	2	2	1	24	0	0	0	0	2	2	0	0	1	0
	6111	0	2	0	1	3	2	0	0	0	0	42	0	0	0	0	0	0	0	0	0
	6886	0	2	0	0	0	3	0	0	0	0	0	41	2	1	0	0	0	0	1	0
	7100	0	0	0	0	2	3	1	0	0	0	0	0	44	0	0	0	0	0	0	0
	7241	0	2	0	6	5	2	2	0	1	0	0	1	1	29	0	0	1	0	0	0
	7754	0	1	0	2	2	3	1	1	0	3	0	2	0	0	31	1	0	0	3	0
	7958	3	0	0	0	0	2	0	0	0	0	0	0	2	0	0	42	0	0	1	0
	8164	0	4	0	1	2	0	0	1	0	0	3	1	1	0	0	1	36	0	0	0
	8487	1	0	0	0	6	1	1	0	0	0	2	0	1	0	0	0	0	36	1	1
	9417	0	4	1	1	0	6	1	1	0	1	1	0	1	0	1	1	0	0	31	0
	9800	0	2	0	1	2	2	3	0	0	0	0	2	2	0	0	0	0	0	0	36

Table 32. Confusion Matrix for 150 Tweets per Author With Five Tweets per Document

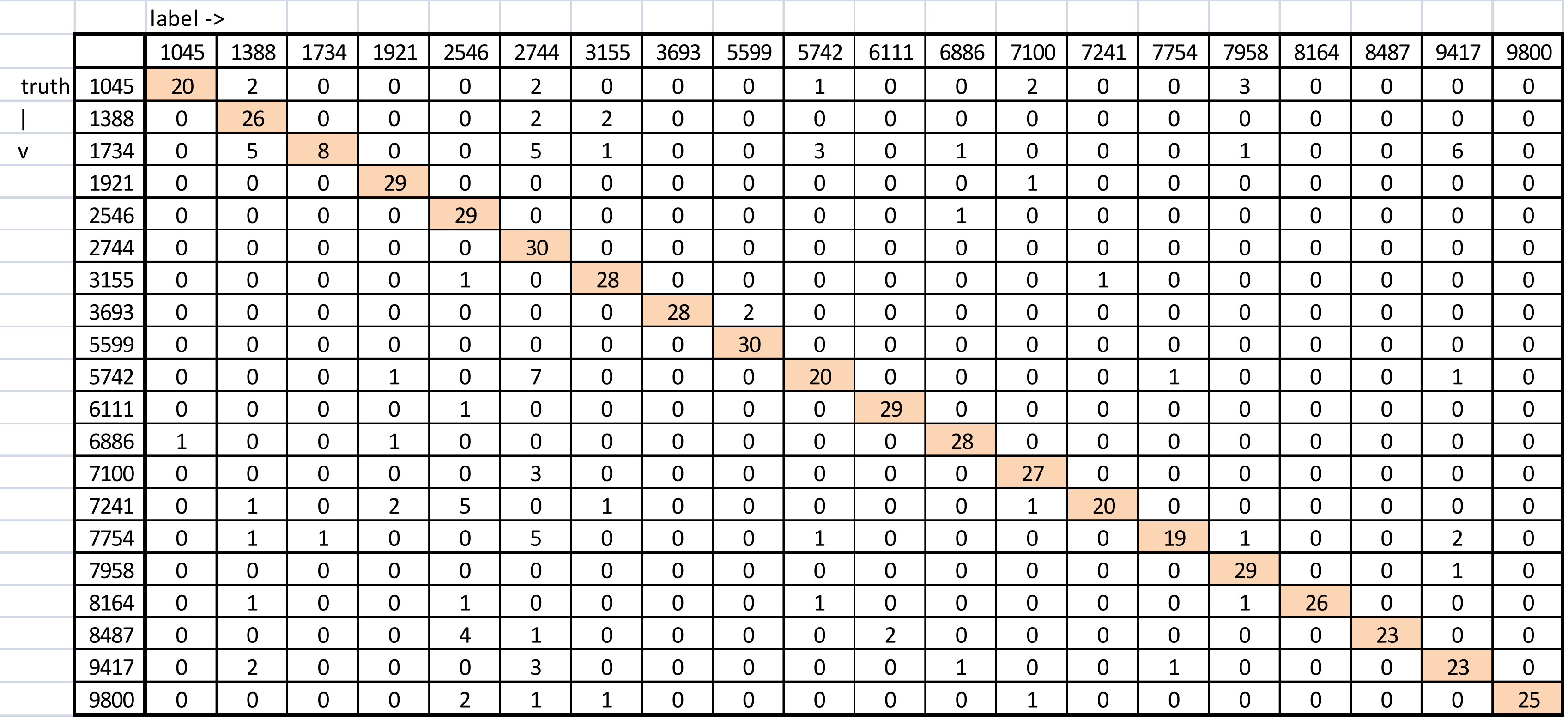

		label ->																			
		1045	1388	1734	1921	2546	2744	3155	3693	5599	5742	6111	6886	7100	7241	7754	7958	8164	8487	9417	9800
truth	1045	20	2	0	0	0	2	0	0	0	1	0	0	2	0	0	3	0	0	0	0
|	1388	0	26	0	0	0	2	2	0	0	0	0	0	0	0	0	0	0	0	0	0
v	1734	0	5	8	0	0	5	1	0	0	3	0	1	0	0	0	1	0	0	6	0
	1921	0	0	0	29	0	0	0	0	0	0	0	0	1	0	0	0	0	0	0	0
	2546	0	0	0	0	29	0	0	0	0	0	0	1	0	0	0	0	0	0	0	0
	2744	0	0	0	0	0	30	0	0	0	0	0	0	0	0	0	0	0	0	0	0
	3155	0	0	0	0	1	0	28	0	0	0	0	0	0	1	0	0	0	0	0	0
	3693	0	0	0	0	0	0	0	28	2	0	0	0	0	0	0	0	0	0	0	0
	5599	0	0	0	0	0	0	0	0	30	0	0	0	0	0	0	0	0	0	0	0
	5742	0	0	0	1	0	7	0	0	0	20	0	0	0	0	1	0	0	0	1	0
	6111	0	0	0	0	1	0	0	0	0	0	29	0	0	0	0	0	0	0	0	0
	6886	1	0	0	1	0	0	0	0	0	0	0	28	0	0	0	0	0	0	0	0
	7100	0	0	0	0	0	3	0	0	0	0	0	0	27	0	0	0	0	0	0	0
	7241	0	1	0	2	5	0	1	0	0	0	0	0	1	20	0	0	0	0	0	0
	7754	0	1	1	0	0	5	0	0	0	1	0	0	0	0	19	1	0	0	2	0
	7958	0	0	0	0	0	0	0	0	0	0	0	0	0	0	0	29	0	0	1	0
	8164	0	1	0	0	1	0	0	0	0	1	0	0	0	0	0	1	26	0	0	0
	8487	0	0	0	0	4	1	0	0	0	0	2	0	0	0	0	0	0	23	0	0
	9417	0	2	0	0	0	3	0	0	0	0	0	1	0	0	1	0	0	0	23	0
	9800	0	0	0	0	2	1	1	0	0	0	0	0	1	0	0	0	0	0	0	25

Table 33. Per Author Accuracy Rates for Various Total Tweets per Author and Tweets per Document

# Tweets	30		50			120			150		
Tweets per Document	1	3	1	3	5	1	3	5	1	3	5
1045	0.133	0.5	0.12	0.294	0.5	0.283	0.525	0.583	0.3	0.5	0.667
1388	0.2	0.6	0.42	0.824	0.9	0.4	0.775	0.958	0.453	0.76	0.867
1734	0.033	0.1	0.08	0.059	0	0.183	0.225	0.292	0.2	0.22	0.267
1921	0.133	0.2	0.3	0.294	0.3	0.508	0.8	0.875	0.527	0.82	0.967
2546	0.367	0.7	0.3	0.647	0.9	0.483	0.75	0.917	0.513	0.86	0.967
2744	0.333	0.6	0.4	0.588	0.9	0.617	0.85	1	0.58	0.92	1
3155	0.267	0.7	0.48	0.765	0.8	0.492	0.8	0.958	0.467	0.84	0.933
3693	0.6	0.7	0.54	0.647	0.8	0.608	0.775	0.917	0.607	0.8	0.933
5599	0.733	0.9	0.74	0.941	1	0.783	0.95	1	0.753	0.92	1
5742	0.067	0.1	0.14	0.294	0.2	0.325	0.45	0.625	0.333	0.48	0.667
6111	0.467	0.6	0.5	0.471	0.8	0.542	0.85	1	0.607	0.84	0.967
6886	0.3	0.4	0.26	0.294	0.4	0.492	0.725	0.833	0.507	0.82	0.933
7100	0.267	0.5	0.36	0.529	0.7	0.533	0.825	0.875	0.613	0.88	0.9
7241	0.167	0.2	0.2	0.353	0.4	0.35	0.575	0.542	0.36	0.58	0.667
7754	0.333	0.3	0.24	0.059	0.2	0.375	0.575	0.625	0.353	0.62	0.633
7958	0.267	0.7	0.44	0.529	0.7	0.475	0.725	0.917	0.54	0.84	0.967
8164	0.467	0.7	0.36	0.471	0.7	0.442	0.75	0.875	0.507	0.72	0.867
8487	0.267	0.4	0.38	0.588	0.7	0.442	0.725	0.792	0.453	0.72	0.767
9417	0.333	0.6	0.26	0.412	0.5	0.342	0.625	0.75	0.32	0.62	0.767
9800	0.167	0.3	0.18	0.235	0.4	0.317	0.475	0.792	0.347	0.72	0.833

APPENDIX C: TWEET SEND TIME ADDITIONAL DATA

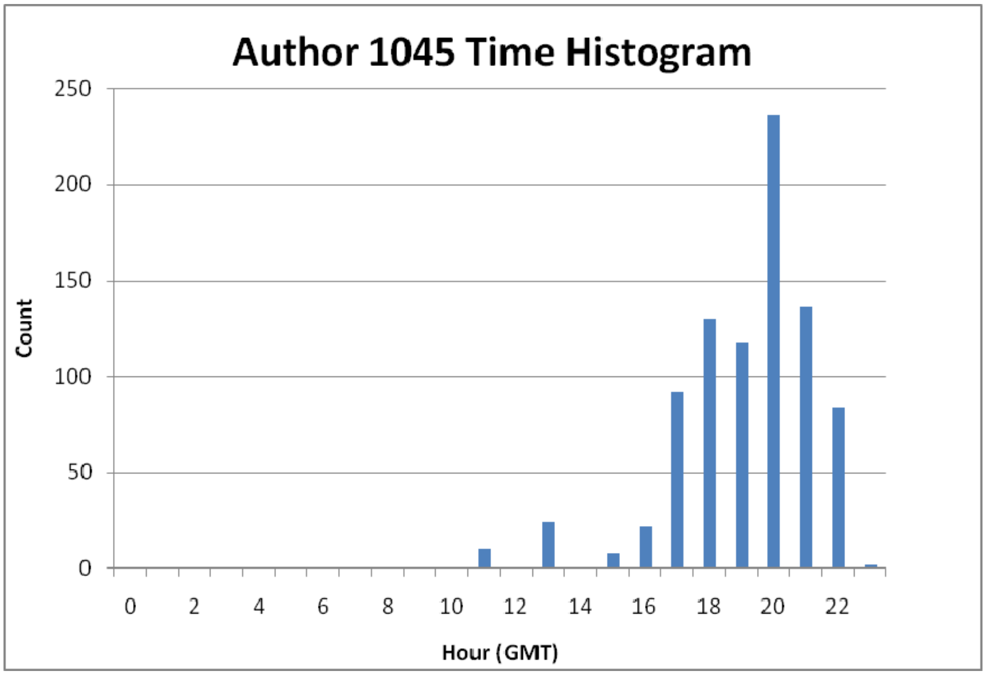

Figure 31. Author 1045 Tweet Send Time Histogram

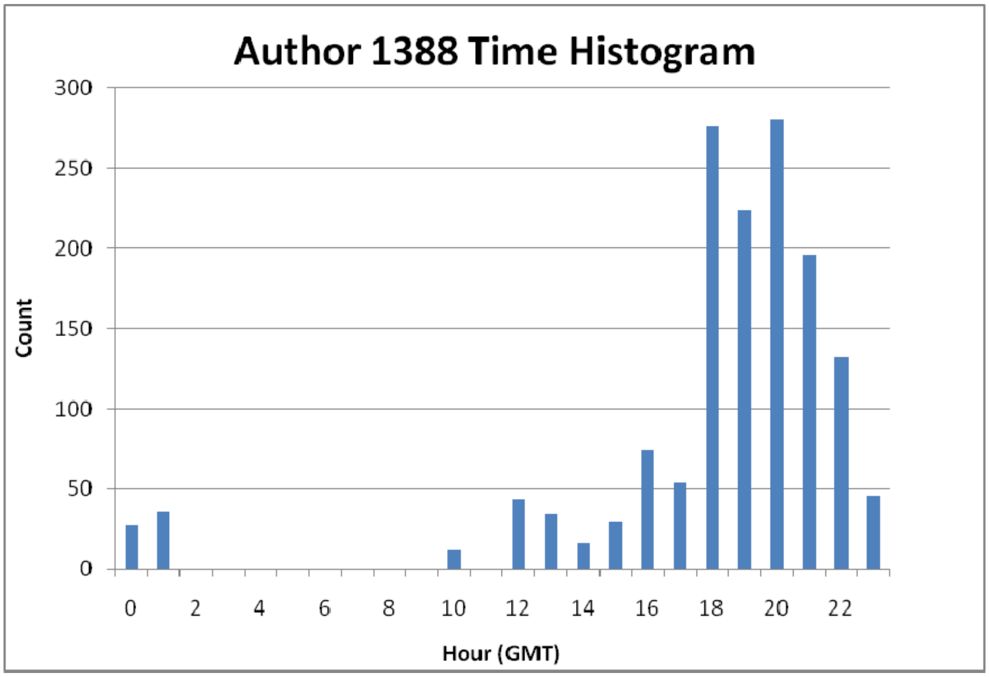

Figure 32. Author 1388 Tweet Send Time Histogram

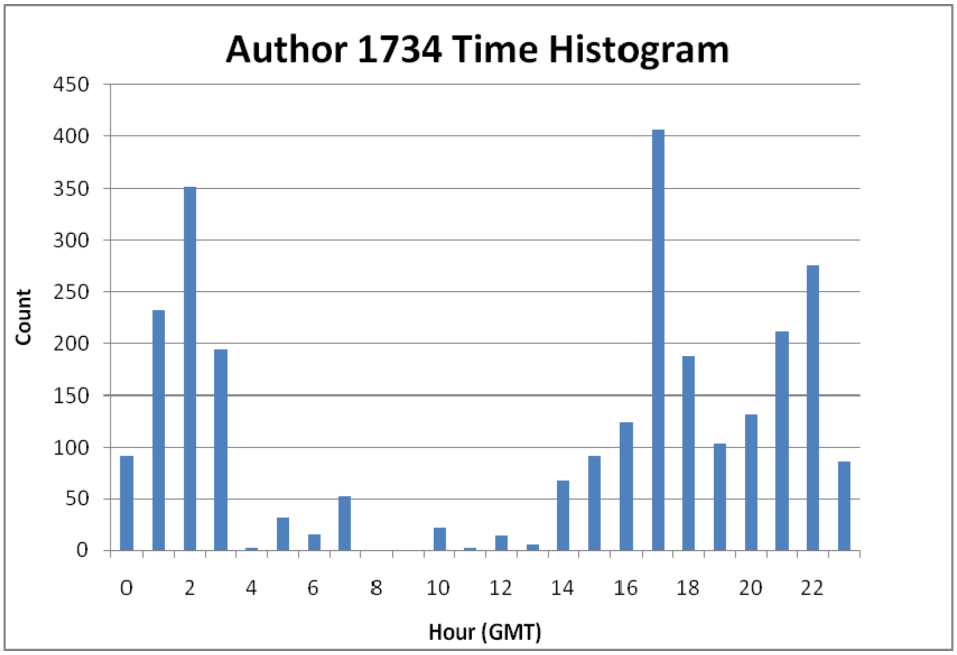

Figure 33. Author 1734 Tweet Send Time Histogram

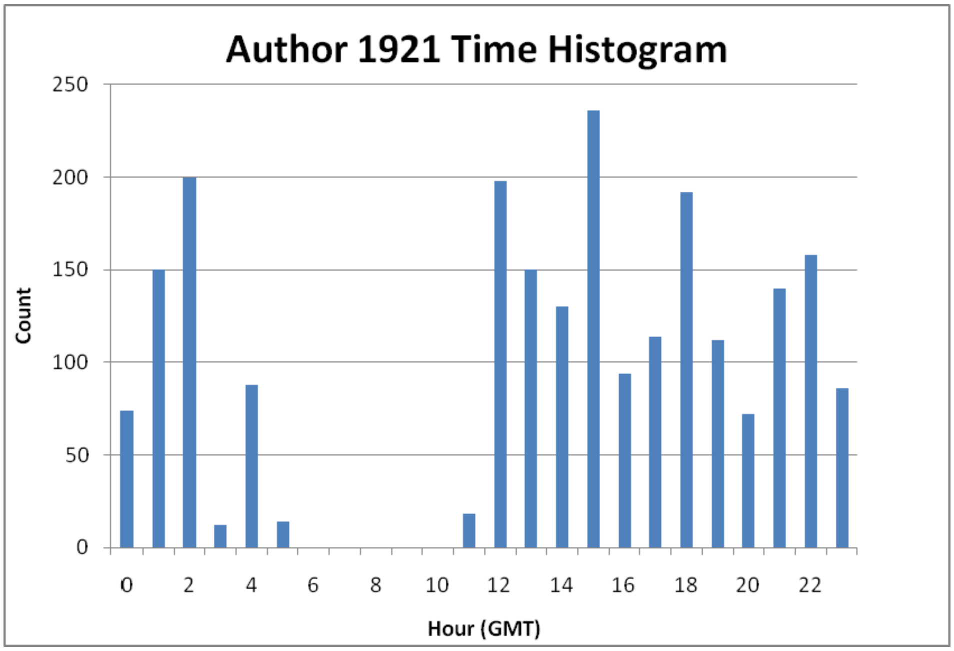

Figure 34. Author 1921 Tweet Send Time Histogram

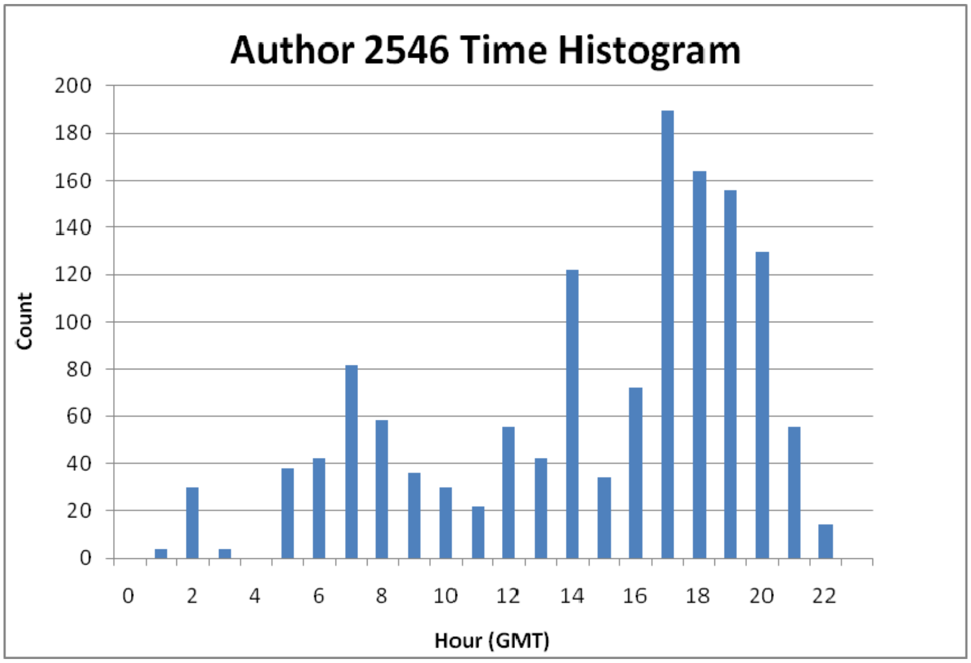

Figure 35. Author 2546 Tweet Send Time Histogram

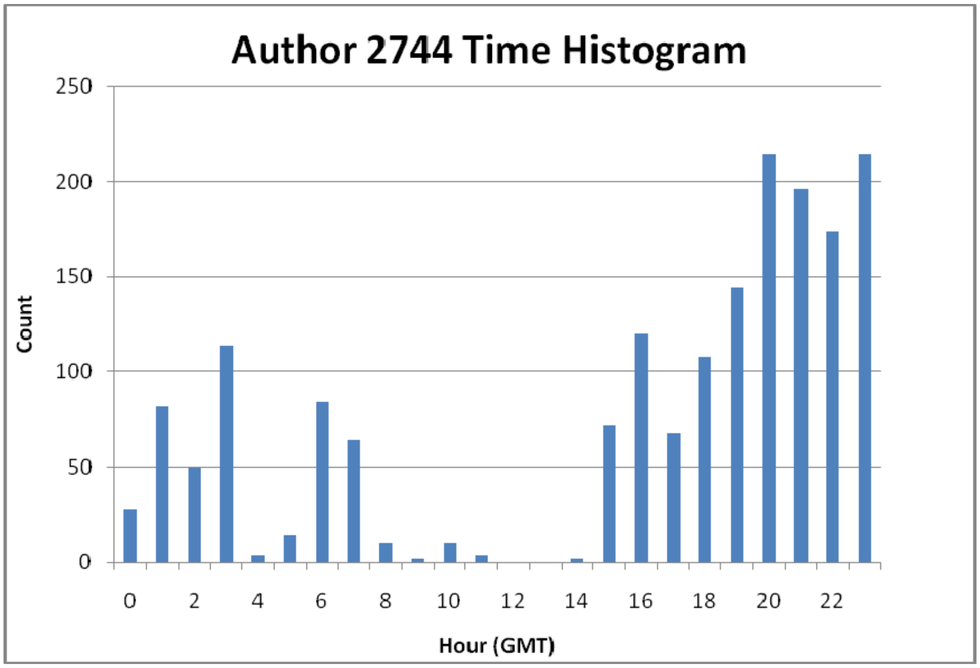

Figure 36. Author 2744 Tweet Send Time Histogram

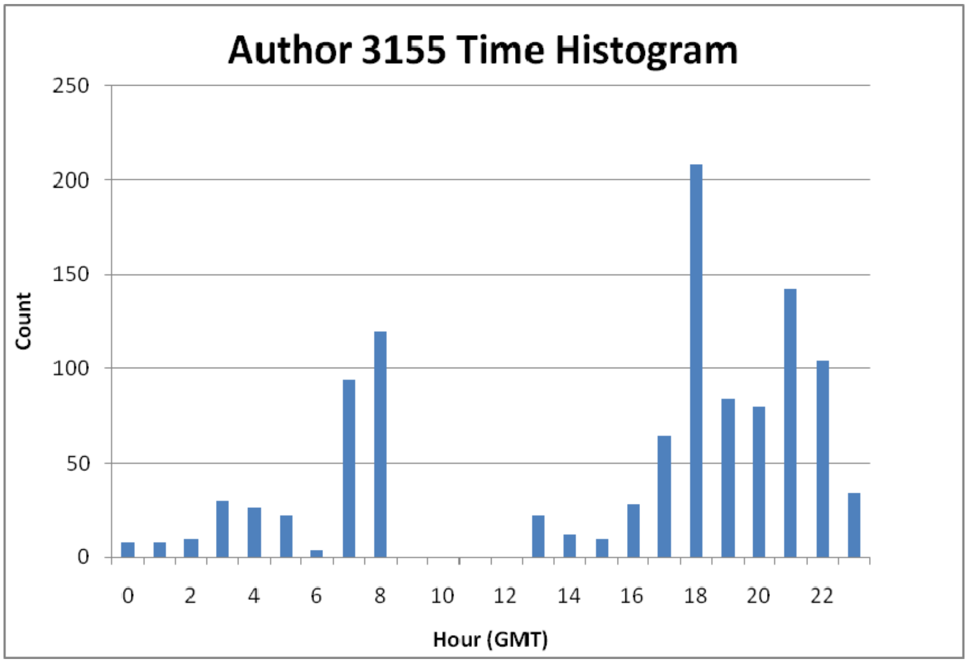

Figure 37. Author 3155 Tweet Send Time Histogram

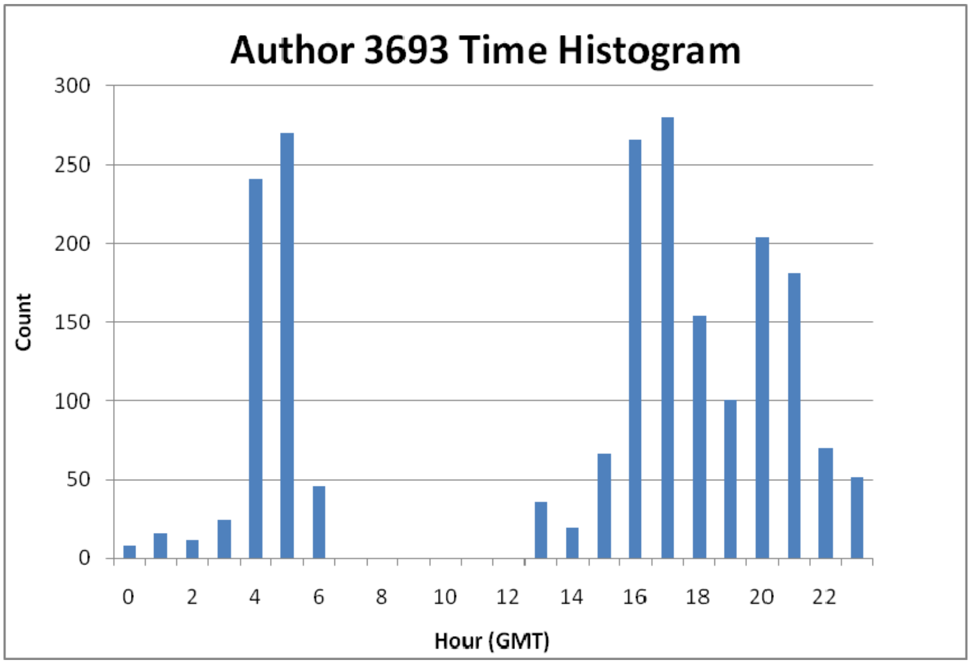

Figure 38. Author 3693 Tweet Send Time Histogram

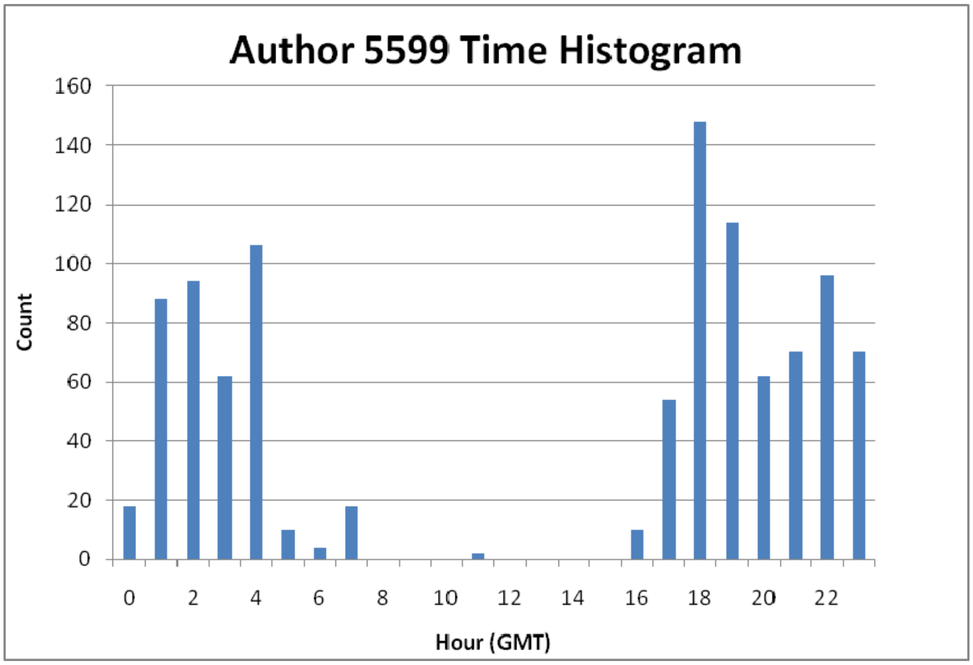

Figure 39. Author 5599 Tweet Send Time Histogram

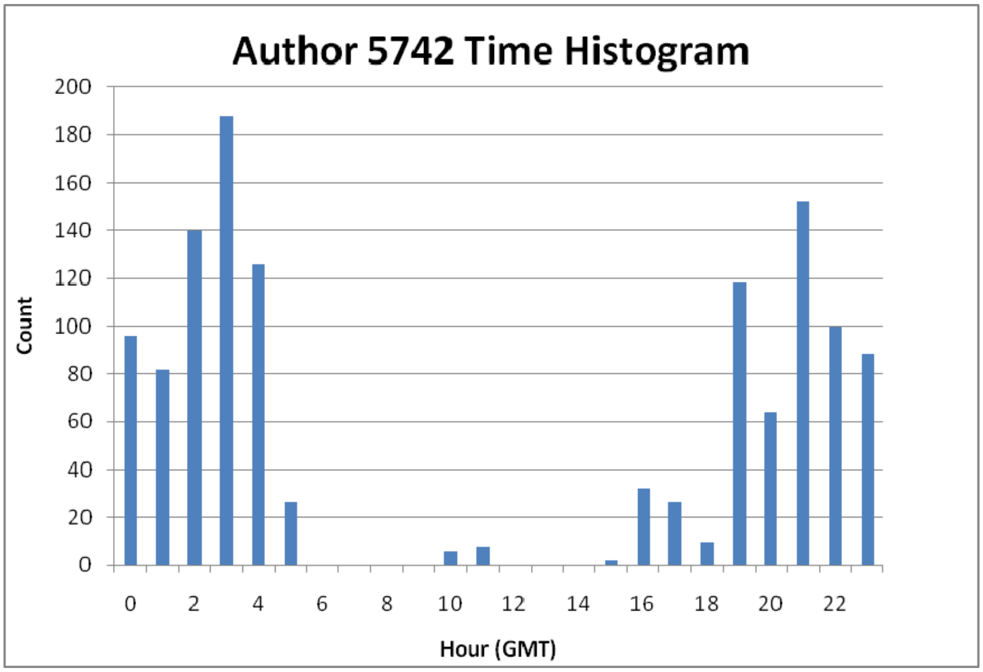

Figure 40. Author 5742 Tweet Send Time Histogram

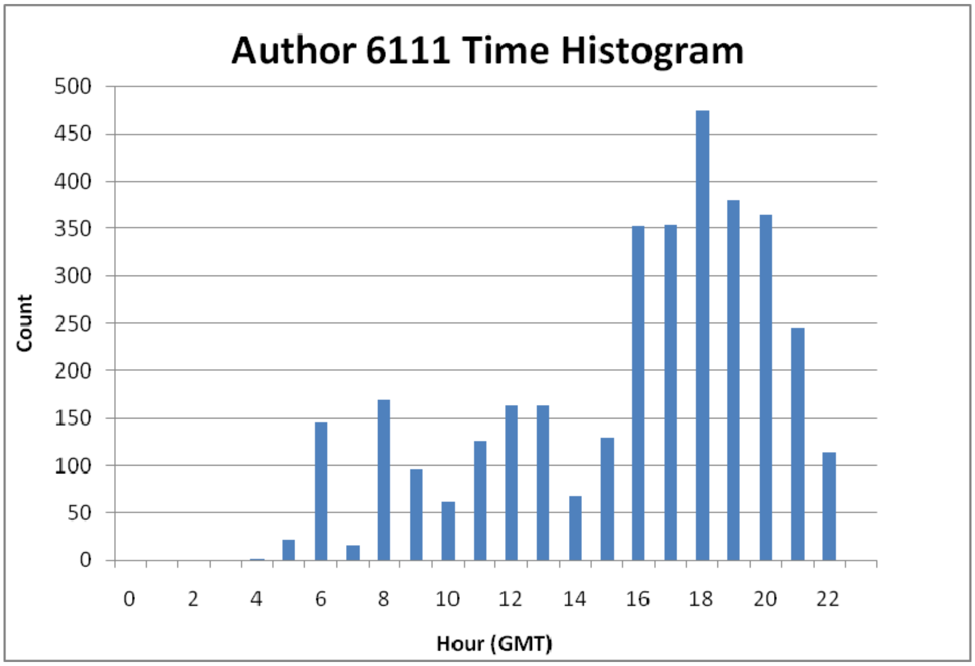

Figure 41. Author 6111 Tweet Send Time Histogram

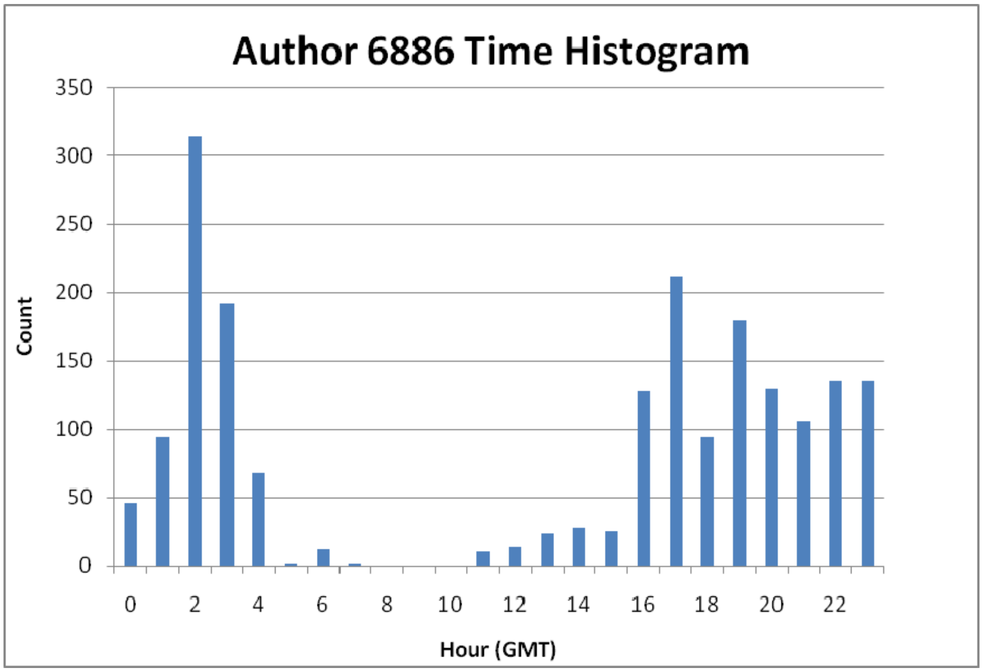

Figure 42. Author 6886 Tweet Send Time Histogram

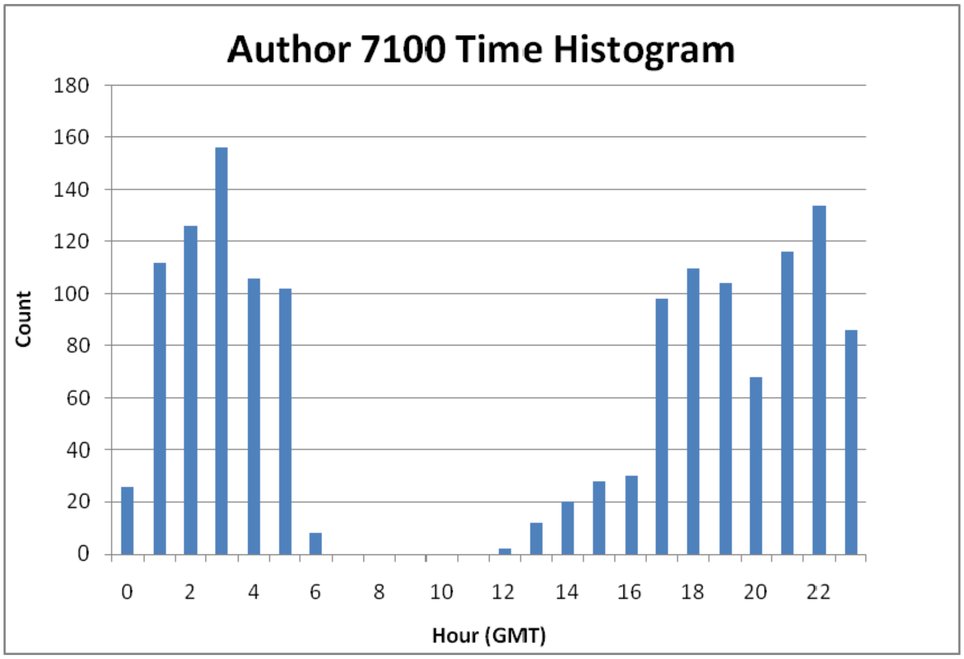

Figure 43. Author 7100 Tweet Send Time Histogram

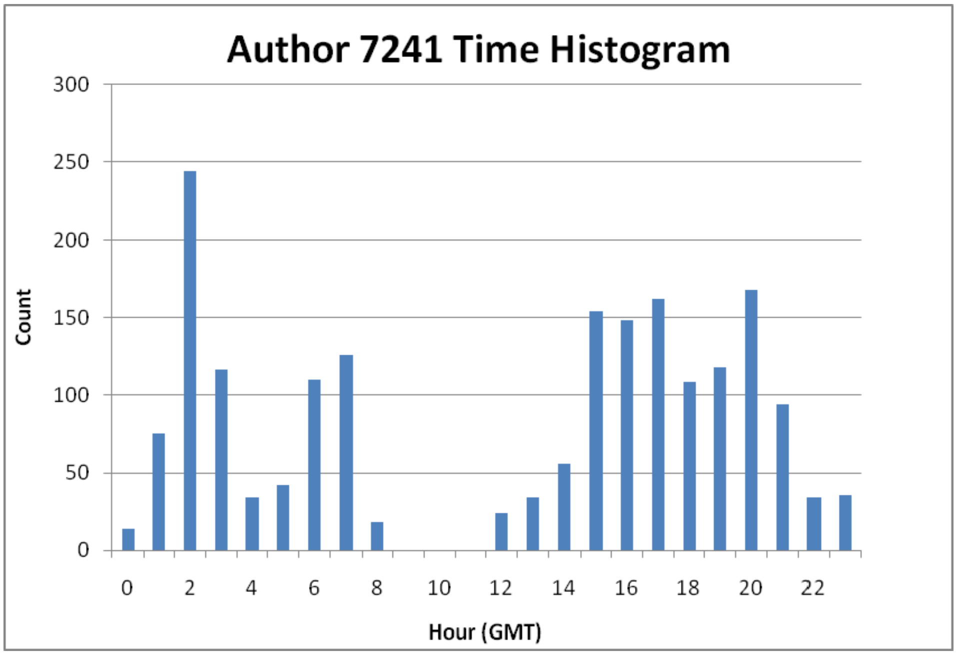

Figure 44. Author 7241 Tweet Send Time Histogram

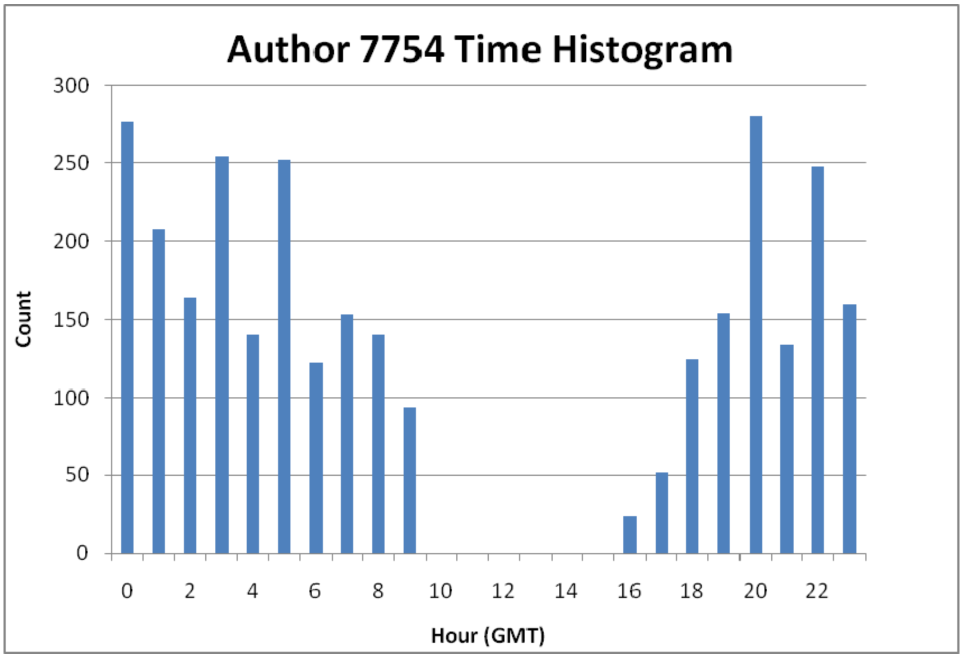

Figure 45.   Author 7754 Tweet Send Time Histogram

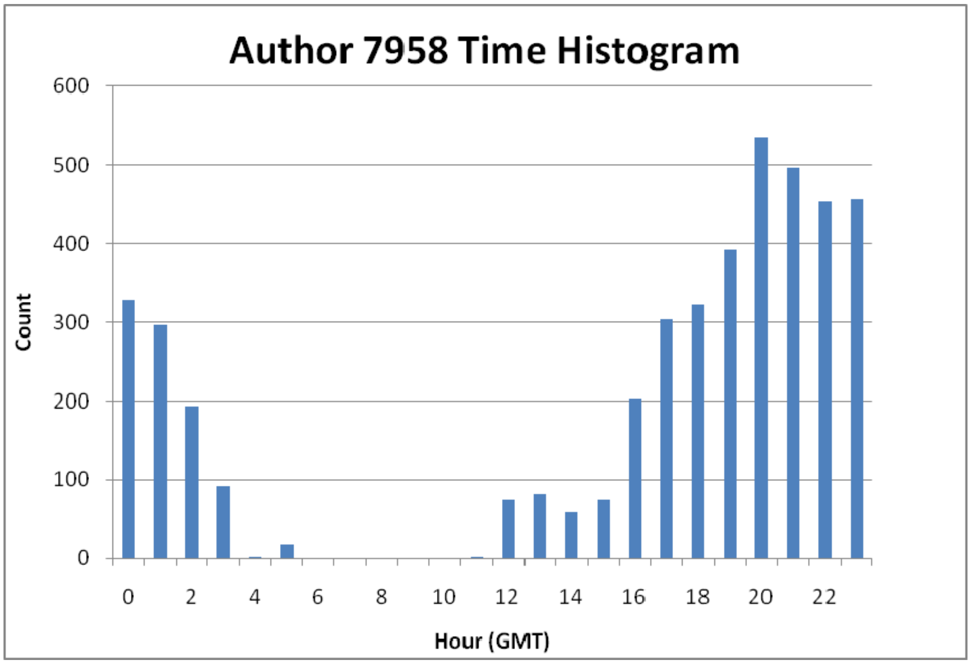

Figure 46.   Author 7958 Tweet Send Time Histogram

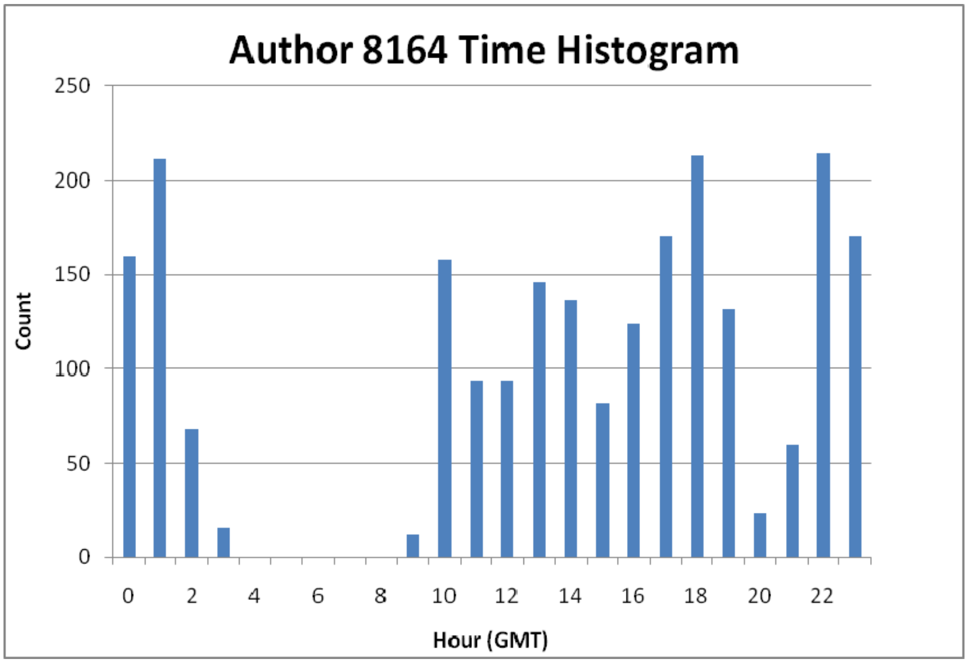

Figure 47. Author 8164 Tweet Send Time Histogram

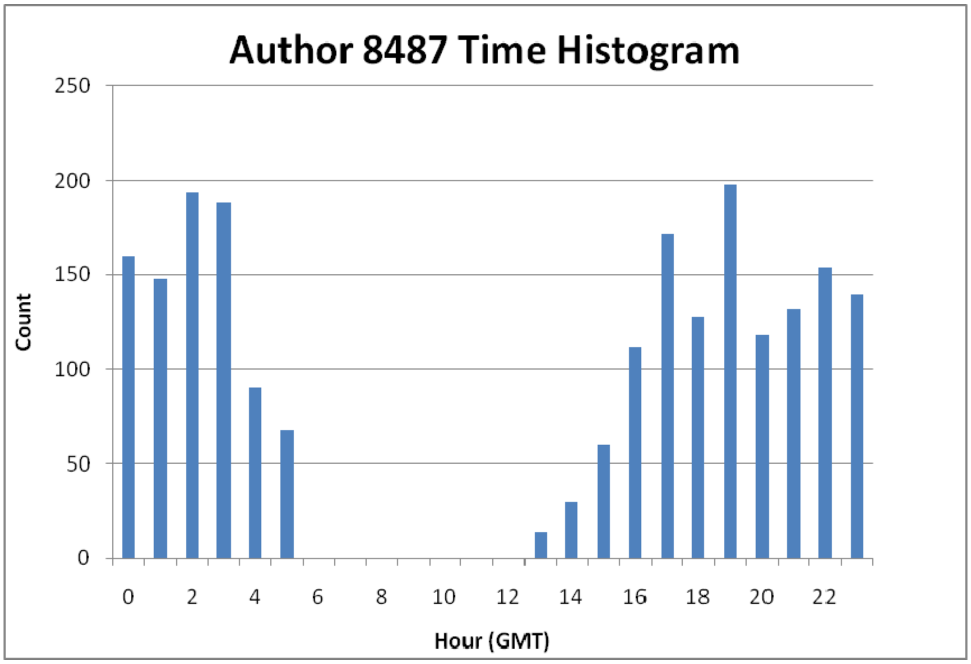

Figure 48. Author 8487 Tweet Send Time Histogram

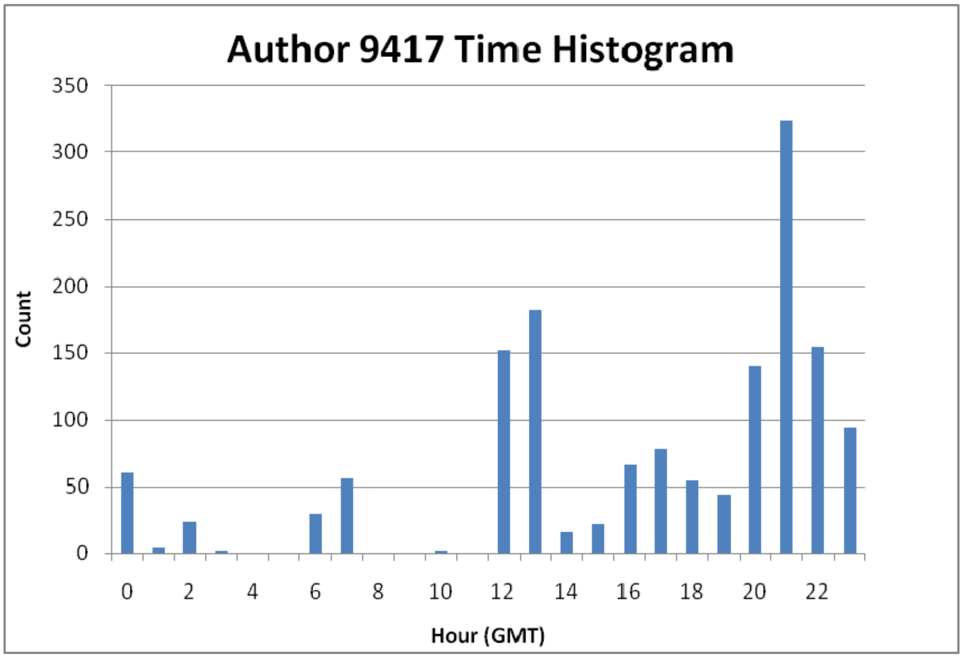

Figure 49. Author 9417 Tweet Send Time Histogram

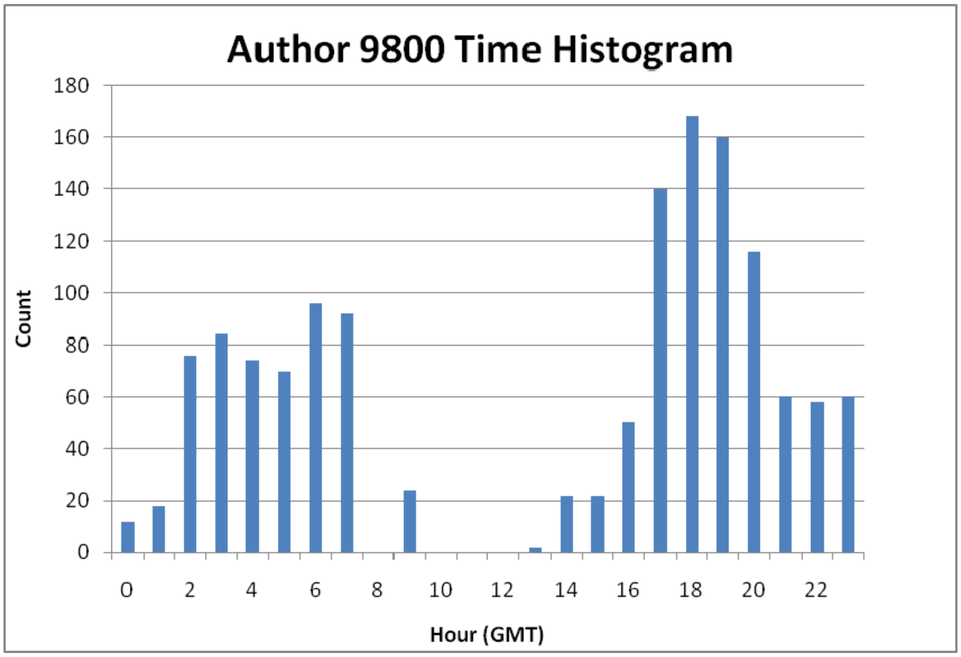

Figure 50. Author 9800 Tweet Send Time Histogram

APPENDIX D: PHONE CLASSIFIER ADDITIONAL DATA

Table 34. Confusion Matrix for 30 Signal Vectors per Phone With One Signal Vector per Training Set

		label																			
truth		bberry	htc371	htc373	htc374	htc375	htc376	htc601	htc_rob	iphone4	iphone5	iphone7	n8_594	n97_430	n97_444	n97_618	n97_620	nok_128	nok_e5	nok_e62	treo
	bberry	29	0	0	0	0	0	0	0	0	0	0	0	0	0	0	1	0	0	0	0
	htc371	0	27	2	0	0	0	0	0	0	0	0	0	0	0	0	0	1	0	0	0
	htc373	0	1	28	0	0	0	0	0	0	0	0	0	0	0	0	0	0	0	2	0
	htc374	0	0	0	25	0	4	0	0	0	0	0	0	0	0	0	0	0	0	1	0
	htc375	0	0	0	0	28	0	0	1	0	0	0	0	0	0	0	0	0	0	0	1
	htc376	1	0	1	5	0	22	0	0	0	0	0	0	0	0	0	0	0	0	1	0
	htc601	0	0	0	0	0	0	30	0	0	0	0	0	0	0	0	0	0	0	0	0
	htc_rob	0	0	0	0	0	0	0	28	0	0	1	0	0	0	0	0	0	0	1	0
	iphone4	1	0	0	0	0	0	0	0	22	3	1	3	0	0	0	0	0	0	0	0
	iphone5	0	0	0	0	0	0	0	0	6	21	3	0	0	0	0	0	0	0	0	0
	iphone7	1	0	0	0	0	0	1	2	3	6	9	0	0	3	2	0	1	2	0	0
	n8_594	0	0	0	0	0	0	0	0	0	0	0	30	0	0	0	0	0	0	0	0
	n97_430	0	0	0	0	0	0	0	0	0	0	0	2	27	0	0	1	0	0	0	0
	n97_444	0	0	0	0	0	0	0	0	0	0	0	2	1	24	0	1	2	0	0	0
	n97_618	0	0	0	0	0	0	0	0	0	0	1	0	0	0	26	0	0	0	3	0
	n97_620	0	0	0	0	0	0	0	0	0	0	0	1	6	2	0	21	0	0	0	0
	nok_128	4	2	0	0	0	0	0	0	0	0	0	1	1	5	4	1	11	1	0	0
	nok_e5	0	0	0	0	0	0	0	0	0	0	0	0	0	0	3	0	0	27	0	0
	nok_e62	0	0	1	1	0	0	0	2	0	0	0	0	0	0	0	0	0	0	26	0
	treo	0	0	0	0	1	0	0	0	0	0	0	0	0	0	0	0	0	0	0	29

Table 35. Confusion Matrix for 30 Signal Vectors per Phone With Two Signal Vectors per Training Set

		label																			
		bberry	htc371	htc373	htc374	htc375	htc376	htc601	htc_rob	iphone4	iphone5	iphone7	n8_594	n97_430	n97_444	n97_618	n97_620	nok_128	nok_e5	nok_e62	treo
truth	bberry	15	0	0	0	0	0	0	0	0	0	0	0	0	0	0	0	0	0	0	0
	htc371	0	11	3	0	0	0	0	0	0	0	0	0	0	1	0	0	0	0	0	0
	htc373	0	2	13	0	0	0	0	0	0	0	0	0	0	0	0	0	0	0	0	0
	htc374	0	0	0	11	0	4	0	0	0	0	0	0	0	0	0	0	0	0	0	0
	htc375	0	0	0	0	14	0	0	0	1	0	0	0	0	0	0	0	0	0	0	0
	htc376	0	0	0	3	0	12	0	0	0	0	0	0	0	0	0	0	0	0	0	0
	htc601	0	0	0	0	0	0	15	0	0	0	0	0	0	0	0	0	0	0	0	0
	htc_rob	0	0	0	0	0	0	0	14	0	0	0	0	0	0	0	0	0	0	1	0
	iphone4	0	0	0	0	0	0	0	0	11	2	2	0	0	0	0	0	0	0	0	0
	iphone5	0	0	0	0	0	0	0	0	1	11	2	0	0	0	0	0	1	0	0	0
	iphone7	0	0	0	0	0	0	0	2	2	6	4	0	0	1	0	0	0	0	0	0
	n8_594	0	0	0	0	0	0	0	0	0	0	0	15	0	0	0	0	0	0	0	0
	n97_430	0	0	0	0	0	0	0	0	0	0	0	0	15	0	0	0	0	0	0	0
	n97_444	0	0	0	0	0	0	0	0	0	0	0	0	0	15	0	0	0	0	0	0
	n97_618	0	0	0	0	0	0	0	0	0	0	0	0	0	0	14	0	0	1	0	0
	n97_620	0	0	0	0	0	0	0	0	0	0	0	1	2	0	0	12	0	0	0	0
	nok_128	0	1	0	0	0	0	0	0	0	0	0	1	0	3	4	1	4	1	0	0
	nok_e5	0	0	0	0	0	0	1	0	0	0	0	0	0	0	2	0	0	12	0	0
	nok_e62	0	0	0	0	0	0	0	0	0	0	0	0	0	0	0	0	0	0	15	0
	treo	0	0	0	0	0	0	0	0	0	0	0	0	0	0	0	0	0	0	0	15

Table 36. Confusion Matrix for 30 Signal Vectors per Phone With Three Signal Vectors per Training Set

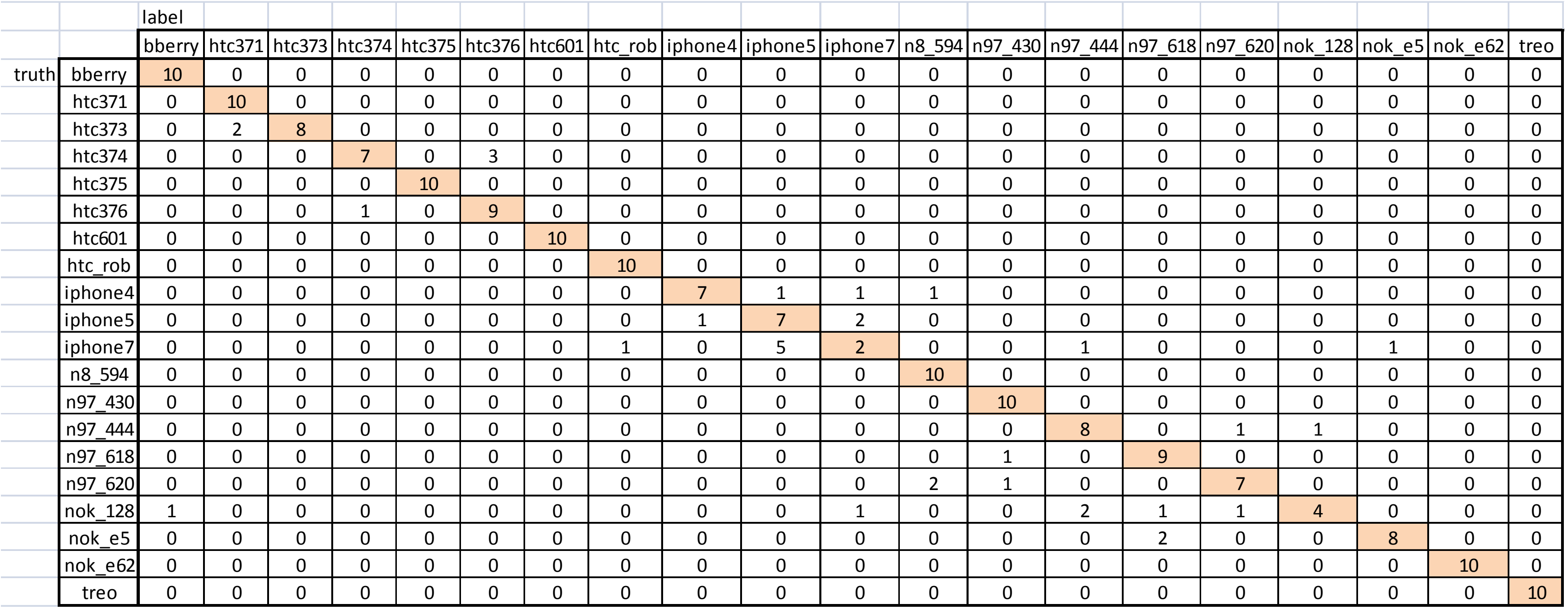

		label																			
		bberry	htc371	htc373	htc374	htc375	htc376	htc601	htc_rob	iphone4	iphone5	iphone7	n8_594	n97_430	n97_444	n97_618	n97_620	nok_128	nok_e5	nok_e62	treo
truth	bberry	10	0	0	0	0	0	0	0	0	0	0	0	0	0	0	0	0	0	0	0
	htc371	0	10	0	0	0	0	0	0	0	0	0	0	0	0	0	0	0	0	0	0
	htc373	0	2	8	0	0	0	0	0	0	0	0	0	0	0	0	0	0	0	0	0
	htc374	0	0	0	7	0	3	0	0	0	0	0	0	0	0	0	0	0	0	0	0
	htc375	0	0	0	0	10	0	0	0	0	0	0	0	0	0	0	0	0	0	0	0
	htc376	0	0	0	1	0	9	0	0	0	0	0	0	0	0	0	0	0	0	0	0
	htc601	0	0	0	0	0	0	10	0	0	0	0	0	0	0	0	0	0	0	0	0
	htc_rob	0	0	0	0	0	0	0	10	0	0	0	0	0	0	0	0	0	0	0	0
	iphone4	0	0	0	0	0	0	0	0	7	1	1	1	0	0	0	0	0	0	0	0
	iphone5	0	0	0	0	0	0	0	0	1	7	2	0	0	0	0	0	0	0	0	0
	iphone7	0	0	0	0	0	0	0	1	0	5	2	0	0	1	0	0	0	1	0	0
	n8_594	0	0	0	0	0	0	0	0	0	0	0	10	0	0	0	0	0	0	0	0
	n97_430	0	0	0	0	0	0	0	0	0	0	0	0	10	0	0	0	0	0	0	0
	n97_444	0	0	0	0	0	0	0	0	0	0	0	0	0	8	0	1	1	0	0	0
	n97_618	0	0	0	0	0	0	0	0	0	0	0	0	1	0	9	0	0	0	0	0
	n97_620	0	0	0	0	0	0	0	0	0	0	0	2	1	0	0	7	0	0	0	0
	nok_128	1	0	0	0	0	0	0	0	0	0	1	0	0	2	1	1	4	0	0	0
	nok_e5	0	0	0	0	0	0	0	0	0	0	0	0	0	0	2	0	0	8	0	0
	nok_e62	0	0	0	0	0	0	0	0	0	0	0	0	0	0	0	0	0	0	10	0
	treo	0	0	0	0	0	0	0	0	0	0	0	0	0	0	0	0	0	0	0	10

Table 37. Confusion Matrix for 50 Signal Vectors per Phone With One Signal Vector per Training Set

		label																			
		bberry	htc_rob	htc371	htc373	htc374	htc375	htc376	htc601	iphone4	iphone5	iphone7	n8_594	n97_430	n97_444	n97_618	n97_620	nok_128	nok_e5	nok_e62	treo
truth	bberry	49	0	1	0	0	0	0	0	0	0	0	0	0	0	0	0	0	0	0	0
	htc_rob	0	47	0	0	0	1	0	0	0	0	1	0	0	0	0	0	0	0	1	0
	htc371	0	0	46	3	0	0	0	0	0	0	0	0	0	1	0	0	0	0	0	0
	htc373	0	0	0	49	1	0	0	0	0	0	0	0	0	0	0	0	0	0	0	0
	htc374	0	0	0	0	43	0	6	0	0	0	0	0	0	0	0	0	0	0	1	0
	htc375	0	1	0	0	0	49	0	0	0	0	0	0	0	0	0	0	0	0	0	0
	htc376	1	0	1	1	14	0	30	0	0	0	0	0	0	0	0	0	0	0	2	1
	htc601	0	0	0	0	0	0	0	50	0	0	0	0	0	0	0	0	0	0	0	0
	iphone4	0	0	0	0	0	0	0	2	43	4	0	1	0	0	0	0	0	0	0	0
	iphone5	0	0	0	0	0	0	0	0	8	36	6	0	0	0	0	0	0	0	0	0
	iphone7	1	1	0	0	0	1	0	0	4	13	23	0	0	2	1	0	2	2	0	0
	n8_594	0	0	0	0	0	0	0	0	0	0	0	47	0	0	0	1	2	0	0	0
	n97_430	0	0	0	0	0	0	0	0	0	0	0	1	47	0	0	2	0	0	0	0
	n97_444	0	0	0	0	0	0	0	0	0	0	0	1	1	45	0	1	2	0	0	0
	n97_618	0	0	0	0	0	0	0	0	0	0	0	0	1	0	43	0	1	5	0	0
	n97_620	0	0	0	0	0	0	0	0	0	0	0	1	7	1	0	41	0	0	0	0
	nok_128	5	0	1	0	0	0	0	0	0	0	4	1	2	11	5	3	16	2	0	0
	nok_e5	0	0	0	0	0	0	0	3	0	0	0	0	0	0	2	0	0	45	0	0
	nok_e62	0	0	0	0	2	1	1	0	0	0	0	0	0	0	0	0	0	0	46	0
	treo	0	0	0	0	0	0	0	0	0	0	0	0	0	0	0	0	0	0	0	50

Table 38. Confusion Matrix for 50 Signal Vectors per Phone With Two Signal Vectors per Training Set

		label																			
		bberry	htc_rob	htc371	htc373	htc374	htc375	htc376	htc601	iphone4	iphone5	iphone7	n8_594	n97_430	n97_444	n97_618	n97_620	nok_128	nok_e5	nok_e62	treo
truth	bberry	24	0	0	0	0	0	0	0	0	0	0	0	0	0	1	0	0	0	0	0
	htc_rob	0	25	0	0	0	0	0	0	0	0	0	0	0	0	0	0	0	0	0	0
	htc371	0	0	25	0	0	0	0	0	0	0	0	0	0	0	0	0	0	0	0	0
	htc373	0	0	1	24	0	0	0	0	0	0	0	0	0	0	0	0	0	0	0	0
	htc374	0	0	0	0	23	0	2	0	0	0	0	0	0	0	0	0	0	0	0	0
	htc375	0	0	0	0	0	24	0	0	1	0	0	0	0	0	0	0	0	0	0	0
	htc376	0	0	0	0	4	0	21	0	0	0	0	0	0	0	0	0	0	0	0	0
	htc601	0	0	0	0	0	0	0	25	0	0	0	0	0	0	0	0	0	0	0	0
	iphone4	0	0	0	0	0	0	0	0	22	3	0	0	0	0	0	0	0	0	0	0
	iphone5	0	0	0	0	0	0	0	0	2	20	3	0	0	0	0	0	0	0	0	0
	iphone7	0	1	0	0	0	0	0	0	1	9	9	0	0	1	0	0	3	1	0	0
	n8_594	0	0	0	0	0	0	0	0	0	0	0	24	1	0	0	0	0	0	0	0
	n97_430	0	0	0	0	0	0	0	0	0	0	0	0	25	0	0	0	0	0	0	0
	n97_444	0	0	0	0	0	0	0	0	0	0	0	0	0	25	0	0	0	0	0	0
	n97_618	0	0	0	0	0	0	0	0	0	0	0	0	0	0	24	0	0	1	0	0
	n97_620	0	0	0	0	0	0	0	0	0	0	0	0	2	0	0	23	0	0	0	0
	nok_128	1	0	0	0	0	0	0	0	0	0	1	0	0	2	4	1	14	2	0	0
	nok_e5	0	0	0	0	0	0	0	0	0	0	0	0	0	0	2	0	0	23	0	0
	nok_e62	0	0	0	0	1	0	0	0	0	0	0	0	0	0	0	0	0	0	24	0
	treo	0	0	0	0	0	0	0	0	0	0	0	0	0	0	0	0	0	0	0	25

Table 39. Confusion Matrix for 50 Signal Vectors per Phone With Three Signal Vectors per Training Set

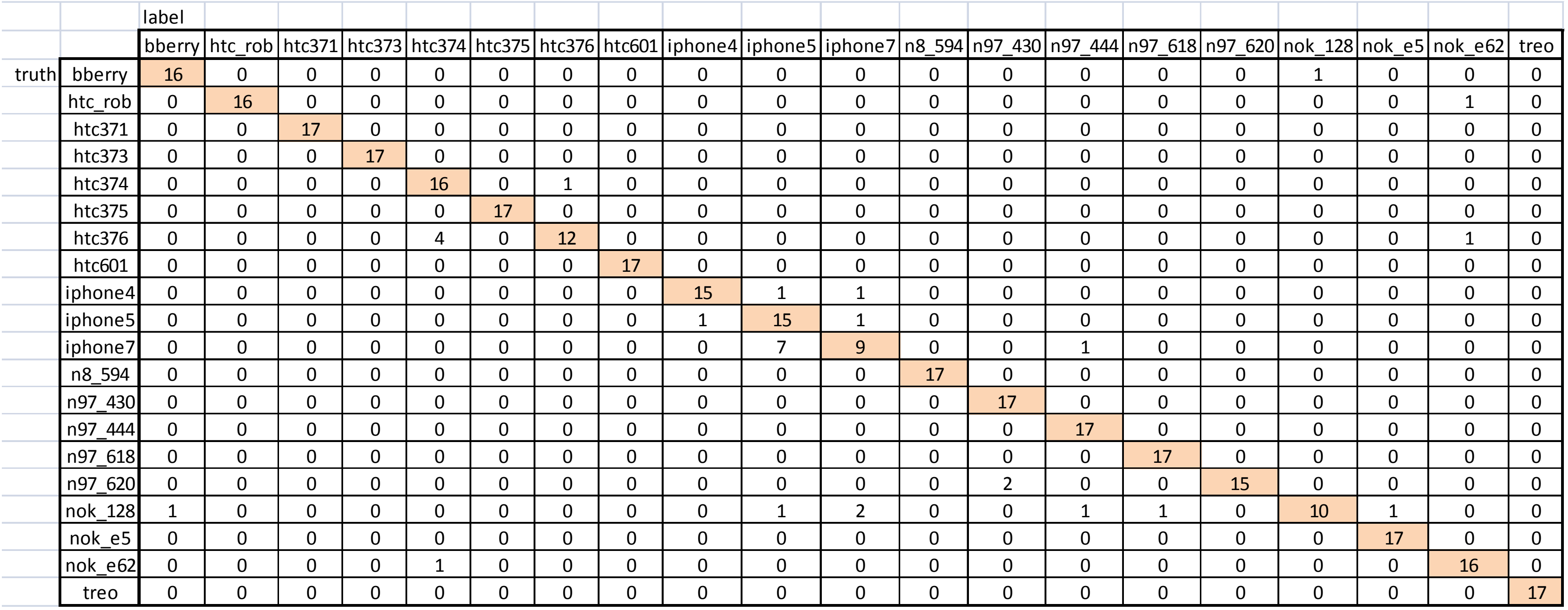

		label																			
		bberry	htc_rob	htc371	htc373	htc374	htc375	htc376	htc601	iphone4	iphone5	iphone7	n8_594	n97_430	n97_444	n97_618	n97_620	nok_128	nok_e5	nok_e62	treo
truth	bberry	16	0	0	0	0	0	0	0	0	0	0	0	0	0	0	0	1	0	0	0
	htc_rob	0	16	0	0	0	0	0	0	0	0	0	0	0	0	0	0	0	0	1	0
	htc371	0	0	17	0	0	0	0	0	0	0	0	0	0	0	0	0	0	0	0	0
	htc373	0	0	0	17	0	0	0	0	0	0	0	0	0	0	0	0	0	0	0	0
	htc374	0	0	0	0	16	0	1	0	0	0	0	0	0	0	0	0	0	0	0	0
	htc375	0	0	0	0	0	17	0	0	0	0	0	0	0	0	0	0	0	0	0	0
	htc376	0	0	0	0	4	0	12	0	0	0	0	0	0	0	0	0	0	0	1	0
	htc601	0	0	0	0	0	0	0	17	0	0	0	0	0	0	0	0	0	0	0	0
	iphone4	0	0	0	0	0	0	0	0	15	1	1	0	0	0	0	0	0	0	0	0
	iphone5	0	0	0	0	0	0	0	0	1	15	1	0	0	0	0	0	0	0	0	0
	iphone7	0	0	0	0	0	0	0	0	0	7	9	0	0	1	0	0	0	0	0	0
	n8_594	0	0	0	0	0	0	0	0	0	0	0	17	0	0	0	0	0	0	0	0
	n97_430	0	0	0	0	0	0	0	0	0	0	0	0	17	0	0	0	0	0	0	0
	n97_444	0	0	0	0	0	0	0	0	0	0	0	0	0	17	0	0	0	0	0	0
	n97_618	0	0	0	0	0	0	0	0	0	0	0	0	0	0	17	0	0	0	0	0
	n97_620	0	0	0	0	0	0	0	0	0	0	0	0	2	0	0	15	0	0	0	0
	nok_128	1	0	0	0	0	0	0	0	0	1	2	0	0	1	1	0	10	1	0	0
	nok_e5	0	0	0	0	0	0	0	0	0	0	0	0	0	0	0	0	0	17	0	0
	nok_e62	0	0	0	0	1	0	0	0	0	0	0	0	0	0	0	0	0	0	16	0
	treo	0	0	0	0	0	0	0	0	0	0	0	0	0	0	0	0	0	0	0	17

Table 40. Confusion Matrix for 50 Signal Vectors per Phone With Four Signal Vectors per Training Set

		label																		
		bberry	htc_rob	htc371	htc373	htc374	htc375	htc376	htc601	iphone4	iphone5	iphone7	n8_594	n97_430	n97_444	n97_618	n97_620	nok_128	nok_e5	nok_e62	treo
truth	bberry	13	0	0	0	0	0	0	0	0	0	0	0	0	0	0	0	0	0	0	0
	htc_rob	0	13	0	0	0	0	0	0	0	0	0	0	0	0	0	0	0	0	0	0
	htc371	0	0	13	0	0	0	0	0	0	0	0	0	0	0	0	0	0	0	0	0
	htc373	0	0	0	13	0	0	0	0	0	0	0	0	0	0	0	0	0	0	0	0
	htc374	0	0	0	0	13	0	0	0	0	0	0	0	0	0	0	0	0	0	0	0
	htc375	0	0	0	0	0	13	0	0	0	0	0	0	0	0	0	0	0	0	0	0
	htc376	0	0	0	0	2	0	11	0	0	0	0	0	0	0	0	0	0	0	0	0
	htc601	0	0	0	0	0	0	0	13	0	0	0	0	0	0	0	0	0	0	0	0
	iphone4	0	0	0	0	0	0	0	0	11	1	1	0	0	0	0	0	0	0	0	0
	iphone5	0	0	0	0	0	0	0	0	1	10	2	0	0	0	0	0	0	0	0	0
	iphone7	0	0	0	0	0	0	0	0	0	5	7	0	0	1	0	0	0	0	0	0
	n8_594	0	0	0	0	0	0	0	0	0	0	0	13	0	0	0	0	0	0	0	0
	n97_430	0	0	0	0	0	0	0	0	0	0	0	0	13	0	0	0	0	0	0	0
	n97_444	0	0	0	0	0	0	0	0	0	0	0	0	0	13	0	0	0	0	0	0
	n97_618	0	0	0	0	0	0	0	0	0	0	0	0	0	0	13	0	0	0	0	0
	n97_620	0	0	0	0	0	0	0	0	0	0	0	0	0	0	0	13	0	0	0	0
	nok_128	0	0	0	0	0	0	0	0	0	0	1	0	0	1	1	0	10	0	0	0
	nok_e5	0	0	0	0	0	0	0	0	0	0	0	0	0	0	0	0	0	13	0	0
	nok_e62	0	0	0	0	1	0	0	0	0	0	0	0	0	0	0	0	0	0	12	0
	treo	0	0	0	0	0	0	0	0	0	0	0	0	0	0	0	0	0	0	0	13

Table 41. Confusion Matrix for 50 Signal Vectors per Phone With Five Signal Vectors per Training Set

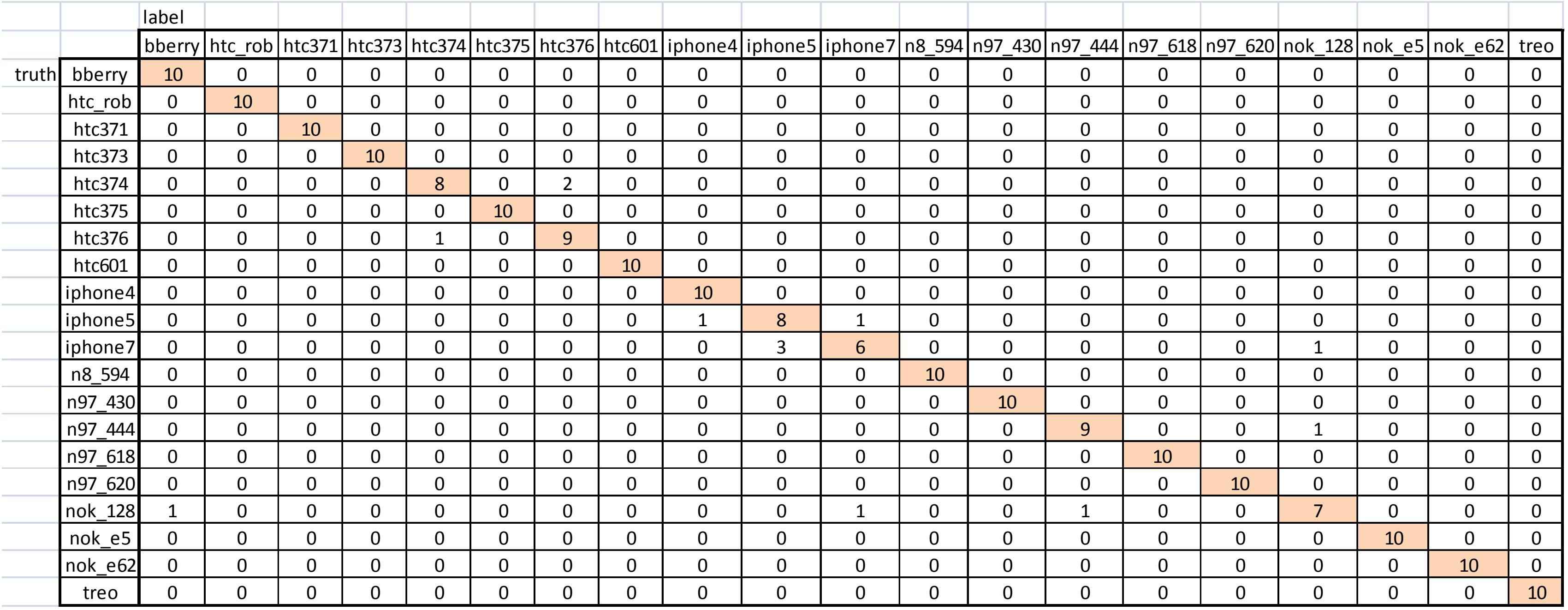

		label																			
		bberry	htc_rob	htc371	htc373	htc374	htc375	htc376	htc601	iphone4	iphone5	iphone7	n8_594	n97_430	n97_444	n97_618	n97_620	nok_128	nok_e5	nok_e62	treo
truth	bberry	10	0	0	0	0	0	0	0	0	0	0	0	0	0	0	0	0	0	0	0
	htc_rob	0	10	0	0	0	0	0	0	0	0	0	0	0	0	0	0	0	0	0	0
	htc371	0	0	10	0	0	0	0	0	0	0	0	0	0	0	0	0	0	0	0	0
	htc373	0	0	0	10	0	0	0	0	0	0	0	0	0	0	0	0	0	0	0	0
	htc374	0	0	0	0	8	0	2	0	0	0	0	0	0	0	0	0	0	0	0	0
	htc375	0	0	0	0	0	10	0	0	0	0	0	0	0	0	0	0	0	0	0	0
	htc376	0	0	0	0	1	0	9	0	0	0	0	0	0	0	0	0	0	0	0	0
	htc601	0	0	0	0	0	0	0	10	0	0	0	0	0	0	0	0	0	0	0	0
	iphone4	0	0	0	0	0	0	0	0	10	0	0	0	0	0	0	0	0	0	0	0
	iphone5	0	0	0	0	0	0	0	0	1	8	1	0	0	0	0	0	0	0	0	0
	iphone7	0	0	0	0	0	0	0	0	0	3	6	0	0	0	0	0	1	0	0	0
	n8_594	0	0	0	0	0	0	0	0	0	0	0	10	0	0	0	0	0	0	0	0
	n97_430	0	0	0	0	0	0	0	0	0	0	0	0	10	0	0	0	0	0	0	0
	n97_444	0	0	0	0	0	0	0	0	0	0	0	0	0	9	0	0	1	0	0	0
	n97_618	0	0	0	0	0	0	0	0	0	0	0	0	0	0	10	0	0	0	0	0
	n97_620	0	0	0	0	0	0	0	0	0	0	0	0	0	0	0	10	0	0	0	0
	nok_128	1	0	0	0	0	0	0	0	0	0	1	0	0	1	0	0	7	0	0	0
	nok_e5	0	0	0	0	0	0	0	0	0	0	0	0	0	0	0	0	0	10	0	0
	nok_e62	0	0	0	0	0	0	0	0	0	0	0	0	0	0	0	0	0	0	10	0
	treo	0	0	0	0	0	0	0	0	0	0	0	0	0	0	0	0	0	0	0	10

Table 42. Confusion Matrix for 100 Signal Vectors per Phone With One Signal Vector per Training Set

		label																			
		bberry	htc_rob	htc371	htc373	htc374	htc375	htc376	htc601	iphone4	iphone5	iphone7	n8_594	n97_430	n97_444	n97_618	n97_620	nok_128	nok_e5	nok_e62	treo
truth	bberry	96	0	1	0	0	0	0	0	0	0	0	0	0	0	0	0	3	0	0	0
	htc_rob	0	100	0	0	0	0	0	0	0	0	0	0	0	0	0	0	0	0	0	0
	htc371	1	0	94	5	0	0	0	0	0	0	0	0	0	0	0	0	0	0	0	0
	htc373	0	0	1	99	0	0	0	0	0	0	0	0	0	0	0	0	0	0	0	0
	htc374	0	0	0	0	89	0	10	0	0	0	0	0	0	0	0	0	0	0	1	0
	htc375	0	1	0	0	0	99	0	0	0	0	0	0	0	0	0	0	0	0	0	0
	htc376	1	1	0	0	29	0	67	0	0	0	0	0	0	0	0	0	0	0	2	0
	htc601	0	0	0	0	1	0	0	97	0	0	0	0	0	0	0	0	0	2	0	0
	iphone4	0	0	0	0	0	0	0	1	84	12	0	0	0	0	0	0	3	0	0	0
	iphone5	0	0	0	0	0	0	0	0	7	83	10	0	0	0	0	0	0	0	0	0
	iphone7	1	0	0	0	0	1	0	2	8	20	59	0	0	2	0	0	4	3	0	0
	n8_594	0	0	0	0	0	0	0	1	0	0	0	98	1	0	0	0	0	0	0	0
	n97_430	0	0	0	0	0	0	0	0	0	0	0	0	98	0	0	2	0	0	0	0
	n97_444	0	0	0	0	0	0	0	0	0	0	0	0	1	91	0	0	8	0	0	0
	n97_618	0	0	1	0	0	0	0	0	0	0	0	0	1	0	89	0	1	8	0	0
	n97_620	0	0	0	0	0	0	0	0	0	0	0	0	4	1	0	95	0	0	0	0
	nok_128	13	0	1	0	0	0	0	0	0	0	4	0	2	20	4	1	51	4	0	0
	nok_e5	0	0	0	0	0	0	0	4	0	0	0	0	0	0	3	0	0	93	0	0
	nok_e62	0	0	0	0	2	2	0	0	0	0	0	0	0	0	0	0	0	0	96	0
	treo	0	0	0	0	0	0	0	0	0	0	0	0	0	0	0	0	0	0	0	100

Table 43. Confusion Matrix for 100 Signal Vectors per Phone With Two Signal Vectors per Training Set

		label																			
		bberry	htc_rob	htc371	htc373	htc374	htc375	htc376	htc601	iphone4	iphone5	iphone7	n8_594	n97_430	n97_444	n97_618	n97_620	nok_128	nok_e5	nok_e62	treo
truth	bberry	49	0	1	0	0	0	0	0	0	0	0	0	0	0	0	0	0	0	0	0
	htc_rob	0	50	0	0	0	0	0	0	0	0	0	0	0	0	0	0	0	0	0	0
	htc371	0	0	50	0	0	0	0	0	0	0	0	0	0	0	0	0	0	0	0	0
	htc373	0	0	0	50	0	0	0	0	0	0	0	0	0	0	0	0	0	0	0	0
	htc374	0	0	0	0	49	0	1	0	0	0	0	0	0	0	0	0	0	0	0	0
	htc375	0	0	0	0	0	50	0	0	0	0	0	0	0	0	0	0	0	0	0	0
	htc376	0	0	0	0	5	0	44	0	0	0	0	0	0	0	0	0	0	0	1	0
	htc601	0	0	0	0	0	0	0	50	0	0	0	0	0	0	0	0	0	0	0	0
	iphone4	0	0	0	0	0	0	0	0	49	1	0	0	0	0	0	0	0	0	0	0
	iphone5	0	0	0	0	0	0	0	0	3	44	3	0	0	0	0	0	0	0	0	0
	iphone7	1	0	0	0	0	0	0	0	1	6	41	0	0	1	0	0	0	0	0	0
	n8_594	0	0	0	0	0	0	0	0	0	0	0	50	0	0	0	0	0	0	0	0
	n97_430	0	0	0	0	0	0	0	0	0	0	0	0	50	0	0	0	0	0	0	0
	n97_444	0	0	0	0	0	0	0	0	0	0	0	0	0	50	0	0	0	0	0	0
	n97_618	0	0	0	0	0	0	0	0	0	0	0	0	0	0	50	0	0	0	0	0
	n97_620	0	0	0	0	0	0	0	0	0	0	0	0	0	0	0	50	0	0	0	0
	nok_128	4	0	0	0	0	0	0	0	0	0	1	0	0	4	1	0	40	0	0	0
	nok_e5	0	0	0	0	0	0	0	0	0	0	0	0	0	0	0	0	0	50	0	0
	nok_e62	0	0	0	0	0	0	0	0	0	0	0	0	0	0	0	0	0	0	50	0
	treo	0	0	0	0	0	0	0	0	0	0	0	0	0	0	0	0	0	0	0	50

Table 44. Confusion Matrix for 100 Signal Vectors per Phone With Three Signal Vectors per Training Set

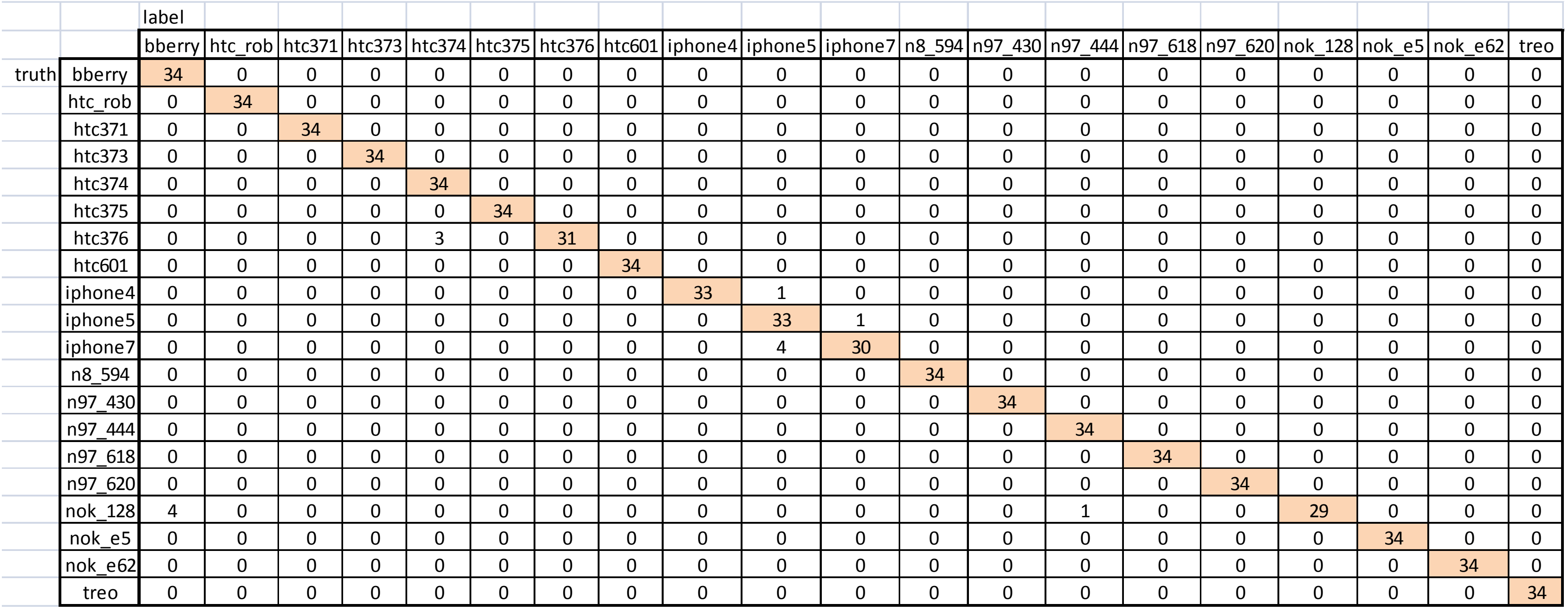

		label																			
		bberry	htc_rob	htc371	htc373	htc374	htc375	htc376	htc601	iphone4	iphone5	iphone7	n8_594	n97_430	n97_444	n97_618	n97_620	nok_128	nok_e5	nok_e62	treo
truth	bberry	34	0	0	0	0	0	0	0	0	0	0	0	0	0	0	0	0	0	0	0
	htc_rob	0	34	0	0	0	0	0	0	0	0	0	0	0	0	0	0	0	0	0	0
	htc371	0	0	34	0	0	0	0	0	0	0	0	0	0	0	0	0	0	0	0	0
	htc373	0	0	0	34	0	0	0	0	0	0	0	0	0	0	0	0	0	0	0	0
	htc374	0	0	0	0	34	0	0	0	0	0	0	0	0	0	0	0	0	0	0	0
	htc375	0	0	0	0	0	34	0	0	0	0	0	0	0	0	0	0	0	0	0	0
	htc376	0	0	0	0	3	0	31	0	0	0	0	0	0	0	0	0	0	0	0	0
	htc601	0	0	0	0	0	0	0	34	0	0	0	0	0	0	0	0	0	0	0	0
	iphone4	0	0	0	0	0	0	0	0	33	1	0	0	0	0	0	0	0	0	0	0
	iphone5	0	0	0	0	0	0	0	0	0	33	1	0	0	0	0	0	0	0	0	0
	iphone7	0	0	0	0	0	0	0	0	0	4	30	0	0	0	0	0	0	0	0	0
	n8_594	0	0	0	0	0	0	0	0	0	0	0	34	0	0	0	0	0	0	0	0
	n97_430	0	0	0	0	0	0	0	0	0	0	0	0	34	0	0	0	0	0	0	0
	n97_444	0	0	0	0	0	0	0	0	0	0	0	0	0	34	0	0	0	0	0	0
	n97_618	0	0	0	0	0	0	0	0	0	0	0	0	0	0	34	0	0	0	0	0
	n97_620	0	0	0	0	0	0	0	0	0	0	0	0	0	0	0	34	0	0	0	0
	nok_128	4	0	0	0	0	0	0	0	0	0	0	0	0	1	0	0	29	0	0	0
	nok_e5	0	0	0	0	0	0	0	0	0	0	0	0	0	0	0	0	0	34	0	0
	nok_e62	0	0	0	0	0	0	0	0	0	0	0	0	0	0	0	0	0	0	34	0
	treo	0	0	0	0	0	0	0	0	0	0	0	0	0	0	0	0	0	0	0	34

Table 45. Confusion Matrix for 120 Signal Vectors per Phone With One Signal Vector per Training Set

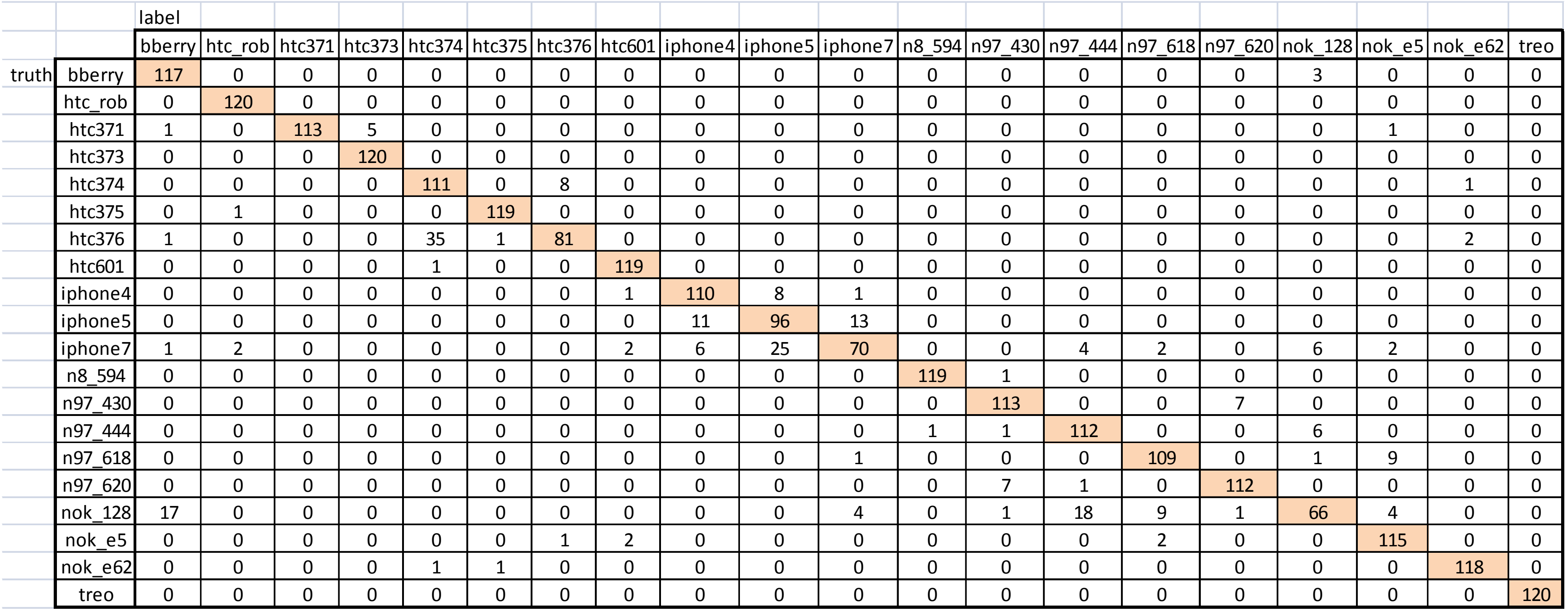

		label																			
		bberry	htc_rob	htc371	htc373	htc374	htc375	htc376	htc601	iphone4	iphone5	iphone7	n8_594	n97_430	n97_444	n97_618	n97_620	nok_128	nok_e5	nok_e62	treo
truth	bberry	117	0	0	0	0	0	0	0	0	0	0	0	0	0	0	0	3	0	0	0
	htc_rob	0	120	0	0	0	0	0	0	0	0	0	0	0	0	0	0	0	0	0	0
	htc371	1	0	113	5	0	0	0	0	0	0	0	0	0	0	0	0	0	1	0	0
	htc373	0	0	0	120	0	0	0	0	0	0	0	0	0	0	0	0	0	0	0	0
	htc374	0	0	0	0	111	0	8	0	0	0	0	0	0	0	0	0	0	0	1	0
	htc375	0	1	0	0	0	119	0	0	0	0	0	0	0	0	0	0	0	0	0	0
	htc376	1	0	0	0	35	1	81	0	0	0	0	0	0	0	0	0	0	0	2	0
	htc601	0	0	0	0	1	0	0	119	0	0	0	0	0	0	0	0	0	0	0	0
	iphone4	0	0	0	0	0	0	0	1	110	8	1	0	0	0	0	0	0	0	0	0
	iphone5	0	0	0	0	0	0	0	0	11	96	13	0	0	0	0	0	0	0	0	0
	iphone7	1	2	0	0	0	0	0	2	6	25	70	0	0	4	2	0	6	2	0	0
	n8_594	0	0	0	0	0	0	0	0	0	0	0	119	1	0	0	0	0	0	0	0
	n97_430	0	0	0	0	0	0	0	0	0	0	0	0	113	0	0	7	0	0	0	0
	n97_444	0	0	0	0	0	0	0	0	0	0	0	1	1	112	0	0	6	0	0	0
	n97_618	0	0	0	0	0	0	0	0	0	0	1	0	0	0	109	0	1	9	0	0
	n97_620	0	0	0	0	0	0	0	0	0	0	0	0	7	1	0	112	0	0	0	0
	nok_128	17	0	0	0	0	0	0	0	0	0	4	0	1	18	9	1	66	4	0	0
	nok_e5	0	0	0	0	0	0	1	2	0	0	0	0	0	0	2	0	0	115	0	0
	nok_e62	0	0	0	0	1	1	0	0	0	0	0	0	0	0	0	0	0	0	118	0
	treo	0	0	0	0	0	0	0	0	0	0	0	0	0	0	0	0	0	0	0	120

Table 46. Confusion Matrix for 120 Signal Vectors per Phone With Two Signal Vectors per Training Set

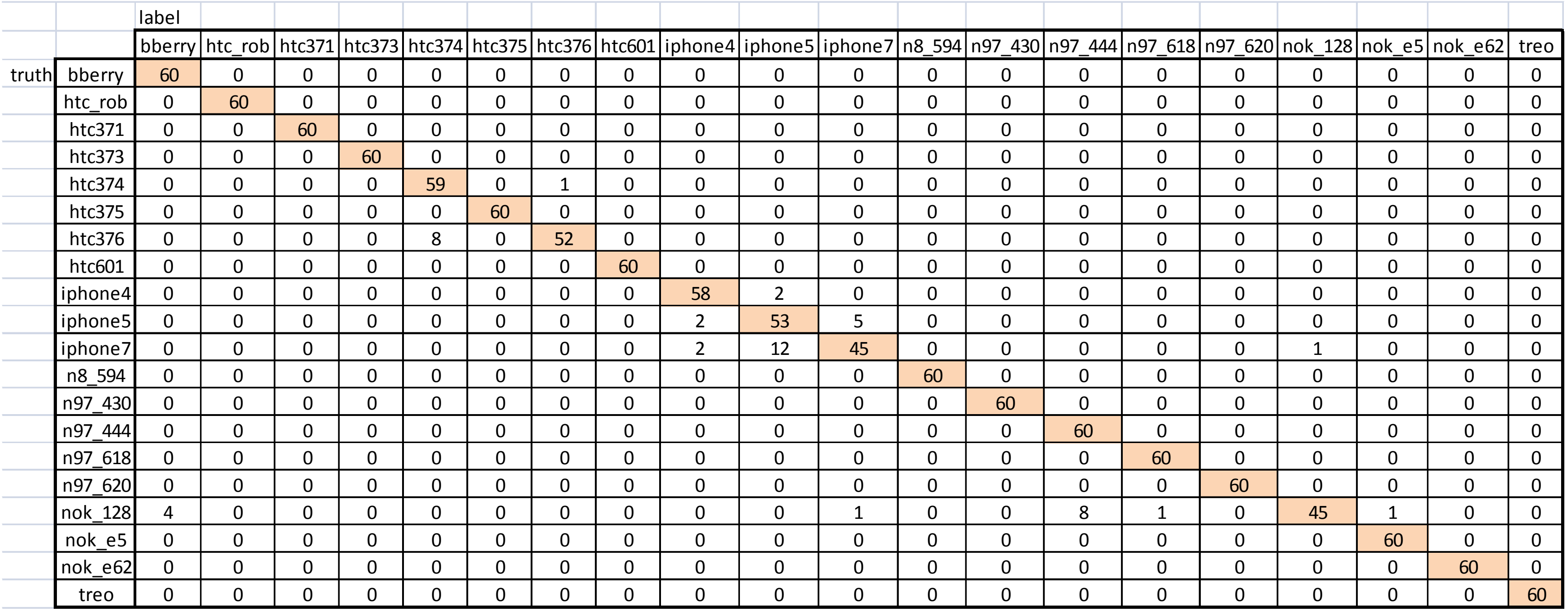

		label																			
		bberry	htc_rob	htc371	htc373	htc374	htc375	htc376	htc601	iphone4	iphone5	iphone7	n8_594	n97_430	n97_444	n97_618	n97_620	nok_128	nok_e5	nok_e62	treo
truth	bberry	60	0	0	0	0	0	0	0	0	0	0	0	0	0	0	0	0	0	0	0
	htc_rob	0	60	0	0	0	0	0	0	0	0	0	0	0	0	0	0	0	0	0	0
	htc371	0	0	60	0	0	0	0	0	0	0	0	0	0	0	0	0	0	0	0	0
	htc373	0	0	0	60	0	0	0	0	0	0	0	0	0	0	0	0	0	0	0	0
	htc374	0	0	0	0	59	0	1	0	0	0	0	0	0	0	0	0	0	0	0	0
	htc375	0	0	0	0	0	60	0	0	0	0	0	0	0	0	0	0	0	0	0	0
	htc376	0	0	0	0	8	0	52	0	0	0	0	0	0	0	0	0	0	0	0	0
	htc601	0	0	0	0	0	0	0	60	0	0	0	0	0	0	0	0	0	0	0	0
	iphone4	0	0	0	0	0	0	0	0	58	2	0	0	0	0	0	0	0	0	0	0
	iphone5	0	0	0	0	0	0	0	0	2	53	5	0	0	0	0	0	0	0	0	0
	iphone7	0	0	0	0	0	0	0	0	2	12	45	0	0	0	0	0	1	0	0	0
	n8_594	0	0	0	0	0	0	0	0	0	0	0	60	0	0	0	0	0	0	0	0
	n97_430	0	0	0	0	0	0	0	0	0	0	0	0	60	0	0	0	0	0	0	0
	n97_444	0	0	0	0	0	0	0	0	0	0	0	0	0	60	0	0	0	0	0	0
	n97_618	0	0	0	0	0	0	0	0	0	0	0	0	0	0	60	0	0	0	0	0
	n97_620	0	0	0	0	0	0	0	0	0	0	0	0	0	0	0	60	0	0	0	0
	nok_128	4	0	0	0	0	0	0	0	0	0	1	0	0	8	1	0	45	1	0	0
	nok_e5	0	0	0	0	0	0	0	0	0	0	0	0	0	0	0	0	0	60	0	0
	nok_e62	0	0	0	0	0	0	0	0	0	0	0	0	0	0	0	0	0	0	60	0
	treo	0	0	0	0	0	0	0	0	0	0	0	0	0	0	0	0	0	0	0	60

Table 47. Confusion Matrix for 120 Signal Vectors per Phone With Three Signal Vectors per Training Set

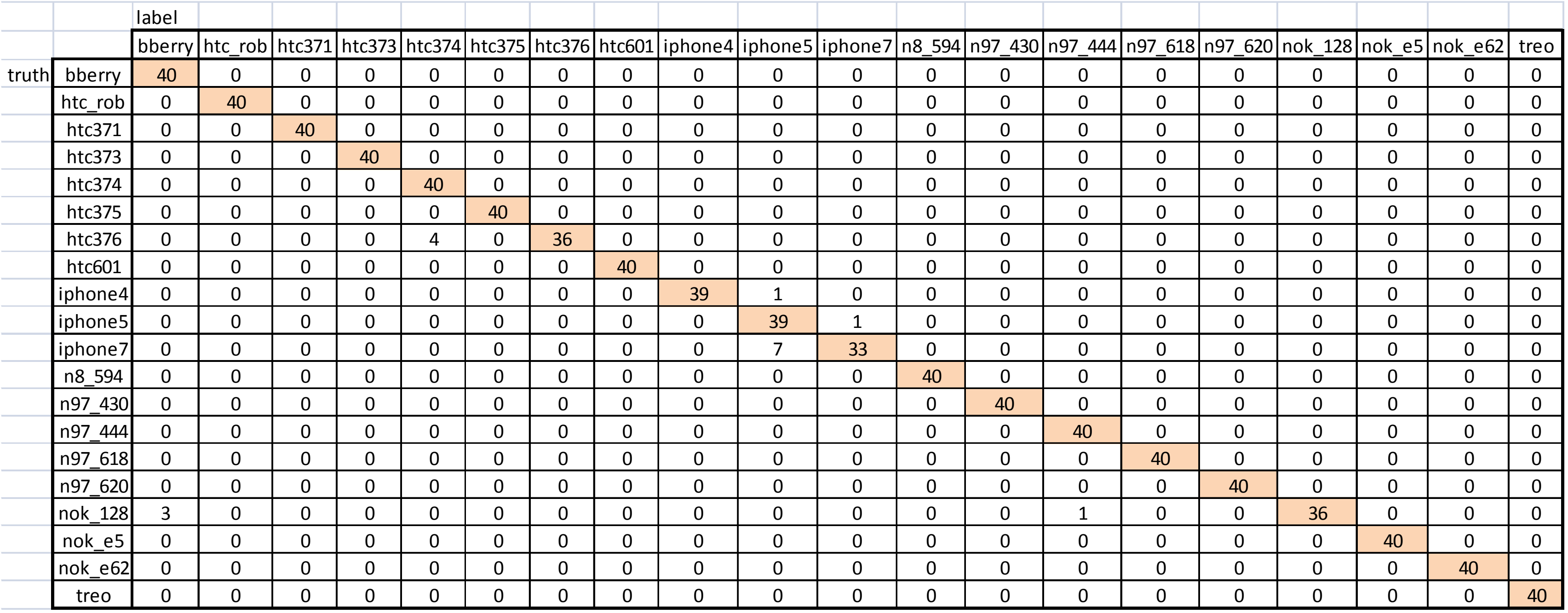

		label																			
		bberry	htc_rob	htc371	htc373	htc374	htc375	htc376	htc601	iphone4	iphone5	iphone7	n8_594	n97_430	n97_444	n97_618	n97_620	nok_128	nok_e5	nok_e62	treo
truth	bberry	40	0	0	0	0	0	0	0	0	0	0	0	0	0	0	0	0	0	0	0
	htc_rob	0	40	0	0	0	0	0	0	0	0	0	0	0	0	0	0	0	0	0	0
	htc371	0	0	40	0	0	0	0	0	0	0	0	0	0	0	0	0	0	0	0	0
	htc373	0	0	0	40	0	0	0	0	0	0	0	0	0	0	0	0	0	0	0	0
	htc374	0	0	0	0	40	0	0	0	0	0	0	0	0	0	0	0	0	0	0	0
	htc375	0	0	0	0	0	40	0	0	0	0	0	0	0	0	0	0	0	0	0	0
	htc376	0	0	0	0	4	0	36	0	0	0	0	0	0	0	0	0	0	0	0	0
	htc601	0	0	0	0	0	0	0	40	0	0	0	0	0	0	0	0	0	0	0	0
	iphone4	0	0	0	0	0	0	0	0	39	1	0	0	0	0	0	0	0	0	0	0
	iphone5	0	0	0	0	0	0	0	0	0	39	1	0	0	0	0	0	0	0	0	0
	iphone7	0	0	0	0	0	0	0	0	0	7	33	0	0	0	0	0	0	0	0	0
	n8_594	0	0	0	0	0	0	0	0	0	0	0	40	0	0	0	0	0	0	0	0
	n97_430	0	0	0	0	0	0	0	0	0	0	0	0	40	0	0	0	0	0	0	0
	n97_444	0	0	0	0	0	0	0	0	0	0	0	0	0	40	0	0	0	0	0	0
	n97_618	0	0	0	0	0	0	0	0	0	0	0	0	0	0	40	0	0	0	0	0
	n97_620	0	0	0	0	0	0	0	0	0	0	0	0	0	0	0	40	0	0	0	0
	nok_128	3	0	0	0	0	0	0	0	0	0	0	0	0	1	0	0	36	0	0	0
	nok_e5	0	0	0	0	0	0	0	0	0	0	0	0	0	0	0	0	0	40	0	0
	nok_e62	0	0	0	0	0	0	0	0	0	0	0	0	0	0	0	0	0	0	40	0
	treo	0	0	0	0	0	0	0	0	0	0	0	0	0	0	0	0	0	0	0	40

Table 48. Confusion Matrix for 150 Signal Vectors per Phone With One Signal Vector per Training Set

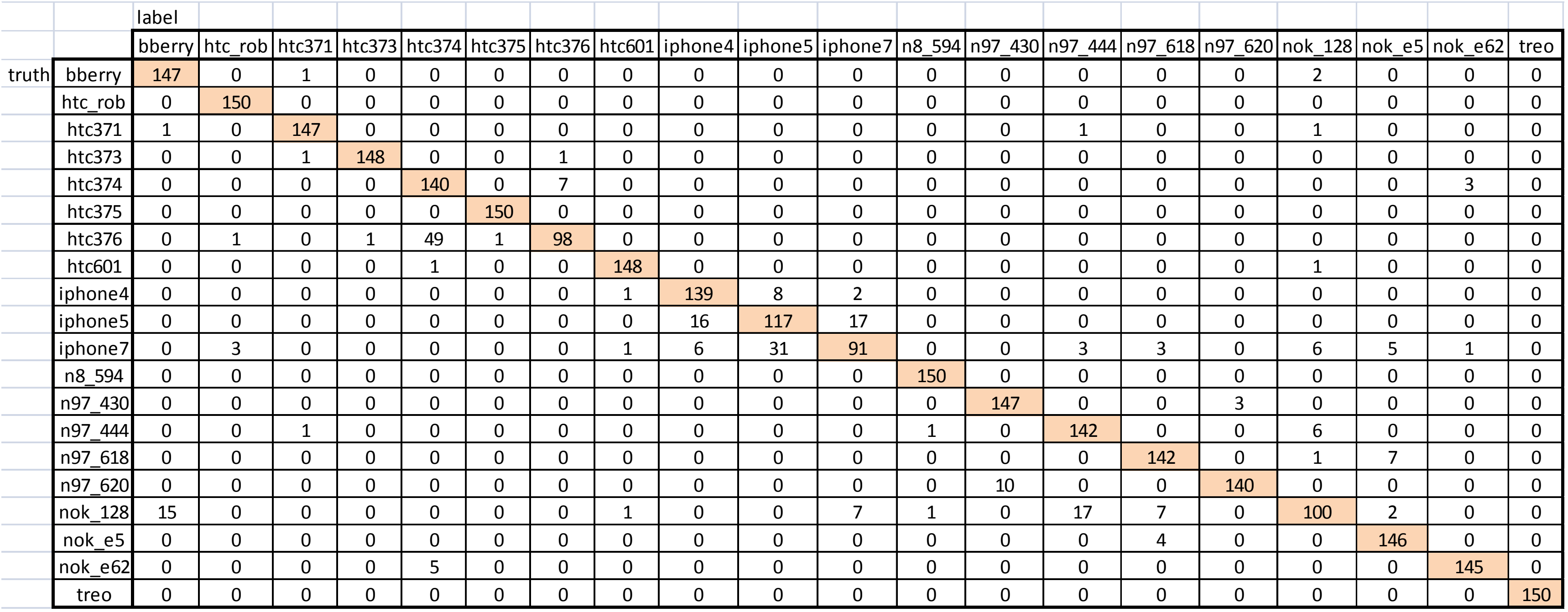

		label																			
		bberry	htc_rob	htc371	htc373	htc374	htc375	htc376	htc601	iphone4	iphone5	iphone7	n8_594	n97_430	n97_444	n97_618	n97_620	nok_128	nok_e5	nok_e62	treo
truth	bberry	147	0	1	0	0	0	0	0	0	0	0	0	0	0	0	0	2	0	0	0
	htc_rob	0	150	0	0	0	0	0	0	0	0	0	0	0	0	0	0	0	0	0	0
	htc371	1	0	147	0	0	0	0	0	0	0	0	0	0	1	0	0	1	0	0	0
	htc373	0	0	1	148	0	0	1	0	0	0	0	0	0	0	0	0	0	0	0	0
	htc374	0	0	0	0	140	0	7	0	0	0	0	0	0	0	0	0	0	0	3	0
	htc375	0	0	0	0	0	150	0	0	0	0	0	0	0	0	0	0	0	0	0	0
	htc376	0	1	0	1	49	1	98	0	0	0	0	0	0	0	0	0	0	0	0	0
	htc601	0	0	0	0	1	0	0	148	0	0	0	0	0	0	0	0	1	0	0	0
	iphone4	0	0	0	0	0	0	0	1	139	8	2	0	0	0	0	0	0	0	0	0
	iphone5	0	0	0	0	0	0	0	0	16	117	17	0	0	0	0	0	0	0	0	0
	iphone7	0	3	0	0	0	0	0	1	6	31	91	0	0	3	3	0	6	5	1	0
	n8_594	0	0	0	0	0	0	0	0	0	0	0	150	0	0	0	0	0	0	0	0
	n97_430	0	0	0	0	0	0	0	0	0	0	0	0	147	0	0	3	0	0	0	0
	n97_444	0	0	1	0	0	0	0	0	0	0	0	1	0	142	0	0	6	0	0	0
	n97_618	0	0	0	0	0	0	0	0	0	0	0	0	0	0	142	0	1	7	0	0
	n97_620	0	0	0	0	0	0	0	0	0	0	0	0	10	0	0	140	0	0	0	0
	nok_128	15	0	0	0	0	0	0	1	0	0	7	1	0	17	7	0	100	2	0	0
	nok_e5	0	0	0	0	0	0	0	0	0	0	0	0	0	0	4	0	0	146	0	0
	nok_e62	0	0	0	0	5	0	0	0	0	0	0	0	0	0	0	0	0	0	145	0
	treo	0	0	0	0	0	0	0	0	0	0	0	0	0	0	0	0	0	0	0	150

Table 49. Confusion Matrix for 150 Signal Vectors per Phone With Two Signal Vectors per Training Set

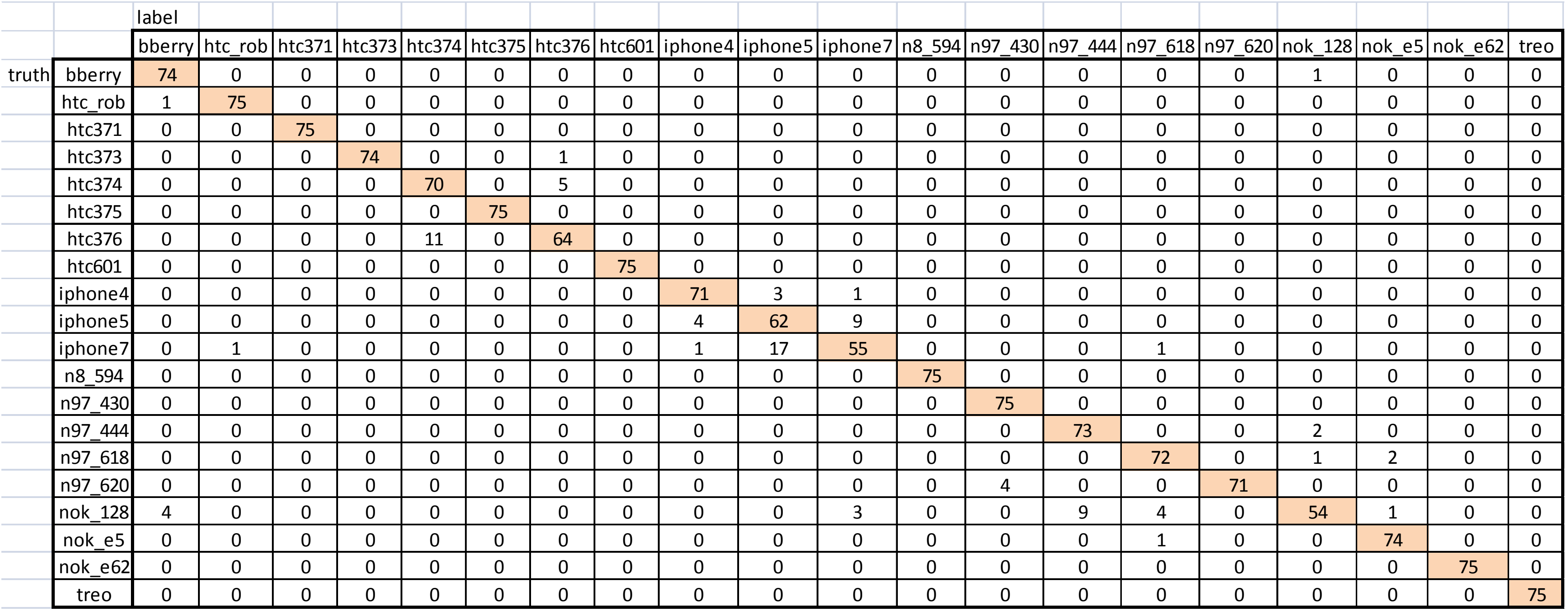

		label																			
		bberry	htc_rob	htc371	htc373	htc374	htc375	htc376	htc601	iphone4	iphone5	iphone7	n8_594	n97_430	n97_444	n97_618	n97_620	nok_128	nok_e5	nok_e62	treo
truth	bberry	74	0	0	0	0	0	0	0	0	0	0	0	0	0	0	0	1	0	0	0
	htc_rob	1	75	0	0	0	0	0	0	0	0	0	0	0	0	0	0	0	0	0	0
	htc371	0	0	75	0	0	0	0	0	0	0	0	0	0	0	0	0	0	0	0	0
	htc373	0	0	0	74	0	0	1	0	0	0	0	0	0	0	0	0	0	0	0	0
	htc374	0	0	0	0	70	0	5	0	0	0	0	0	0	0	0	0	0	0	0	0
	htc375	0	0	0	0	0	75	0	0	0	0	0	0	0	0	0	0	0	0	0	0
	htc376	0	0	0	0	11	0	64	0	0	0	0	0	0	0	0	0	0	0	0	0
	htc601	0	0	0	0	0	0	0	75	0	0	0	0	0	0	0	0	0	0	0	0
	iphone4	0	0	0	0	0	0	0	0	71	3	1	0	0	0	0	0	0	0	0	0
	iphone5	0	0	0	0	0	0	0	0	4	62	9	0	0	0	0	0	0	0	0	0
	iphone7	0	1	0	0	0	0	0	0	1	17	55	0	0	0	1	0	0	0	0	0
	n8_594	0	0	0	0	0	0	0	0	0	0	0	75	0	0	0	0	0	0	0	0
	n97_430	0	0	0	0	0	0	0	0	0	0	0	0	75	0	0	0	0	0	0	0
	n97_444	0	0	0	0	0	0	0	0	0	0	0	0	0	73	0	0	2	0	0	0
	n97_618	0	0	0	0	0	0	0	0	0	0	0	0	0	0	72	0	1	2	0	0
	n97_620	0	0	0	0	0	0	0	0	0	0	0	0	4	0	0	71	0	0	0	0
	nok_128	4	0	0	0	0	0	0	0	0	0	3	0	0	9	4	0	54	1	0	0
	nok_e5	0	0	0	0	0	0	0	0	0	0	0	0	0	0	1	0	0	74	0	0
	nok_e62	0	0	0	0	0	0	0	0	0	0	0	0	0	0	0	0	0	0	75	0
	treo	0	0	0	0	0	0	0	0	0	0	0	0	0	0	0	0	0	0	0	75

Table 50. Confusion Matrix for 150 Signal Vectors per Phone With Three Signal Vectors per Training Set

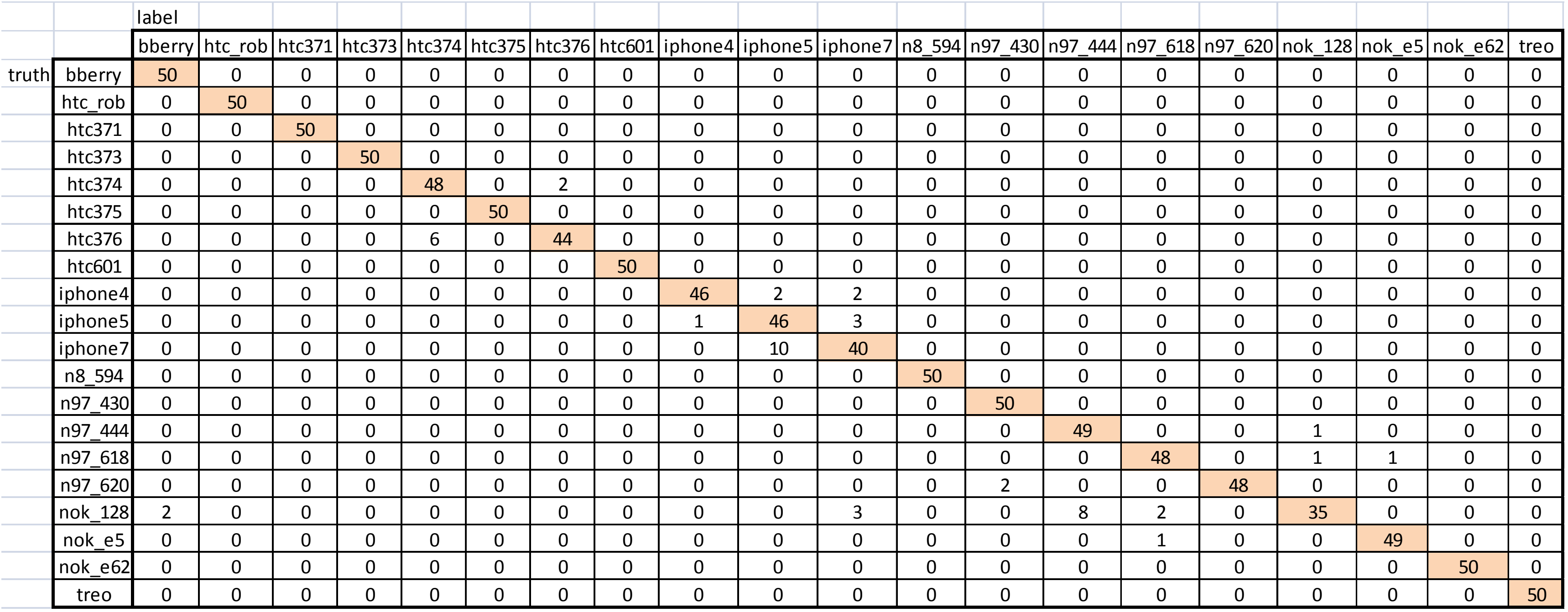

		label																			
		bberry	htc_rob	htc371	htc373	htc374	htc375	htc376	htc601	iphone4	iphone5	iphone7	n8_594	n97_430	n97_444	n97_618	n97_620	nok_128	nok_e5	nok_e62	treo
truth	bberry	50	0	0	0	0	0	0	0	0	0	0	0	0	0	0	0	0	0	0	0
	htc_rob	0	50	0	0	0	0	0	0	0	0	0	0	0	0	0	0	0	0	0	0
	htc371	0	0	50	0	0	0	0	0	0	0	0	0	0	0	0	0	0	0	0	0
	htc373	0	0	0	50	0	0	0	0	0	0	0	0	0	0	0	0	0	0	0	0
	htc374	0	0	0	0	48	0	2	0	0	0	0	0	0	0	0	0	0	0	0	0
	htc375	0	0	0	0	0	50	0	0	0	0	0	0	0	0	0	0	0	0	0	0
	htc376	0	0	0	0	6	0	44	0	0	0	0	0	0	0	0	0	0	0	0	0
	htc601	0	0	0	0	0	0	0	50	0	0	0	0	0	0	0	0	0	0	0	0
	iphone4	0	0	0	0	0	0	0	0	46	2	2	0	0	0	0	0	0	0	0	0
	iphone5	0	0	0	0	0	0	0	0	1	46	3	0	0	0	0	0	0	0	0	0
	iphone7	0	0	0	0	0	0	0	0	0	10	40	0	0	0	0	0	0	0	0	0
	n8_594	0	0	0	0	0	0	0	0	0	0	0	50	0	0	0	0	0	0	0	0
	n97_430	0	0	0	0	0	0	0	0	0	0	0	0	50	0	0	0	0	0	0	0
	n97_444	0	0	0	0	0	0	0	0	0	0	0	0	0	49	0	0	1	0	0	0
	n97_618	0	0	0	0	0	0	0	0	0	0	0	0	0	0	48	0	1	1	0	0
	n97_620	0	0	0	0	0	0	0	0	0	0	0	0	2	0	0	48	0	0	0	0
	nok_128	2	0	0	0	0	0	0	0	0	0	3	0	0	8	2	0	35	0	0	0
	nok_e5	0	0	0	0	0	0	0	0	0	0	0	0	0	0	1	0	0	49	0	0
	nok_e62	0	0	0	0	0	0	0	0	0	0	0	0	0	0	0	0	0	0	50	0
	treo	0	0	0	0	0	0	0	0	0	0	0	0	0	0	0	0	0	0	0	50

Table 51. Per Phone Accuracy Rates for Various Total Signal Vectors per Phone and Vectors per Training Set

# Vectors	30			50					100					120					150				
Training Set	1	2	3	1	2	3	4	5	1	2	3	4	5	1	2	3	4	5	1	2	3	4	5
bberry	0.967	1.000	1.000	0.980	0.960	0.941	1.000	1.000	0.960	0.980	1.000	1.000	1.000	0.975	1.000	1.000	1.000	1.000	0.980	0.987	1.000	0.947	1.000
htc371	0.900	0.733	1.000	0.940	1.000	0.941	1.000	1.000	1.000	1.000	1.000	1.000	1.000	1.000	1.000	1.000	1.000	1.000	1.000	0.987	1.000	1.000	1.000
htc373	0.933	0.867	0.800	0.920	1.000	1.000	1.000	1.000	0.940	1.000	1.000	1.000	1.000	0.942	1.000	1.000	1.000	1.000	0.980	1.000	1.000	1.000	1.000
htc374	0.833	0.733	0.700	0.980	0.960	1.000	1.000	1.000	0.990	1.000	1.000	1.000	1.000	1.000	1.000	1.000	1.000	1.000	0.987	0.987	1.000	0.921	0.933
htc375	0.933	0.933	1.000	0.860	0.920	0.941	1.000	0.800	0.890	0.980	1.000	1.000	1.000	0.925	0.983	1.000	1.000	1.000	0.933	0.933	0.960	1.000	1.000
htc376	0.733	0.800	0.900	0.980	0.960	1.000	1.000	1.000	0.990	1.000	1.000	1.000	1.000	0.992	1.000	1.000	1.000	0.958	1.000	1.000	1.000	0.947	1.000
htc601	1.000	1.000	1.000	0.600	0.840	0.706	0.846	0.900	0.670	0.880	0.912	1.000	0.950	0.675	0.867	0.900	1.000	1.000	0.653	0.853	0.880	0.974	1.000
htc_rob	0.933	0.933	1.000	1.000	1.000	1.000	1.000	1.000	0.970	1.000	1.000	1.000	1.000	0.992	1.000	1.000	1.000	1.000	0.987	1.000	1.000	1.000	1.000
iphone4	0.733	0.733	0.700	0.860	0.880	0.882	0.846	1.000	0.840	0.980	0.971	1.000	1.000	0.917	0.967	0.975	1.000	1.000	0.927	0.947	0.920	0.947	0.967
iphone5	0.700	0.733	0.700	0.720	0.800	0.882	0.769	0.800	0.830	0.880	0.971	1.000	1.000	0.800	0.883	0.975	1.000	1.000	0.780	0.827	0.920	0.842	0.867
iphone7	0.300	0.267	0.200	0.460	0.360	0.529	0.538	0.600	0.590	0.820	0.882	0.840	0.950	0.583	0.750	0.825	0.933	0.917	0.607	0.733	0.800	0.868	0.767
n8_594	1.000	1.000	1.000	0.940	0.960	1.000	1.000	1.000	0.980	1.000	1.000	1.000	1.000	0.992	1.000	1.000	1.000	1.000	1.000	1.000	1.000	1.000	1.000
n97_430	0.900	1.000	1.000	0.940	1.000	1.000	1.000	1.000	0.980	1.000	1.000	1.000	1.000	0.942	1.000	1.000	1.000	1.000	0.980	1.000	1.000	1.000	1.000
n97_444	0.800	1.000	0.800	0.900	1.000	1.000	1.000	0.900	0.910	1.000	1.000	1.000	1.000	0.933	1.000	1.000	1.000	1.000	0.947	0.973	0.980	0.974	1.000
n97_618	0.867	0.933	0.900	0.860	0.960	1.000	1.000	1.000	0.890	1.000	1.000	1.000	1.000	0.908	1.000	1.000	1.000	1.000	0.947	0.960	0.960	1.000	1.000
n97_620	0.700	0.800	0.700	0.820	0.920	0.882	1.000	1.000	0.950	1.000	1.000	1.000	1.000	0.933	1.000	1.000	1.000	1.000	0.933	0.947	0.960	1.000	0.967
nok_128	0.367	0.267	0.400	0.320	0.560	0.588	0.769	0.700	0.510	0.800	0.853	0.960	1.000	0.550	0.750	0.900	0.967	1.000	0.667	0.720	0.700	0.816	0.800
nok_e5	0.900	0.800	0.800	0.900	0.920	1.000	1.000	1.000	0.930	1.000	1.000	1.000	1.000	0.958	1.000	1.000	1.000	1.000	0.973	0.987	0.980	1.000	1.000
nok_e62	0.867	1.000	1.000	0.920	0.960	0.941	0.923	1.000	0.960	1.000	1.000	1.000	1.000	0.983	1.000	1.000	1.000	1.000	0.967	1.000	1.000	1.000	1.000
treo	0.967	1.000	1.000	1.000	1.000	1.000	1.000	1.000	1.000	1.000	1.000	1.000	1.000	1.000	1.000	1.000	1.000	1.000	1.000	1.000	1.000	1.000	1.000

APPENDIX E: COMBINED CLASSIFIER ADDITIONAL DATA

Table 52. Phone to Author Pairing Matrix

		Authors																			
	matrix	1	2	3	4	5	6	7	8	9	10	11	12	13	14	15	16	17	18	19	20
Phones	bberry	1045	1388	1734	1921	2546	2744	3155	3693	5599	5742	6111	6886	7100	7241	7754	7958	8164	8487	9417	9800
	htc371	1388	1734	1921	2546	2744	3155	3693	5599	5742	6111	6886	7100	7241	7754	7958	8164	8487	9417	9800	1045
	htc373	1734	1921	2546	2744	3155	3693	5599	5742	6111	6886	7100	7241	7754	7958	8164	8487	9417	9800	1045	1388
	htc374	1921	2546	2744	3155	3693	5599	5742	6111	6886	7100	7241	7754	7958	8164	8487	9417	9800	1045	1388	1734
	htc375	2546	2744	3155	3693	5599	5742	6111	6886	7100	7241	7754	7958	8164	8487	9417	9800	1045	1388	1734	1921
	htc376	2744	3155	3693	5599	5742	6111	6886	7100	7241	7754	7958	8164	8487	9417	9800	1045	1388	1734	1921	2546
	htc601	3155	3693	5599	5742	6111	6886	7100	7241	7754	7958	8164	8487	9417	9800	1045	1388	1734	1921	2546	2744
	htc_rob	3693	5599	5742	6111	6886	7100	7241	7754	7958	8164	8487	9417	9800	1045	1388	1734	1921	2546	2744	3155
	iphone4	5599	5742	6111	6886	7100	7241	7754	7958	8164	8487	9417	9800	1045	1388	1734	1921	2546	2744	3155	3693
	iphone5	5742	6111	6886	7100	7241	7754	7958	8164	8487	9417	9800	1045	1388	1734	1921	2546	2744	3155	3693	5599
	iphone7	6111	6886	7100	7241	7754	7958	8164	8487	9417	9800	1045	1388	1734	1921	2546	2744	3155	3693	5599	5742
	n8_594	6886	7100	7241	7754	7958	8164	8487	9417	9800	1045	1388	1734	1921	2546	2744	3155	3693	5599	5742	6111
	n97_430	7100	7241	7754	7958	8164	8487	9417	9800	1045	1388	1734	1921	2546	2744	3155	3693	5599	5742	6111	6886
	n97_444	7241	7754	7958	8164	8487	9417	9800	1045	1388	1734	1921	2546	2744	3155	3693	5599	5742	6111	6886	7100
	n97_618	7754	7958	8164	8487	9417	9800	1045	1388	1734	1921	2546	2744	3155	3693	5599	5742	6111	6886	7100	7241
	n97_620	7958	8164	8487	9417	9800	1045	1388	1734	1921	2546	2744	3155	3693	5599	5742	6111	6886	7100	7241	7754
	nok_128	8164	8487	9417	9800	1045	1388	1734	1921	2546	2744	3155	3693	5599	5742	6111	6886	7100	7241	7754	7958
	nok_e5	8487	9417	9800	1045	1388	1734	1921	2546	2744	3155	3693	5599	5742	6111	6886	7100	7241	7754	7958	8164
	nok_e62	9417	9800	1045	1388	1734	1921	2546	2744	3155	3693	5599	5742	6111	6886	7100	7241	7754	7958	8164	8487
	treo	9800	1045	1388	1734	1921	2546	2744	3155	3693	5599	5742	6111	6886	7100	7241	7754	7958	8164	8487	9417

Table 53. Confusion Matrix for Normalized Combined Classifier Matrix Pairing 1 Using 30 Tweets/Signal Vectors With One Tweet/Signal Vector per Training Set

		label ->																			
		1045	1388	1734	1921	2546	2744	3155	3693	5599	5742	6111	6886	7100	7241	7754	7958	8164	8487	9417	9800
truth	1045	28	0	0	0	0	0	0	0	0	0	0	1	0	0	0	0	1	0	0	0
|	1388	1	25	4	0	0	0	0	0	0	0	0	0	0	0	0	0	0	0	0	0
v	1734	0	1	27	0	0	0	0	0	0	0	0	0	0	0	0	0	0	0	2	0
	1921	0	0	0	25	0	4	0	0	0	0	0	0	0	0	0	0	0	0	1	0
	2546	0	0	0	0	29	0	0	0	0	0	0	0	0	0	0	0	0	0	1	0
	2744	1	1	0	4	0	23	0	0	0	0	0	0	0	0	0	0	0	0	1	0
	3155	0	0	0	0	0	0	30	19	0	0	0	0	0	0	0	0	0	0	1	0
	3693	0	0	0	0	0	0	0	10	0	0	0	0	0	0	0	0	0	0	0	0
	5599	0	0	0	0	0	0	0	0	26	1	2	1	0	0	0	0	0	0	0	0
	5742	0	0	0	0	0	0	0	0	7	23	0	0	0	0	0	0	0	0	0	0
	6111	1	0	0	0	0	1	0	1	5	4	17	0	0	0	0	0	0	1	0	0
	6886	0	0	0	0	0	0	0	0	0	0	0	30	0	0	0	0	0	0	0	0
	7100	0	0	0	0	0	0	0	0	0	0	0	1	28	0	0	1	0	0	0	0
	7241	0	1	0	0	0	0	0	0	0	0	1	2	1	25	0	0	0	0	0	0
	7754	0	0	0	0	0	0	0	0	0	0	0	0	0	0	27	0	0	3	0	0
	7958	0	0	0	0	0	0	0	0	0	0	0	1	5	1	0	23	0	0	0	0
	8164	3	1	0	0	0	0	0	0	0	0	1	0	2	6	3	0	13	1	0	0
	8487	0	0	0	0	0	0	0	0	0	0	0	0	0	0	2	0	0	28	0	0
	9417	0	0	0	1	1	1	0	0	0	0	0	0	0	0	0	0	0	0	27	0
	9800	0	0	0	0	1	0	0	0	0	0	0	0	0	0	0	0	0	0	0	29

Table 54. Confusion Matrix for Non-normalized Combined Classifier Matrix Pairing 1 Using 30 Tweets/Signal Vectors With One Tweet/Signal Vector per Training Set

		label ->																			
		1045	1388	1734	1921	2546	2744	3155	3693	5599	5742	6111	6886	7100	7241	7754	7958	8164	8487	9417	9800
truth	1045	9	2	0	2	2	0	0	1	3	0	1	3	1	1	1	3	0	1	0	0
|	1388	0	6	0	2	1	4	2	1	4	1	2	2	0	1	0	1	0	1	0	2
v	1734	1	5	4	0	1	0	3	3	0	1	1	3	0	0	0	4	0	0	3	1
	1921	0	5	3	4	1	4	5	0	0	0	0	0	1	2	1	3	0	1	0	0
	2546	0	0	0	4	11	8	1	0	2	0	1	0	1	0	0	0	0	0	1	1
	2744	0	2	1	2	4	10	0	0	3	1	1	0	1	0	0	1	0	1	2	1
	3155	0	0	1	6	6	9	11	7	3	0	0	1	1	1	1	0	1	2	0	0
	3693	0	0	0	1	1	0	0	7	0	0	0	0	0	0	0	0	1	0	0	0
	5599	0	0	0	0	0	0	0	0	27	0	2	0	1	0	0	0	0	0	0	0
	5742	3	1	1	0	1	0	4	0	4	10	1	1	1	0	0	1	0	0	2	0
	6111	0	0	0	2	0	0	1	0	8	1	16	0	0	1	0	0	0	0	1	0
	6886	0	2	0	0	1	1	2	0	2	0	1	17	1	0	0	2	1	0	0	0
	7100	0	1	3	0	2	2	2	1	4	0	0	0	15	0	0	0	0	0	0	0
	7241	0	1	0	0	2	1	5	0	3	0	4	2	0	10	0	2	0	0	0	0
	7754	0	1	0	0	1	1	1	0	0	0	0	4	0	1	11	3	0	0	5	2
	7958	0	1	2	1	0	1	3	0	0	1	1	1	2	1	0	14	0	0	2	0
	8164	0	1	0	2	0	1	2	0	0	0	3	0	1	0	0	1	18	0	0	1
	8487	1	2	0	2	2	0	1	1	3	0	1	0	0	0	1	1	0	15	0	0
	9417	1	1	0	0	0	2	3	1	2	0	0	2	0	0	2	2	0	1	13	0
	9800	0	0	0	1	4	2	1	0	0	0	2	1	3	0	0	0	1	1	0	14

Table 55. Confusion Matrix for Normalized Combined Classifier Matrix Pairing 1 Using 30 Tweets/Signal Vectors With Three Tweets/Signal Vectors per Training Set

		label ->																			
		1045	1388	1734	1921	2546	2744	3155	3693	5599	5742	6111	6886	7100	7241	7754	7958	8164	8487	9417	9800
truth	1045	10	0	0	0	0	0	0	0	0	0	0	0	0	0	0	0	0	0	0	0
|	1388	0	10	0	0	0	0	0	0	0	0	0	0	0	0	0	0	0	0	0	0
v	1734	0	2	8	0	0	0	0	0	0	0	0	0	0	0	0	0	0	0	0	0
	1921	0	0	0	7	0	3	0	0	0	0	0	0	0	0	0	0	0	0	0	0
	2546	0	0	0	0	10	0	0	0	0	0	0	0	0	0	0	0	0	0	0	0
	2744	0	0	0	1	0	9	0	0	0	0	0	0	0	0	0	0	0	0	0	0
	3155	0	0	0	0	0	0	10	0	0	0	0	0	0	0	0	0	0	0	0	0
	3693	0	0	0	0	0	0	0	10	0	0	0	0	0	0	0	0	0	0	0	0
	5599	0	0	0	0	0	0	0	0	9	0	1	0	0	0	0	0	0	0	0	0
	5742	0	0	0	0	0	0	0	0	1	9	0	0	0	0	0	0	0	0	0	0
	6111	0	0	0	0	0	0	0	1	0	0	8	0	0	1	0	0	0	0	0	0
	6886	0	0	0	0	0	0	0	0	0	0	1	10	1	0	0	0	0	0	0	0
	7100	0	0	0	0	0	0	0	0	0	0	0	0	10	0	0	0	0	0	0	0
	7241	0	0	0	0	0	0	0	0	0	0	0	1	0	8	0	0	1	0	0	0
	7754	0	0	0	0	0	0	0	0	0	0	0	0	0	0	10	0	0	0	0	0
	7958	0	0	0	0	0	0	0	0	0	0	0	0	1	0	0	9	0	0	0	0
	8164	1	0	0	0	0	0	0	0	0	0	1	0	0	1	0	1	6	0	0	0
	8487	0	0	0	0	0	0	0	0	0	0	0	0	0	0	2	0	0	8	0	0
	9417	0	0	0	0	0	0	0	0	0	0	0	0	0	0	0	0	0	0	10	0
	9800	0	0	0	0	0	0	0	0	0	0	0	0	0	0	0	0	0	0	1	10

Table 56. Confusion Matrix for Non-normalized Combined Classifier Matrix Pairing 1 Using 30 Tweets/Signal Vectors With Three Tweets/Signal Vectors per Training Set

		label ->																			
		1045	1388	1734	1921	2546	2744	3155	3693	5599	5742	6111	6886	7100	7241	7754	7958	8164	8487	9417	9800
truth	1045	6	0	0	0	0	0	1	0	0	0	0	1	1	0	0	1	0	0	0	0
|	1388	0	5	0	1	0	3	1	0	0	0	0	0	0	0	0	0	0	0	0	0
v	1734	0	4	2	0	0	0	1	0	0	0	0	0	1	0	0	1	1	0	0	0
	1921	0	4	1	0	0	3	2	0	0	0	0	0	0	0	0	0	0	0	0	0
	2546	0	0	0	0	7	1	1	0	0	0	0	0	0	0	0	1	0	0	0	0
	2744	0	2	0	1	2	5	0	0	0	0	0	0	0	0	0	0	0	0	0	0
	3155	0	0	0	3	0	2	5	0	0	0	0	0	0	0	0	0	0	0	0	0
	3693	0	0	0	0	1	0	0	6	3	0	0	0	0	0	0	0	0	0	0	0
	5599	0	0	0	0	0	0	0	0	10	0	0	0	0	0	0	0	0	0	0	0
	5742	0	0	1	0	0	1	2	0	2	4	0	0	0	0	0	0	0	0	0	0
	6111	0	1	0	0	0	0	1	0	2	0	6	0	0	0	0	0	0	0	0	0
	6886	0	1	0	0	1	1	1	0	0	0	0	6	0	0	0	0	0	0	0	0
	7100	0	0	0	0	0	0	1	0	0	0	0	0	9	0	0	0	0	0	0	0
	7241	0	0	0	0	0	0	0	0	1	0	0	2	0	6	0	1	0	0	0	0
	7754	0	0	0	0	0	0	1	0	0	0	0	1	0	0	6	1	0	0	1	0
	7958	0	0	0	0	0	0	0	0	0	0	0	0	1	0	0	9	0	0	0	0
	8164	0	0	0	1	0	0	0	0	0	0	0	0	1	0	0	0	8	0	0	0
	8487	0	0	0	0	0	0	0	0	1	0	0	0	0	0	0	0	0	9	0	0
	9417	0	0	0	0	0	1	0	0	0	0	0	0	0	0	1	0	0	0	8	0
	9800	0	0	0	1	2	0	0	0	0	0	1	0	2	0	0	0	0	0	0	4

Table 57. Confusion Matrix for Normalized Combined Classifier Matrix Pairing 1 Using 50 Tweets/Signal Vectors With One Tweet/Signal Vector per Training Set

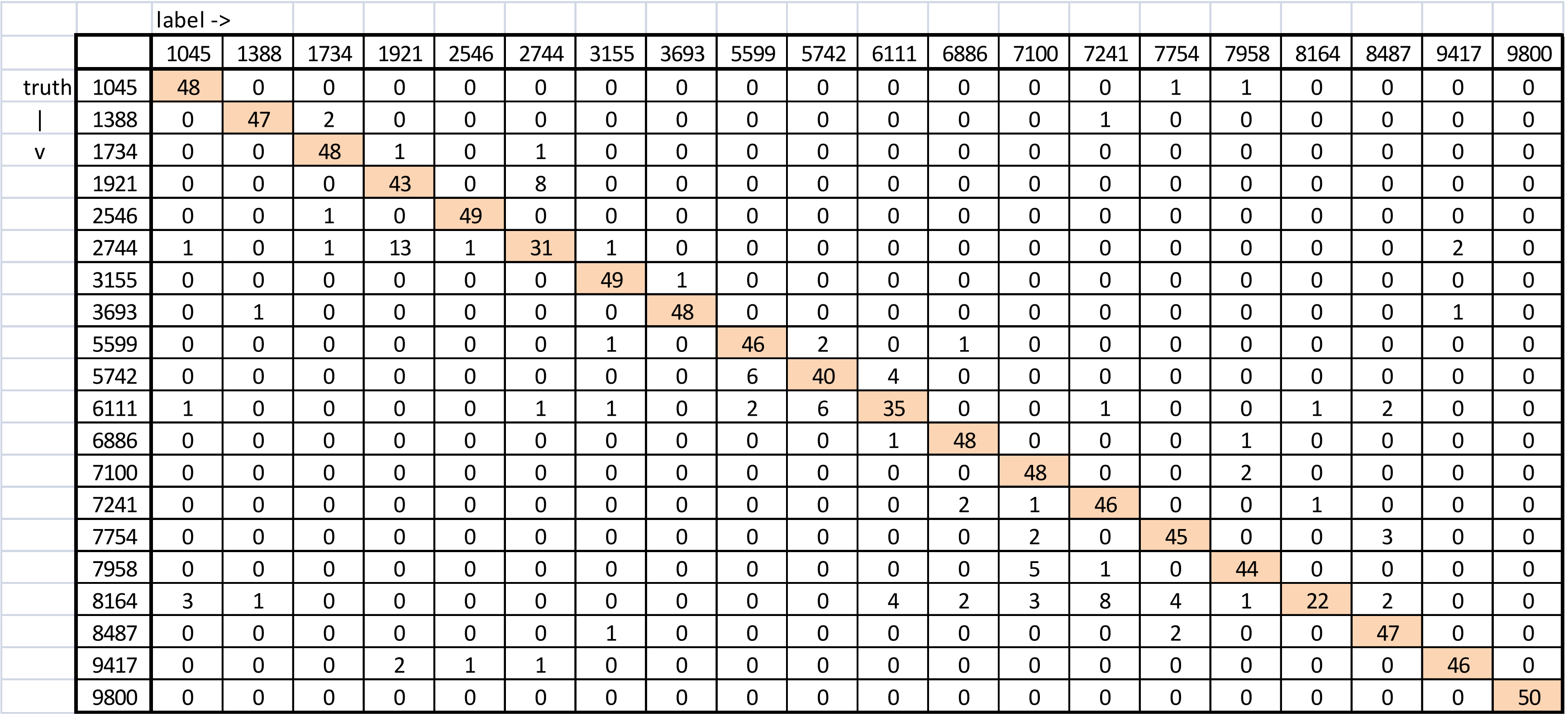

		label ->																			
		1045	1388	1734	1921	2546	2744	3155	3693	5599	5742	6111	6886	7100	7241	7754	7958	8164	8487	9417	9800
truth	1045	48	0	0	0	0	0	0	0	0	0	0	0	0	0	1	1	0	0	0	0
|	1388	0	47	2	0	0	0	0	0	0	0	0	0	0	1	0	0	0	0	0	0
v	1734	0	0	48	1	0	1	0	0	0	0	0	0	0	0	0	0	0	0	0	0
	1921	0	0	0	43	0	8	0	0	0	0	0	0	0	0	0	0	0	0	0	0
	2546	0	0	1	0	49	0	0	0	0	0	0	0	0	0	0	0	0	0	0	0
	2744	1	0	1	13	1	31	1	0	0	0	0	0	0	0	0	0	0	0	2	0
	3155	0	0	0	0	0	0	49	1	0	0	0	0	0	0	0	0	0	0	0	0
	3693	0	1	0	0	0	0	0	48	0	0	0	0	0	0	0	0	0	0	1	0
	5599	0	0	0	0	0	0	1	0	46	2	0	1	0	0	0	0	0	0	0	0
	5742	0	0	0	0	0	0	0	0	6	40	4	0	0	0	0	0	0	0	0	0
	6111	1	0	0	0	0	1	1	0	2	6	35	0	0	1	0	0	1	2	0	0
	6886	0	0	0	0	0	0	0	0	0	0	1	48	0	0	0	1	0	0	0	0
	7100	0	0	0	0	0	0	0	0	0	0	0	0	48	0	0	2	0	0	0	0
	7241	0	0	0	0	0	0	0	0	0	0	0	2	1	46	0	0	1	0	0	0
	7754	0	0	0	0	0	0	0	0	0	0	0	0	2	0	45	0	0	3	0	0
	7958	0	0	0	0	0	0	0	0	0	0	0	0	5	1	0	44	0	0	0	0
	8164	3	1	0	0	0	0	0	0	0	0	4	2	3	8	4	1	22	2	0	0
	8487	0	0	0	0	0	0	1	0	0	0	0	0	0	0	2	0	0	47	0	0
	9417	0	0	0	2	1	1	0	0	0	0	0	0	0	0	0	0	0	0	46	0
	9800	0	0	0	0	0	0	0	0	0	0	0	0	0	0	0	0	0	0	0	50

Table 58. Confusion Matrix for Non-normalized Combined Classifier Matrix Pairing 1 Using 50 Tweets/Signal Vectors With One Tweet/Signal Vector per Training Set

		label ->																			
		1045	1388	1734	1921	2546	2744	3155	3693	5599	5742	6111	6886	7100	7241	7754	7958	8164	8487	9417	9800
truth	1045	19	4	0	0	2	3	1	2	3	3	3	1	2	2	0	3	1	0	0	1
|	1388	0	16	0	3	1	9	2	1	5	3	4	2	0	0	0	0	1	0	2	1
v	1734	0	13	10	1	0	2	3	5	0	3	1	2	0	2	0	3	2	0	1	2
	1921	1	15	4	14	0	8	1	0	1	1	2	0	0	0	0	1	1	0	2	0
	2546	0	0	0	4	13	17	4	0	4	0	2	0	1	1	0	2	0	2	0	0
	2744	0	2	1	3	14	20	0	0	2	1	2	1	2	0	0	0	0	0	1	1
	3155	0	1	1	4	3	12	25	0	0	0	1	1	0	1	0	0	0	0	1	0
	3693	0	0	0	0	4	1	5	24	3	0	1	3	0	0	1	0	3	3	1	1
	5599	0	0	0	0	1	0	1	0	45	1	2	0	0	0	0	0	0	0	0	0
	5742	3	4	0	0	2	3	3	2	2	20	2	3	3	1	1	0	0	0	1	0
	6111	0	4	0	1	1	5	2	0	4	0	29	0	1	1	0	1	0	0	0	1
	6886	1	5	0	0	1	2	1	0	1	3	2	23	2	0	0	8	0	0	1	0
	7100	0	1	0	1	4	3	2	0	4	1	1	2	29	0	1	1	0	0	0	0
	7241	0	4	0	1	2	1	2	0	3	1	4	2	0	26	0	1	2	0	0	1
	7754	0	2	0	1	2	4	2	0	0	2	0	2	4	0	27	0	1	1	2	0
	7958	0	2	0	1	0	3	1	0	0	0	2	7	2	3	1	28	0	0	0	0
	8164	0	6	0	0	0	2	0	0	2	1	5	2	2	2	0	0	23	2	2	1
	8487	1	2	0	0	1	3	4	1	4	0	3	0	0	0	2	0	0	28	0	1
	9417	1	5	2	4	2	1	1	3	1	2	0	0	2	0	1	0	0	0	25	0
	9800	0	1	0	2	11	2	2	0	2	0	3	1	3	0	0	0	0	0	0	23

Table 59. Confusion Matrix for Normalized Combined Classifier Matrix Pairing 1 Using 50 Tweets/Signal Vectors With Three Tweets/Signal Vectors per Training Set

		label ->																			
		1045	1388	1734	1921	2546	2744	3155	3693	5599	5742	6111	6886	7100	7241	7754	7958	8164	8487	9417	9800
truth	1045	16	0	0	0	0	0	0	0	0	0	0	0	0	0	1	0	0	0	0	0
|	1388	0	17	0	0	0	0	0	0	0	0	0	0	0	0	0	0	0	0	0	0
v	1734	0	0	17	0	0	0	0	0	0	0	0	0	0	0	0	0	0	0	0	0
	1921	0	0	0	16	0	1	0	0	0	0	0	0	0	0	0	0	0	0	0	0
	2546	0	0	0	0	17	0	0	0	0	0	0	0	0	0	0	0	0	0	0	0
	2744	0	0	0	2	0	15	0	0	0	0	0	0	0	0	0	0	0	0	0	0
	3155	0	0	0	0	0	0	17	0	0	0	0	0	0	0	0	0	0	0	0	0
	3693	0	0	0	0	0	0	0	17	0	0	0	0	0	0	0	0	0	0	0	0
	5599	0	0	0	0	0	0	0	0	17	0	0	0	0	0	0	0	0	0	0	0
	5742	0	0	0	0	0	0	0	0	1	16	0	0	0	0	0	0	0	0	0	0
	6111	0	0	0	0	0	0	0	0	0	3	12	0	0	1	0	0	1	0	0	0
	6886	0	0	0	0	0	0	0	0	0	0	0	16	0	0	0	1	0	0	0	0
	7100	0	0	0	0	0	0	0	0	0	0	0	0	17	0	0	0	0	0	0	0
	7241	0	0	0	0	0	0	0	0	0	0	0	0	0	17	0	0	0	0	0	0
	7754	0	0	0	0	0	0	0	0	0	0	0	0	0	0	17	0	0	0	0	0
	7958	0	0	0	0	0	0	0	0	0	0	0	0	2	0	0	15	0	0	0	0
	8164	0	0	0	0	0	0	0	0	0	0	4	0	0	1	0	0	12	0	0	0
	8487	0	0	0	0	0	0	0	0	0	0	0	0	0	0	0	0	0	17	0	0
	9417	0	0	0	0	0	0	0	0	0	0	0	0	0	0	0	0	0	0	17	0
	9800	0	0	0	0	0	0	0	0	0	0	0	0	0	0	0	0	0	0	0	17

Table 60. Confusion Matrix for Non-normalized Combined Classifier Matrix Pairing 1 Using 50 Tweets/Signal Vectors With Three Tweets/Signal Vectors per Training Set

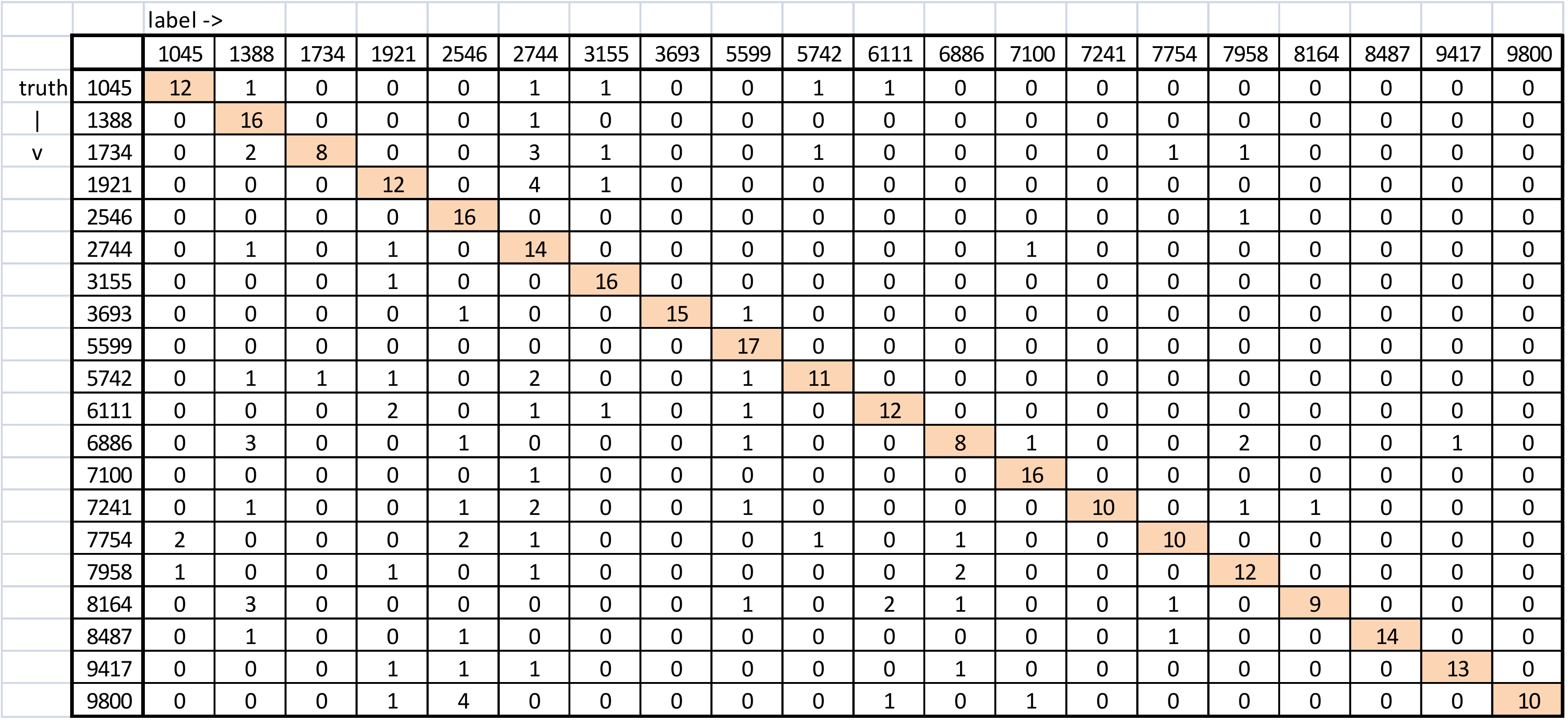

		label ->																			
		1045	1388	1734	1921	2546	2744	3155	3693	5599	5742	6111	6886	7100	7241	7754	7958	8164	8487	9417	9800
truth	1045	12	1	0	0	0	1	1	0	0	1	1	0	0	0	0	0	0	0	0	0
|	1388	0	16	0	0	0	1	0	0	0	0	0	0	0	0	0	0	0	0	0	0
v	1734	0	2	8	0	0	3	1	0	0	1	0	0	0	0	1	1	0	0	0	0
	1921	0	0	0	12	0	4	1	0	0	0	0	0	0	0	0	0	0	0	0	0
	2546	0	0	0	0	16	0	0	0	0	0	0	0	0	0	0	1	0	0	0	0
	2744	0	1	0	1	0	14	0	0	0	0	0	0	1	0	0	0	0	0	0	0
	3155	0	0	0	1	0	0	16	0	0	0	0	0	0	0	0	0	0	0	0	0
	3693	0	0	0	0	1	0	0	15	1	0	0	0	0	0	0	0	0	0	0	0
	5599	0	0	0	0	0	0	0	0	17	0	0	0	0	0	0	0	0	0	0	0
	5742	0	1	1	1	0	2	0	0	1	11	0	0	0	0	0	0	0	0	0	0
	6111	0	0	0	2	0	1	1	0	1	0	12	0	0	0	0	0	0	0	0	0
	6886	0	3	0	0	1	0	0	0	1	0	0	8	1	0	0	2	0	0	1	0
	7100	0	0	0	0	0	1	0	0	0	0	0	0	16	0	0	0	0	0	0	0
	7241	0	1	0	0	1	2	0	0	1	0	0	0	0	10	0	1	1	0	0	0
	7754	2	0	0	0	2	1	0	0	0	1	0	1	0	0	10	0	0	0	0	0
	7958	1	0	0	1	0	1	0	0	0	0	0	2	0	0	0	12	0	0	0	0
	8164	0	3	0	0	0	0	0	0	1	0	2	1	0	0	1	0	9	0	0	0
	8487	0	1	0	0	1	0	0	0	0	0	0	0	0	0	1	0	0	14	0	0
	9417	0	0	0	1	1	1	0	0	0	0	0	1	0	0	0	0	0	0	13	0
	9800	0	0	0	1	4	0	0	0	0	0	1	0	1	0	0	0	0	0	0	10

Table 61. Confusion Matrix for Normalized Combined Classifier Matrix Pairing 1 Using 120 Tweets/Signal Vectors With One Tweet/Signal Vector per Training Set

		label ->																			
		1045	1388	1734	1921	2546	2744	3155	3693	5599	5742	6111	6886	7100	7241	7754	7958	8164	8487	9417	9800
truth	1045	118	0	0	0	0	0	0	0	0	0	0	0	0	0	0	0	2	0	0	0
|	1388	1	113	5	0	0	0	0	0	0	0	0	0	0	0	0	0	0	1	0	0
v	1734	0	0	120	0	0	0	0	0	0	0	0	0	0	0	0	0	0	0	0	0
	1921	0	0	0	111	0	8	0	0	0	0	0	0	0	0	0	0	0	0	1	0
	2546	0	0	0	0	119	1	0	0	0	0	0	0	0	0	0	0	0	0	0	0
	2744	1	0	0	26	0	91	0	0	0	0	0	0	0	0	0	0	0	0	2	0
	3155	0	0	0	1	0	0	119	0	0	0	0	0	0	0	0	0	0	0	0	0
	3693	0	0	0	0	0	0	0	120	0	0	0	0	0	0	0	0	0	0	0	0
	5599	0	0	0	0	0	0	1	0	115	3	1	0	0	0	0	0	0	0	0	0
	5742	0	0	0	0	0	0	0	0	7	106	7	0	0	0	0	0	0	0	0	0
	6111	0	0	0	0	0	0	1	0	4	8	102	0	0	1	0	0	2	2	0	0
	6886	0	0	0	0	0	0	0	0	0	0	0	118	1	0	0	1	0	0	0	0
	7100	0	0	0	0	0	0	0	0	0	0	0	0	118	0	0	2	0	0	0	0
	7241	0	0	0	0	0	0	0	0	0	0	0	0	1	114	0	1	4	0	0	0
	7754	0	0	0	0	0	0	0	0	0	0	0	0	0	0	117	0	0	3	0	0
	7958	0	0	0	0	0	0	0	0	0	0	0	0	5	1	0	114	0	0	0	0
	8164	12	1	0	0	0	0	1	0	0	0	3	0	1	13	9	1	78	1	0	0
	8487	0	0	0	0	0	1	0	0	0	0	0	0	0	0	0	0	0	119	0	0
	9417	0	0	0	1	2	0	0	0	0	0	0	0	0	0	0	0	0	0	117	0
	9800	0	0	0	0	0	0	0	0	0	0	0	0	0	0	0	0	0	0	0	120

Table 62. Confusion Matrix for Non-normalized Combined Classifier Matrix Pairing 1 Using 120 Tweets/Signal Vectors With One Tweet/Signal Vector per Training Set

		label ->																			
		1045	1388	1734	1921	2546	2744	3155	3693	5599	5742	6111	6886	7100	7241	7754	7958	8164	8487	9417	9800
truth	1045	67	10	0	0	2	4	2	8	5	2	4	1	4	3	0	5	2	1	0	0
|	1388	0	39	0	7	0	22	8	2	9	5	7	0	2	1	1	0	1	0	14	2
v	1734	0	45	31	1	0	6	2	11	1	4	1	3	1	4	1	4	3	0	1	1
	1921	0	27	18	44	5	13	6	0	0	0	2	1	0	1	0	1	0	0	1	1
	2546	0	1	0	20	39	45	2	0	7	1	1	1	0	0	0	1	0	0	2	0
	2744	0	2	1	1	38	62	0	1	5	2	1	0	1	0	0	0	0	2	1	3
	3155	0	0	1	12	8	41	49	1	0	0	1	0	1	0	1	0	0	1	1	3
	3693	3	0	0	0	0	3	16	65	14	3	2	2	1	0	2	0	1	7	0	1
	5599	1	1	0	0	4	1	0	0	109	0	2	0	0	0	0	0	0	0	1	1
	5742	1	5	0	3	0	15	5	10	5	66	3	1	0	1	1	0	0	0	3	1
	6111	0	7	0	3	2	9	2	0	3	3	86	3	0	0	0	0	1	0	1	0
	6886	1	2	0	1	0	1	0	4	3	0	2	92	2	1	0	10	0	0	1	0
	7100	0	3	0	0	2	9	1	0	1	1	1	1	90	0	3	7	1	0	0	0
	7241	0	8	1	2	3	2	0	0	3	2	4	1	3	84	0	3	4	0	0	0
	7754	2	5	0	1	1	8	2	4	2	3	1	2	5	2	79	2	1	0	0	0
	7958	0	4	1	0	0	2	0	4	2	0	2	6	3	2	2	91	0	0	0	1
	8164	4	7	0	2	3	1	1	1	4	2	10	2	2	2	5	2	70	1	0	1
	8487	1	2	0	0	2	8	3	3	1	2	4	0	1	0	2	0	0	89	1	1
	9417	1	2	5	4	1	15	1	8	0	1	1	0	0	1	0	1	0	0	79	0
	9800	0	1	0	5	7	5	2	0	0	0	1	2	4	0	0	3	0	0	0	90

Table 63. Confusion Matrix for Normalized Combined Classifier Matrix Pairing 1 Using 120 Tweets/Signal Vectors With Three Tweets/Signal Vectors per Training Set

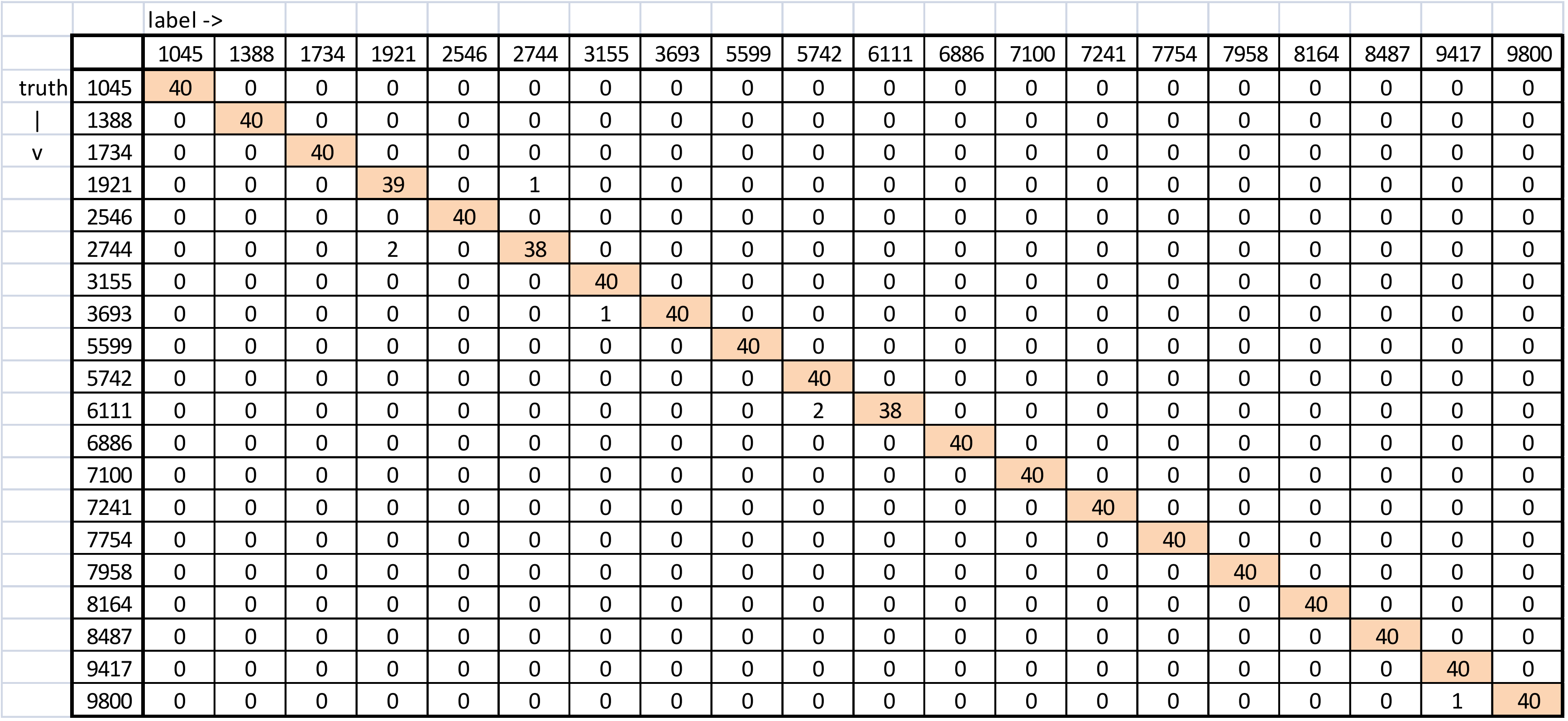

		label ->																			
		1045	1388	1734	1921	2546	2744	3155	3693	5599	5742	6111	6886	7100	7241	7754	7958	8164	8487	9417	9800
truth	1045	40	0	0	0	0	0	0	0	0	0	0	0	0	0	0	0	0	0	0	0
|	1388	0	40	0	0	0	0	0	0	0	0	0	0	0	0	0	0	0	0	0	0
v	1734	0	0	40	0	0	0	0	0	0	0	0	0	0	0	0	0	0	0	0	0
	1921	0	0	0	39	0	1	0	0	0	0	0	0	0	0	0	0	0	0	0	0
	2546	0	0	0	0	40	0	0	0	0	0	0	0	0	0	0	0	0	0	0	0
	2744	0	0	0	2	0	38	0	0	0	0	0	0	0	0	0	0	0	0	0	0
	3155	0	0	0	0	0	0	40	0	0	0	0	0	0	0	0	0	0	0	0	0
	3693	0	0	0	0	0	0	1	40	0	0	0	0	0	0	0	0	0	0	0	0
	5599	0	0	0	0	0	0	0	0	40	0	0	0	0	0	0	0	0	0	0	0
	5742	0	0	0	0	0	0	0	0	0	40	0	0	0	0	0	0	0	0	0	0
	6111	0	0	0	0	0	0	0	0	0	2	38	0	0	0	0	0	0	0	0	0
	6886	0	0	0	0	0	0	0	0	0	0	0	40	0	0	0	0	0	0	0	0
	7100	0	0	0	0	0	0	0	0	0	0	0	0	40	0	0	0	0	0	0	0
	7241	0	0	0	0	0	0	0	0	0	0	0	0	0	40	0	0	0	0	0	0
	7754	0	0	0	0	0	0	0	0	0	0	0	0	0	0	40	0	0	0	0	0
	7958	0	0	0	0	0	0	0	0	0	0	0	0	0	0	0	40	0	0	0	0
	8164	0	0	0	0	0	0	0	0	0	0	0	0	0	0	0	0	40	0	0	0
	8487	0	0	0	0	0	0	0	0	0	0	0	0	0	0	0	0	0	40	0	0
	9417	0	0	0	0	0	0	0	0	0	0	0	0	0	0	0	0	0	0	40	0
	9800	0	0	0	0	0	0	0	0	0	0	0	0	0	0	0	0	0	0	1	40

Table 64. Confusion Matrix for Non-normalized Combined Classifier Matrix Pairing 1 Using 120 Tweets/Signal Vectors With Three Tweets/Signal Vectors per Training Set

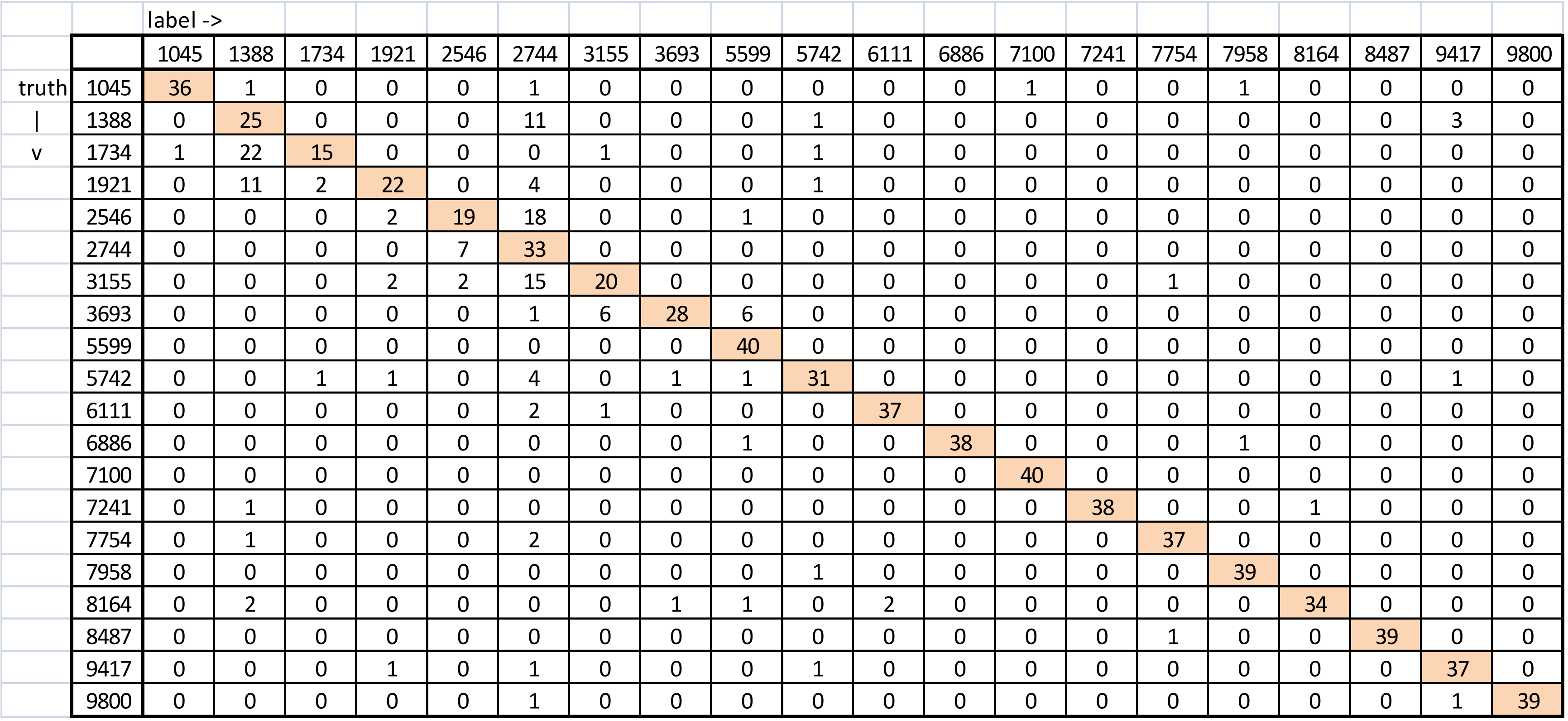

		label ->																			
		1045	1388	1734	1921	2546	2744	3155	3693	5599	5742	6111	6886	7100	7241	7754	7958	8164	8487	9417	9800
truth	1045	36	1	0	0	0	1	0	0	0	0	0	0	1	0	0	1	0	0	0	0
|	1388	0	25	0	0	0	11	0	0	0	1	0	0	0	0	0	0	0	0	3	0
v	1734	1	22	15	0	0	0	1	0	0	1	0	0	0	0	0	0	0	0	0	0
	1921	0	11	2	22	0	4	0	0	0	1	0	0	0	0	0	0	0	0	0	0
	2546	0	0	0	2	19	18	0	0	1	0	0	0	0	0	0	0	0	0	0	0
	2744	0	0	0	0	7	33	0	0	0	0	0	0	0	0	0	0	0	0	0	0
	3155	0	0	0	2	2	15	20	0	0	0	0	0	0	0	1	0	0	0	0	0
	3693	0	0	0	0	0	1	6	28	6	0	0	0	0	0	0	0	0	0	0	0
	5599	0	0	0	0	0	0	0	0	40	0	0	0	0	0	0	0	0	0	0	0
	5742	0	0	1	1	0	4	0	1	1	31	0	0	0	0	0	0	0	0	1	0
	6111	0	0	0	0	0	2	1	0	0	0	37	0	0	0	0	0	0	0	0	0
	6886	0	0	0	0	0	0	0	0	1	0	0	38	0	0	0	1	0	0	0	0
	7100	0	0	0	0	0	0	0	0	0	0	0	0	40	0	0	0	0	0	0	0
	7241	0	1	0	0	0	0	0	0	0	0	0	0	0	38	0	0	1	0	0	0
	7754	0	1	0	0	0	2	0	0	0	0	0	0	0	0	37	0	0	0	0	0
	7958	0	0	0	0	0	0	0	0	0	1	0	0	0	0	0	39	0	0	0	0
	8164	0	2	0	0	0	0	0	1	1	0	2	0	0	0	0	0	34	0	0	0
	8487	0	0	0	0	0	0	0	0	0	0	0	0	0	0	1	0	0	39	0	0
	9417	0	0	0	1	0	1	0	0	0	1	0	0	0	0	0	0	0	0	37	0
	9800	0	0	0	0	0	1	0	0	0	0	0	0	0	0	0	0	0	0	1	39

Table 65. Confusion Matrix for Normalized Combined Classifier Matrix Pairing 1 Using 120 Tweets/Signal Vectors With Five Tweets/Signal Vectors per Training Set

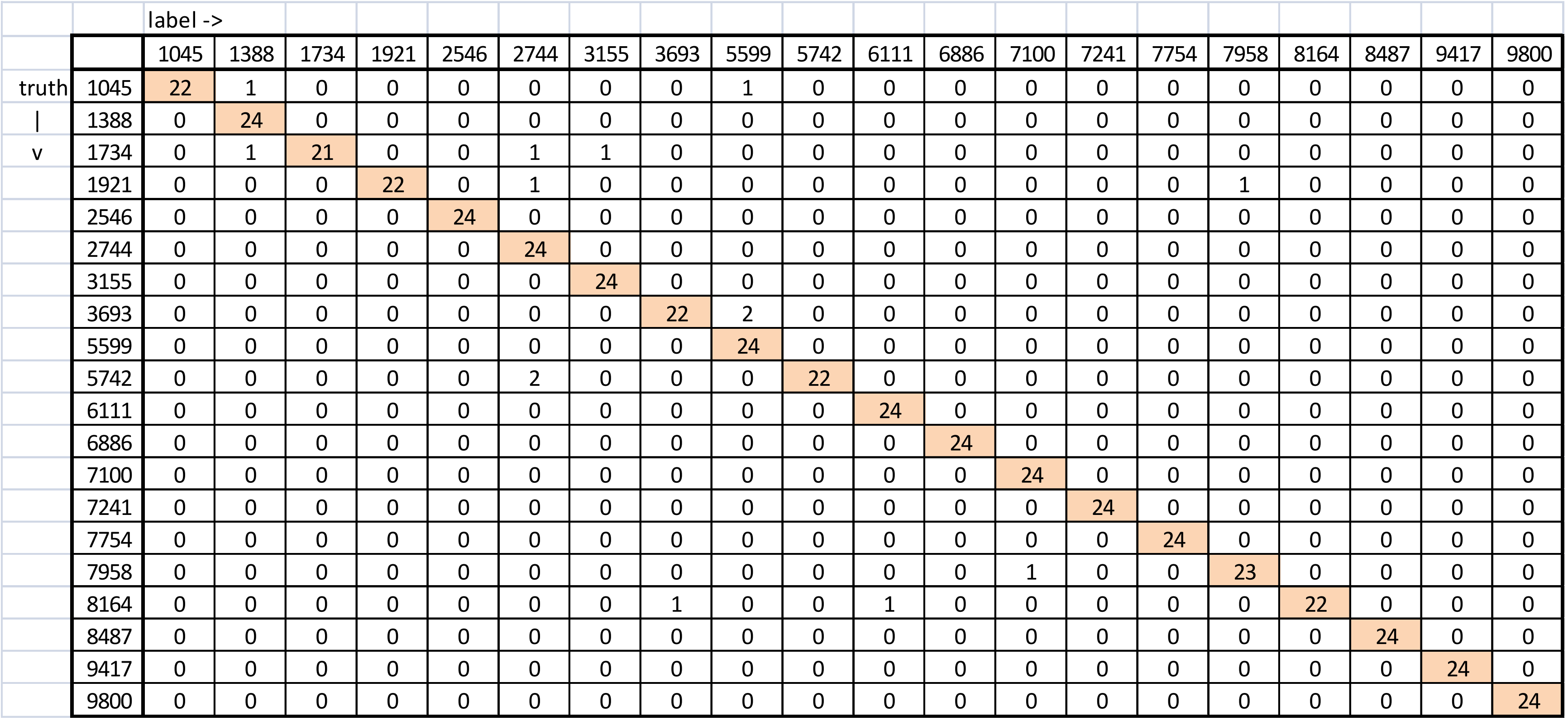

		label ->																			
		1045	1388	1734	1921	2546	2744	3155	3693	5599	5742	6111	6886	7100	7241	7754	7958	8164	8487	9417	9800
truth	1045	22	1	0	0	0	0	0	0	1	0	0	0	0	0	0	0	0	0	0	0
|	1388	0	24	0	0	0	0	0	0	0	0	0	0	0	0	0	0	0	0	0	0
v	1734	0	1	21	0	0	1	1	0	0	0	0	0	0	0	0	0	0	0	0	0
	1921	0	0	0	22	0	1	0	0	0	0	0	0	0	0	0	1	0	0	0	0
	2546	0	0	0	0	24	0	0	0	0	0	0	0	0	0	0	0	0	0	0	0
	2744	0	0	0	0	0	24	0	0	0	0	0	0	0	0	0	0	0	0	0	0
	3155	0	0	0	0	0	0	24	0	0	0	0	0	0	0	0	0	0	0	0	0
	3693	0	0	0	0	0	0	0	22	2	0	0	0	0	0	0	0	0	0	0	0
	5599	0	0	0	0	0	0	0	0	24	0	0	0	0	0	0	0	0	0	0	0
	5742	0	0	0	0	0	2	0	0	0	22	0	0	0	0	0	0	0	0	0	0
	6111	0	0	0	0	0	0	0	0	0	0	24	0	0	0	0	0	0	0	0	0
	6886	0	0	0	0	0	0	0	0	0	0	0	24	0	0	0	0	0	0	0	0
	7100	0	0	0	0	0	0	0	0	0	0	0	0	24	0	0	0	0	0	0	0
	7241	0	0	0	0	0	0	0	0	0	0	0	0	0	24	0	0	0	0	0	0
	7754	0	0	0	0	0	0	0	0	0	0	0	0	0	0	24	0	0	0	0	0
	7958	0	0	0	0	0	0	0	0	0	0	0	0	1	0	0	23	0	0	0	0
	8164	0	0	0	0	0	0	0	1	0	0	1	0	0	0	0	0	22	0	0	0
	8487	0	0	0	0	0	0	0	0	0	0	0	0	0	0	0	0	0	24	0	0
	9417	0	0	0	0	0	0	0	0	0	0	0	0	0	0	0	0	0	0	24	0
	9800	0	0	0	0	0	0	0	0	0	0	0	0	0	0	0	0	0	0	0	24

Table 66. Confusion Matrix for Non-normalized Combined Classifier Matrix Pairing 1 Using 120 Tweets/Signal Vectors With Five Tweets/Signal Vectors per Training Set

		label ->																			
		1045	1388	1734	1921	2546	2744	3155	3693	5599	5742	6111	6886	7100	7241	7754	7958	8164	8487	9417	9800
truth	1045	24	0	0	0	0	0	0	0	0	0	0	0	0	0	0	0	0	0	0	0
|	1388	0	24	0	0	0	0	0	0	0	0	0	0	0	0	0	0	0	0	0	0
v	1734	0	0	24	0	0	0	0	0	0	0	0	0	0	0	0	0	0	0	0	0
	1921	0	0	0	24	0	0	0	0	0	0	0	0	0	0	0	0	0	0	0	0
	2546	0	0	0	0	24	0	0	0	0	0	0	0	0	0	0	0	0	0	0	0
	2744	0	0	0	0	0	24	0	0	0	0	0	0	0	0	0	0	0	0	0	0
	3155	0	0	0	0	0	0	24	0	0	0	0	0	0	0	0	0	0	0	0	0
	3693	0	0	0	0	0	0	0	24	0	0	0	0	0	0	0	0	0	0	0	0
	5599	0	0	0	0	0	0	0	0	24	0	0	0	0	0	0	0	0	0	0	0
	5742	0	0	0	0	0	0	0	0	0	24	0	0	0	0	0	0	0	0	0	0
	6111	0	0	0	0	0	0	0	0	0	2	22	0	0	0	0	0	0	0	0	0
	6886	0	0	0	0	0	0	0	0	0	0	0	24	0	0	0	0	0	0	0	0
	7100	0	0	0	0	0	0	0	0	0	0	0	0	24	0	0	0	0	0	0	0
	7241	0	0	0	0	0	0	0	0	0	0	0	0	0	24	0	0	0	0	0	0
	7754	0	0	0	0	0	0	0	0	0	0	0	0	0	0	24	0	0	0	0	0
	7958	0	0	0	0	0	0	0	0	0	0	0	0	0	0	0	24	0	0	0	0
	8164	0	0	0	0	0	0	0	0	0	0	0	0	0	0	0	0	24	0	0	0
	8487	0	0	0	0	0	0	0	0	0	0	0	0	0	0	0	0	0	24	0	0
	9417	0	0	0	0	0	0	0	0	0	0	0	0	0	0	0	0	0	0	24	0
	9800	0	0	0	0	0	0	0	0	0	0	0	0	0	0	0	0	0	0	0	24

Table 67. Per Pair Combined Classifier Accuracy Results by Total Tweets/Signal Vectors and Tweets/Signal Vectors per Training Set

		Normalized							Non-normalized						
		30		50		120			30		50		120		
Phone	Author	1	3	1	3	1	3	5	1	3	1	3	1	3	5
bberry	1045	0.933	1.000	0.960	0.941	0.983	1.000	0.917	0.300	0.600	0.380	0.706	0.558	0.900	1.000
htc371	1388	0.833	1.000	0.940	1.000	0.942	1.000	1.000	0.200	0.500	0.320	0.941	0.325	0.625	1.000
htc373	1734	0.900	0.800	0.960	1.000	1.000	1.000	0.875	0.133	0.200	0.200	0.471	0.258	0.375	1.000
htc374	1921	0.833	0.700	0.843	0.941	0.925	0.975	0.917	0.133	0.000	0.275	0.706	0.367	0.550	1.000
htc375	2546	0.967	1.000	0.980	1.000	0.992	1.000	1.000	0.367	0.700	0.260	0.941	0.325	0.475	1.000
htc376	2744	0.767	0.900	0.620	0.882	0.758	0.950	1.000	0.333	0.500	0.400	0.824	0.517	0.825	1.000
htc601	3155	0.600	1.000	0.980	1.000	0.992	1.000	1.000	0.220	0.500	0.500	0.941	0.408	0.500	1.000
htc_rob	3693	1.000	1.000	0.960	1.000	1.000	0.976	0.917	0.700	0.600	0.480	0.882	0.542	0.683	1.000
iphone4	5599	0.867	0.900	0.920	1.000	0.958	1.000	1.000	0.900	1.000	0.900	1.000	0.908	1.000	1.000
iphone5	5742	0.767	0.900	0.800	0.941	0.883	1.000	0.917	0.333	0.400	0.400	0.647	0.550	0.775	1.000
iphone7	6111	0.567	0.800	0.700	0.706	0.850	0.950	1.000	0.533	0.600	0.580	0.706	0.717	0.925	0.917
n8_594	6886	1.000	0.833	0.960	0.941	0.983	1.000	1.000	0.567	0.600	0.460	0.471	0.767	0.950	1.000
n97_430	7100	0.933	1.000	0.960	1.000	0.983	1.000	1.000	0.500	0.900	0.580	0.941	0.750	1.000	1.000
n97_444	7241	0.833	0.800	0.920	1.000	0.950	1.000	1.000	0.333	0.600	0.520	0.588	0.700	0.950	1.000
n97_618	7754	0.900	1.000	0.900	1.000	0.975	1.000	1.000	0.367	0.600	0.540	0.588	0.658	0.925	1.000
n97_620	7958	0.767	0.900	0.880	0.882	0.950	1.000	0.958	0.467	0.900	0.560	0.706	0.758	0.975	1.000
nok_128	8164	0.433	0.600	0.440	0.706	0.650	1.000	0.917	0.600	0.800	0.460	0.529	0.583	0.850	1.000
nok_e5	8487	0.933	0.800	0.940	1.000	0.992	1.000	1.000	0.500	0.900	0.560	0.824	0.742	0.975	1.000
nok_e62	9417	0.900	1.000	0.920	1.000	0.975	1.000	1.000	0.433	0.800	0.500	0.765	0.658	0.925	1.000
treo	9800	0.967	0.909	1.000	1.000	1.000	0.976	1.000	0.467	0.400	0.460	0.588	0.750	0.951	1.000

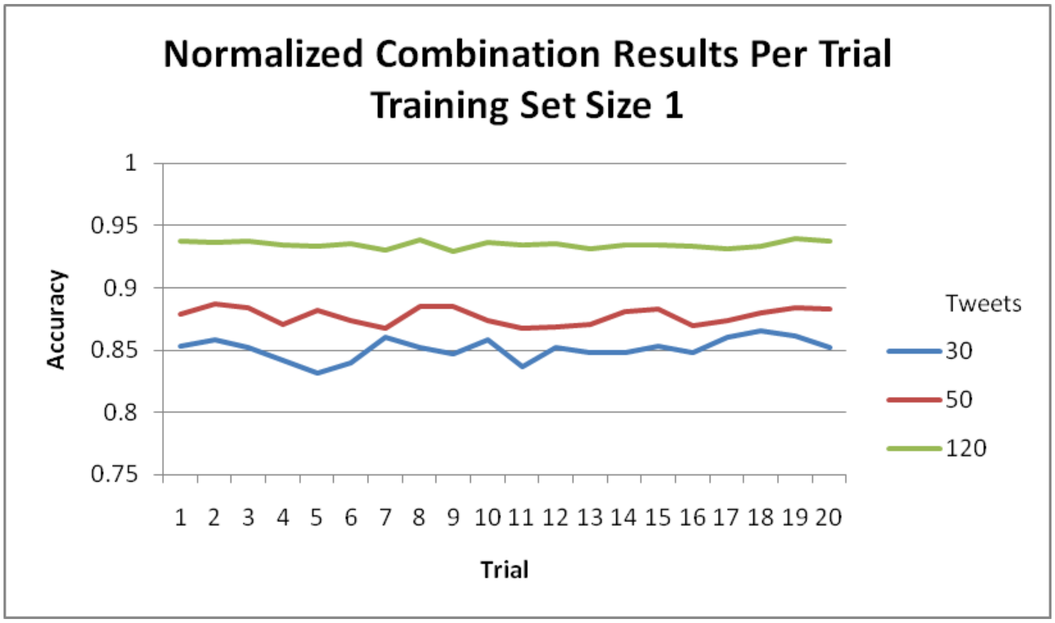

Figure 51. Averaged Accuracy Results of Normalized Combined Classifiers for Each Phone-Author Pairing Matrix Using One Tweet per Training Set

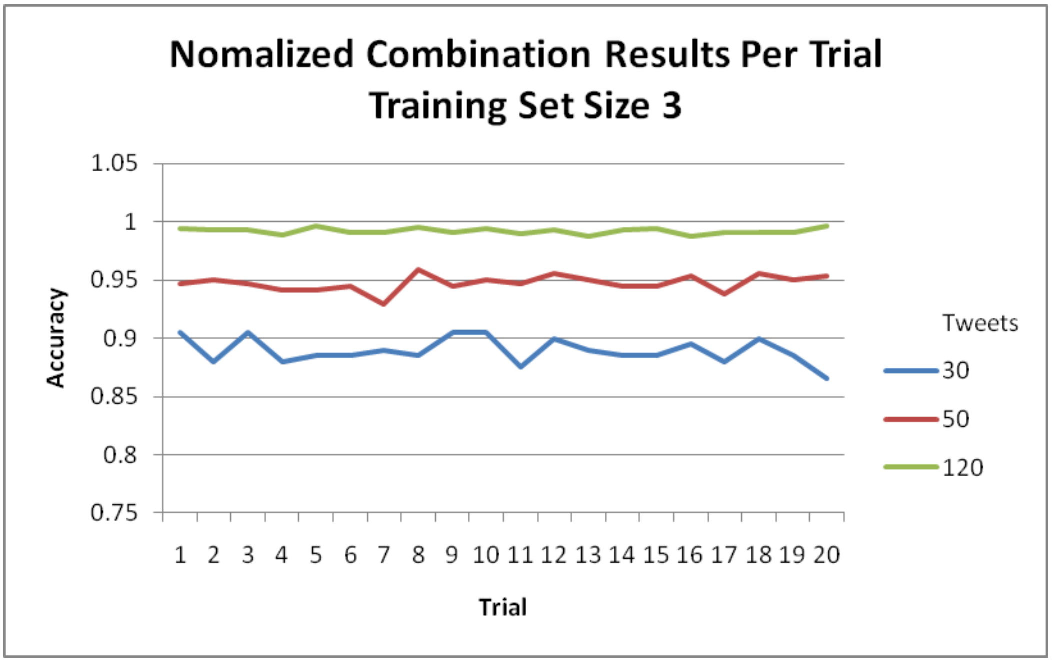

Figure 52. Averaged Accuracy Results of Normalized Combined Classifiers for Each Phone-Author Pairing Matrix Using Three Tweets per Training Set

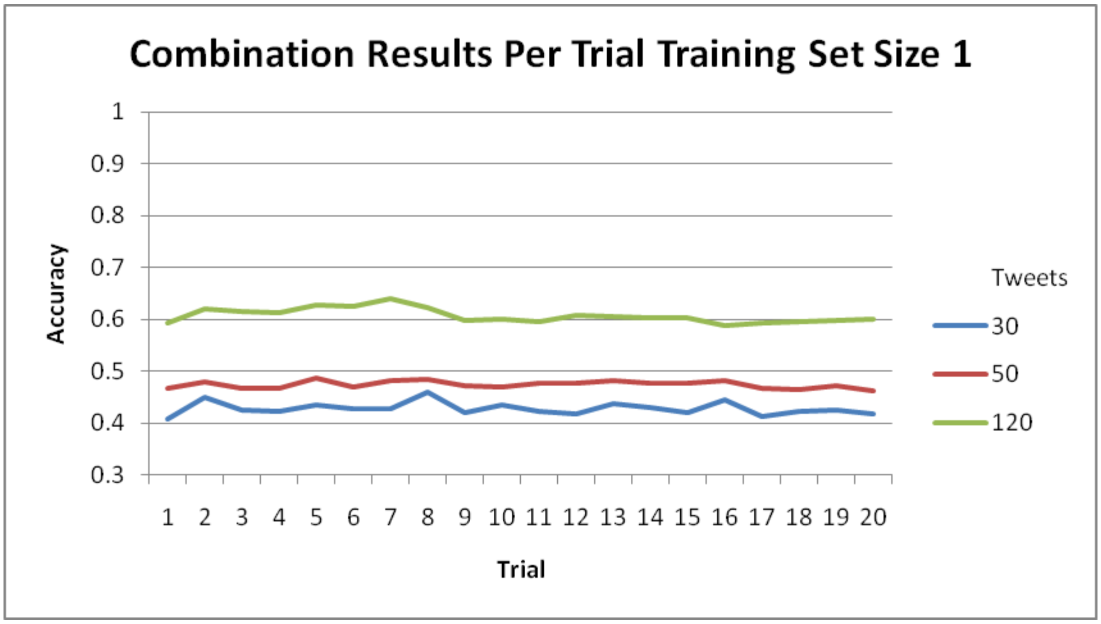

Figure 53. Averaged Accuracy Results of Non-Normalized Combined Classifiers for Each Phone-Author Pairing Matrix Using One Tweet per Training Set

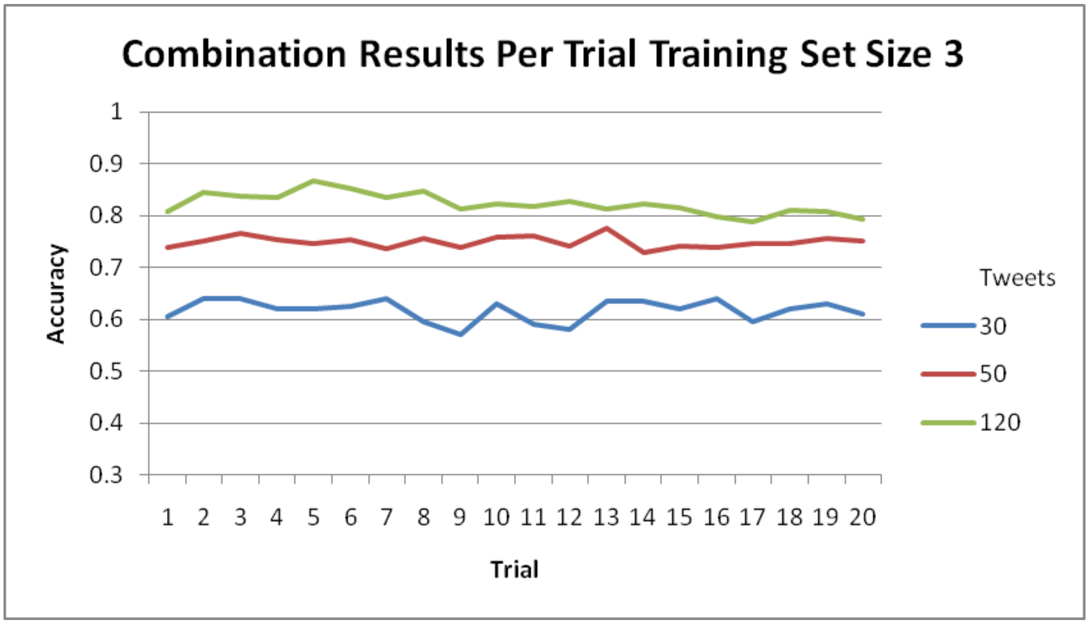

Figure 54. Averaged Accuracy Results of Non-Normalized Combined Classifiers for Each Phone-Author Pairing Matrix Using Three Tweets per Training Set

LIST OF REFERENCES

[1] CTIA – The Wireless Association. Wireless Quick Facts, Mid-Year Figures. June 2010. [Online]. Available: http://www.ctia.org/advocacy/research/index.cfm/aid/10323 (accessed March 6, 2011).

[2] L. Castillo. Sale of SIM cards to be regulated and monitored. *Mindanao Current* 30 January 2011. [Online]. Available: http://themindanaocurrent.blogspot.com/2011/01/sale-of-sim-cards-to-be-regulated-and.html (accessed March 10, 2011).

[3] R. Layton, P. Watters and R. Dazeley, "Authorship Attribution for Twitter in 140 Characters or Less," in *Cybercrime and Trustworthy Computing Workshop (CTC), 2010 Second,* 2010, p. 1.

[4] V. Brik, S. Banerjee, M. Gruteser and S. Oh, "Wireless Device Identification with Radiometric Signatures," in *MobiCom '08: Proceedings of the 14th ACM International Conference on Mobile Computing and Networking,* San Francisco, California, USA, 2008, pp. 116-127.

[5] Twitter. About Twitter. 13 December 2010. [Online]. Available: https://twitter.com/about (accessed December 13, 2010).

[6] 3GPP TS 03.40, "Technical Realization of the Short Message Service (SMS) (Release 1998)".

[7] D. Boyd, S. Golder, and G. Lotan, "Tweet, Tweet, Retweet: Conversational Aspects of Retweeting on Twitter," in *Proceedings of the 43rd Hawaii International Conference on System Sciences*, Kauai, HI, January 6, 2010.

[8] IANA, "Uniform Resource Locators (URL)", RFC 1738, December 1994.

[9] E. Stamatatos, "A survey of modern authorship attribution methods," *Journal of the American Society for Information Science and Technology,* vol. 60, pp. 538-556, March 2009.

[10] J. Lin, “Automatic Author Profiling of Online Chat Logs,” M.S. thesis, Naval Postgraduate School, Monterey, CA, 2007.

[11] V. Keselj, F. Peng, N. Cercone and C. Thomas, "N-gram-based Author Profiles for Authorship Attribution," In Proceedings of the Conference Pacific Association for Computational Linguistics, PACLING ’03, 2003, p. 255.

[12] G. Frantzeskou, E. Stamatatos, S. Gritzalis and S. Katsikas, "Effective Identification of Source Code Authors Using Byte-level Information," in *Proceedings of the 28th International Conference on Software Engineering,* Shanghai, China, 2006, pp. 893-896.

[13] L. E. Langley, "Specific Emitter Identification (SEI) and Classical Parameter Fusion Technology," in *WESCON/'93. Conference Record,* 1993, p. 377.

[14] B. Danev and S. Capkun, "Transient-based Identification of Wireless Sensor Nodes," in *IPSN '09: Proceedings of the 2009 International Conference on Information Processing in Sensor Networks,* 2009, pp. 25-36.

[15] A. Candore, O. Kocabas and F. Koushanfar, "Robust Stable Radiometric Fingerprinting for Wireless Devices," in *IEEE International Workshop on Hardware-Oriented Security and Trust, 2009, HOST '09,* 2009, p. 43.

[16] T. Kohno, A. Broido and K. C. Claffy, "Remote Physical Device Fingerprinting," *IEEE Transactions on Dependable and Secure Computing,* vol. 2, p. 93, April–June 2005.

[17] GSM World. Market Data Summary ~ GSM World. 15 December 2010. [Online]. Available: http://www.gsmworld.com/newsroom/market-data/market_data_summary.htm (accessed December 15, 2010).

[18] M. Rahnema, "Overview of the GSM System and Protocol Architecture," *Communications Magazine, IEEE,* vol. 31, p. 92, April 1993.

[19] Wikimedia Commons. File:Gsm structures.svg. 15 December 2010. [Online]. Available: https://secure.wikimedia.org/wikipedia/commons/wiki/File:Gsm_structures.svg (accessed December 15, 2010).

[20] C. Peersman, S. Cvetkovic, P. Griffiths and H. Spear, "The Global System for Mobile Communications Short Message Service," *Personal Communications, IEEE,* vol. 7, p. 15, June 2000.

[21] J. Scourias. "Overview of the Global System for Mobile Communications." December 15, 2010. [Online]. Available: http://ccnga.uwaterloo.ca/~jscouria/GSM/gsmreport.html (accessed December 15, 2010).

[22] K. Murota and K. Hirade, "GMSK Modulation for Digital Mobile Radio Telephony," *IEEE Transactions on Communications,* vol. 29, p. 1044, July 1981.

[23] T. Turletti, "GMSK in a nutshell," Technical Notes, Cambridge, MA, April 1996.

[24] D. Lewis, “Naïve (Bayes) at Forty: The Independence Assumption in Information Retrieval,” in *Proceedings of the 10th European Conference on Machine Learning, ECML ’98*, London, UK, 1998.

[25] E. Alpaydin, *Introduction to Machine Learning*. Cambridge, MA: MIT Press, 2004.

[26] D. Jurafsky and J. H. Martin, *Speech and Language Processing: An Introduction to Natural Language Processing, Speech Recognition, and Computational Linguistics.* Prentice-Hall, 2009.

[27] I. H. Witten and T. C. Bell, "The Zero-frequency Problem: Estimating the Probabilities of Novel Events in Adaptive Text Compression," *IEEE Transactions on Information Theory,* vol. 37, p. 1085, July 1991.

[28] J. Kittler, M. Hatef, R. P. W. Duin and J. Matas, "On Combining Classifiers," *IEEE Transactions on Pattern Analysis and Machine Intelligence,* vol. 20, p. 226, March 1998.

[29] L. Xu, A. Krzyzak, C. Y. Suen, “Methods of Combining Multiple Classifiers and Their Applications to Handwriting Recognition,” *IEEE Transactions on Systems, Man, and Cybernetics*, vol. 22, p. 418, May/June 1992.

[30] C. J. van Rijsbergen. Information. 1979. Retrieval. [Online]. Available: http://www.dcs.gla.ac.uk/Keith/Chapter.7/Ch.7.html (accessed December 17, 2010).

[31] Twitter Development. Streaming API Documentation. January 9, 2011. [Online]. Available: http://dev.twitter.com/pages/streaming_api (accessed January 9, 2011).

[32] A. Schein. The Naval Postgraduate School Machine Learning Library. Monterey, CA. 2010. [Online]. Available: http://sourceforge.net/projects/npsml/ [Accessed: January 15, 2011].

[33] 3GPP TS 05.05, “Radio Transmission and Reception (Release 1999)”.

[34] 3GPP TS 11.21, “Base Station System (BSS) equipment specification; Radio aspects (Release 1999)”.

[35] Agilent Technologies, “User’s Guide, Agilent Technologies 8922M/S GSM Test Set,” Agilent Part No. 08922-90211, January 1998.

[36] R. Honaker, “Novel Topic Authorship Attribution,” M.S. thesis, Naval Postgraduate School, Monterey, CA, 2011.

[37] P. Kimuli, ”Introduction to GSM and GSM mobile RF transceiver derivation,” *RF Design*, June 2003.

[38] Agilent Technologies, “Understanding GSM/EDGE Transmitter and Receiver Measurements for Base Transceiver Stations and their Components,” Application Note 1312, August 24, 2008.

INITIAL DISTRIBUTION LIST

1. Defense Technical Information Center
   Ft. Belvoir, Virginia

2. Dudley Knox Library
   Naval Postgraduate School
   Monterey, California

3. Dr. Robert Beverly
   Naval Postgraduate School
   Monterey, California

4. Dr. Craig Martell
   Naval Postgraduate School
   Monterey, California

5. Sarah Boutwell
   Naval Postgraduate School
   Monterey, California